FINE COAL DEWATERING USING HYPERBARIC FILTER CENTRIFUGATION

by

Serhat Keles

Dissertation submitted to the faculty of the
Virginia Polytechnic Institute and State University
in partial fulfillment of the requirements for the degree of

Doctor of Philosophy
in
Mining and Minerals Engineering

Gerald H. Luttrell, Chairman
Roe-Hoan Yoon, Co-Chairman
Gregory T. Adel
Ricky Q. Honaker

May 5, 2010
Blacksburg, Virginia

Keywords: Dewatering, Centrifugation, Hyperbaric, Filtration

FINE COAL DEWATERING USING HYPERBARIC FILTER CENTRIFUGATION

by

Serhat Keles

ABSTRACT

The solid-solid separation processes employed by modern coal preparation plants require large amounts of process water that must be removed from the surfaces of particles using mechanical dewatering equipment. Unfortunately, the existing processes that are used to dewater fine particles are inefficient in terms of moisture reduction and/or solids recovery. Many coal preparation plants are forced to discard fine coal particles because of the inability of existing technologies to reduce the moisture content of this product to an acceptable level. In light of this problem, a new ultrafine dewatering process called hyperbaric filter centrifugation (HFC) has been developed. This novel method combines centrifugation and pressure filtration within a single process to substantially reduce moistures over what can be achieved using conventional dewatering systems.

In the current study, empirical and theoretical dewatering models were developed in order to be able to simulate the behavior of the HFC technology. The empirical model was based on grain-size properties. On the other hand, the theoretical model was based on fundamental theories of filtration and centrifugation. Although the theoretical model provided a better understanding of the working principles of the process, the empirical model produced more accurate equilibrium moisture predictions. Therefore, the empirical model was used to further investigate the effects of several parameters on cake moistures. As such, the empirical model was useful for scale up and design purposes.

The empirical dewatering model was also used to perform an economical analysis of potential applications of the HFC technology. The model was used to investigate a variety of new circuit designs that have the potential to be commercially applied in the coal industry. The results clearly showed that this new technology would allow coal companies to process difficult-to-dewater ultrafines using the HFC process, while coarser solids would be more appropriately dewatered using conventional technologies such as vacuum filters or screenbowl centrifuges. This "split dewatering" concept would provide substantially higher profitability due to lower moistures and higher recoveries of ultrafine solids than could be achieved using a single dewatering process.

Laboratory- and pilot-scale versions of this technology has been constructed and tested at the facilities of Mining & Minerals Engineering Department of Virginia Tech. Results of this testing program showed that 30-50% lower moisture values than the ones obtained using conventional mechanical dewatering processes could be achieved with the HFC technology. Based on these promising results, a pilot-scale prototype unit, which was tested successfully at several commercial U.S. coal plants, was also constructed by Decanter Machine, Inc. Finally, the process of developing of this novel technology was successfully completed with the sale of the first full-scale commercial unit by Decanter Machine, Inc. to a major U.S. coal producer.

ACKNOWLEDGEMENTS

I would like to express my deepest gratitude and thanks to my advisor and my mentor Dr. Jerry Luttrell for his guidance and valuable insight throughout this research. He supervised this dissertation with great patience and keen interest. He contributed to it through his invaluable suggestions and criticism. The valuable comments and suggestions of the committee members Dr. Roe-Hoan Yoon, Dr. Greg Adel and Dr. Rick Honaker are also gratefully acknowledged.

The financial support from the U.S. Department of Energy and Mining and Minerals Engineering Department is greatly appreciated.

I would like to extend my sincere appreciation to Mr. Jim Waddell for helping me build all the machines that were needed for testing and for fixing things that were constantly broken. Also, many thanks to Mr. Bob Bratton for his help with my experiments and for staying late in the office many times to help me figure out mistakes made in Excel spreadsheets.

I wish to express my appreciation to Dr. Kerem Eraydin for his help with the experiments, for his valuable input and suggestions about chemicals, and for keeping me in shape.

Alpha Natural Resources, Arch Coal, Inc. and their employees are also acknowledged for providing much needed coal samples for my experiments.

Finally, I would like to thank my parents, my brother and my fiancé for their love, continuous moral support and encouragements throughout this study. It would not have been possible to complete this dissertation without them.

TABLE OF CONTENTS

LIST OF FIGURES

LIST OF TABLES

CHAPTER 1 GENERAL INTRODUCTION

Preamble

The United States has the world's largest reported coal reserve with approximately 263 billion tons of coal, which represents about 29% of the total proved global coal reserves (see Figure 1.1). In 2008, the U.S. coal production reached a record level of 1,171.5 million tons (see Table 1.2) and 96% of the coal produced was used domestically (BP, 2009; Freme, 2009). Therefore, if the consumption continues at the same rate, there is enough coal to meet the domestic consumption for more than 200 years. In 2008, more than 90% of the coal produced was used for electric power generation. Moreover, coal was the largest source of electrical power generation, with a share of almost 50% (Figure 1.1).

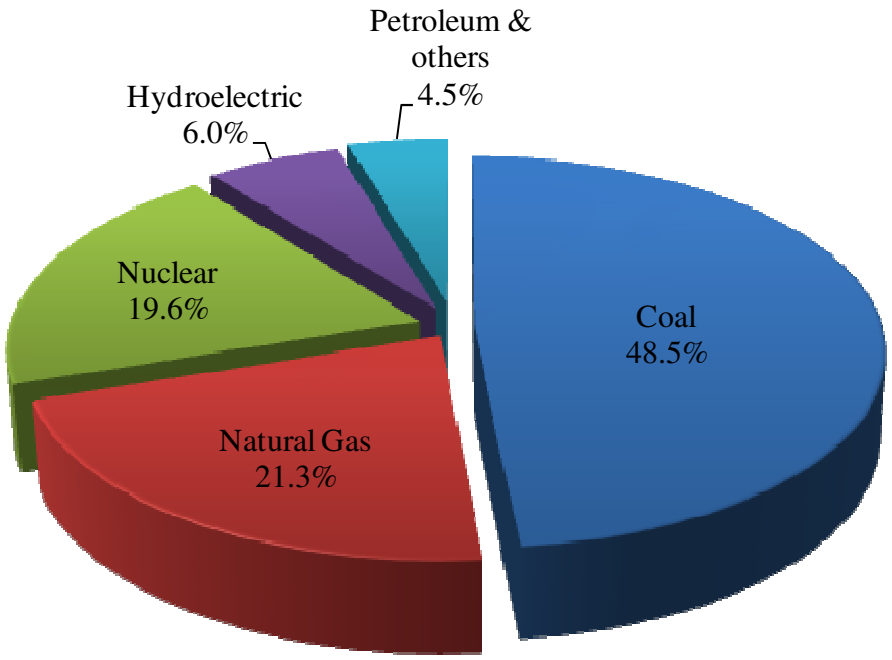

Figure 1.1 Electric power generation by energy source in the U.S. in 2008 (EIA, 2010)

Table 1.1 Recoverable coal reserves at the end of 2008 (BP, 2009)

Country	Recoverable Reserve (Million short tons)
United States	262,689
Russia	173,073
China	126,214
Australia	83,996
India	64,595
Ukraine	37,339
Kazakhstan	34,502
South Africa	33,519
Poland	8,269
Brazil	7,781

Table 1.2 Leading coal producers of the world and their production numbers in 2008 (Thousand short tons) (EIA, 2010)

	Anthracite	Bituminous	Lignite
China	539,454	2,197,069	111,461
United States	1,701	1,094,098	75,684
India	0	532,782	35,541
Australia	218	358,480	79,807
Indonesia	0	304,997	8,234
Africa	1,434	264,601	0
Russia	10,828	261,533	83,824
South Africa	1,414	258,182	0
Kazakhstan	0	115,100	4,708
Poland	0	92,217	65,665

Even though the global coal consumption increase slowed in 2008, coal still was the fastest growing fossil fuel with 3.1% growth among the other fuels. While the domestic coal consumption decreased as a consequence of the slowing domestic economy and poor weather in 2008, production and exports increased to levels not seen in 30 years as a result of the increased international demand (Figure 1.2). Furthermore, coal prices also increased because of rising international demand and the increased cost of transportation due to elevated oil prices (Freme,

2009). Therefore, coal is likely to remain as one of the most important energy sources in the U.S. and in the world.

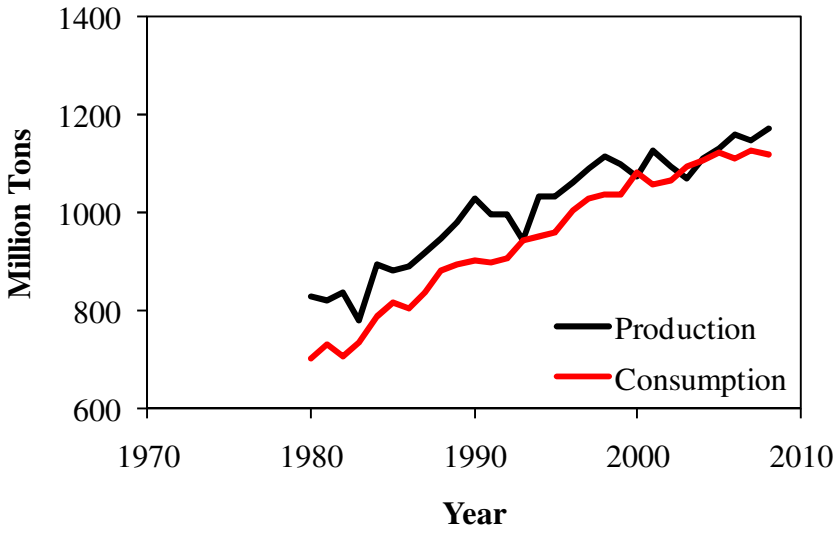

Figure 1.2 Coal production and consumption in the United States (EIA, 2010)

Much of the coal consumed in the U.S. is pretreated using coal preparation operations. These facilities are used to remove unwanted mineral matter that otherwise would decrease coal heating value, increase transportation costs, and adversely impact environmental emissions. Unfortunately, most of the cleaning processes used in modern coal preparation facilities are performed in an aqueous medium. As such, a variety of dewatering processes are used in coal preparation plants to remove excess surface moisture from clean coal products. Coarser particles can be readily dewatered using simple screening systems, while finer particles require costly unit operations such as centrifuges and filters (Osborne, 1988). Moisture that is not removed by these processes reduces the heating value and increases the cost of transporting the clean coal. Excess moisture can also create unacceptable handling problems for both the coal producer and downstream consumers by plugging chutes, bins, and rail cars. In colder regions, coal handling

can be particularly severe during winter months because of freezing (Kaytaz, Acarkan, & Halvorsen, 1994; L. R. Lyons, 1950).

The dewatering of fine (minus 0.150 mm) coal is particularly difficult due to the large surface area of particles in this size fraction (Sandy, Matoney, & Dahlstrom, 1991). At present, there are no mechanical dewatering processes that can inexpensively reduce the surface moisture of fine coal to a level that is acceptable for most industrial consumers. This shortcoming often forces U.S. coal producers to deslime their fine coal streams and to discard the ultrafine (minus 0.044 mm) fraction into refuse impoundments. Recent estimates for the U.S. coal industry suggest that approximately 2 billion tons of fine coal has been discarded in abandoned ponds and 500-800 million tons are in active ponds (Orr, 2002). In addition, U.S. preparation plants discard 30-40 million tons of additional fresh fine coal to ponds each year. This activity represents a loss of valuable natural resources, loss of profit for coal producers, and the creation of a potential environmental liability.

1.1 Literature Review

1.1.1 Coal Dewatering

The solid-solid separation processes employed by modern coal preparation plants require large amounts of process water. After cleaning, the unwanted water must be removed from the surfaces of the particles. Only about less than 10% of the existing U.S. coal plants still utilizes thermal dryers for moisture control (Bratton, 2010) because obtaining new permits for new thermal dryers is very difficult. Therefore, dewatering operations are mostly conducted by mechanical dewatering devices in modern coal preparation plants. Depending on the size of the coal, several types of mechanical devices are employed for coal dewatering. Coal particles larger than 5 mm are dewatered using screens. Shaking and vibrating screens are commonly used for

this purpose. Moreover, sieve bends are generally used for preliminary dewatering of coal prior to vibrating screens and centrifuges. 5 mm x 0.5 mm size range is sent to basket type centrifuges for dewatering. Screenbowl centrifuges are widely used in coal industry to dewater 1 mm x 0 size range of clean coal coming from froth flotation and spirals. However, the biggest disadvantage of screenbowl centrifuges is that they discard approximately 50% of the minus 0.044 mm material. If high coal recovery is desirable, then the fine coal (0.5 mm x 0) can be dewatered using vacuum filters. Two types of vacuum filters traditionally used are drum filters and disc filters. Vacuum disc filters are the most commonly employed type in coal preparation due to their large filter areas and small footprint (Dahlstrom & Klepper, 1982; Kaytaz, et al., 1994; Sandy, et al., 1991).

While clean coal is dewatered using the above mentioned units, coal tailings also have to be dewatered. The first step in fines tailing dewatering is sedimentation, which is done by thickeners. In the second step, thickened refuse sludge is sent to a dewatering device for further dewatering. Among all the available units, belt filter presses are the most commonly used devices to dewater fine coal refuse due to their good performance with very fine clay, which is often the main component of fine coal refuse. While the solid refuse material obtained is discarded to a refuse pond, clarified water recovered from thickeners and filters is recycled back to the plant to meet the water requirements of different processes (Dahlstrom & Klepper, 1982; Osborne, 1988).

1.1.2 Filtration theory

Filtration is used to separate liquids from solids by passing the solid-liquid mixture through a permeable medium, which accumulates most of the solid particles while permeating the liquid. There are two types of filters:

- Surface filters accumulate solids in the form of a cake atop a thin filter medium. Filtration conducted using surface filters is also called cake filtration.
- Depth filters accumulate the solids inside a thicker filter medium.

Surface filters are the most commonly used type of filters in coal preparation. Although, the filter medium is very thin, the cake formed on top of the filter medium becomes an extension to the original medium. Consequently, the cake acts as a depth filter and continues to accumulate particles inside and on the top as the slurry flow continues (Osborne, 1988; Svarovsky, 1990).

Cake filtration consists of several stages. First, initial bridging of particles occurs across the filter medium (Figure 1.3(a)). Then, cake formation starts and the cake gradually grows, while single-phase flow of water passes through the filter medium (Figure 1.3(b)). After the cake is formed (Figure 1.3(c)), cake compression occurs if the material is compressible (Figure 1.3(d)). This stage is often not important for coal applications because fine (i.e., 0.5 mm x 0) coal is not considered compressible (Condie, Hinkel, & Veal, 1996). Up to this point, the process is called filtration, as there is only single-phase flow of water. After that, the dewatering part of the process begins. Two-phase flow of air and water empties the largest pores (Figure 1.3(e)) and finally air breakthrough occurs (Figure 1.3(f)). In this stage, small pores still contain water. If there is a significant amount of cake cracking as result of the air breakthrough, dewatering stops because the vacuum pressure is lost (Condie, et al., 1996; Gala, Kakwani, Chiang, Tierney, & Klinzing, 1981).

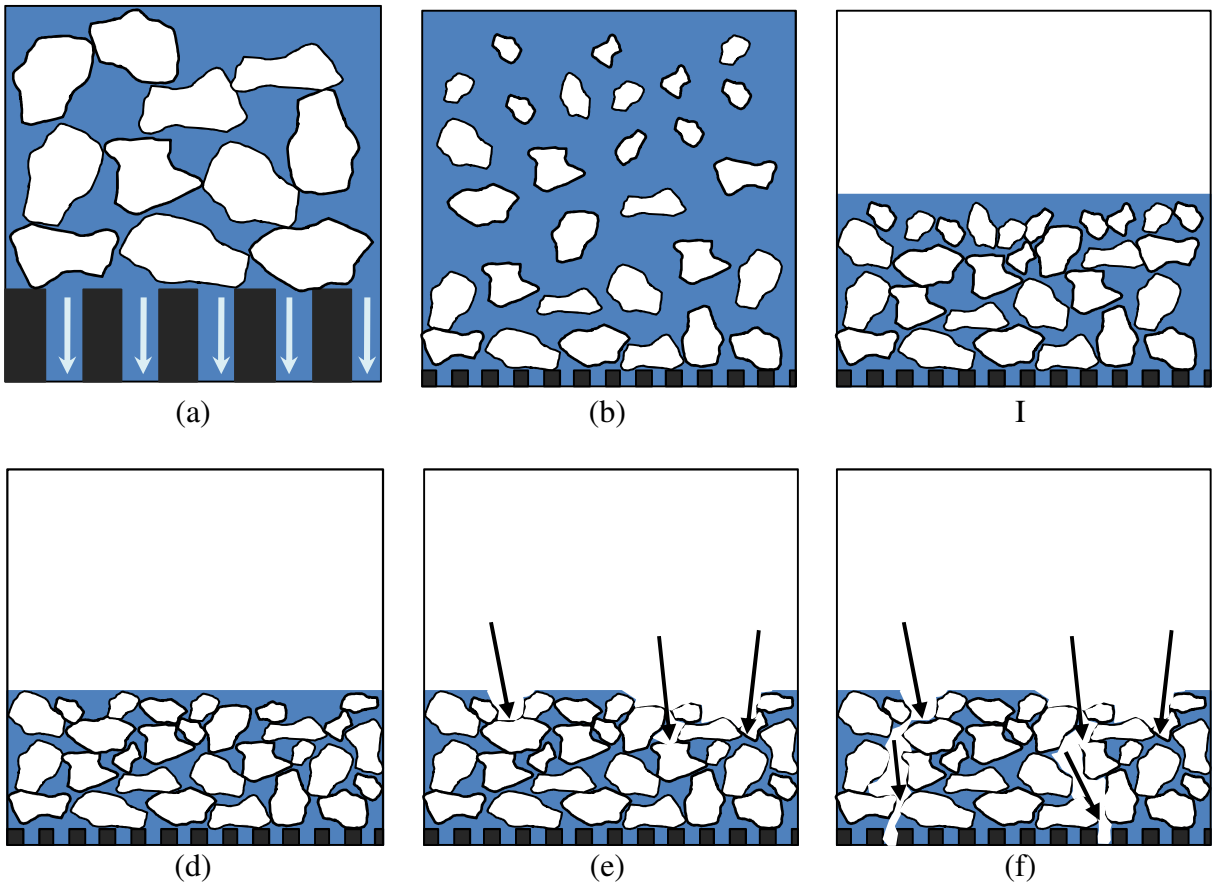

Figure 1.3 Stages of filtration

1.1.2.1 Kinetics of Filtration

Darcy (1856) defined filtration with the following basic equation, which relates the liquid flow rate through a filter cake to several parameters:

$$\frac{dV}{dt} = \frac{K\Delta PA}{\eta L} \qquad [1.1]$$

where V is the volume of liquid passing through the cake, t is the filtration time, K is the permeability of the bed, ΔP is the pressure drop across the cake, A is the cross-sectional area of the cake, η is the viscosity of the fluid and H is the cake thickness. In this equation ΔP is the most important parameter, as it is the driving force for liquid flow and dewatering.

Eq. [1.1] contains the permeability term K, which was defined by Kozeny (1927) using the following equation:

$$K = \frac{\varepsilon^3}{k(1-\varepsilon)^2 {S_v}^2} \quad [1.2]$$

where S_v is the specific surface area of the cake (m^2/m^3), ε is the porosity of the cake and k is the Kozeny constant, which normally takes value of 5 in fixed or slowly moving beds. For many industrial filter cakes formed in the presence of flocculants, k is often greater than 5 and can be as large as several thousands (Gray, 1958). Substituting Eq. [1.2] into Eq. [1.1] gives the Kozeny-Carman equation (Carman, 1956):

$$\frac{dV}{dt} = \frac{\Delta P A}{\eta L} \frac{\varepsilon^3}{k(1-\varepsilon)^2 {S_v}^2} \quad [1.3]$$

In vacuum filtration and pressure filtration, the liquid filtered is subjected to medium resistance, R_m, and cake resistance, R_c. The medium resistance is assumed to stay more or less constant, while the cake resistance changes with time. The L/K term in Eq. [1.1] can be expressed in terms of these two resistance values, and the equation becomes:

$$\frac{dV}{dt} = \frac{\Delta P A}{\eta (R_c + R_m)} \quad [1.4]$$

If the cake formed is assumed to be incompressible, then R_c can be expressed as:

$$R_c = \alpha W \quad [1.5]$$

where α is the specific cake resistance (m/kg) and W is the cake mass accumulated per unit area (kg/m^2). W can also be expressed as:

$$W = c\frac{V}{A} \quad [1.6]$$

where c is the concentration of solids in slurry (kg/m^3). Therefore, substituting Eq. [1.5] and Eq. [1.6] into Eq. [1.4] results in:

$$\frac{dV}{dt} = \frac{\Delta PA}{\eta\left(\alpha c\frac{V}{A} + R_m\right)} \quad [1.7]$$

$$\frac{dt}{dV} = \frac{\alpha\eta cV}{\Delta PA^2} + \frac{\eta R_m}{\Delta PA} \quad [1.8]$$

Integration of Eq. [1.8] for constant-pressure filtration condition gives:

$$\frac{t}{V} = \left(\frac{\alpha\eta c}{2\Delta PA^2}\right)V + \left(\frac{\eta R_m}{\Delta PA}\right) \quad [1.9]$$

which produces a straight line when *t/V* is plotted against *V*, as shown in Figure 1.4(a). The parameter *a* is the slope of the line and *b* is the y-axis intercept of the line. Moreover, for constant-rate filtration, *V/t* is constant and ΔP varies as follows:

$$\Delta P = \left(\frac{\alpha\eta cV}{A^2 t}\right)V + \left(\frac{\eta R_m}{A}\frac{V}{t}\right) \quad [1.10]$$

Similarly, plotting volume of liquid collected, V, versus filtration time, t, results in a straight line relationship such as that shown in Figure 1.4(b) (Dahlstrom, 1985; Osborne, 1988; Ranjan & Hogg, 1996; Rushton, Ward, & Holdich, 2000b; Wakeman & Tarleton, 1999).

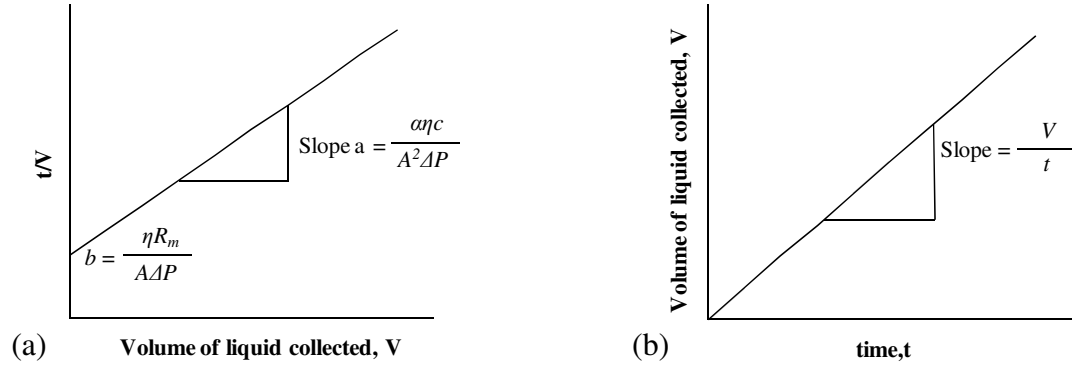

Figure 1.4 Plots of (a) t/V versus filtrate volume V for constant-pressure filtration and (b) ΔP versus filtration time, t for constant-rate filtration

Another fundamental equation of filtration was developed by Poiseuille (1841), which defines the flow of a liquid through a capillary tube with circular cross-section:

$$\frac{dV}{dt} = \frac{\Delta P \pi r^4}{8\eta L} \qquad [1.11]$$

where r is the capillary radius (Akers & Ward, 1977).

1.1.2.2 Thermodynamics of Filtration

In order to move a liquid contained in a capillary tube, the capillary pressure, *P*, defined by the Laplace equation (1806) given below has to be overcome (Ralston & Newcombe, 1992).

$$P = \frac{2\gamma_{LV} \cos\theta}{r} \qquad [1.12]$$

where γ_{LV} is the surface tension of the liquid, θ is the water contact angle and r is the radius of the capillary. Eq. [1.12] indicates that P can be reduced by decreasing γ_{LV}, increasing r or increasing θ. Therefore, the Laplace equation suggests that a cake with coarser size distribution would be easier to dewater than a finer cake, as the coarser cake would have larger capillaries.

Surface tension and contact angle values can be changed in favor of dewatering by addition of appropriate surface-active dewatering aids to the feed slurry. Figure 1.5 shows a liquid droplet attached to a solid surface. Surface tension vectors for solid-liquid (γ_{SL}), solid-vapor (γ_{SV}) and liquid-vapor (γ_{LV}) interfaces and the contact angle which is measured between the solid and the liquid interfaces are shown in the figure. The relationship between surface tensions and the contact angle can be quantified using Young's equation (Erbil, 2006; Ralston & Newcombe, 1992; Young, 1805):

$$\gamma_{SL} + \gamma_{LV} \cos\theta = \gamma_{SV} \quad [1.13]$$

The work of adhesion, which can be defined as the energy required to separate the liquid droplet from the solid surface, is defined by the following equation:

$$W_{adh} = \gamma_{SV} + \gamma_{LV} - \gamma_{SL} \quad [1.14]$$

Combining Eq. [1.13] and Eq. [1.14] gives the Young-Dupré equation (Dupré, 1869; Erbil, 2006; Ralston & Newcombe, 1992):

$$W_{adh} = \gamma_{LV}(1 + \cos\theta) \quad [1.15]$$

According to Eq. [1.15], the work of adhesion reaches its maximum value when θ is 0°, while at

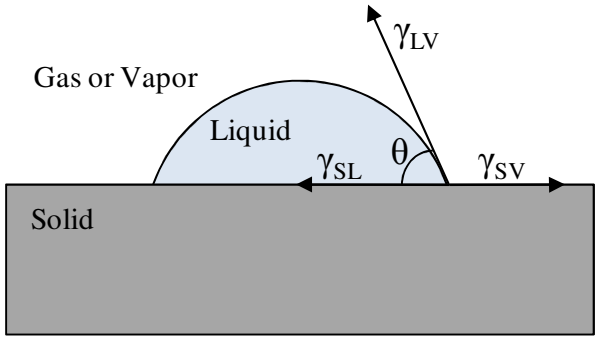

Figure 1.5 Representation of contact angles between solid, liquid and vapor phases

a 180°, the work of adhesion would be minimum. Therefore, the addition of proper surface-active dewatering aids which increase the contact angle and reduce the surface tension can help to reduce the work of adhesion, resulting in better dewatering performance.

1.1.3 Centrifugal Dewatering Theory

Centrifugal dewatering is a solid-liquid separation technique in which solid particles are separated from a liquid by means of a combination of sedimentation and filtration mechanisms driven by centrifugal force. Although gravitational sedimentation and centrifugation employs the same basic principle, which is density separation, centrifugation is a much faster process because of the magnitude of the centrifugal force applied. Most of the centrifugal dewatering devices used in coal industry operate at 50-3000 times of gravitational force (Osborne, 1988).

Under the effect of centrifugal force, particles in suspension move away tangentially from the rotation axis until they are stopped by the inner surface of the centrifuge, thus forming an annular cake. If the centrifuge has a perforated wall, the cake acts as filter medium and allows liquid to flow out; thus sedimentation and filtration are combined in this case. However, if the centrifuge has a solid wall, then only sedimentation occurs (Osborne, 1988; Rushton, Ward, & Holdich, 2000a).

Generally, the centrifugal force created by a centrifuge is expressed in terms of the number of times this force exceeds the gravitational force, or “the number of g's”, and it is formulated as follows:

$$F_C = \frac{4\pi^2 r N^2}{g} \qquad [1.16]$$

Where F_c is the centrifugal force, r is the centrifuge radius, N is the number of rotations per second and g is the gravitational acceleration.

The particulate bed, or the cake, formed inside a centrifuge contains three types of water: surface water, structure water and chemical water (Lowry, 1963). Chemical water is held in the chemical structure of the solids and cannot be removed. Surface water that lies on the particle surfaces can be removed easily by centrifugation, while the structure water that is found inside the capillary structure of the cake is more difficult to remove (Wakeman, 1984).

The liquid content of a cake is the most important factor among the factors that induce the capillary pressure. The liquid can be contained in a particulate bed in three states, i.e. pendular, funicular and capillary states as shown in Figure 1.6 States of a liquid in particulate bed. The relationship given in Figure 1.7 shows the capillary pressure for different states. As seen from the figure, capillary pressure is the smallest at the capillary state. As some of the liquid is drained from the cake, the capillary pressure increases and becomes far larger in magnitude at the funicular state than at the capillary state. If liquid drainage is continued, the capillary pressure increases rapidly and when the saturation of the particulate bed decreases to a certain level. Under this condition, the centrifugal force will not be large enough to overcome the capillary pressure; therefore, drainage of the liquid will stop (Hwang, Chu, & Lu, 2001).

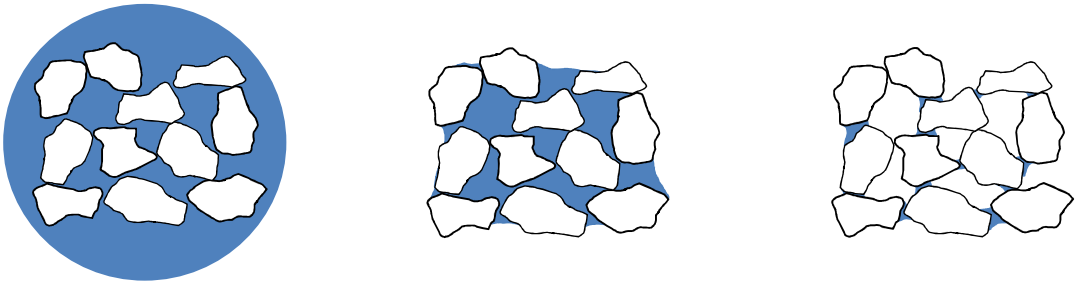

(a) Capillary State (b) Funicular state (c) Pendular State

Figure 1.6 States of a liquid in particulate bed

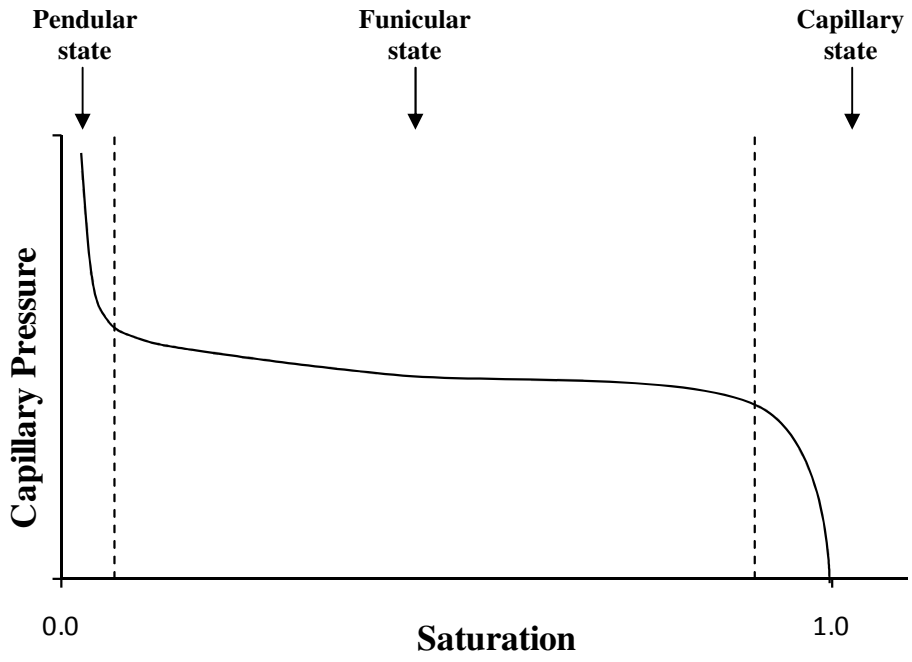

Figure 1.7 Relationship between capillary pressure and saturation of a particulate cake

1.1.4 Centrifugal Dewatering Equipment

Industrial centrifuges can be divided into two main categories, namely, continuously fed machines and batch machines. Centrifuges employed in coal industry are all continuously fed type machines, which can treat particle sizes from 50 mm to a few micrometers. Available feed capacities range from 0.25 to 100 tons of dry solids per hour (tph). However, no single machine can handle this entire particle size range.

In general, continuously fed centrifuges can be divided into two types (Osborne, 1988; Rushton, et al., 2000a; Wills, 2006; Zeitsch, 1990)

1) Perforate basket centrifuges (horizontal or vertical axis of rotation);
2) Bowl type centrifuges (horizontal axis of rotation);

Each main group has many types of machines as follows:

- Perforate basket type
    - Without a transport device
    - With a transport device
        - With positive discharge system
    - Vibrating basket
- Bowl type
    - Solid-bowl
    - Screen-bowl

1.1.4.1 Perforate Basket Centrifuges

Perforate basket centrifuges without transport devices are the simplest centrifuge designs. They consist of a conical perforated basket with an upward pointed apex of the cone. The coal is accelerated by the rotating bowl and the water is drained through the perforations of the basket. Coal slides down the inclined wall and is discharged at the base of the bowl. These centrifuges can handle 10 mm to 1 mm size range at capacities up to 50 tph, producing 6-8% moistures by weight (Osborne, 1988; Sandy, et al., 1991).

Perforate basket centrifuges with transport devices are commonly used in coal industry. They consist of a positive discharge mechanism, which is a solid cone with helical flights, inside a conical perforated bowl. Wet coal enters the apex of the bowl and is transported by the rotating flights towards the base of the bowl where it is discharged. These centrifuges can handle 10 mm to 0.5 mm size range at 80 tph capacity, producing 6-7% moisture by weight. Another design with a transport device, which is a horizontally rotated machine, can handle finer coal feeds of

minus 0.5 mm at 35 tph capacity and can produce a cake containing 10-12% moisture (Osborne, 1988; Sandy, et al., 1991).

Vibrating basket centrifuges, which can have either a vertical or a horizontal cone shaped basket, are also very commonly employed in coal industry. Perforated basket of the centrifuge vibrates in such a way that causes the coal particles move towards the discharge point. These machines do not rotate at as high speeds as the previously mentioned centrifuges. In the vertical axis type, the coal particles enter the centrifuge from the top through a hopper, and travel upwards on the perforated side walls by the vibrating action. Feed size for this type of centrifuge can be as coarse as 75 x 6.7 mm, which can be handled at 200 tph to produce 2% moisture by weight. A finer feed of 6.7 x 0.5 mm can also be handled at up to 110 tph capacity to produce about 7.5% moisture by weight. In the horizontal axis type, the coal particles enter the apex of the basket and the water is drained through the perforations on the walls. The vibrating action of the basket distributes and transports the coal through the machine. The horizontal axis type machines have the similar capabilities to vertical types (Osborne, 1988; Sandy, et al., 1991).

1.1.4.2 Bowl Type Centrifuges

Bowl type centrifuges, which are also called as decanter centrifuges, were started being used in the coal industry in mid 1960s with the introduction of solid-bowl centrifuge (Figure 1.8) for treating coal refuse. These centrifuges contain two rotating elements, namely the conveyor and the bowl. The bowl consists of a long cylindrical shaped region and a shorter cone shaped region. The conveyor with one or more helical flights that follow the contour of the bowl rotates at a slightly slower or faster speed than the bowl to transport the material. The transport speed is controlled by a mechanical gear reducer that operates at a fixed gear ratio. Clearance between the flights and the bowl is kept to a minimum. Solid particles are transported by the conveyor up the

slope of the cone above the liquid level, which is controlled by weirs at the other end of the centrifuge. Since solid particles can be very abrasive, conveyor flights are usually lined with a wear resistant material (Osborne, 1988; Sanders & Sutherland, 2001; Sandy, et al., 1991).

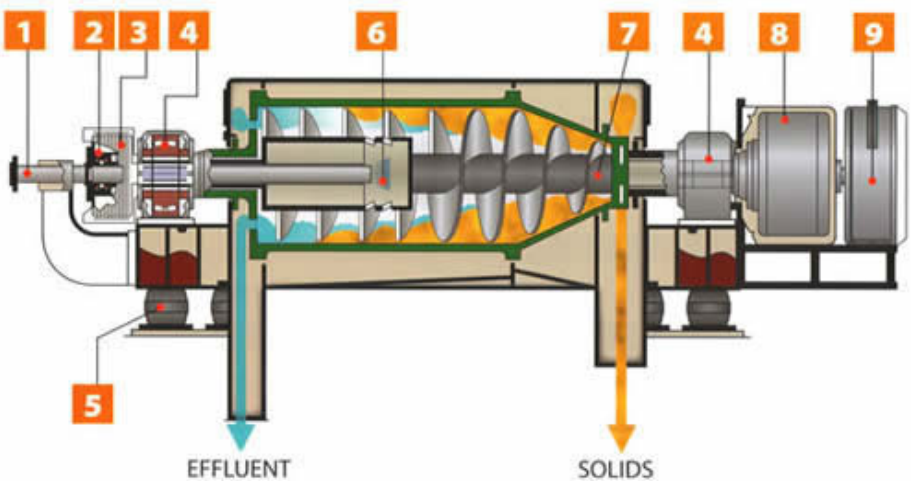

1. Feed Pipe
2. Thrust Bearings
3. Driven Sheave
4. Main Bearings
5. Vibration Isolators
6. Feed Compartment
7. Screw Conveyor
8. Planetary Gearbox
9. Back drive

Figure 1.8 Components of a solid-bowl centrifuge (Decanter Machine, 2010)

A bowl centrifuge can have either a concurrent or a countercurrent feed arrangement. In the concurrent feed design, the material enters the centrifuge at the larger cylindrical section of the bowl and the cake moves in the same direction as the centrate towards the conical end. Concurrent machines operate at slower speeds than countercurrent machines, therefore they are found to be attractive in disposal of coal tailings where higher product moistures (35-45%) can be accepted. In the countercurrent design, the material enters the centrifuge near where the conical section starts and the cake moves in the opposite direction to centrate flow. Higher wear and more power consumption are unavoidable with countercurrent centrifuges due to the higher speeds at which they operate. However, lower moistures can be achieved as a result of the much higher speeds they operate.

A screenbowl centrifuge (Figure 1.9) has an added cylindrical screen section to the solid bowl that allows for further water drainage. The screen is made up of tungsten carbide bars that have wedge profiles to prevent near size solid particles from getting stuck between the bars. By design, a screenbowl centrifuge is a countercurrent machine. Feed slurry enters the acceleration chamber, where it is brought up to speed, through a stationary pipe. Then, it is distributed inside the bowl through the feed ports. Solids settled under the acceleration force are carried up the slope of the cone by the helical conveyor, as in solid-bowl centrifuges. However, unlike solid-bowl centrifuges, thickened cake of solids pass over a screen section where the remaining excess water is filtered through the cake and discarded by the screen openings. Since the liquid drained through the screen section has such a small volume compared to the feed slurry and it can contain useful material, this liquid is usually recycled back to the feed (Osborne, 1988; Policow & Orphanos, 1983).

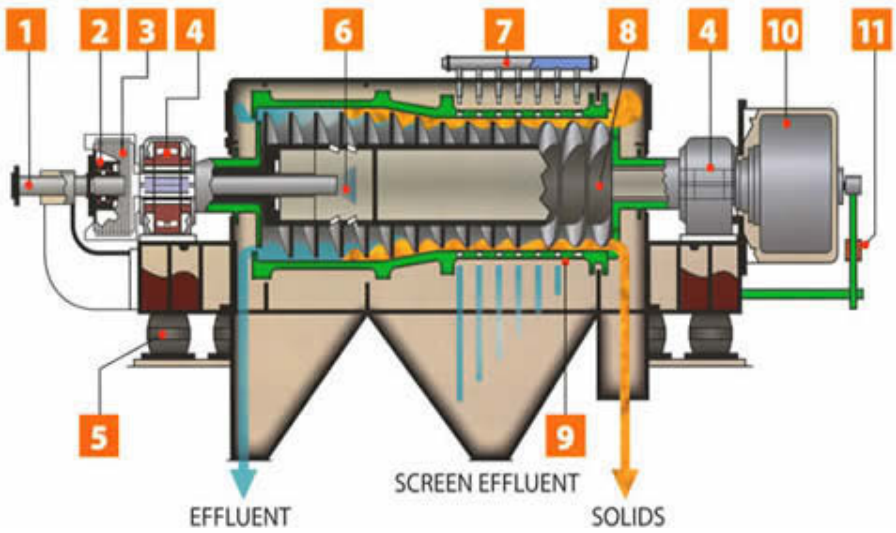

1. Feed Pipe
2. Thrust Bearings
3. Driven Sheave
4. Main Bearings
5. Vibration Isolators
6. Feed Compartments
7. Screen Wash Header
8. Screw Conveyor
9. Dewatering Screen
10. Planetary Gearbox
11. Torque Sensor

Figure 1.9 Components of a screenbowl centrifuge (Decanter Machine, 2010)

1.1.5 Hyperbaric Centrifugation

Injection of air into a centrifuge to improve dewatering performance was first described in the literature by Veal et al. (1998, 1999). This technology consists of the injection of a turbulent stream of high velocity air through the coal bed formed inside a vibrating basket centrifuge. The turbulent flow strips water from the surface of the particles. This technique can be effective when used with a particle size range of 0.5 to 50 mm. However, it is not applicable for fine coal.

Friedmann et al. (2004) conducted hyperbaric centrifugation experiments with a beaker centrifuge using EPDM elastomer particles (ethylene-propylene-diene-polymethylene elastomers), which form a highly compressible filter cake. They concluded that the hyperbaric centrifugation can provide better results in solid-liquid separation for highly compressible materials. They obtained the best results with respect to dewatering rate when a superimposed static pressure was used at lower centrifugal accelerations.

According to Darcy's law (Eq. [1.1]) the driving force for the flow is the pressure differential. In vacuum filtration, the pressure differential is less than 1 atm, while in pressure filtration it can be as high as 10 atm or more. In centrifugal filtration, the layer of water atop the filter cake creates the pressure differential needed to dewater the particle bed. This pressure can be calculated using:

$$\Delta P = \frac{1}{2}\rho\omega^2 h \qquad [1.17]$$

in which ρ is the density of water, ω the angular velocity, and h is the thickness of the water above the cake surface. One can see that ΔP becomes zero when h becomes zero (i.e., when the water disappears from the cake surface). In fact, the pressure inside the filter cake becomes lower than the ambient pressure when the water level drops below the surface of the cake as

shown in the example given in Figure 1.10 (Zeitsch, 1990). In the figure, the horizontal axis represents the distance from the axis of rotation and vertical axis shows the pressure differential across the filter cake. The cake surface is 0.6 m away from the axis of rotation. The water level first forms close to the center of rotation and proceeds towards the cake surface with time. Pressure differentials for three cases are provided in the figure. The top line represents the case when the water level is 0.5 m away from the center of rotation. The middle and the bottom lines show the pressures when the water level is 0.55 m and 0.60 m away from the center of rotation, respectively. As can be seen, the pressure profile across the cake decreases as the water level moves towards the cake surface. Eventually, the pressure drops below ambient, essentially creating a negative pressure, when the water level reaches the cake surface (at 0.60 m). This phenomenon greatly reduces the rate of dewatering during the drainage period of the centrifugal filtration process. In order to compensate the loss of the pressure, a higher centrifugal acceleration is typically recommended. Unfortunately, this action has practical limitations and

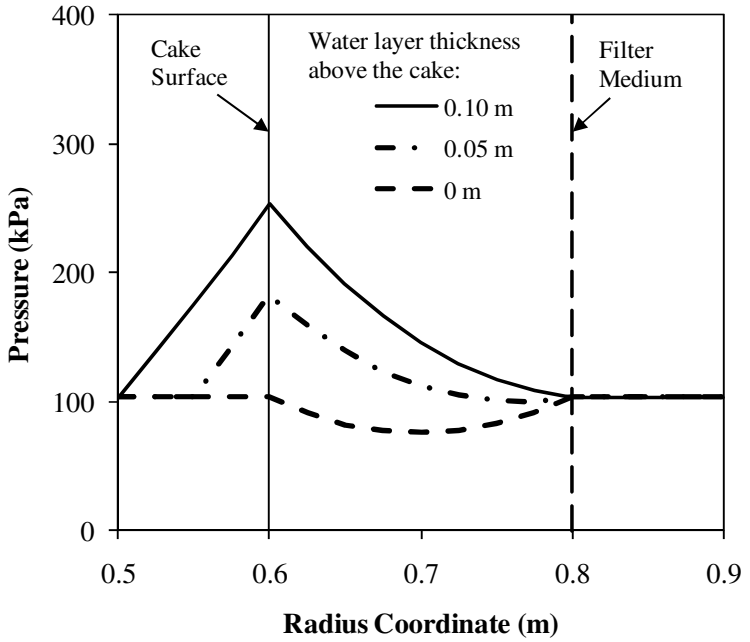

Figure 1.10 Pressure in a centrifuge filter cake under ambient pressure (Zeitsch, 1990)

typically leads to higher machine wear and maintenance requirements.

Another method of increasing the driving force for dewatering is to introduce compressed gas into the centrifuge chamber. The compressed gas increases the pressure differential across the filter cake and increases the rate of dewatering in accordance with Darcy's law (Eq. [1.1]). A larger pressure differential is useful for increasing the rate of dewatering during the drainage period, which is critical in achieving lower cake moistures.

Using the concepts introduced in the preceding paragraphs, Yoon and Asmatulu (2002) developed a novel centrifugal dewatering device for fine coal dewatering. The novel feature of this device is the use of air pressure as an additional driving force to the centrifugal force for removing water from a fine coal cake. With this technology, the rate of dewatering increases due to the increased driving force. Consequently, laboratory test results showed that hyperbaric centrifugation could provide substantially better moisture reductions than with air pressure or centrifugation alone (Asmatulu, Luttrell, & Yoon, 2005).

1.2 Objectives

The objectives of this study are:

- To fully develop a novel fine coal dewatering technology which can be employed commercially to recover the finest coal particles that were once discarded due to their high moisture content and lack of economic value. This goal has been achieved by:
    - conducting laboratory-scale parametric studies with batch test units so that an improved understanding of the parameters affecting hyperbaric centrifugation could be fully investigated,
    - conducting semi-continuous bench-scale and fully-continuous pilot-scale tests to establish engineering criteria for the design and operation of a prototype unit, and

- conducting a demonstration of the technology at an industrial site using a full-scale continuous prototype constructed by a commercial partner.

- To successfully develop a dewatering model that can be used to accurately simulate the hyperbaric centrifugation process by extending and improving existing centrifugal dewatering models, and
- To demonstrate the capability of this novel technology for reducing environmental impacts associated with coal production while simultaneously creating a potential source of new revenue and profit for coal producers.

1.3 Organization

This dissertation consists of seven chapters. The first chapter gives an introduction to the research and provides detailed background information obtained from various literature sources. While the second chapter represents and discusses all the laboratory-scale test results obtained, the third chapter gives details of the pilot-scale test program. The fourth chapter provides the details and results of field tests conducted with a prototype unit. The fifth chapter discusses the theoretical basis of this research project and provides two models developed in order to simulate this novel dewatering process. The sixth chapter provides an economical evaluation of this novel process via a case study. Finally, the seventh chapter summarizes all the findings of this research and development project.

1.4 References

1. Akers, R. J., & Ward, A. S. (1977). *Filtration: Principles and Practices Part 1* (Vol. 10). New York and Basel: Marcel Dekker, Inc.
2. Asmatulu, R., Luttrell, G., & Yoon, R.-H. (2005). Dewatering of Fine Coal Using Hyperbaric Centrifugation. *Coal Preparation, 25*, 117-127.
3. BP. (2009). Statistical Review of World Energy, from http://www.bp.com/statisticalreview
4. Bratton, R. (2010). [Personal Communication].
5. Carman, P. C. (1956). *Flow of Gases Through Porous Media*. London: Butterworths.
6. Condie, D. J., Hinkel, M., & Veal, C. J. (1996). Modelling the vacuum filtration of fine coal. *Filtration & Separation, 33*(9), 825-834.
7. Dahlstrom, D. A. (1985). Filtration. In N. L. Weiss (Ed.), *SME Mineral Processing Handbook*. New York, N. Y.: Society of Mining Engineers of the American Institute of Mining, Metallurgical, and Petroleum Engineers.
8. Dahlstrom, D. A., & Klepper, R. P. (1982). Practical Aspects of Filtration and Dewatering in Physical Cleaning of Fine Coal. In Y. A. Liu (Ed.), *Pyhsical Cleaning of Coal: Present and Developing Methods*. New York: M. Dekker.
9. Darcy, H. (1856). *Les fontaines publiques de la ville de Dijon*. Paris.
10. Decanter Machine, I. (2010), from http://www.decantermachine.com
11. Dupré, A. (1869). *Theorie Mecanique de la Chaleur*. Paris: Gauthier-Villars.
12. EIA. (2010). International Energy Statistics, from http://www.eia.doe.gov
13. Erbil, H. Y. (2006). Contact Angle of Liquid Drops on Solids. In H. Y. Erbil (Ed.), *Surface Chemistry of Solid and Liquid Interfaces* (pp. 308-334). India: Blackwell Publishing.
14. Freme, F. (2009). U. S. Coal Supply and Demand: 2008 Review, from http://eia.doe.gov

15. Friedmann, T., Lustenberger, C., & Windhab, E. J. (2004). Filtration experiments with compressible filter cakes in centrifugal fields with superimposed static pressure. *International Journal of Mineral Processing, 73*(2-4), 261-267.
16. Gala, H. B., Kakwani, R., Chiang, S. H., Tierney, J. W., & Klinzing, G. E. (1981). Filtration and Dewatering of Fine Coal. *Separation Science and Technology, 16*(10), 1611 - 1632.
17. Gray, V. R. (1958). The Dewatering of Fine Coal. *Journal of the Energy Institute, 31*, 96-108.
18. Hwang, K.-J., Chu, W.-T., & Lu, W.-M. (2001). A Method To Determine The Cake Properties In Centrifugal Dewatering. *Separation Science and Technology, 36*(12), 2693 - 2706.
19. Kaytaz, Y., Acarkan, N., & Halvorsen, W. J. (1994). Dewatering of Coal. In O. Kural (Ed.), *Coal: Resources, Properties, Utilization, Pollution* (pp. 239-245).
20. Kozeny, J. (1927). Uber Kapillare Leitung Des Wassers in Boden (Vol. 136(2a), pp. 271-306): Wien Akad. Wiss.
21. Laplace, P. S. (1806). Théorie de l'Action Capillaire *Supplement au livre dixième de la Mechanique Celeste*. Paris.
22. Lowry, H. H. (1963). *Chemistry of Coal Utilization*. New York: Wiley.
23. Lyons, L. R. (1950). Dewatering and Thermal Drying. In D. R. Mitchell (Ed.), *Coal Preparation* (2nd ed.). New York: American Institute of Mining and Metallurgical Engineers.
24. Orr, F. M. (2002). Coal Waste Impoundments: Risks, Responses and Alternatives. Washington, D. C.: National Research Council.

25. Osborne, D. G. (1988). Solid-Liquid Separation *Coal Preparation Technology* (Vol. 1, pp. 478-542). London; Boston: Graham & Trotman.

26. Poiseuille, J. L. M. (1841). *Comptes Rendus, 12*, 1041.

27. Policow, N. D., & Orphanos, J. S. (1983). Development of the Screen Bowl Centrifuge for Dewatering Fine Coals. *Mining Engineering, 35*(4), 333-336.

28. Ralston, J., & Newcombe, G. (1992). Static and Dynamic Contact Angles. In J. S. Laskowski & J. Ralston (Eds.), *Colloid Chemistry in Mineral Processing*. Amsterdam: Elsevier.

29. Ranjan, S., & Hogg, R. (1996). The Role of Cake Structure in the Dewatering of Fine Coal by Filtration. *Coal Preparation, 17*(1), 71 - 87.

30. Rushton, A., Ward, A. S., & Holdich, R. G. (2000a). Centrifugal Separation *Solid-Liquid Filtration and Separation Technology* (pp. 295-365). Weinhheim: Wiley-VCH.

31. Rushton, A., Ward, A. S., & Holdich, R. G. (2000b). Filtration Fundamentals *Solid-Liquid Filtration and Separation Technology* (pp. 295-365). Weinhheim: Wiley-VCH.

32. Sanders, A., & Sutherland, K. (2001). *Decanter Centrifuge Handbook*: Elsevier.

33. Sandy, E. J., Matoney, J. P., & Dahlstrom, D. A. (1991). Dewatering. In J. W. Leonard (Ed.), *Coal Preparation* (5th ed.). Littleton, Colorado: Society for Mining, Metallurgy, and Exploration.

34. Svarovsky, L. (1990). Filtration Fundamentals. In L. Svarovsky (Ed.), *Solid-Liquid Separation* (3rd ed.). London; Boston: Butterworths.

35. Veal, C. J., Nicol, S. k., & Johnston, K. (1998). USA Patent No. 5771601.

36. Veal, C. J., Nicol, S. k., & Johnston, K. (1999). USA Patent No. 5956858.

37. Wakeman, R. J. (1984). Residual saturation and dewatering of fine coals and filter cakes. *Powder Technology, 40*(1-3), 53-63.

38. Wakeman, R. J., & Tarleton, E. S. (1999). *Filtration: Equipment Selection Modelling and Process Simulation* (1st ed.): Elsevier.

39. Wills, B. A. (2006). *Wills' Mineral Processing Technology: An Introduction to the Practical Aspects of Ore Treatment and Mineral Recovery* (7th ed.). Amsterdam, London: BH.

40. Yoon, R.-H., & Asmatulu, R. (2002). USA Patent No. 6440316 B1.

41. Young, T. (1805). *Philosophical Transactions of the Royal Society (London), 95*(1805), 65.

42. Zeitsch, K. (1990). Centrifugal Filtration. In L. Svarovsky (Ed.), *Solid-Liquid Separation* (3 ed.). London; Boston: Butterworths.

CHAPTER 2 A LABORATORY STUDY OF HYPERBARIC CENTRIFUGATION

2.1 Introduction

Yoon et al. (2001; 2005) performed several series of laboratory tests to demonstrate the effectiveness of hyperbaric centrifugation for fine coal dewatering. Based on the results obtained, a pilot-scale test unit was constructed to study this novel technology furthermore. However, as it will be explained in Chapter 3, the originally planned complete testing program could not be finished because of the many technical problems faced with the pilot-scale unit. To overcome this problem, Decanter Machine, Inc., which is the largest producer of screenbowl centrifuges in the U.S., was chosen and licensed as a partner for developing a pilot-scale prototype hyperbaric centrifuge. While construction of the pilot-scale prototype was being completed, it was decided to conduct a more detailed laboratory-scale testing program to fully understand the hyperbaric centrifugation process. For this purpose, several laboratory-scale test units were constructed and tested using various coal samples obtained from different coal preparation plants.

2.2 Experimental

2.2.1 Samples

All slurry samples used for laboratory studies were clean coal samples (i.e. screenbowl feed or flotation product) obtained from different commercial coal plants. These samples typically contained 8-12% ash. A low-ash (<10%) unprocessed dry coal sample from Cucumber Mine in West Virginia was also obtained for testing. All slurry samples were split upon receipt by a custom-made slurry splitter (Figure 2.1) down to the amount required. This step was found to be essential to have a representative sample of the slurry so that reproducible results could be

obtained. Past experience showed that when dealing with a coarser sample (i.e. 1 mm topsize), sampling from a mixed bucket was not a trustworthy method and often resulted in biased results. The use of a hand-held scoop to collect feed samples was found to produce erroneous and non-reproducible results. The dry coal sample was also split using a riffle sample divider. After splitting, all samples were screened to determine size distributions. Slurry samples were tested within 2-3 weeks upon receipt to avoid changing of the sample due to surface oxidization.

Figure 2.1 Slurry splitter

2.2.2 Equipment Design and Setup

2.2.2.1 Hyperbaric Centrifuge Apparatus

Figure 2.2 shows a schematic of the batch test unit used in the laboratory-scale test program. The unit was constructed with a 4-inch diameter and 3-inch height using stainless steel. Evenly spaced holes with 3.0, 2.4 and 1.6 mm diameters were drilled on the sidewalls for water drainage from the cake. The unit was used in two different setups with two different pressure lids for a variety of tests.

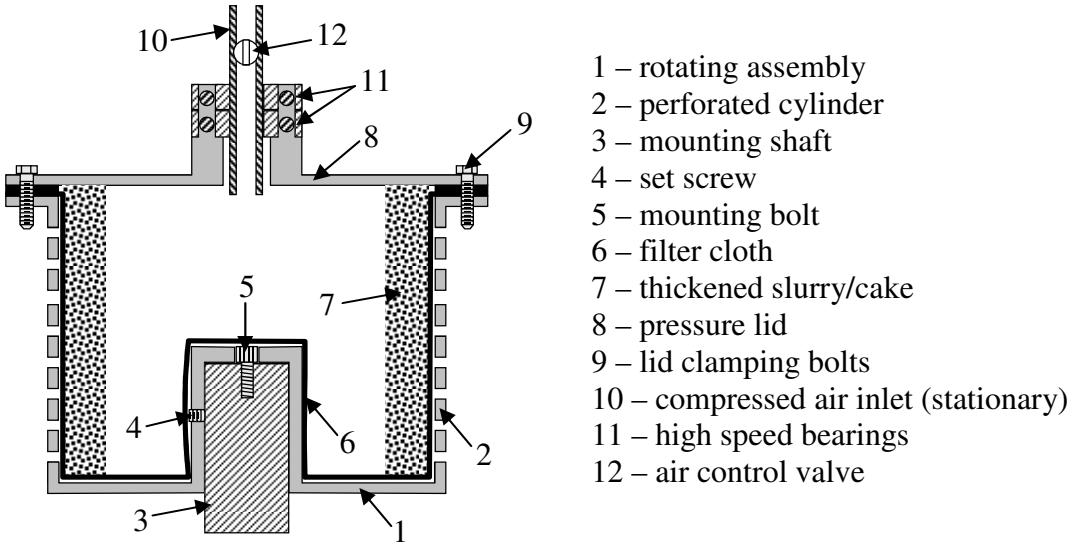

Figure 2.2 Schematic of the hyperbaric centrifuge unit used in standard batch tests

The first setup was used for the standard batch tests described in Section 2.3.1. For this setup, the centrifuge basket was placed inside in a Beckman variable-speed centrifuge machine (Figure 2.3). This "ultracentrifuge" is capable of high rotational speeds of up to approximately 20,000 rpm. The basket was attached to the rotating shaft by means of a mounting bolt. Also, a set screw was used to secure the basket in place to avoid any balancing issues that might arise at high rotation speeds. Since the basket was sealed inside the centrifuge machine (Figure 2.4), very high rotation speeds (and high-g levels) were possible without any safety concerns. Two high-speed ball bearings were attached to the lid in order to insert and support a pressurized air line. The air line was equipped with an on/off valve and a pressure gauge for monitoring and controlling air pressure. Since, this test setup did not also allow for collecting the effluent, coal recovery values could not be determined from these batch experiments.

Figure 2.3 Beckman centrifuge machine

Figure 2.4 Sealed compartment of the Beckman centrifuge machine

The second setup (see Figure 2.5) was used for the modified batch tests described in Section 2.3.2. In this setup, the unit was mounted on a vertical rotor shaft and fixed in place using a set screw. A variable speed motor was used to control the rotational speed of the centrifuge. In order to pressurize the unit, a bearing and a sealed connector were used to attach a compressed air line to the center of the lid. The air-line was equipped with an on/off valve and a pressure gauge so that the air pressure can be monitored and controlled. A container suspended from a digital balance was used to collect water removed during kinetic testing. The balance continuously recorded the mass of water accumulated via a data acquisition computer. As such, this setup made it possible to monitor the kinetics of dewatering.

Figure 2.5 The test setup used for modified batch tests

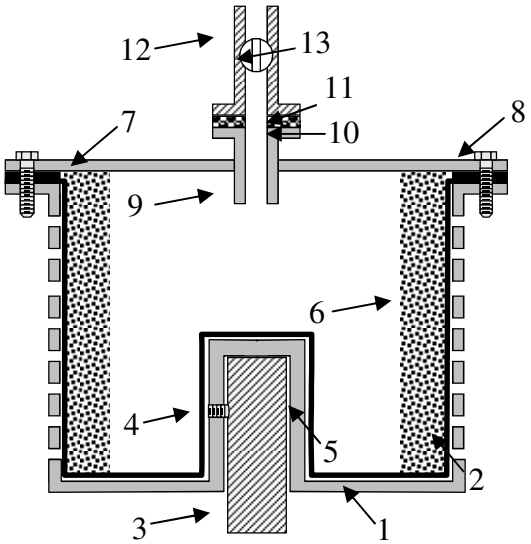

1 – rotating assembly
2 – perforated cylinder
3 – mounting shaft
4 – set screw
5 – filter cloth (or mesh)
6 – cake
7 – pressure lid
8 – lid clamping bolts
9 – compressed air inlet
10 – rotating seal face
11 – rotating pressure seal
12 – stationary inlet
13 – air control valve

Figure 2.6 Schematic of the hyperbaric centrifuge unit used in modified batch tests

In most of the tests, the centrifuge basket was lined with a filter cloth that had a 0.015 mm aperture size. However, a somewhat coarser filter cloth (unknown aperture size) and a 1.5 mm screen mesh were also used to study the effect of filter medium on product moisture and solid recovery. The first test setup described above did not allow for feeding the unit while the basket was rotating. Therefore, the basket was filled with coal slurry before the lid was securely closed in every test. Since only a limited amount of slurry could fit inside the basket, all the excess water contained in slurries had to be removed before testing. This was accomplished by allowing solid particles to settle followed by removing the excess water using a syringe. On the other hand, in the second test setup, the coal slurry could be fed to the unit while the basket was rotating. A peristaltic pump was used for this purpose so as to minimize degradation of particle size.

2.2.3 Hyperbaric Centrifuge Apparatus with Screen Bars

2.2.3.1 Screen Section

After experimenting with the hyperbaric batch filter centrifuge, another small scale batch unit was built using tungsten carbide bars in the screen section. These bars were the same as those employed in commercial screenbowl centrifuges. The aim of this study was to replace the screen mesh or the filter cloth, which cannot be used commercially, with a wear resistant part that is widely used in the industry. The test unit, which is shown in Figure 2.7, was constructed from aluminum with 4.25-inch height, 5-inch outside diameter and 3.9-inch inside diameter. Slots of approximately 1/8-inch wide were cut on the sidewalls of the basket for water removal. T-shaped tungsten carbide bars (Figure 2.8) were glued inside the basket. These bars were designed by the manufacturer in such a way that when two of them are put together, the gap between them expands towards the outside (i.e., similar to the configuration used in a wedge-

wire sieve). This arrangement reduces the probability of near-size particles getting trapped between the bars.

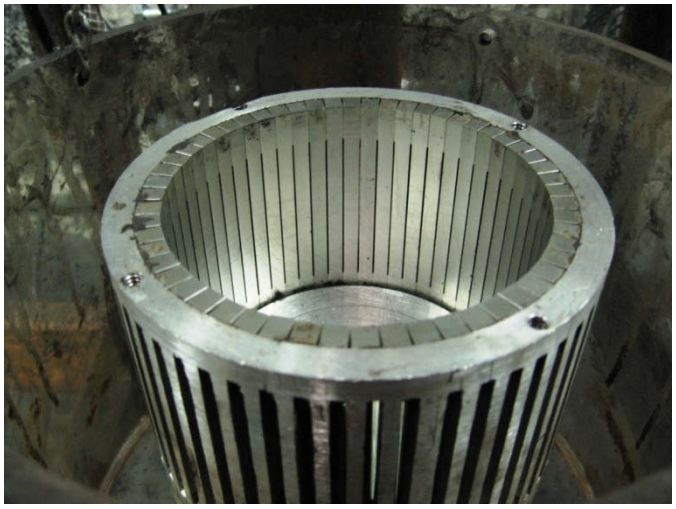

Figure 2.7 Hyperbaric centrifuge constructed with screen bars

Figure 2.8 Different sides of tungsten carbide bars used to build the screen section

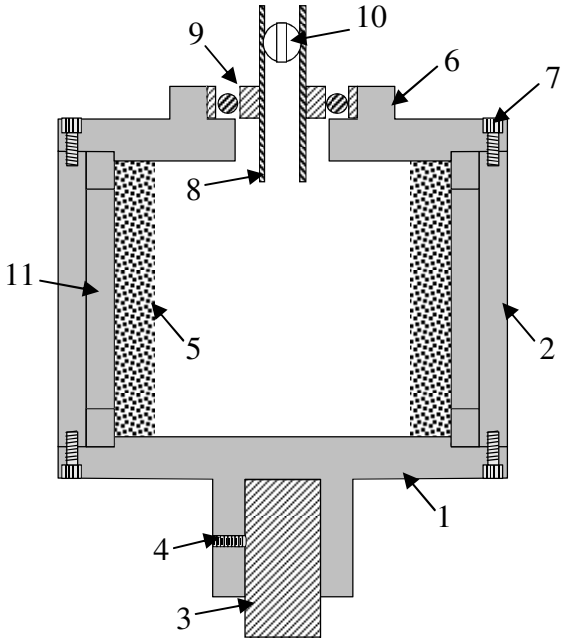

1 – rotating assembly
2 – cylinder with slots
3 – mounting shaft
4 – set screw
5 – thickened slurry/cake
6 – pressure lid
7 – lid clamping bolts
8– compressed air inlet (stationary)
9 – high speed bearing
10 – air control valve
11 – tungsten carbide bars

Figure 2.9 Schematic of the batch bench-scale centrifuge unit used in standard batch tests

The test unit was mounted on a vertical rotor shaft and fixed in place using a set screw (Figure 2.9). A variable speed motor was used to control the rotational speed of the centrifuge. A high-speed bearing was attached to the lid, in order to connect a pressurized air line. The air-line was equipped with an on/off valve and a pressure gauge so that the air pressure could be accurately monitored and controlled.

2.2.3.2 Solid-Bowl Section

One of the aims of this project was to use a feed finer than what is normally used with screenbowl centrifuges. Some preliminary tests were run with the batch bench-scale unit with screen bars using minus 0.15 mm flotation product, but all the particles passed through the openings. Trials with flocculant addition also failed, because the agglomerates formed were not large enough to be retained in the centrifuge. Commercially available screenbowl centrifuges contain a solid-bowl section before the screen-section so that the feed can be thickened and excessive water and ultrafine particles can be discarded for more efficient dewatering. Based on this fact, a separate solid-bowl centrifuge was constructed to produce a thickened-feed for the batch bench-scale centrifuge with screen bars.

The solid-bowl unit (Figure 2.10) was constructed from aluminum with 4.25-inch height, 5-inch outside diameter and 4.4-inch inside diameter. The unit was mounted on a vertical shaft and fixed in place using a set screw. A variable-speed motor was used to control the rotational speed of the centrifuge. A high-speed bearing was attached to the lid, in order to connect a slurry feed line. Slurry was gravity fed into the unit. The lid of the unit (Figure 2.11) was designed in such a way that excess water could escape the unit easily while solid particles form a cake under the lid. Also, four small threaded-holes were drilled on the sides near the top of the centrifuge, in

order to discard the water that could not be discarded through the lid. These holes were covered with small pieces of filter cloth to prevent solid particles from escaping the unit.

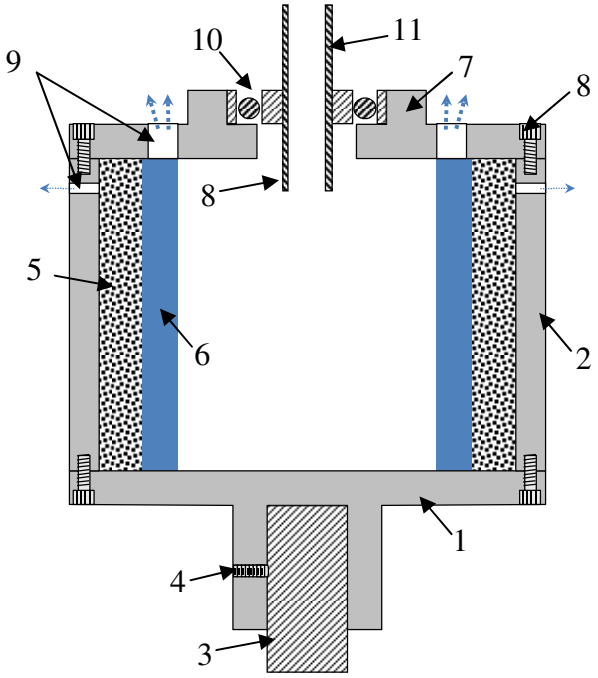

1 – rotating assembly
2 – solid cylinder
3 – mounting shaft
4 – set screw
5 – thickened slurry/cake
6 – excess water
7 – lid with slots for water removal
8 – lid clamping bolts
8– compressed air inlet (stationary)
9 – threaded-holes for water removal
10 – high speed bearing
11 – feed line
11 – tungsten carbide bars

Figure 2.10 Schematic of the solid-bowl centrifuge unit used in standard batch tests.

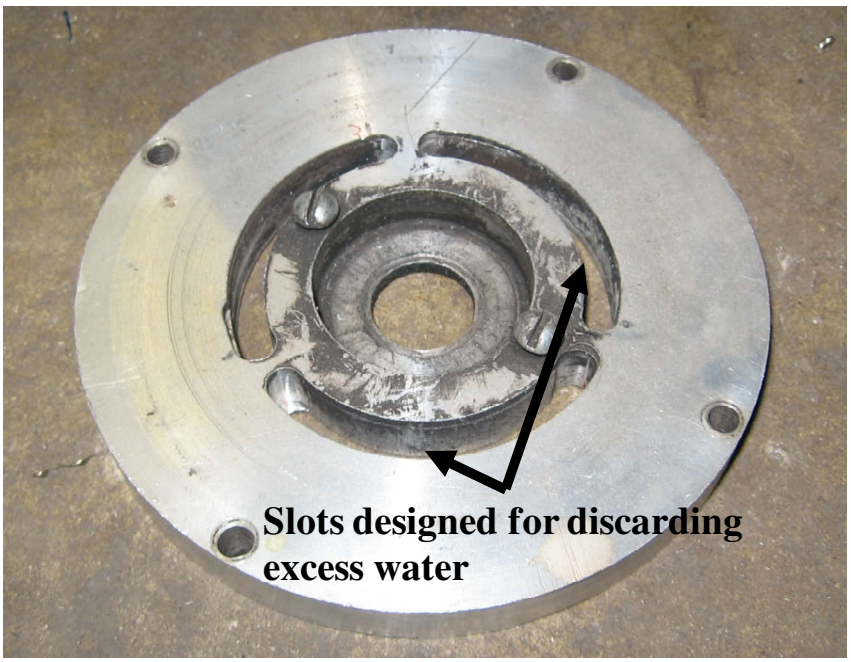

Figure 2.11 Specially designed lid of the solid-bowl unit

All tests that were conducted with this unit consisted of two steps. In the first step, threaded holes on the sides of the bowl were sealed using bolts, so that the water could only go out of the holes on the top, and the centrifuge was run until there was no water leaving. Then, in the second step, bolts on the sides were unscrewed and the centrifuge was run again to let the remaining free water leave the unit.

2.3 Results

2.3.1 Standard Batch Tests

2.3.1.1 Effect of Coal Type

This parametric study of hyperbaric centrifugation was carried out using coal samples from various coal preparation plants. Screenbowl feed samples taken from Tom's Creek, Moss No. 3, Coal Clean and Weatherby coal plants, all of which process different coal seams, were used for these tests. Tests were run as function of centrifugal acceleration (i.e. 1500, 2000 and 2700 g), rotation time (i.e. 30, 60 and 120 second) and air pressure (with and without air pressure of 200 kPa). Air pressure was on for the whole duration of the tests with air. The particle size distributions of all the different coal samples were determined by wet screening (see Table 2.1). After sizing, an anionic flocculant was added to all samples for the purpose of thickening. The

Table 2.1 Size distributions of the screenbowl feed samples obtained from different plants.

Size	Tom's Creek Coal Plant (Mass, %)	Coal Clean Coal Plant (Mass, %)	Weatherby Coal Plant (Mass, %)	Moss #3 Coal Plant (Mass, %)
+0.5 mm	39.05	45.40	53.83	1.80
0.5 x 0.25 mm	21.43	17.22	18.43	7.81
0.25 x 0.15 mm	6.21	5.44	5.76	6.04
0.15 x 0.075 mm	10.40	8.58	8.62	13.24
0.075 x 0.044 mm	5.99	5.63	4.69	13.91
-0.044 mm	16.92	17.74	8.67	57.20

excess water was decanted and discarded.

Test results obtained with the Tom's Creek coal sample are given in Table 2.2. The data showed that single-digit moistures were easily achievable when 1500 g's or more of centrifugal acceleration was used, even without applying air pressure. The baseline product moisture without air was 11.5% for the lowest g level and shortest rotation time. This value was reduced down to 7.3% moisture at the highest g level and the longest rotation time. These values were further reduced from 11.5% to 8.3% and from 7.3% down to 6.2%, respectively, when air pressure was applied. The results also showed that the effect of air pressure on moisture reduction was more significant at lower rotation speeds (lower g levels). For example, at 1500 g's and 60 seconds of rotation time, the moisture was reduced from 9.9% down to 8.1% with air, corresponding to a 1.8 percentage point reduction. However, at 2700 g's, the moisture was reduced from 8.5% down to 7.0% with air, corresponding to a lower moisture reduction of 1.5 percentage points. Also, the moisture reduction dropped for all g levels as the rotation time increased from 30 to 120 seconds.

Table 2.2 Test results obtained with Tom's Creek coal plant screenbowl feed (1 mm x 0).

	Cake Moisture					
	Without Air			**With Air**		
Rotation Time (s)	**1500 g's (%)**	**2000 g's (%)**	**2700 g's (%)**	**1500 g's (%)**	**2000 g's (%)**	**2700 g's (%)**
0	47.7	47.7	47.7	47.7	47.7	47.7
30	11.5	10.3	9.6	8.3	8.1	8.1
60	9.9	9.4	8.5	8.1	7.7	7.0
120	8.9	7.8	7.3	7.0	7.1	6.2

The Coal Clean sample had a very similar size distribution to that of the Tom's Creek sample. Even though the samples were taken from coal plants that were processing different coal

seams, the test results were very similar owning to the similar size distributions. As shown in Table 2.3, baseline moistures obtained ranged from 11.5% for the lowest g level and shortest rotation time down to 8.1% for highest g level with the longest rotation time. Moreover, similar to the results obtained with Tom's Creek sample, the moisture reduction obtained by applying air pressure dropped with increased g levels. For example, the moisture at 1500 g's and 60 seconds of rotation time was reduced from 11.0% down to 8.5% with air, corresponding to a 2.5 percentage point moisture reduction. Whereas, at 2700 g's, the moisture was reduced from 8.9% down to 7.4%, corresponding to a lower moisture reduction of 1.5 percentage points.

Table 2.3 Test results obtained with Coal Clean coal plant screenbowl feed (1 mm x 0, Eagle Seam).

	Cake Moisture					
	Without Air			**With Air**		
Rotation Time (s)	**1500 g's (%)**	**2000 g's (%)**	**2700 g's (%)**	**1500 g's (%)**	**2000 g's (%)**	**2700 g's (%)**
0	50.0	50.0	50.0	50.0	50.0	50.0
30	11.5	10.8	10.0	9.3	8.8	8.0
60	11.0	9.9	8.9	8.5	7.8	7.4
120	9.9	9.1	8.1	7.4	7.1	6.8

The coal sample from the Weatherby plant was partially deslimed at 0.044 mm as a result of the use of fine classifying cyclones utilized in the plant circuitry. Because the sample was deslimed, all the moisture values obtained with this coal product were less than 10%. While the baseline moisture for the lowest centrifugal field of 1500 g's and the shortest rotation time of 30 seconds was 9.4%, for the highest centrifugal field of 2700 g's and the longest rotation time of 120, it was 7.4%. When air pressure was introduced, moistures decreased down to only 8.7% and 6.5%, respectively, for the same conditions. Therefore, the lack of fines reduced the moisture

drop and severely limited the impact of air injection on moisture reduction. The smallest moisture drop, which was 0.3 percentage points, was obtained with 2700 g's and 30 seconds rotation time. The largest moisture drop was only about 1.0 percentage point at 2000 g's and 120 seconds rotation time.

Table 2.4 Test results obtained with Weatherby coal plant screenbowl feed (1 mm x 0, Deslimed, Stockton Seam).

	Cake Moisture					
	Without Air			**With Air**		
Rotation Time (s)	**1500 g's (%)**	**2000 g's (%)**	**2700 g's (%)**	**1500 g's (%)**	**2000 g's (%)**	**2700 g's (%)**
0	42.0	42.4	42.4	42.4	42.4	42.4
30	9.4	9.1	8.5	8.7	8.1	8.2
60	9.0	8.4	8.2	8.2	7.9	7.2
120	8.4	8.1	7.4	7.4	7.1	6.5

The Moss No. 3 sample was a finer sample compared to the other samples with 57.2% minus 0.044 mm particles. As a result of the increased surface area, product moistures also increased to values more than two times the values obtained with the other samples (see Table 2.5). For the lowest g level and the shortest rotation time, the baseline cake moisture was 26.5%. This value was reduced down to 20.2% for the highest g level and the longest rotation time. When air pressure was introduced, these values decreased further from 26.5% down to 21.0% and from 20.2% down to 15.5%, respectively. Greater moisture reductions compared to the other samples were also observed as a consequence of the increased surface area. For example, at 1500 g’s and 60 seconds of rotation time, the moisture was reduced from 25.3% to 19.0% with air, corresponding to a 6.3 percentage point reduction. Similar to the tests with other samples, moisture reductions with air were dropped at higher g levels. For instance, at 2700 g’s and 60

seconds of rotation time, the moisture was reduced from 21.7% to 16.7% with air, corresponding to a lower moisture reduction of 5.0 percentage points.

Table 2.5 Test results obtained with Moss No. 3 coal plant screenbowl feed (1 mm x 0).

	Cake Moisture					
	Without Air			With Air		
Rotation Time (s)	**1500 g's (%)**	**2000 g's (%)**	**2700 g's (%)**	**1500 g's (%)**	**2000 g's (%)**	**2700 g's (%)**
0	67.3	67.3	67.3	67.3	67.3	67.3
30	26.5	24.3	22.6	21.0	19.6	18.0
60	25.3	23.4	21.7	19.0	18.4	16.7
120	24.0	22.1	20.2	17.6	16.1	15.5

2.3.1.2 Effect of Dewatering Aids

Two sets of flotation concentrate samples (nominally 0.15 x 0 mm) obtained from the East Gulf Plant of United Coal Company and the Cardinal Plant of Arch Coal Company, both located in West Virginia, were used to test the effect of dewatering aids on cake moistures. The main difference between the samples was the size distribution, as the East Gulf sample was much finer than the Cardinal sample (see Table 2.6). While the East Gulf sample contained 43.24%

Table 2.6 Size distributions of the flotation concentrate samples obtained from two plants for dewatering aid tests.

Size	East Gulf Coal Plant (Mass, %)	Cardinal Coal Plant (Mass, %)
+0.3 mm	0.34	5.04
0.3 x 0.15 mm	1.61	30.57
0.15 x 0.075 mm	17.47	30.43
0.075 x 0.044 mm	17.33	11.93
0.044 x 0.025 mm	20.01	9.74
-0.025 mm	43.24	12.29

minus 0.025 mm material, the Cardinal sample's minus 0.025 mm material content was only 12.29%. All the centrifuge tests were run at a relatively lower centrifugal acceleration level of 500 g's to show the effect of dewatering aids, because higher centrifugal accelerations tend to reduce the effect of other parameters. Also, rotation time was kept at 60 seconds and the air pressure was kept at 200 kPa for the tests with air. For comparison, vacuum filtration tests were conducted using the same samples. Several dewatering aids (i.e., reagents U, V and W) and proprietary shear resistant flocculants (i.e., Nalco 71300, 71303, 71306 and 71321) were used in several of the experiments.

Table 2.7 Effect of dewatering aids on moisture (East Gulf Coal Plant flotation concentrate sample).

Air Pressure (kPa)	Chemical Type	Chemical Dosage* (lbs/t)	Moisture (%)	Moisture Reduction (%)
0	-	0	40.8	0.0
200	-	0	25.1	38.5
0	RU	1	40.2	1.3
0	RU	2	38.6	5.4
0	RU	4	29.7	27.3
200	RU	1	24.0	41.0
200	RU	2	20.1	50.8
200	RU	4	18.4	54.8
0	RV	1	41.7	-2.4
0	RV	2	41.7	-2.4
0	RV	4	39.8	2.4
200	RV	1	24.7	39.3
200	RV	2	24.8	39.1
200	RV	4	23.6	42.1
0	RW	1	39.6	2.9
0	RW	2	39.7	2.6
0	RW	4	37.7	7.5
200	RW	1	22.8	44.0
200	RW	2	20.0	50.9
200	RW	4	17.5	56.9

* Dosage of active chemical

Centrifugation test results obtained with the East Gulf sample are given in Table 2.7. All the tests were conducted using 1, 2 and 4 lbs/t dosages of reagents U, V and W. Tests without any chemical addition were also performed. Moisture reductions compared to the baseline test, which was run without dewatering aids and without air pressure, are shown in the same table, as well. While the baseline test produced 40.8% moisture, the lowest moisture value of 27.9% without air injection was obtained using 4 lbs/t of reagent U corresponding to 27.3% moisture reduction. While reagent W slightly reduced the moisture down to 37.7%, reagent V had almost no effect and it produced 39.8% moisture at 4 lbs/t dosage. In fact, at the lower dosages of reagent V, moisture slightly increased compared to the baseline. When air pressure was applied, 25.1% cake moisture, which corresponds to 38.5% moisture reduction, was obtained without any dewatering aids. Reagents U and W had similar impacts on water removal and produced 18.4% and 17.5% moistures, respectively. This level of performance corresponds to moisture reductions of about 55-56%. Reagent V, on the other hand, caused only a slight moisture reduction compared to the no chemical case and produced 23.6% cake moisture at the highest dosage.

Vacuum filtration test results obtained with the East Gulf Plant sample are shown in Table 2.8. Since reagent V did not have any effect in centrifuge tests, it was not included in filtration tests. Vacuum pressure was kept at 133 kPa for all the tests. Two cake thicknesses of 12 mm and 22-24 mm were tested. Since reagent U gave the best results in centrifuge tests and since there was a limited amount of coal sample left, only reagent U was tested with both cake thicknesses. Test results given in Table 2.8 show that when the cake thickness was 12 mm, moisture was reduced to about 25% with both reagents U and W compared to the baseline moisture of 30.3%. Also, when a 22-24 mm cake thickness was produced, the baseline moisture of 36.5% was reduced to 31.5% with reagent U.

Table 2.8 Vacuum filtration test results (East Gulf Plant flotation concentrate sample)

Vacuum Pressure (kPa)	Chemical Type	Chemical Dosage (lbs/t)	Cake Thickness (mm)	Filtration Time (s)	Moisture (%)
133	-	0	11	120	30.3
133	RU	2	12	120	26.3
133	RU	4	12	120	24.9
133	RW	2	12	120	25.7
133	RW	4	12	120	25.0
133	-	0	22-24	300	36.5
133	RU	2	22-24	240	32.8
133	RU	4	22-24	240	31.5

Several series of centrifugation tests were conducted using samples from the Cardinal Plant. The first set was performed to study the effect of reagents U, V and W on cake moisture. Table 2.9 shows the test results obtained. Since this sample was coarser than the East Gulf sample, the need for the chemical dosage reduced due to the smaller specific surface area (surface area per unit weight) of the sample. Therefore, 0.3, 1.0 and 1.7 lbs/t dosages were used for these experiments. While the baseline test produced 20.0% moisture, similar moisture values of approximately 15-16% and 11.5% were obtained when no air pressure was applied with all dewatering aids at the lowest and the highest dosages, respectively. When air pressure was applied, reagents U and W produced similar moisture values at all dosages. However, the lowest moisture value of 7.8% was obtained using reagent W at the highest dosage of 1.7 lbs/t. Moistures produced using reagent V were slightly higher than the ones with reagents U and W, but still lower than the moisture of 13.4%, which was produced without chemicals.

Table 2.9 Effect of dewatering aids on moisture (Cardinal Coal Plant flotation concentrate sample)

Air Pressure (kPa)	Chemical Type	Chemical Dosage* (lbs/t)	Moisture (%)	Moisture Reduction (%)
0	-	0	20.0	0.00
200	-	0	13.4	33.19
0	RU	0.3	14.9	25.7
0	RU	1.0	12.2	38.9
0	RU	1.7	11.7	41.5
200	RU	0.3	10.4	47.9
200	RU	1.0	8.4	58.2
200	RU	1.7	8.3	58.6
0	RV	0.3	14.9	25.8
0	RV	1.0	12.9	35.6
0	RV	1.7	11.4	43.1
200	RV	0.3	11.1	44.4
200	RV	1.0	10.4	48.0
200	RV	1.7	8.9	55.7
0	RW	0.3	16.1	19.5
0	RW	1.0	11.3	43.3
0	RW	1.7	11.6	42.0
200	RW	0.3	10.5	47.4
200	RW	1.0	8.8	55.9
200	RW	1.7	7.8	60.8

* Dosage of active chemical

Another set of tests was run with the Cardinal sample to study the effect of different rotation times when a dewatering aid was used. Since reagents U, V and W had similar effects in the previous set of tests, only reagent U at a mid-dosage of 1 lbs/t was used. Moreover, all the tests were run without air. Test results given in Table 2.10 showed that when no chemical was used, the moisture content was highly correlated to rotation time, as the moisture decreased from 35.9% at 15 seconds rotation time down to 21.7% at 60 seconds rotation time. However, when reagent U was added to the feed slurry, even at the shortest rotation time, moisture was reduced down to 14.8%, which corresponds to about 21 percentage points difference compared to no chemical case. Even though the difference was less at the highest rotation time, reagent U still

produced a lower moisture value of 12.7% compared to the no chemical case. Therefore, while the product moistures were reduced by using a dewatering aid, the amount of time required for dewatering was also lowered.

Table 2.10 Effect of rotation time with 1 lbs/t Reagent U addition

Rotation Time (s)	Chemical Type	Chemical Dosage* (lbs/t)	Moisture (% by weight)
15	-	0	35.9
30	-	0	28.1
60	-	0	21.7
15	RU	1	14.8
30	RU	1	12.6
60	RU	1	12.7

* Dosage of active chemical

The last set of centrifugation tests with the Cardinal Plant sample were conducted using proprietary shear resistant flocculants 71300, 713003, 71306 and 71321 obtained from Nalco Company. Test results given in Table 2.11 showed that using a proper dosage is of utmost importance when dealing with flocculants. When no air was used, employing flocculants reduced the moisture compared to the no chemical case at even the lowest dosage. However, while an additional moisture reduction was obtained with all flocculants when the dosage increased from 0.00033 to 0.00055 lbs/t, increasing the dosage further to 0.0011 lbs/t resulted in elevated moistures. For example, when 71321 was used, the baseline moisture of 22.2% was reduced to 17.1% and 16.8%, at 0.00033 lbs/t and 0.00055 lbs/t dosages, respectively. However, the moisture value increased to 17.3% when 0.0011 lbs/t dosage employed. The same trend was also observed when air pressure was used, only lower overall moistures were obtained due to the elevated air pressure.

Similar moisture values ranging from 16.8% to 20.9% were obtained with flocculants when no air was used. However, the best results were achieved using the flocculant 71321. The lowest moisture obtained was 16.8% at 0.00055 lbs/t dosage, which corresponds to about 5.4 percentage points moisture reduction compared to the baseline case. When air pressure was applied, moistures produced with flocculants were still in a narrow range of 10.9% - 14.6%. The flocculant 71321 once more produced the lowest moisture value of 10.9% at 0.00033 lbs/t dosage, which corresponds to 11.3 percentage points or 51% moisture reduction.

Table 2.11 Effect of flocculant addition

Air Pressure (kPa)	Chemical Type	Chemical Dosage (lbs/t)	Moisture (% by weight)
0	-	0	22.2
200	-	0	13.6
0	71300	0.00033	18.6
0	71300	0.00055	18.1
0	71300	0.00110	19.1
200	71300	0.00033	13.1
200	71300	0.00055	12.8
200	71300	0.00110	14.6
0	71303	0.00033	18.7
0	71303	0.00055	17.7
0	71303	0.00110	18.7
200	71303	0.00033	12.9
200	71303	0.00055	12.9
200	71303	0.00110	13.0
0	71306	0.00033	20.9
0	71306	0.00055	18.6
0	71306	0.00110	18.7
200	71306	0.00033	13.8
200	71306	0.00055	12.4
200	71306	0.00110	13.5
0	71321	0.00033	17.1
0	71321	0.00055	16.8
0	71321	0.00110	17.3
200	71321	0.00033	10.9
200	71321	0.00055	11.3
200	71321	0.00110	11.4

Several series of vacuum filtration tests were conducted with the Cardinal Plant sample. The first and second sets were performed to provide a comparison to the results given in Table 2.9. While reagents U, V and W were used in the first set of tests, reagent U was not used in the second set of tests because of the limited amount of sample available for testing. Also, only 0.3 and 1 lbs/t dosages were used in the second series of tests. The first set of tests was conducted at 120 seconds of filtration time, whereas the second set was performed at 60 seconds of filtration time. As expected, the former produced lower moisture values due to the longer filtration time. At 120 seconds of filtration time, reagent W produced the lowest moistures, ranging from 11.2% at the highest chemical dosage to 12.7% at the lowest chemical dosage. Generally, moistures decreased as the dosage increased from 0.3 to 1.7 lbs/t for all the chemicals tested. In fact, all moistures produced with chemicals were lower than the baseline moisture of 15.0%. At 60 seconds filtration time, moistures decreased as the chemical dosage increased, resembling the trends observed in the first set of tests. While reagent W produced the lowest moisture of 14.2% at 1 lbs/t dosage, the moisture obtained with reagent V was 16.7% at the same dosage. The baseline moisture of 18.7% was the highest value obtained.

Results showed that when 120 seconds filtration time was used, vacuum filtration produced lower moistures than centrifugation alone at the lowest chemical dosage. For instance, at the lowest dosage of reagent W, centrifugation alone produced 16.1% moisture. Whereas, a lower moisture value of 12.7% was produced with vacuum filtration at the same conditions. However, moisture values obtained at higher dosages with centrifugation were either similar to or lower than the ones obtained with vacuum filtration. For example, for the same conditions given above, centrifugation with air pressure produced 10.5% moisture. When 60 seconds

filtration time was employed, even the moistures produced with only centrifugation were lower than vacuum filtration.

The last set of vacuum filtration tests were performed with flocculants described earlier. Again, because of the limited amount of available samples, only flocculants 71303 and 71321, which performed the best at centrifugation tests, were evaluated at 0.00033 and 0.00055 lbs/t dosages. As in the case with the centrifugation tests, flocculant 71321 produced the lowest moistures. However, this time, the lowest moistures were obtained at 0.00033 lbs/t dosage, rather than 0.00055 lbs/t, which was the optimum dosage in the centrifuge tests. The application of flocculants made an improvement over the baseline moisture of 18.3%. For this particular sample, moistures of 15.3% and 17.2% were produced using flocculants 71321 and 71303, respectively, at a dosage of 0.00033 lbs/t. While the moistures obtained with vacuum filtration were generally lower than centrifugation only results, the application of air pressure together with centrifugation improved moistures and resulted in 25-30% moisture reductions compared to vacuum filtration.

Table 2.12 Vacuum filtration test results at 120 s filtration time (Cardinal Plant flotation concentrate sample)

Vacuum Pressure (kPa)	Chemical Type	Chemical Dosage (lbs/t)	Cake Thickness (mm)	Filtration Time (s)	Moisture (%)
133	-	0	12	120	15.0
133	RU	0.3	12	120	13.4
133	RU	1.0	12	120	12.1
133	RU	1.7	12	120	12.7
133	RV	0.3	12	120	13.8
133	RV	1.0	12	120	13.3
133	RV	1.7	12	120	13.4
133	RW	0.3	12	120	12.7
133	RW	1.0	12	120	12.1
133	RW	1.7	12	120	11.2

Table 2.13 Vacuum filtration test results at 60 s filtration time (Cardinal Plant flotation concentrate sample)

Vacuum Pressure (kPa)	Chemical Type	Chemical Dosage (lbs/t)	Cake Thickness (mm)	Filtration Time (s)	Moisture (%)
133	-	0	12	60	18.7
133	RV	0.3	13	60	17.2
133	RV	1.0	13	60	16.7
133	RW	0.3	13	60	14.5
133	RW	1.0	13	60	14.2

Table 2.14 Vacuum filtration test results with flocculants (Cardinal Plant flotation concentrate sample)

Vacuum Pressure (kPa)	Chemical Type	Chemical Dosage (lbs/t)	Cake Thickness (mm)	Filtration Time (s)	Moisture (%)
133	-	0	12	60	18.3
133	71321	0.00033	13	60	15.4
133	71321	0.00055	13	60	15.9
133	71303	0.00033	13	60	17.8
133	71303	0.00055	13	60	18.4

2.3.1.3 Effect of Air Pressure

To study the effect of air pressure on cake moisture, an additional set of dewatering tests was conducted using the East Gulf Plant sample. The tests were performed as a function of centrifugal acceleration and air pressure. Rotation time was held constant at 60 seconds for all tests. The results given in Table 2.15 showed that increasing air pressure beyond 100-200 kPa at 500 g's decreased the product moisture from 26.1% to 23.4%. Since this improvement corresponds to only about 2.7 percentage point moisture reduction, the use of high air pressures may not be necessary for effective dewatering. Moreover, at 3000 g's, moistures obtained at

different air pressures were practically identical. Therefore, 100-200 kPa of air pressure appears to be adequate for hyperbaric centrifugation.

Table 2.15 Effect of air pressure on cake moisture

Centrifugal Acceleration (g's)	Air Pressure (kPa)	Moisture (% by weight)
500	0	40.8
500	100	26.1
500	200	25.8
500	400	23.4
3000	100	15.4
3000	200	14.2
3000	400	15.8

2.3.1.4 Effect of Particle Size Distribution

Another set of laboratory tests was performed to investigate the effect of feed particle size distribution on cake moisture. To minimize the impacts of heterogeneities, a low-ash unprocessed coal sample taken from Cucumber Mine in West Virginia was used in these experiments. The sample was screened at 1.2 mm to eliminate large chunks of coal. After screening, the dry sample was split down to about 400 grams. Each split was then ground in a laboratory ball mill for different periods of time, varying from 30 seconds to 2 hours, to obtain progressively smaller size distributions. Using these samples, hyperbaric centrifuge tests were run at 500 and 2700 g's. These centrifugal accelerations were purposely chosen to imitate the accelerations applied by the standard screenbowl centrifuges and the new Decanter Centribaric™ centrifuge (described later in this document). An air pressure of about 200 kPa was applied during the tests. The air injection and rotation time was held constant at 120 seconds for all the tests.

The data given in Table 2.16 showed that moisture correlated very well with particle size. For instance, when the centrifugal acceleration was 500 g's, the coarsest product had 9.8% moisture with air and 13.8% moisture without air, while the moisture went up to 37.7% with air and 44.9% without air with the finest cake. The effect of different size fractions on final moisture is more clearly illustrated in Figure 2.12 and Figure 2.13. These plots show the total moisture content obtained as a function of the dry mass percentage below a given particle top-size. As seen from the plots, the correlation between final product moisture and mass percent passing was the poorest for the coarsest (i.e., minus 0.6 mm) size fraction (Figure 2.12(a) and Figure 2.13(a)). The best correlation was obtained with the finest (minus 0.025 mm) size fraction (Figure 2.12(f) and Figure 2.13(f)). Therefore, this fraction was chosen to further investigate the impact of size distribution on cake moisture.

Figure 2.13(f) shows that at 2700 g's, when no air pressure was used, the moisture content increased linearly with an increase in the amount of minus 0.025 mm particles. When air pressure was applied, there was a constant 2 percentage-point moisture improvement until the minus 0.025 mm solids accounted for about 60% of the total sample mass. After this point, the moisture remained steady around 25% with air injection, while it kept increasing without air injection. The absolute difference between adding air and not adding air was about 12 absolute percentage points when the amount of minus 0.025 mm size fraction reached 99%.

Figure 2.12(f) shows that, at 500 g's, all the moisture values increased due to the decrease in centrifugal acceleration. The moisture difference between with and without air cases started at about 4 percentage points for the coarsest cake and increased up to about 17 percentage points when the minus 0.025 mm solids accounted for about 70% of the total sample mass. After this point, the difference started to decrease, because of the rapid change in moisture when air

Table 2.16 Effect of size distribution on moisture

Air Pressure (kPa)	Centrifugal Force (g's)	Size Distribution (% by weight) -0.6 mm (%)	-0.3 mm (%)	-0.15 mm (%)	-0.074 mm (%)	-0.044 mm (%)	-0.025 mm (%)	Moisture (%)
0	500	66.83	48.62	33.04	23.29	18.88	13.84	13.8
0	500	66.83	48.62	33.04	23.29	18.88	13.84	13.7
0	500	100.00	100.00	95.52	71.98	58.00	43.62	31.4
0	500	100.00	100.00	99.89	96.93	88.60	70.04	40.2
0	500	100.00	100.00	99.87	99.06	96.98	85.00	42.1
0	500	100.00	100.00	99.87	99.06	96.98	85.00	42.4
0	500	100.00	100.00	100.00	99.93	99.59	97.82	44.7
0	500	100.00	100.00	100.00	99.93	99.59	97.82	44.9
200	500	66.83	48.62	33.04	23.29	18.88	13.84	9.8
200	500	100.00	100.00	95.52	71.98	58.00	43.62	20.3
200	500	100.00	100.00	99.89	96.93	88.60	70.04	23.6
200	500	100.00	100.00	99.87	99.06	96.98	85.00	30.1
200	500	100.00	100.00	99.87	99.06	96.98	85.00	30.5
200	500	100.00	100.00	100.00	99.93	99.59	97.82	38.3
200	500	100.00	100.00	100.00	99.93	99.59	97.82	37.7
0	2700	69.28	48.67	33.45	24.44	20.61	15.76	9.2
0	2700	88.74	65.43	44.72	31.48	26.28	19.99	11.0
0	2700	97.19	81.59	57.79	43.42	35.62	27.69	14.8
0	2700	99.86	97.93	83.72	62.60	52.69	39.99	18.8
0	2700	99.94	99.30	90.70	71.63	60.14	46.03	20.4
0	2700	100.00	99.50	96.15	86.38	77.58	63.26	28.3
0	2700	99.98	99.46	92.79	76.60	66.31	52.36	21.7
0	2700	99.96	99.65	98.26	86.28	74.75	55.46	24.5
0	2700	100.00	99.92	99.64	98.70	95.62	85.35	32.1
0	2700	100.00	99.92	99.64	98.70	95.62	85.35	32.0
0	2700	100.00	99.74	99.55	99.52	99.13	97.24	40.0
200	2700	68.38	49.19	34.08	24.25	20.54	15.85	7.9
200	2700	88.74	65.43	44.72	31.48	26.28	19.99	9.6
200	2700	97.19	81.59	57.79	43.42	35.62	27.69	11.9
200	2700	99.86	97.93	83.72	62.60	52.69	39.99	16.1
200	2700	99.94	99.30	90.70	71.63	60.14	46.03	17.2
200	2700	100.00	99.50	96.15	86.38	77.58	63.26	23.7
200	2700	99.98	99.46	92.79	76.60	66.31	52.36	19.8
200	2700	99.96	99.65	98.26	86.28	74.75	55.46	22.1
200	2700	100.00	99.92	99.64	98.70	95.62	85.35	21.4
200	2700	100.00	99.92	99.64	98.70	95.62	85.35	22.5
200	2700	100.00	99.74	99.55	99.52	99.13	97.24	28.0
200	2700	100.00	99.74	99.55	99.52	99.13	97.24	27.2

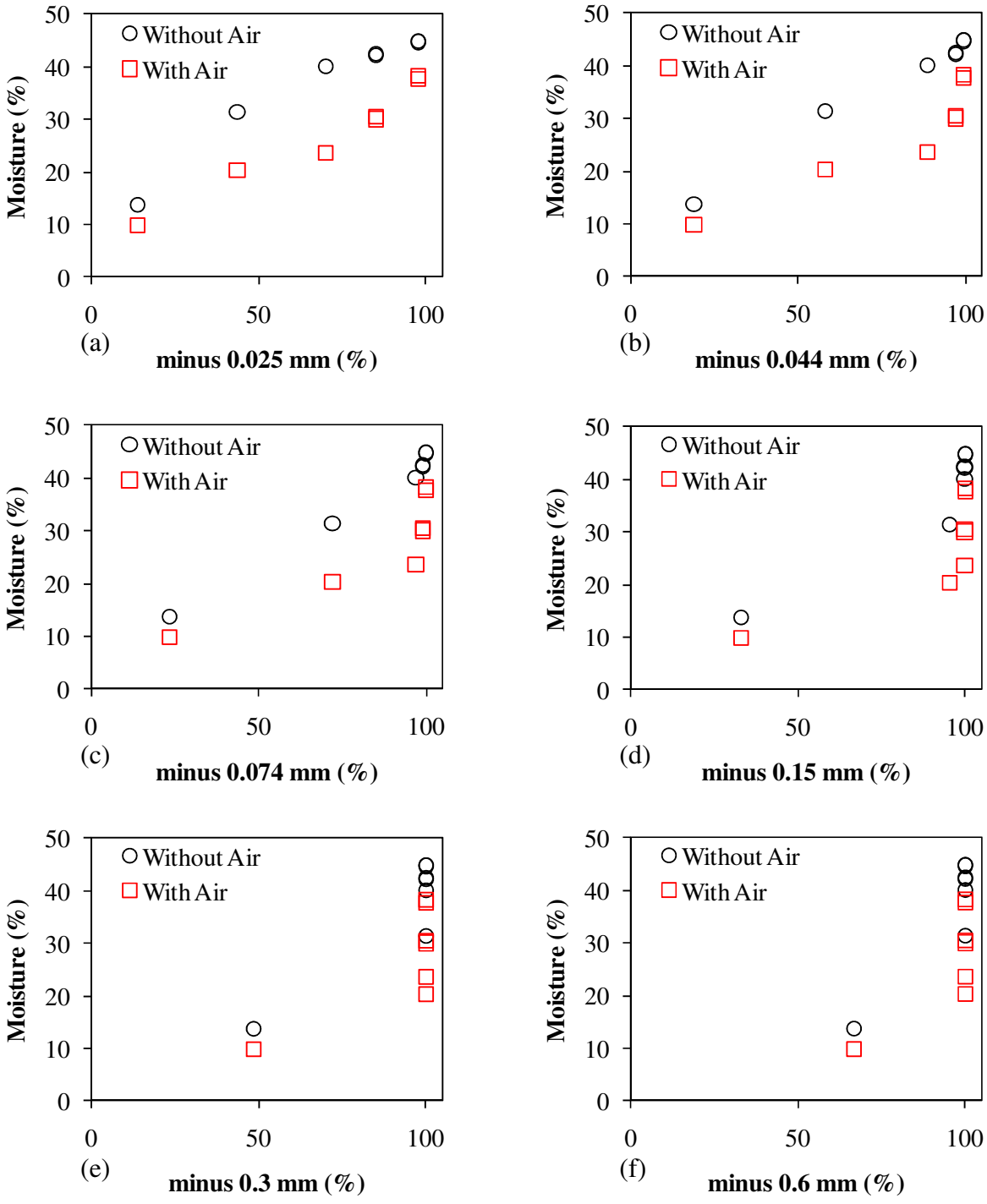

Figure 2.12 The effect of size distribution on moisture at 500 g's

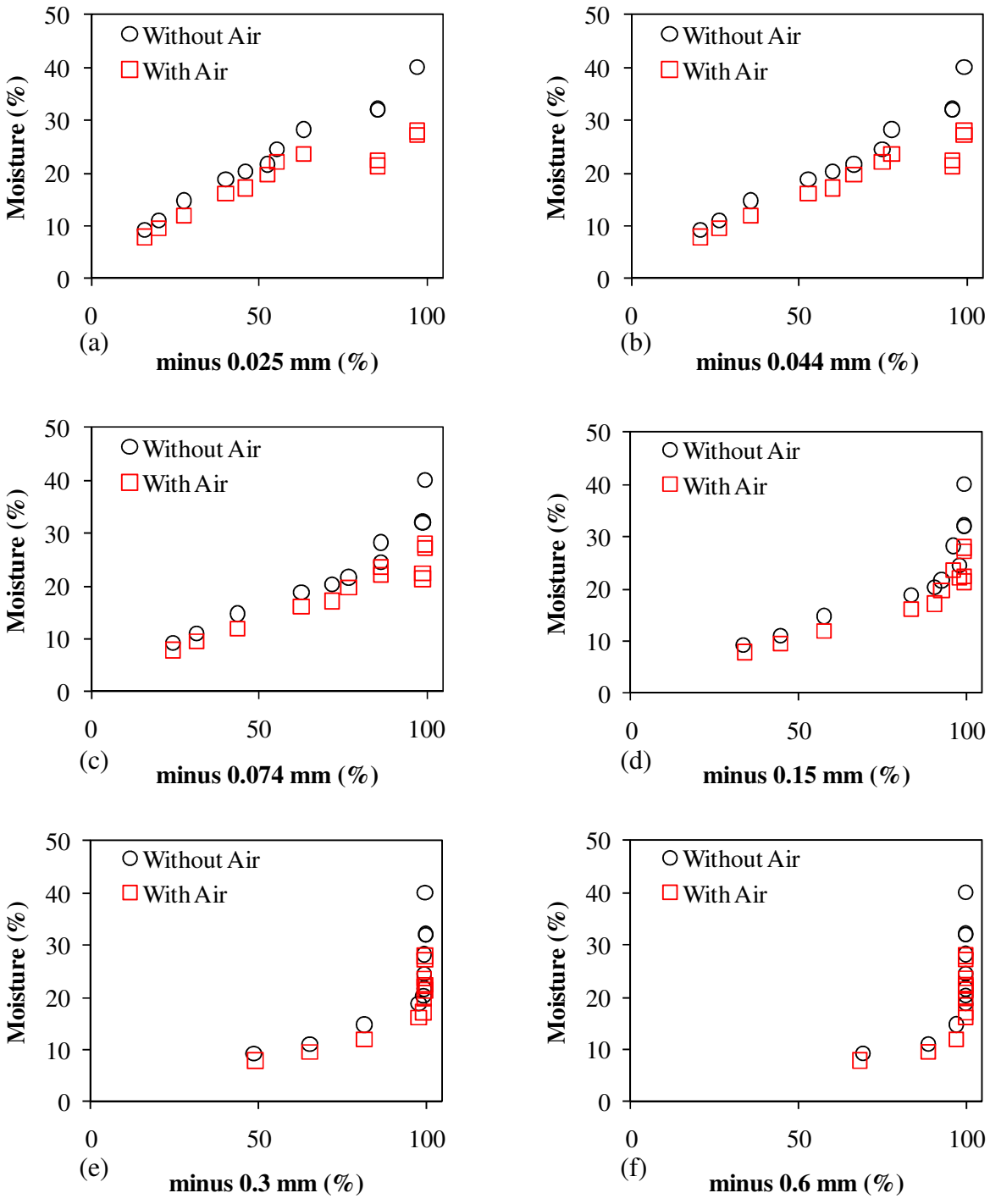

Figure 2.13 The effect of size distribution on moisture at 2700 g's

pressure was applied. As a result, decreasing the centrifugal acceleration from 2700 to 500 g's rendered air less effective when the cake was too fine, thus causing the two performance curves to merge.

2.3.2 Modified Batch Tests

2.3.2.1 Effect of Media Type and Dewatering Kinetics

Several series of tests were run to examine the kinetics of hyperbaric centrifugation. The coal used for these tests was the screenbowl feed sample (1 mm x 0 mm) taken from Tom's Creek Coal Plant, which was described in section 2.2.1. The first two sets were run with either a standard filter cloth, while a screen mesh with 1.5 mm aperture was used as the filter media for the last set of runs. The feed charge was held relatively constant at 485-495 gm using either 29% or 35% solids contents. Two different levels of centrifugal acceleration (i.e., 300 and 800 g's) were used during the tests. Flocculant and coagulant were added to all test samples, in order to increase the solids recovery. Air pressure was also varied from 0 to 200 kPa.

After a few trial tests, it was seen that the test setup was not precise enough to record the small amount of water weight removed from the cake by air injection. Therefore, in the first set of tests, instead of recording the weight continuously, the drum was removed and weighed every 10 to 20 seconds after the air injection started until the end of the test run. Since this procedure was time consuming and the curves needed were obtained using the first set of tests, only the final weight of the drum was measured for the rest of the tests.

The test results given in Tables 2.17-2.19 compare the cake moisture and solid recovery values under different conditions. The biggest impact of air injection was achieved when filter cloth was used, due to higher solid recoveries. While the maximum moisture drop was 6

percentage points when filter cloth was used as the filter media, it was about 1 percentage point with the larger-aperture screen mesh.

Table 2.17 Equilibrium moistures obtained at (a) the first and (b) the second sets of kinetic tests with filter cloth, and (c) the third set of kinetic tests with screen mesh

(a)

Run Number	Feed Solids (%)	Feed Charge (g)	Air Pressure (kPa)	Centrifugal Force (g's)	Moisture (%)	Recovery (%)
K1-1	34.70	494.5	0	300	26.8	90.7
K1-2	34.70	494.5	0	800	22.5	92.4
K1-3	34.70	494.5	100	300	22.8	86.9
K1-4	34.70	494.5	200	300	20.8	92.9

(b)

Run Number	Feed Solids (%)	Feed Charge (g)	Air Pressure (kPa)	Centrifugal Force (g's)	Moisture (%)	Recovery (%)
K2-1	28.76	486.3	0	300	27.6	86.3
K2-2	28.76	486.3	0	800	22.6	90.2
K2-3	28.76	486.3	100	300	25.4	82.7
K2-4	28.76	486.3	100	800	18.9	92.2

(c)

Run Number	Feed Solids (%)	Feed Charge (g)	Air Pressure (kPa)	Centrifugal Force (g's)	Moisture (%)	Recovery (%)
K3-1	28.76	486.3	0	300	21.87	64.0
K3-2	28.76	486.3	0	800	17.38	56.3
K3-3	28.76	486.3	100	300	19.94	59.2
K3-4	28.76	486.3	100	800	16.75	68.5
K3-5	28.76	486.3	166	300	22.63	71.1
K3-6	28.76	486.3	166	800	16.61	66.4

Figures 2.14-2.16 indicate that the greatest moisture drop took place in the first 50-60 seconds of centrifugation. After 60 seconds, the rate of dewatering decreased dramatically. Also, Figure 2.14(d) and Figure 2.14(f) show that only the first 10 seconds of air injection was effective in reducing moisture. This finding is encouraging since it shows that cakes need not be

subjected to long periods of air pressure in a production machine in order to obtain low cake moistures during hyperbaric centrifugation.

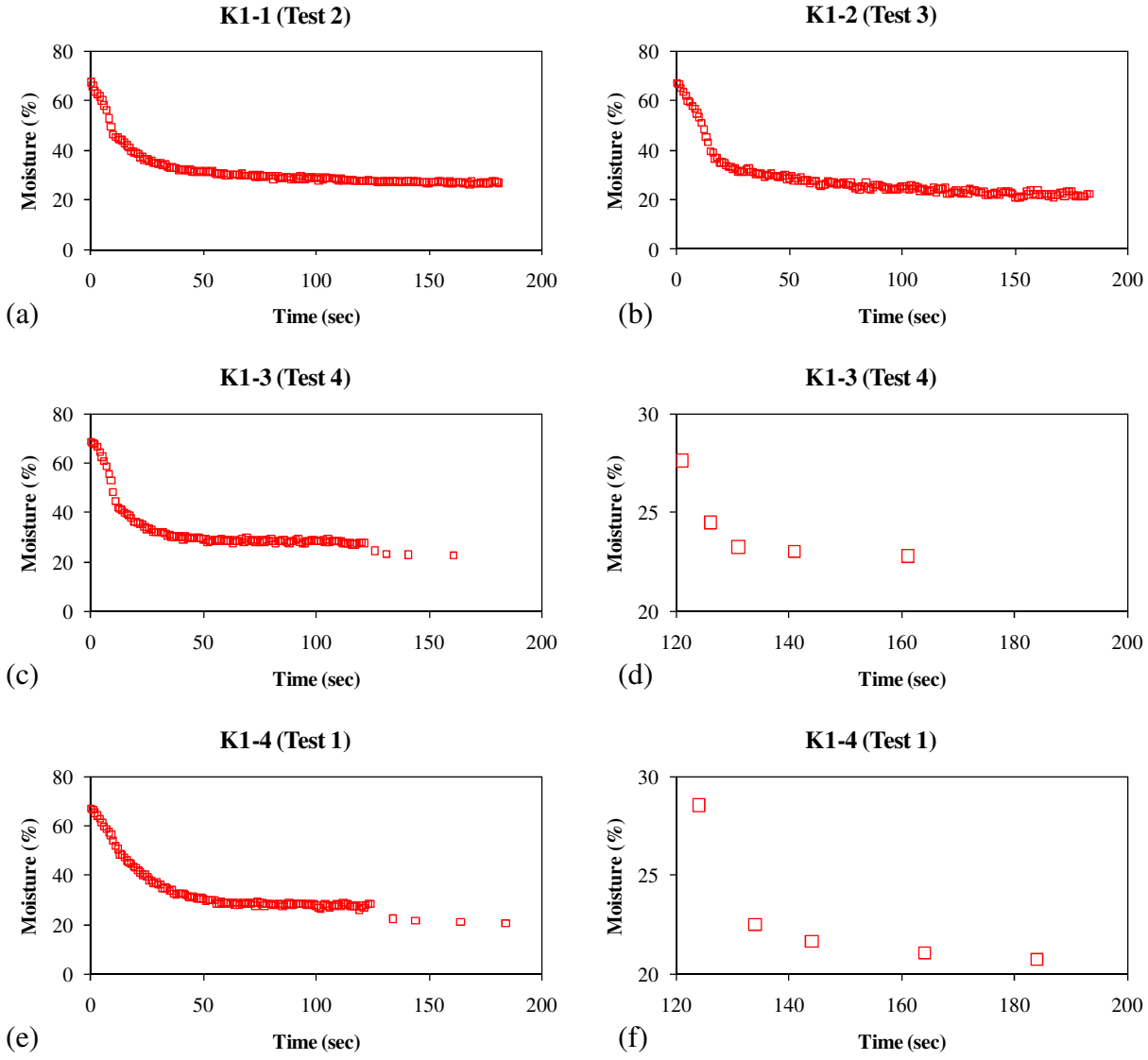

Figure 2.14 The first set of kinetic tests with filter cloth and closer looks to air injection parts of the curves ((d) and (f))

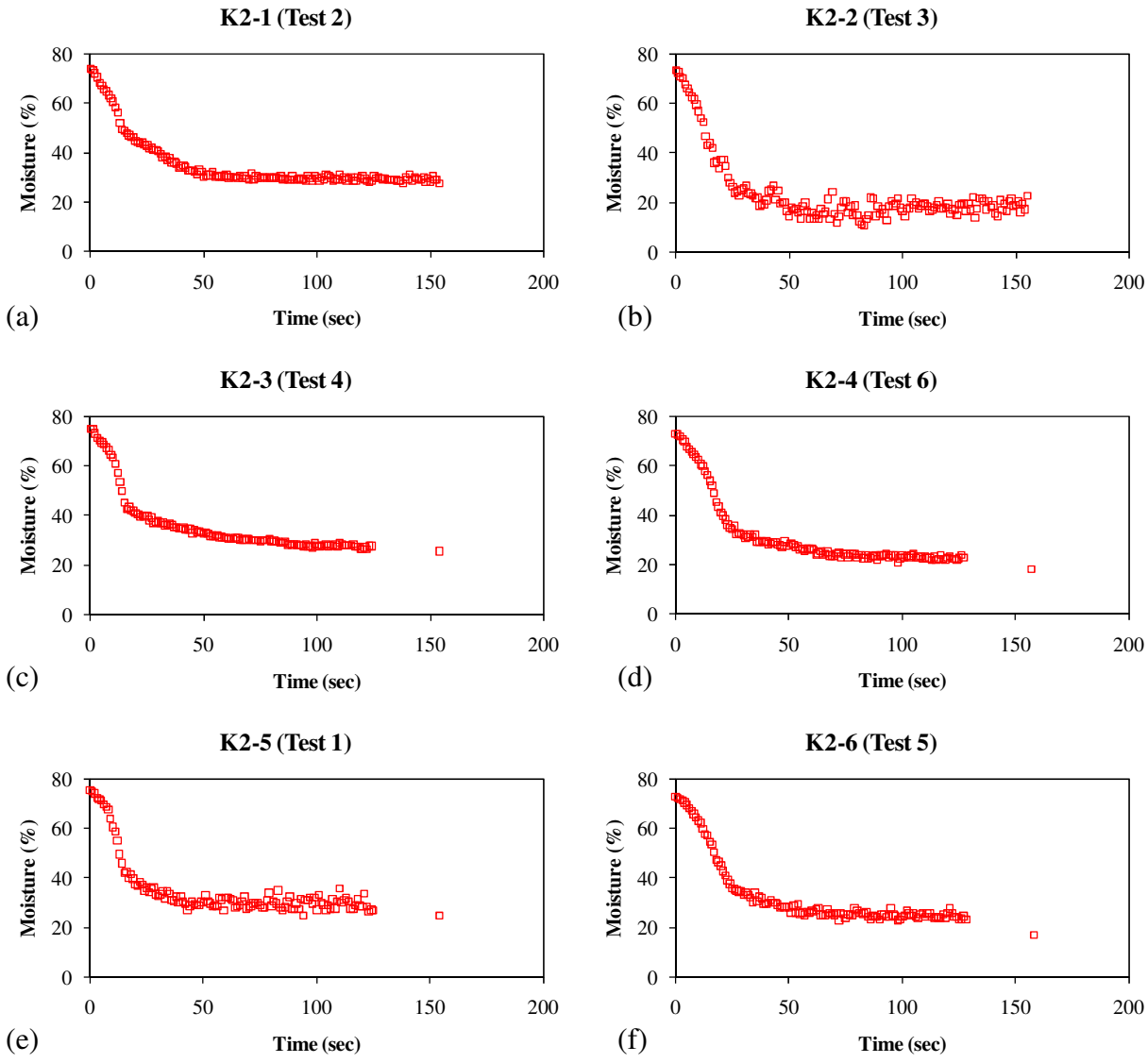

Figure 2.15 The second set of kinetic tests with filter cloth

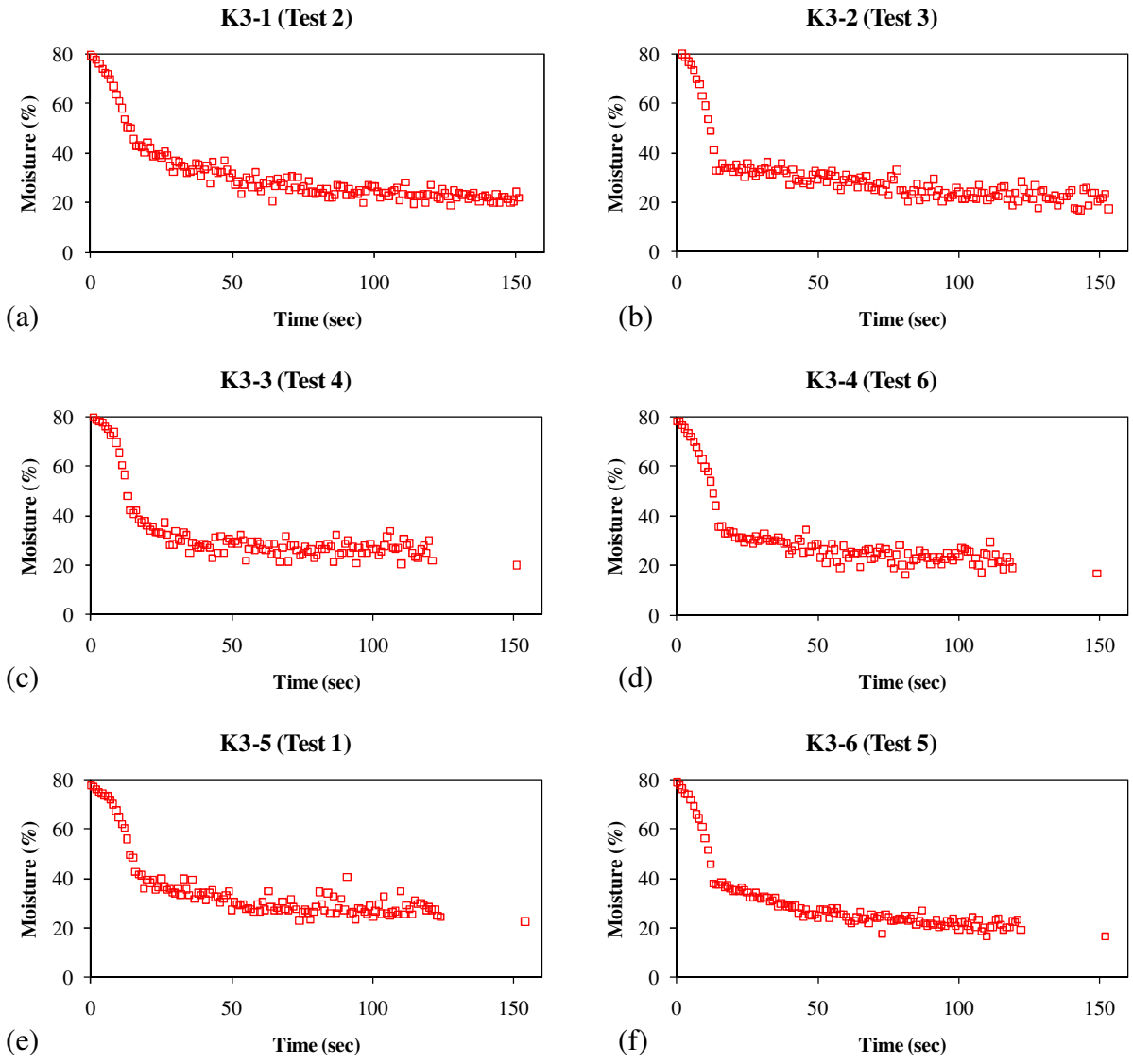

Figure 2.16 The third set of kinetic tests with 1.5 mm screen mesh

2.3.2.2 Solid Bowl Tests

This set of tests was run to identify optimum conditions for producing a thickened feed in a solid-bowl centrifuge. Ideally, this material would be passed to a filter-screen section at a high solids content to ensure that a high recovery of solids could be maintained. The test unit described previously in section 2.2.3.2 was used for this portion of the experimentation. Parameters examined in the study included feed charge, feed rate, feed percent solids and centrifugal acceleration. A flotation product sample (0.15 x 0 mm) taken from Tom's Creek coal plant was used for the tests.

The results given in Table 2.18 and Figures 2.17-2.24 showed that changing the amount of feed charge had almost no effect on either the percent solids of the product or the solids loss to

Table 2.18 Solid bowl test results

Feed Charge (l)	Feed Charge (dry g)	Centrifugal Force (g's)	Feed Rate (%)	Feed Solid Content (%)	Product Solid Content (%)	Solids loss to Effluent (%)
0.50	78.03	760	10	15.0	64.3	3.0
0.70	109.25	760	10	15.0	64.1	2.8
1.00	156.07	760	10	15.0	64.3	2.8
1.25	195.09	760	10	15.0	65.9	2.8
1.50	234.10	760	10	15.0	62.9	2.9
1.00	156.07	100	10	15.0	N/A	100.0
1.00	156.07	365	10	15.0	64.7	3.6
1.00	156.07	760	10	15.0	67.0	2.7
1.00	156.07	1045	10	15.0	66.0	2.0
1.00	156.07	1080	10	15.0	67.3	1.5
1.00	156.07	760	10	15.0	65.3	2.6
1.00	156.07	760	30	15.0	67.4	4.0
1.00	156.07	760	50	15.0	64.2	4.0
1.00	156.07	760	70	15.0	64.7	2.9
1.00	156.07	760	100	15.0	74.4	5.5
3.13	156.07	760	10	5.0	66.8	3.8
1.52	156.07	760	10	10.0	65.4	2.8
1.00	156.07	760	10	15.0	64.7	2.6
0.58	156.07	760	10	25.0	62.6	0.7
0.35	156.07	760	10	40.0	66.0	0.4

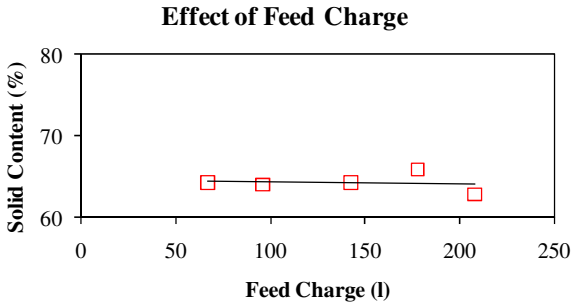

Figure 2.17 Effect of feed charge on product solid content

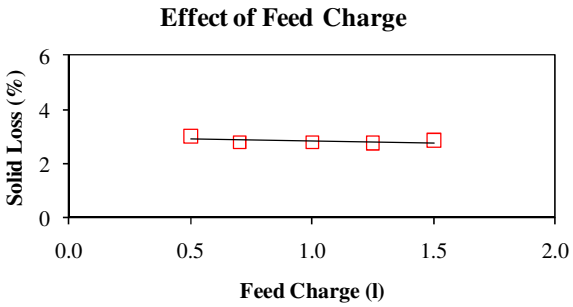

Figure 2.18 Effect of feed charge on solids loss to effluent

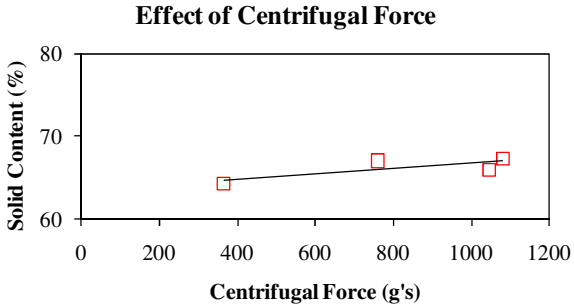

Figure 2.19 Effect of centrifugal force on product solid content

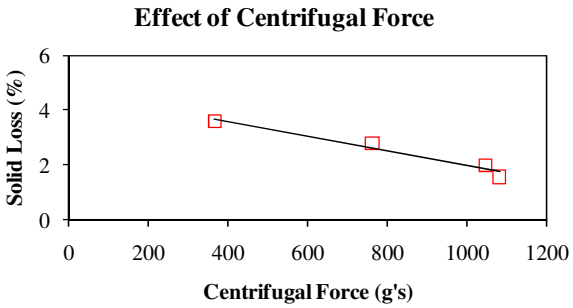

Figure 2.20 Effect of centrifugal force on solids loss to effluent

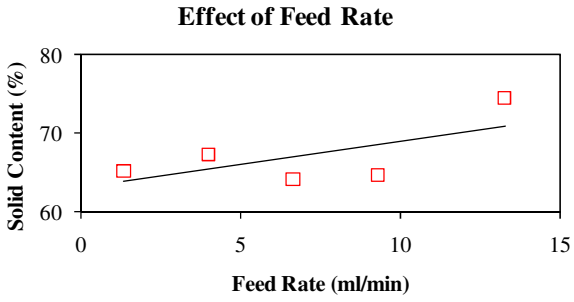

Figure 2.21 Effect of feed rate on product solids content

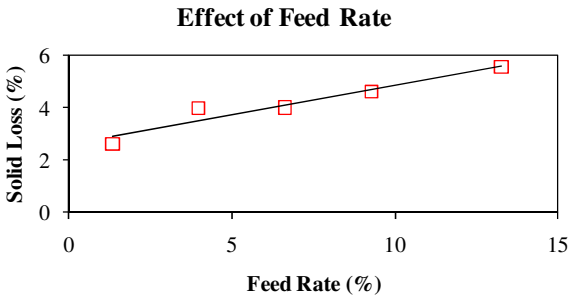

Figure 2.22 Effect of feed rate on solids loss to effluent

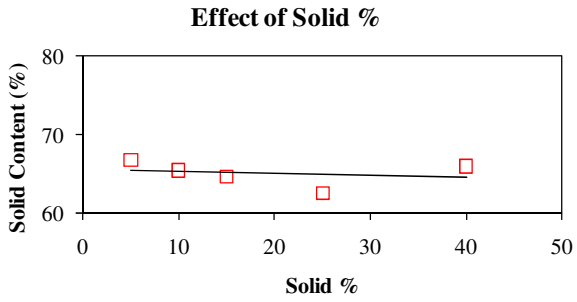

Figure 2.23 Effect of feed solid content on product solid content

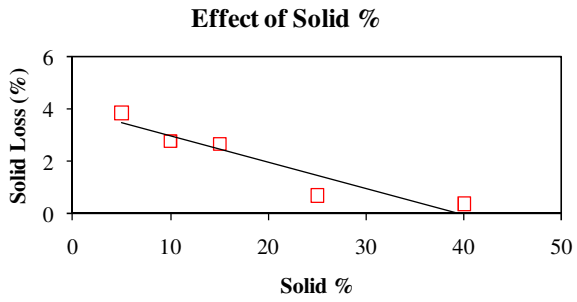

Figure 2.24 Effect of feed solid content on solids loss to effluent

the effluent. In contrast, the loss of solids to effluent significantly decreased from about 4% down to 1.5% when the centrifugal acceleration was increased. At the same time, the solids content of the product slightly increased from about 64% to 67%, while the loss of solids increased significantly from about 2.5% to 5.5%, due to the increasing feed rate. Finally, increasing the feed solids content decreased the solids loss from about 4% down to nearly zero, while the product solids content held constant at about 65%.

2.4 Discussion

2.4.1 Solids Recovery and Product Moisture

Standard batch tests conducted with different coal types showed that the product moisture greatly depended on particle size distribution of the feed slurry. Employing finer feed samples resulted in higher product moistures as a result of the increased specific surface area. Moreover, the application of air pressure was more effective when the feed was finer, which suggests that the higher capillary pressure created by smaller capillaries due to finer particle sizes could only be overcome by applying pressurized air in addition to the centrifugal acceleration.

Moisture reductions obtained using slurries with different size distributions at various levels of centrifugal accelerations are given in Figure 2.25. According to these plots, similar

moisture reductions were obtained using 500 and 2700 g's when the product contained less than 40% minus 0.025 mm material (compared to the baseline moisture obtained at 500 g's without using air pressure). Therefore, it may be unnecessary to use a costly high-g machine when the same level of performance can be obtained using a cost effective lower-g machine for products containing less than 60% minus 0.025 mm material. However, when the product contained more than 60% minus 0.025 mm material, applying 2700 g's with air was more effective than the other options. These results indicate that the hyperbaric centrifuge is best suited for the dewatering of coals containing substantial amounts of ultrafine solids.

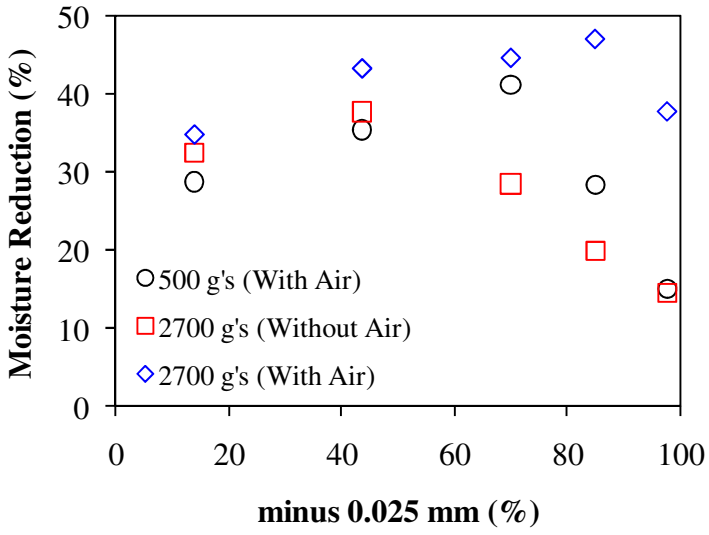

Figure 2.25 Effect of amount of fines on moisture reduction

Tests conducted with various filter media showed that solid recovery can drop dramatically (down to 50-60%) when a conventional screenbowl feed is used with a coarse screen mesh. Fortunately, solids recoveries were improved by using filter cloth without greatly impacting moisture. However, since it is not possible to use filter cloth in industrial applications,

employing a method such as pre-thickening appears to be the best option for increasing solids recoveries.

Pre-thickening is usually performed in the solid bowl section of a screenbowl centrifuge. Hence, a separate lab scale solid bowl centrifuge was built and tested to optimize the feed to the hyperbaric centrifuge. Figure 2.26 shows the effect of residence time on the amount of solids

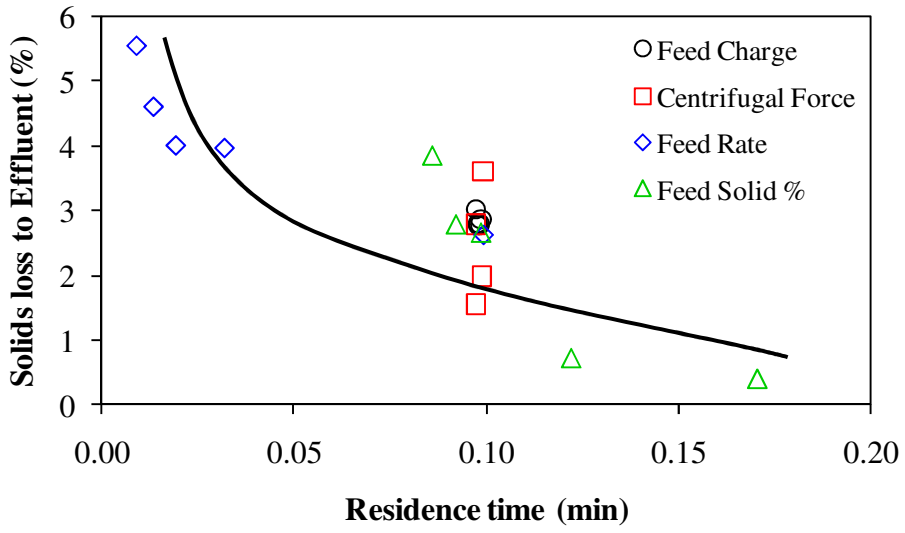

Figure 2.26 Effect of residence time on solids loss to effluent

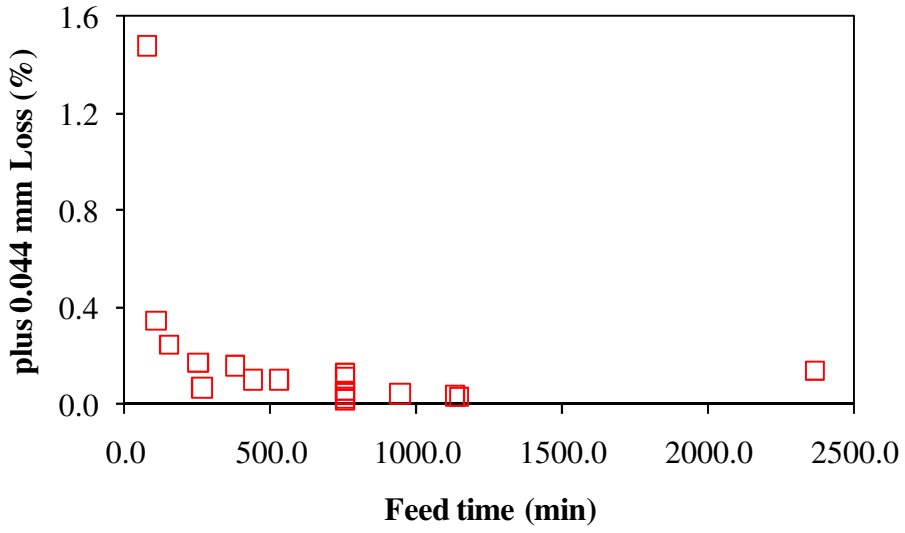

Figure 2.27 Effect of feed time on plus 0.044 mm particle loss

reported to effluent at all the conditions tested. Generally, solids loss to the effluent increased as the residence time decreased. Also, as shown in Figure 2.27, the loss of plus 0.044 mm particles to effluent was found to be correlated to the feed time and, therefore, the feed rate. While the loss was lower than 0.2% at feed times longer than 0.25 minutes, it increased up to 1.5% as the feed time became shorter.

2.4.2 Reproducibility of Test Results

Although a full experimental design was not performed for a complete statistical analysis, some of the tests described in section 2.3.1.4 were repeated to determine the reproducibility of the data. Average moisture values were calculated for each repeated test and these values were used in the charts given in Figure 2.28. Error bars for each repeated test were then determined by adding and subtracting three times the standard deviation value to this average value, which gave a 99.7% confidence interval. As can be seen, the reproducibility of results without air pressure was high. The calculated relative errors approximately 0.3 percentage points for 2700 g's and 0.7 percentage points for 500 g's when no air was used. Although the addition of air pressure

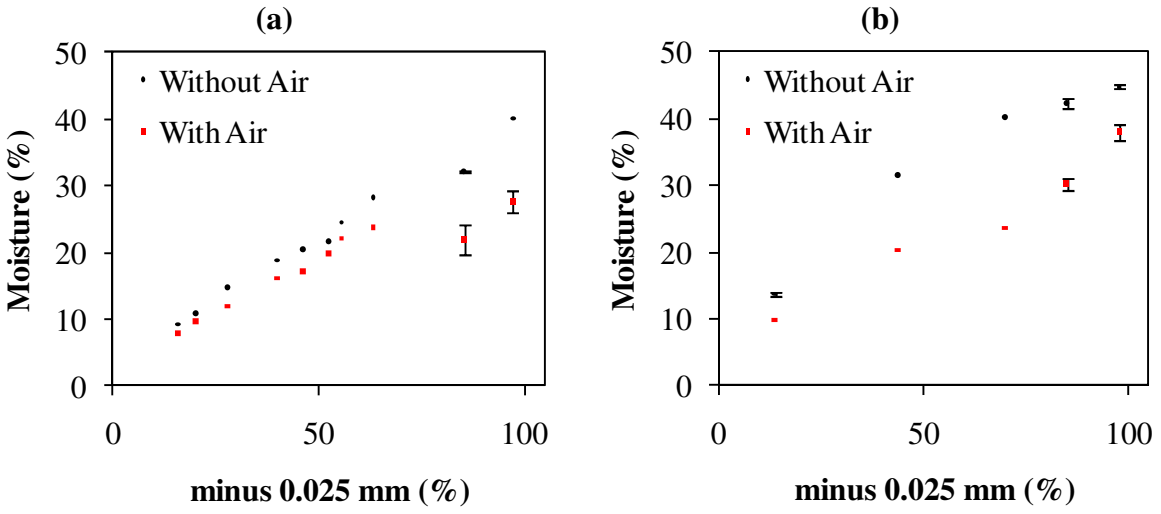

Figure 2.28 Charts showing reproducibility of test results at (a) 2700 g's and (b) 500 g's

increased the relative error values to about 0.7 and 1.2 percentage points for 2700 g's and 500 g's, respectively, these variations were still far from being very significant when compared to variations resulting from manual changes to air pressure or centrifugal acceleration.

2.4.3 Engineering Criteria for Machine Design

2.4.3.1 Rate Constants

The kinetic tests run with different filter media showed that the kinetics of centrifugal dewatering is quite different than filtering. The following filtration equation was derived by Dahlstrom from the commonly employed Poiseuille equation (Dahlstrom, 1985):

$$\frac{t}{V/A} = \frac{\mu a w V}{2\Delta P A} + \frac{\mu r}{\Delta P} \qquad [2.1]$$

where V is the volume of filtrate, A is the area of filtration, t is the time, ΔP is the pressure drop across the filter, μ is the liquid viscosity, a is the specific cake resistance, w is the weight of dry cake solids per unit volume of filtrate and r is the resistance of filter cloth and drainage network.

Eq. [2.1] yields a straight line plot of t/V/A vs. V/A as given in Figure 2.29. However, when the same plot was created using the data obtained from centrifugal kinetics tests (Figure 2.30), it was not possible to obtain a straight line relationship, because centrifugal acceleration

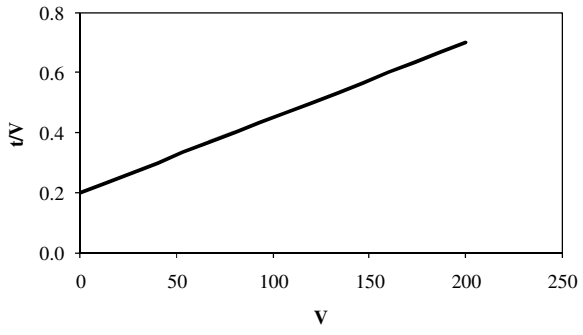

Figure 2.29 t/V/A vs. V/A (filtration theory)

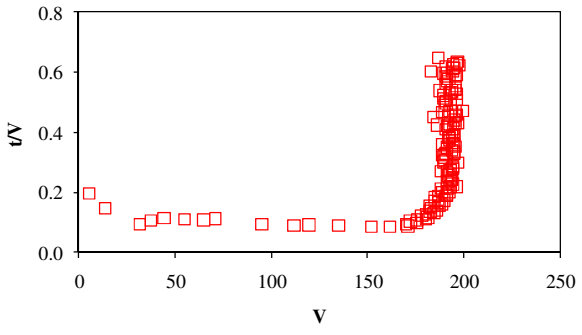

Figure 2.30 t/V/A vs. V/A (Measured)

changes with time as opposed to the constant pressure used in conventional filtering. Therefore, the Dahlstrom filtration equation cannot be used directly to describe hyperbaric centrifugation.

In the current study, a multiple-term rate equation was used to describe the centrifugal dewatering process. The model assumes that a portion of water was removed quickly from the cake, while another portion was removed slower. Also, another portion of water was assumed to be non-removable by mechanical means, thus staying inside the cake as final product moisture. The resultant dewatering equation can be expressed as:

$$W/W_0 = \emptyset_s \cdot exp(-K_s \cdot t) + \emptyset_f \cdot exp\left(-K_f \cdot t\right) + \emptyset_n \qquad [2.2]$$

where W is the weight of water remaining in cake, W_0 is the initial weight of water in feed, K_s and K_t are the rate constants for slow removed and fast removed water from the cake, respectively; φ_s, φ_f and φ_n, are the proportions of slow removed, fast removed and not removed water and t is the time. In general, this expression provided a good correlation between the weight of water remaining in the cake and the dewatering time.

During all of the kinetic tests, the centrifuge was run for a certain amount of time to remove most of the water that could be removed by only centrifugation. Then, air pressure was applied to remove an additional amount of residual water. Therefore, curve fitting was done for every centrifugal acceleration applied using all available data in the relevant set by simply eliminating the values obtained with air. The results of curve fitting based on Eq. [2.2] are given in Figures 2.30-2.32. Even though the moisture and recovery values were reasonable for Tests 3 of the first and second sets, kinetic data recorded were not in agreement with rest of the tests run at the same speed. Also, data for Test 3 of the second set of tests contained an excess amount of scatter. This problem can attributed to the difficulty of recording data with a sensitive digital balance connected to centrifuge running at thousands of rpm. Therefore, the data for Test 3 from

both sets were not included in the plots, since, possibly, for these particular tests, the weights recorded were not accurate.

The kinetic test results showed that the first and second sets of tests that were run with filter cloth had only one dewatering rate, while the third set run with the screen mesh had two rates. More solids and more fines were recovered during the tests with filter cloth, because filter cloth had a much smaller opening size than screen mesh. After a certain amount of time, fines blinded the filter cloth and dewatering rate diminished; thus, there was no slow rate. On the other hand, the screen mesh was coarse enough for dewatering not to stop, but continue at a slower rate. Therefore, the tests with screen mesh had two different dewatering rates.

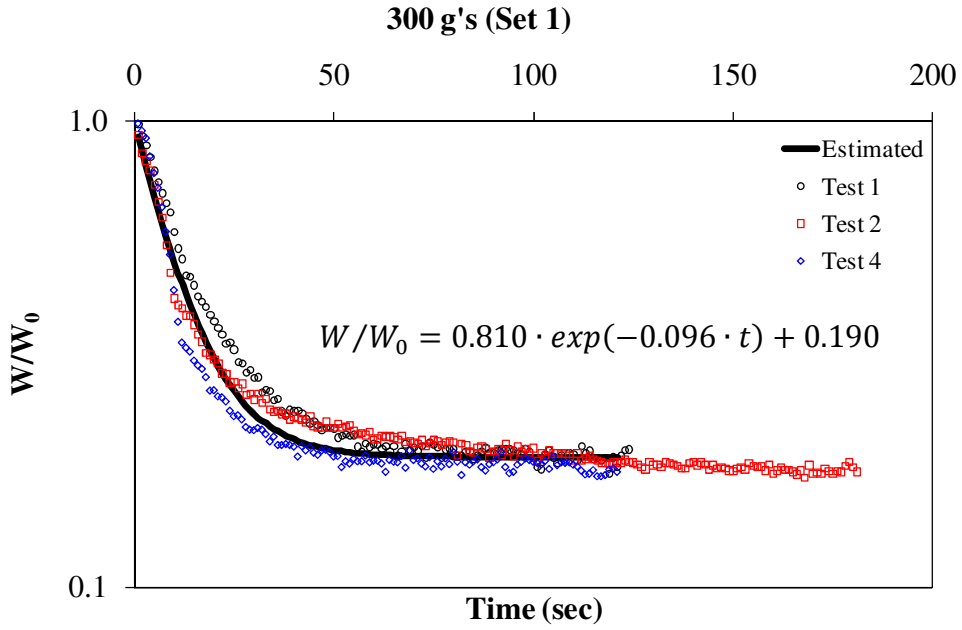

Figure 2.31 Rate curve fit for the first set of kinetic tests at 300 g's

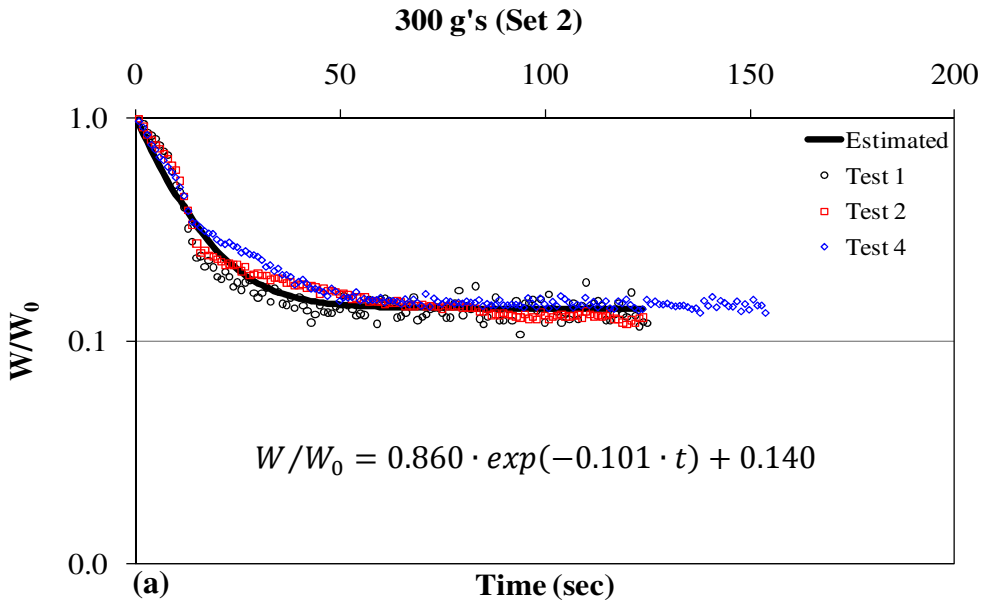

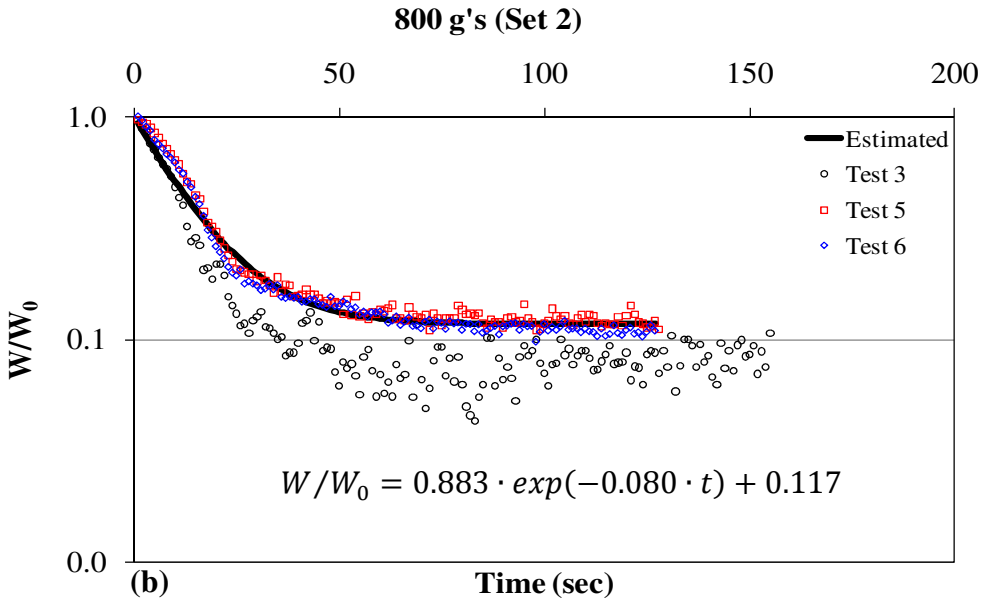

Figure 2.32 Rate curve fits for the second set of kinetic tests at (a) 300 g's and (b) 800g's

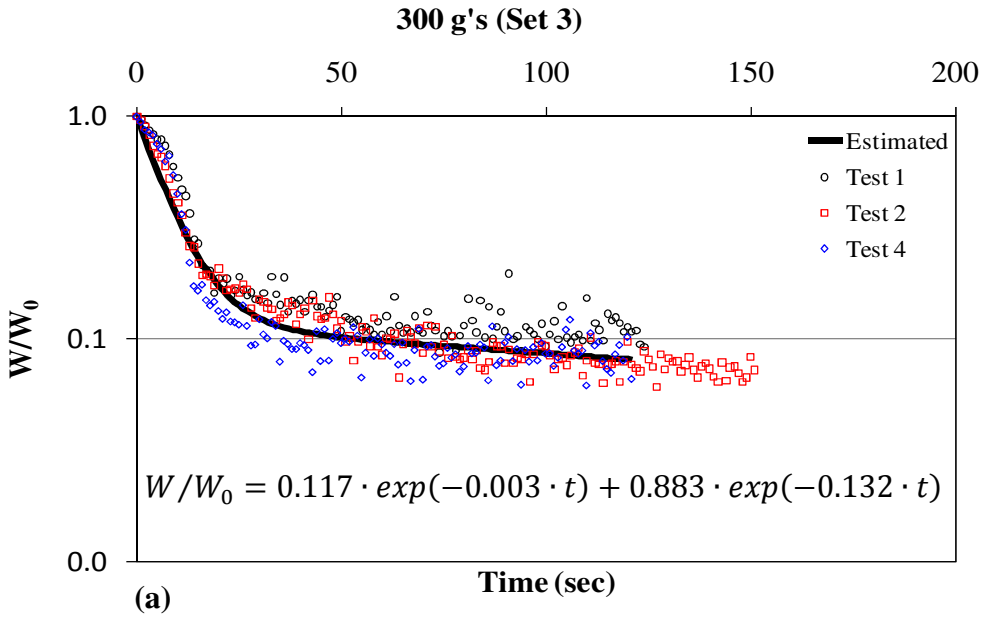

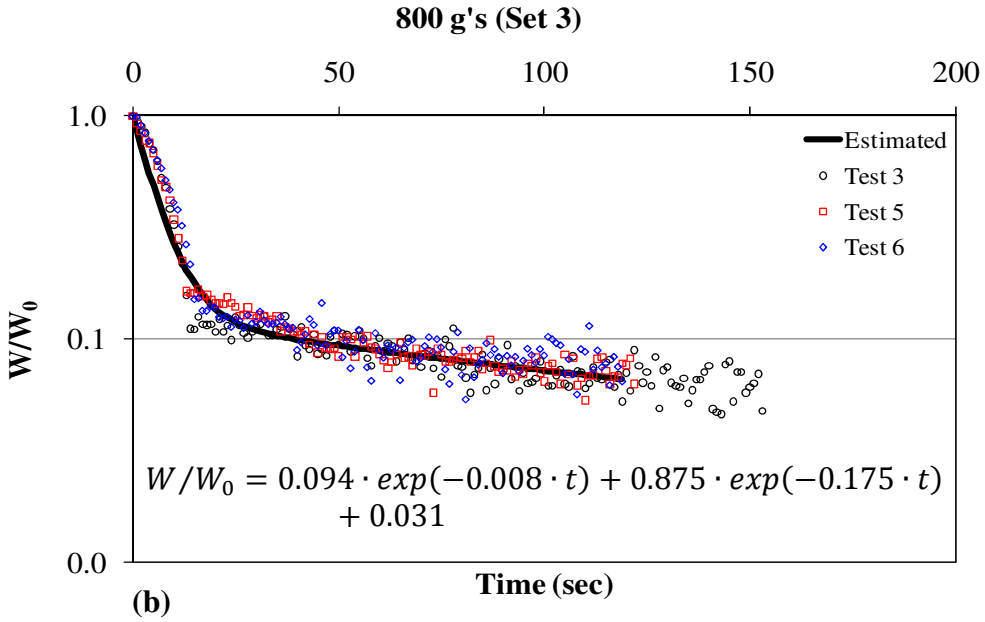

Figure 2.33 Rate curve fits for the third set of kinetic tests at (a) 300 g's and (b) 800g's

As explained in Section 2.3.2.1, the effect of pressurized air injection was studied by measuring cake weight at every 10-20 seconds (Figure 2.14(d) and (f)) at 300 g's. These tests readily demonstrated that air injection provided a further decrease in product moisture. Eq. [2.2] was applied to these data to determine the kinetics of water removal by pressurized air injection during centrifugation. The results given in Figure 2.34 suggest that this process was also a two-rate process. The bulk of the water was removed quickly during the first 10 seconds of air injection with a very high rate constant of 9.0 sec^{-1}. After 10 seconds, air lost its effectiveness and the rate constant declined dramatically down to about 0.2 sec^{-1}. Therefore, these results indicate that injecting air for a short amount of time can be just as efficient as applying air pressure during the entire centrifugation time.

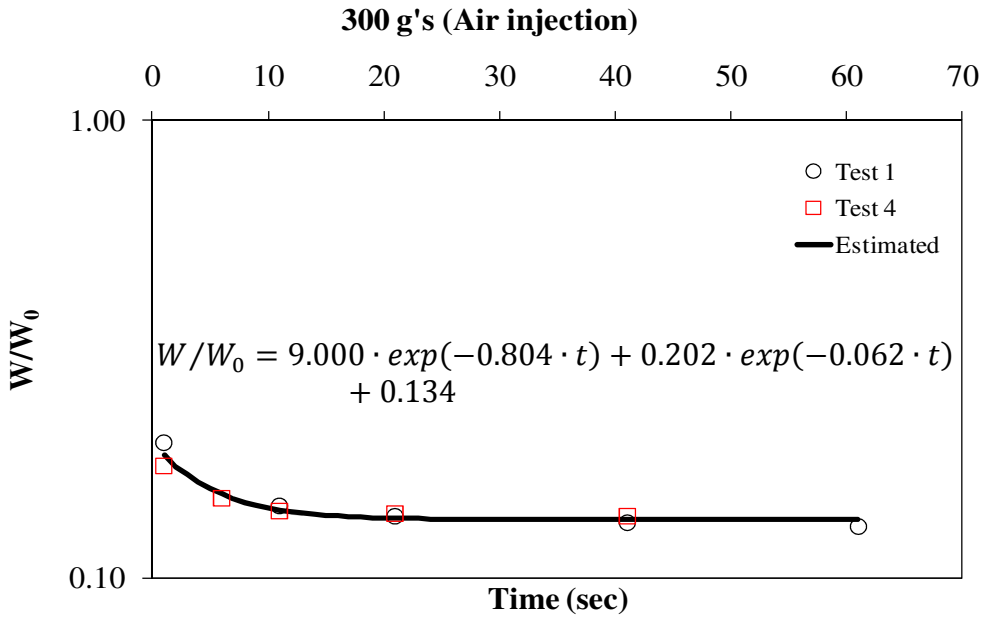

Figure 2.34 Rate curve fit for the air injection part of the kinetic tests at 300 g's

2.5 Conclusions

A detailed parametric study of hyperbaric centrifugation was conducted using several laboratory-scale test units. Tests performed with different coal types showed that it was possible to achieve very low moistures using hyperbaric centrifugation. Moreover, tests performed using different size distributions showed that as long as the product contained less than about 60% minus 0.025 mm particles, a lower centrifugal acceleration of about 500 g's with air pressure was as effective as employing a high centrifugal acceleration of 2700 g's. Therefore, it was concluded that when the fines content of a product was below a certain amount, the use of a high-g centrifuge is probably not necessary. However, when the minus 0.025 mm particle content was above 60%, the use of a high centrifugal acceleration together with air pressure was found to be essential to achieve good moisture values.

Tests conducted using several surface active dewatering aids and flocculants showed that moisture reductions as much as about 60% (compared to no-chemical and no-air cases) were possible when dewatering aids were used along with air pressure. Although it was not possible to measure solid recoveries because of the limitations of the test setups, it was visually observed that the use of chemical additives (especially flocculants) vastly improved solids recoveries.

Test results obtained with the modified batch test setup showed that centrifugal dewatering process could be described as a kinetic process. While the bulk of the water was removed quickly from the cake during centrifugation, a smaller amount was removed at a slower rate and a certain amount was not removed at all, which represented the final moisture content of the product. Therefore, it was necessary to employ a rate equation with multiple rate constants to represent the different stages of cake formation and moisture removal.

2.6 References

1. Asmatulu, R. (2001). *Advanced Chemical-Mechanical Dewatering of Fine Particles.* Doctor of Philosophy, Virginia Polytechnic Institute and State University, Blacksburg.
2. Asmatulu, R., Luttrell, G., & Yoon, R.-H. (2005). Dewatering of Fine Coal Using Hyperbaric
3. Dahlstrom, D. A. (1985). Filtration. In N. L. Weiss (Ed.), *SME Mineral Processing Handbook*. New York, N. Y.: Society of Mining Engineers of the American Institute of Mining, Metallurgical, and Petroleum Engineers.
4. Lynch, A. J., Johnson, N. W., Manlapig, E. V., & Thorne, C. G. (1981). *Mineral and Coal Flotation Circuits: Their Simulation and Control*. Amsterdam: Elsevier Scientific Publishing Company.

CHAPTER 3 A PILOT-SCALE STUDY OF HYPERBARIC CENTRIFUGATION

3.1 Introduction

In the light of previous studies done on hyperbaric centrifugation at Virginia Tech (Asmatulu et. al., 2005), a two-stage pilot-scale unit was designed and built. The design of the pilot-scale unit incorporated two integrated processes: (i) filtration in a pressurized rotating filter basket (pressure chamber) with scraper discharge and (ii) slurry pre-thickening and retreatment of recycled fines in an intermittent feed tank. The rotating pressure chamber is mounted along the central axis of a hollow shaft. This shaft is driven by a variable speed motor. A second hollow shaft is located within the drive shaft to allow feed and air to enter the pressure chamber. The second shaft is also connected to two sets of end plates that serve to seal the pressure chamber on one end and to discharge the cake on the other. A conceptual drawing of the rotating filter basket is shown in Figure 3.1. For comparison, a photograph of the assembled pilot-scale unit is provided in Figure 3.2.

3.2 Experimental

During a typical production cycle, the basket (see Figure 3.4) is rotated at speeds up to 319 g's using a variable speed motor and drive belt (see Figure 3.5). Slurry from the feed tank is pumped into a distributor pipe located within the center of the shaft of the rotating basket. The basket is constructed using wedge-shaped tungsten carbide bars spaced at 0.1 mm intervals. All particles larger than the bar spacing are retained along with most of the fines (via entrapment in the cake). The feeding cycle is continued until a desired cake thickness is achieved (Figure 3.3(a)). The feed flow is then diverted back to the feed tank via an automated three-way valve

(see Figure 3.6). Compressed air is then introduced into the filter chamber to create a differential pressure across the cake. The combined force of the centrifugal field and air pressure drives out nearly all of the surface moisture and some ultrafine solids through the spacing between the basket bars (Figure 3.3(b)). This effluent stream is passed back to the feed tank where the solids are concentrated by flocculation and recycled back to centrifuge to maintain a high recovery of solids. After this pressure drying cycle, the air pressure is released and the cake is discharged by a pneumatically driven scraper (Figure 3.3(c)). The edges of the scraper are sealed by rubber O-Rings to provide an excellent seal and to serve as a replaceable wear element. After discharge is completed, the scraper returns to its original position and the entire cycle of dewatering is repeated. The entire operation requires 30-120 seconds, depending on the range of operating conditions selected, feed particle size distribution, and target moisture level. The entire sequencing of the feeding, drying and discharge cycles is fully automated and controlled using a programmable logic controller (see Figure 3.7).

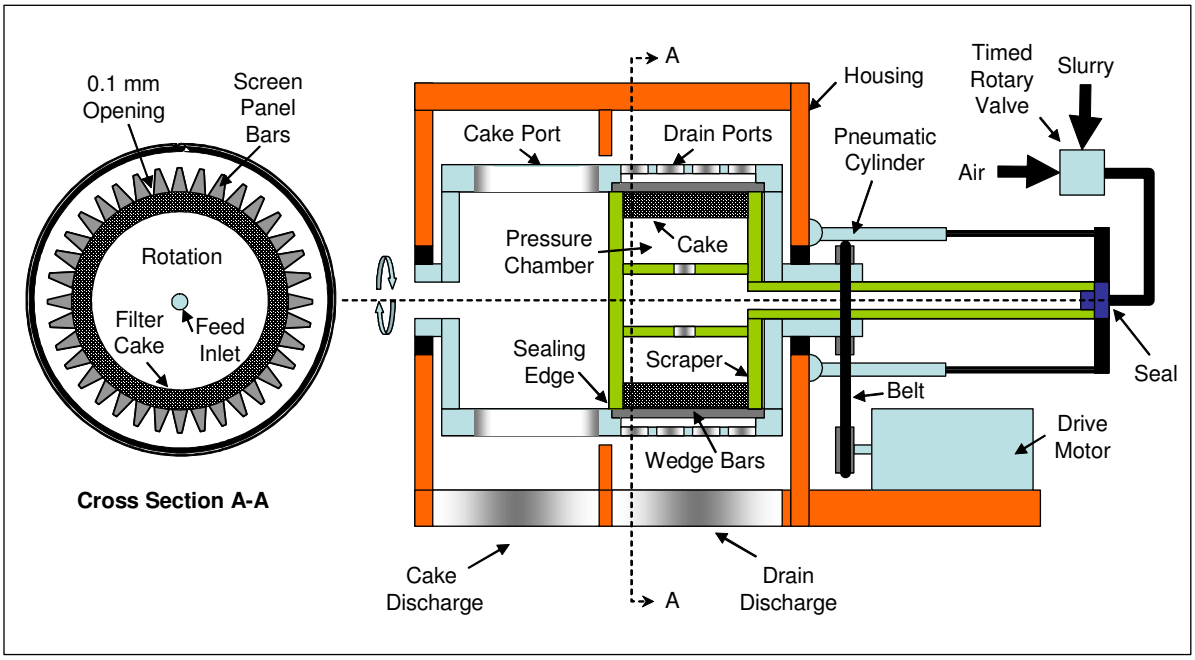

Figure 3.1 Simplified schematic of the hyperbaric filter centrifuge

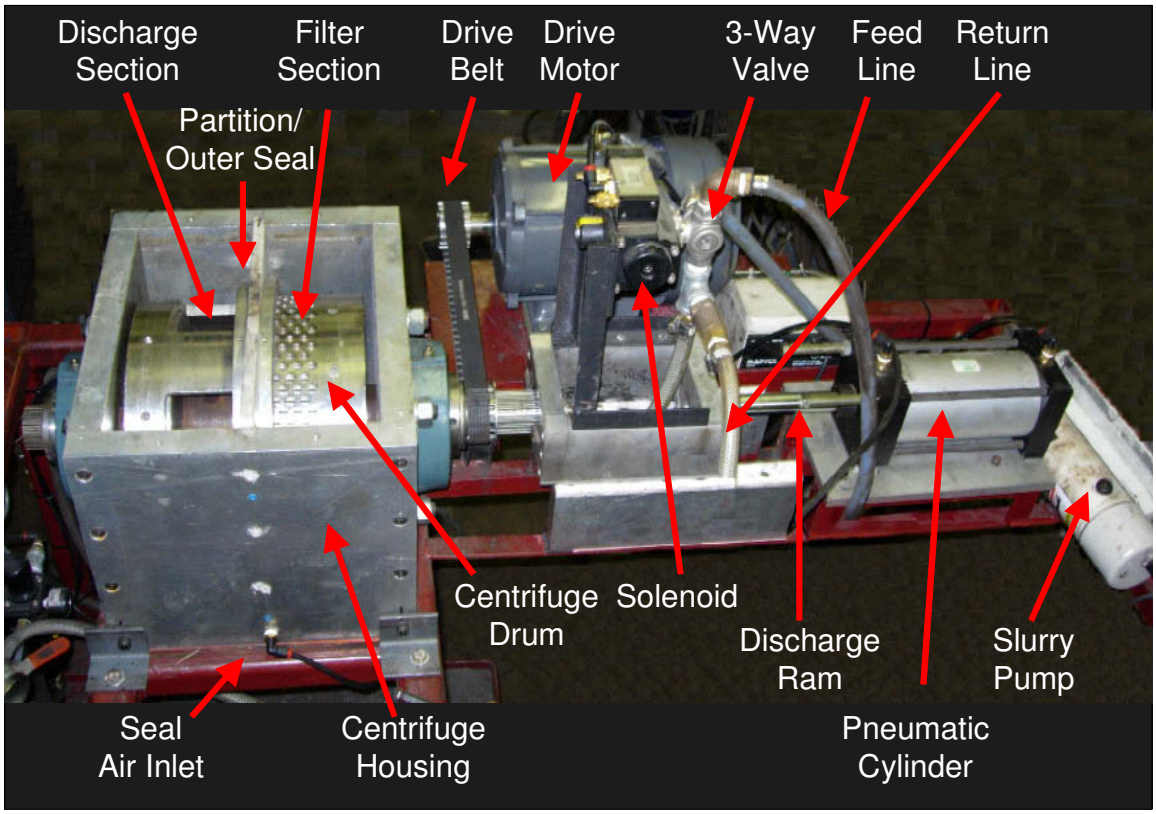

Figure 3.2 HFC with identification labels for key components

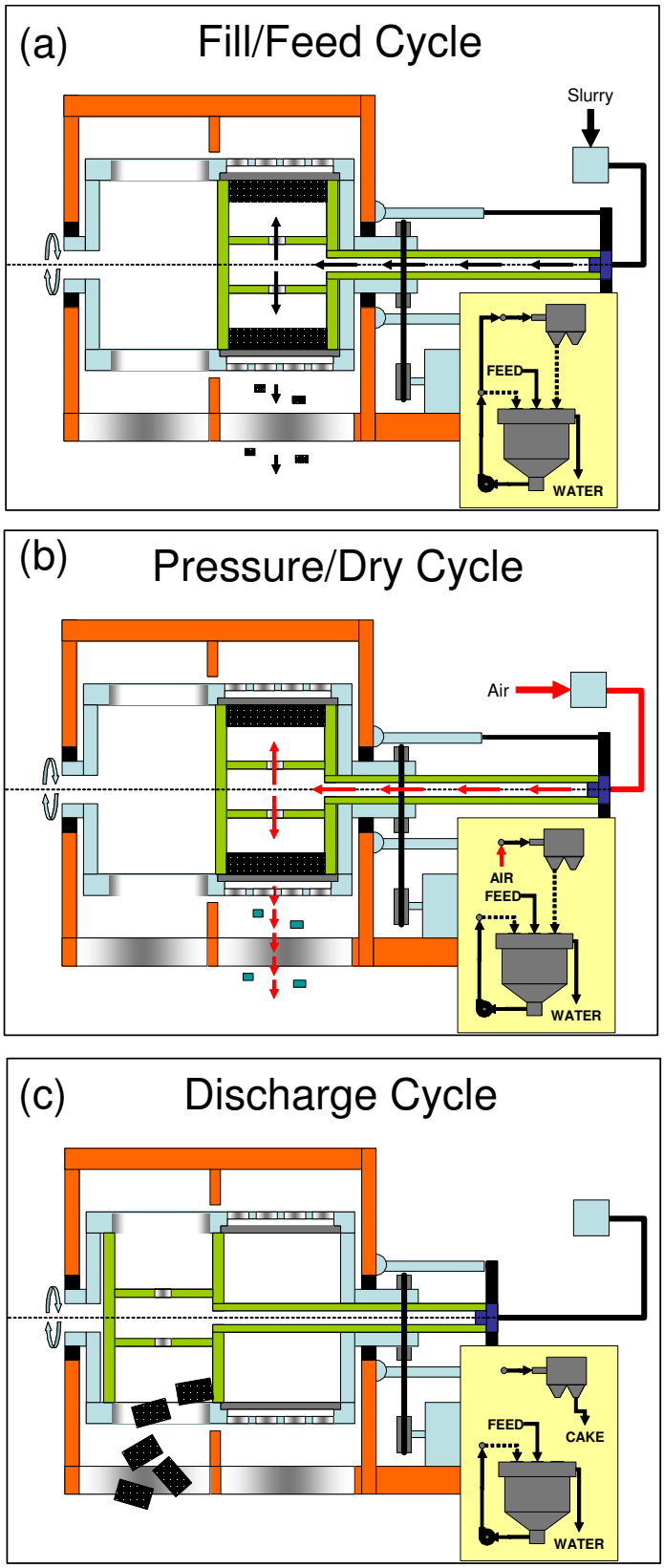

Figure 3.3 Process steps utilized by the hyperbaric filter centrifuge

Figure 3.4 Rotating drum assembly for the pilot-scale centrifuge

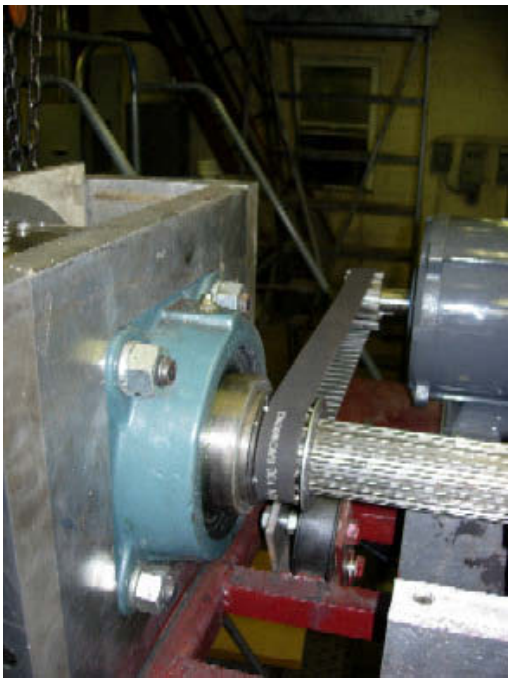

Figure 3.5 Motor, drive belt and shaft assembly for the pilot-scale centrifuge

Figure 3.6 Valve system for the introduction of feed slurry and air

Figure 3.7 Electronic control panel for the pilot-scale centrifuge

After conducting the tests that are given in sections 3.3.1 through 3.3.3 with the setup mentioned above, the feeding mechanism was modified to allow recycling of the effluent slurry that drains through the screen section back to the feed inlet of the pilot-scale unit. The recycling of the effluent for a certain amount of time was found to be necessary in order to increase the capture of fine solids by the cake. With this system, a known amount of coal slurry was pumped from a 6-inch diameter by 17-inch tall feed tank to the centrifuge unit. Effluent was collected in the same tank and was pumped back to the centrifuge. After the effluent became clear, the valve at the bottom of the tank was closed and pumping stopped.

Coal samples from two different coal plants were used to test the pilot-scale unit. The first sample, which was used with tests described in sections 3.3.1 through 3.3.4, was a non-deslimed screenbowl centrifuge feed (nominally 1 mm x 0) obtained from Tom's Creek Coal Preparation Plant. The second sample, which was used with the tests mentioned in section 3.3.5, was a deslimed screenbowl centrifuge feed (nominally 1 mm x 0.15 mm) from Pinnacle Pond Reclamation Plant. The size distributions of the samples are given in Table 3.1.

Table 3.1 Size distributions of samples tested with the pilot-scale unit

Size	**Tom's Creek (%)**	**Pinnacle (%)**
+0.6 mm	26.54	16.08
0.6 x 0.15 mm	33.53	72.38
0.15 x 0.044 mm	17.76	5.48
-0.044 mm	22.17	6.06

3.3 Results and Discussion

3.3.1 Effect of Rotation Speed and Rotation Time

Filling time, which controls the amount of feed slurry entering the test unit, was kept constant at 15 seconds for all test runs. Unfortunately, the baseline tests (without air injection) could not be run due to plugging of the feed line that occurred when no air was introduced. Therefore, air was on for the whole duration of each test. Tests were performed as a function of centrifugal acceleration (i.e. 142 and 319 g's) and rotation time (i.e. 10, 60 and 120 s).

The results from the pilot-scale tests are summarized in Table 3.2. The data show that the moisture dropped from just over 20% at the lowest air injection time and rotation speed to below 11% at the largest air injection time and rotation speed. The data are plotted in Figure 3.8 for comparison. This plot shows that an increase in rotation time from 10 to 120 s incrementally improved the moisture removal by about 5 percentage points for the lowest centrifugal acceleration of 142 g's. The incremental improvement was somewhat smaller (i.e., about 3 percentage points) for the higher centrifugal acceleration of 319 g's. Moreover, increasing centrifugal acceleration from 142 g's to 319 g's caused the moisture to decrease about 7 percentage points for the lowest rotation time and 4 percentage points for the highest rotation time.

Table 3.2 Effect of Rotation Speed and Rotation Time

Rotation Time (s)	Rotation Speed (rpm)	Centrifugal Acceleration (g's)	Moisture Content (%)
10	1000	142	20.2
60	1000	142	18.3
120	1000	142	15.0
10	1500	319	13.9
60	1500	319	13.2
120	1500	319	10.9

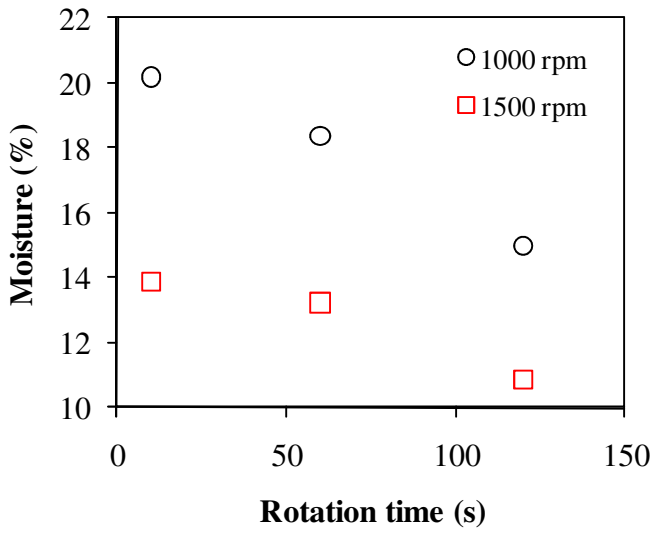

Figure 3.8 Effect of Rotation Speed and Rotation Time

3.3.2 Effect of Rotation Time and Air Injection

Several test runs were also conducted to investigate the effects of rotation time (i.e. 5, 10, 30, and 120 s) and air pressure (i.e. with and without air) on the performance of the pilot-scale test unit. The centrifugal acceleration was kept at 319 g's during these tests. The results are summarized in Table 3.3. A comparison of the data is also provided in Figure 3.9. The test data indicate that the injection of air provided approximately 2 percentage points reduction in moisture with rotation times of 5, 10 and 30 seconds. However, all of the moisture values obtained in these tests were already very low (around 12% or less). In fact, the values obtained with air injection at centrifugation drying times of 30 s or greater were all single-digit values. This can be explained by low solid recovery values obtained. Because the coal slurry was not thickened before it was fed to the unit, most of the fine solids were lost during centrifugation. Therefore, only 55-60% of solids were recovered during all the tests. The absence of fines drove moisture values down to below 12%. Moreover, since moisture values obtained at 120 s rotation

time with and without air were similar (i.e. 9.7%, 9.6%), the effect of air injection on moisture may have diminished due to long rotation time.

Table 3.3 Effect of rotation time and air injection

Rotation Time (s)	Air Injection	Moisture Content (%)	Solid Recovery (%)
5	No	12.6	56.37
10	No	11.2	58.34
30	No	10.8	57.15
120	No	9.6	55.79
5	Yes	10.6	60.76
10	Yes	10.3	60.61
30	Yes	9.6	60.46
120	Yes	9.7	59.17

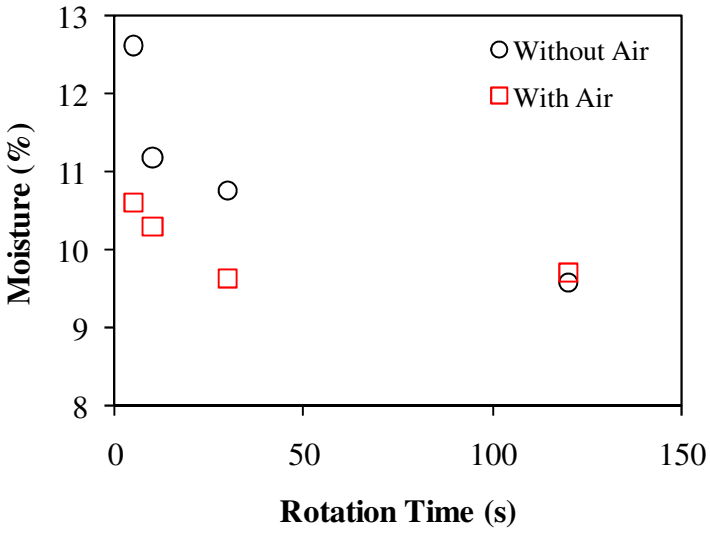

Figure 3.9 Effect of rotation time and air injection on product moisture

3.3.3 Effect of Thickening

Test results given in the previous section showed that only low solid recoveries could be achieved when dilute coal slurry was directly fed to the centrifuge. Therefore, for the next set of tests, the coal slurry was thickened by addition of an anionic flocculant before it was fed to the

centrifuge. Although, a more extensive test program with several cake thicknesses and with and without air injection was planned for this section, only a fraction of these tests could actually be conducted because of several mechanical failures occurred during testing. Tests were conducted as a function of centrifugal acceleration (i.e. 142 g's and 319 g's), rotation time (i.e. 15, 30, 60 and 120 s) and air pressure (i.e. with and without air).

The test results given in Table 3.4 and Figure 3.10 show that the moisture of 18.7% obtained at the shortest rotation time of 15 seconds with 142 g's reduced to 16.1% when the centrifugal acceleration increased to 319 g's. A further moisture reduction down to 13.2% was achieved when air was injected. While the same trend continued at the other rotation speeds, all moisture values improved as the rotation time increased. At the longest rotation time of 120 seconds, 14.1% moisture value obtained with 142 g's reduced down to 10.0% at 319 g's with air injection.

As a result of thickening the feed slurry, higher solid recoveries of more than 90% were obtained. Since no effluent sample was collected during testing, solid recovery values were

Table 3.4 Equilibrium moistures and solids recoveries obtained when samples were thickened

Rotation Time (s)	Rotation Speed (rpm)	Centrifugal Acceleration (g's)	Air Injection	Moisture Content (%)	Solid Recovery (%)
15	1000	142	No	18.7	92.9
30	1000	142	No	16.3	97.5
60	1000	142	No	15.1	96.0
120	1000	142	No	14.1	96.2
15	1500	319	No	16.1	68.6
30	1500	319	No	14.6	89.4
60	1500	319	No	13.0	88.4
120	1500	319	No	12.3	73.7
15	1500	319	Yes	13.2	98.6
30	1500	319	Yes	11.9	72.5
60	1500	319	Yes	11.2	91.4
120	1500	319	Yes	10.0	96.8

calculated by dividing the dry cake weight by dry feed weight. However, this approach created potentially inaccurate recovery values, because feed samples were not taken for all the tests. Therefore, although the solid recoveries seem to be generally improved by thickening, the accuracy of these values is arguable.

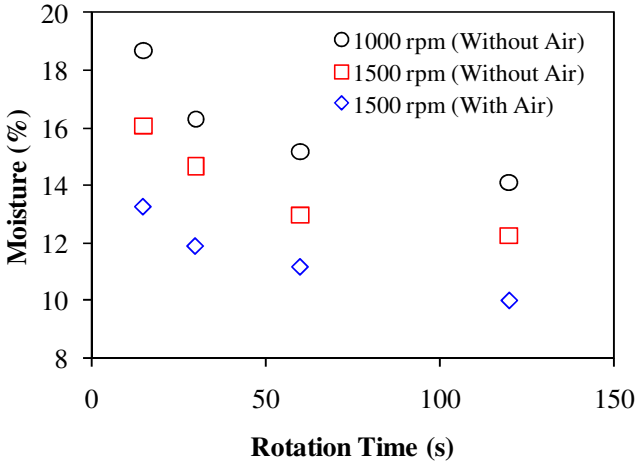

Figure 3.10 Effect of thickening on product moisture

3.3.4 Effect of Feed Size Distribution

Screenbowl centrifuges are widely used in coal industry to dewater fine coal feeds containing nominally 1 mm x 0 size particles. However, a screenbowl centrifuge can only recover about 50% of the minus 0.044 mm size fraction. Therefore, one of the expectations from the hyperbaric centrifuge technology was the ability of dewatering the minus 0.044 mm size fraction effectively while keeping solid recoveries high. To examine this possibility, the effect of feed size distribution was one of the major parameters examined in the pilot-scale tests. Unfortunately, all the test attempts with finer size feeds failed due to several factors. First of all, when a feed finer than 0.5 mm was used, all the particles passed through the screen openings and a cake could not be formed. Secondly, although flocculant addition seemed to be effective with

the coarser feed as explained in the previous section, the sizes of the particle aggregates formed with finer feeds were not sufficiently big to facilitate a cake formation. Even though a shear-resistant flocculant was used, the high shear forces introduced by the feed pump caused these particle aggregates to break, thus they were not able reach the size needed for cake formation. Therefore, the recirculation of the screen effluent appeared to be the only viable option for improving solids recoveries.

3.3.5 Effect of Recirculation

After running the tests that were given in previous sections, the test setup was changed to allow recirculation of screen effluent back to the feed port. This was done using the feeding arrangement explained in section 3.2. Recirculation was considered to be necessary to maximize the solid recovery. First, the non-deslimed Tom's Creek sample (Table 3.1) was tested. However, none of the tests could be completed, because recirculation caused fine particles to form a slime coating atop the cake. This coating prevented the passage of pressurized air through the cake, thus causing the airline to plug and burst several times. Moreover, using a flocculant to form larger agglomerates did not work either, since these weak agglomerates broke after passing through the feed pump several times. Consequently, it was decided to use a deslimed sample to see the effect of recirculation. The results are described in the next section.

3.3.6 Effect of Desliming

These tests were conducted using the deslimed screenbowl feed obtained from the Pinnacle Pond Reclamation plant. The size distribution of the sample is given in Table 3.1. The centrifugal acceleration was maintained at 319 g’s for all tests. After 30 seconds of recirculation, the cake was centrifuged for an additional 30 seconds before ending the test run. The test results

given in Table 3.5 indicate that the use of the deslimed sample, which contained very few particles finer than 0.044 mm, resulted in very low values of cake moisture (i.e., 5-7%). Also, by recycling the effluent, very high solid recoveries were achieved (i.e., 97-99%). Moreover, injecting air at different pressures lowered the moistures by 1-2 percentage points compared to the baseline values. Therefore, single-digit moistures could be achieved by desliming ahead of the filter centrifuge.

Table 3.5 Effect of desliming and recirculation

Air Pressure (kPa)	Moisture Content (%)	Solid Recovery (%)
0	6.9	97.7
93	5.9	97.2
107	5.6	99.1
133	5.1	97.4

3.4 Discussion

3.4.1 Solids Recovery and Product Moisture

The tests conducted with the pilot-scale unit showed that thickening the feed slurry is a necessity for achieving high solid recoveries. Also, recirculation of the effluent stream back to the feed stream gave a chance to fine particles to be captured by the cake, thus increasing the recovery of solids. However, increased solid recovery caused product moisture to escalate about 2.7 to 5.4 percentage points depending on centrifugation period (see Table 3.3 and Table 3.4). Considering the increased moisture values were still below 20% and higher recoveries will help with the capacity requirements, the somewhat higher moisture values were found to be acceptable.

3.4.2 Engineering Criteria for Machine Design

Ability of running a continuous operation is essential for maximizing the capacity in industrial applications. However, the design of the pilot-scale unit did not allow for a truly continuous operation. First of all, it was not possible to feed the unit continuously because of the unit's cyclic operation procedure that was explained in section 3.2. Secondly, coal slurry had to be thickened outside and pumped into the unit, which caused problems with flocculation since the agglomerates broke due to the high shear forces inside the feed pump.

The pilot-scale unit consisted of two sections, a screen section, which was also used as a pressure chamber, and a discharge section. The need for thickening the slurry outside the unit could be eliminated by adding a third "solid" section to the rotating unit, which is similar to the solid-bowl part of a screenbowl centrifuge. Therefore, coal slurry would be fed directly into the unit and be thickened inside. Integrating the thickening operation to the centrifuge would have many advantages over using a conventional thickener. First of all, the space required for a thickening tank would be eliminated. Also, thickening can be done much faster and more efficiently with centrifugation. Furthermore, feeding slurry directly to the unit can effectively reduce the amount of chemicals needed for thickening. Also, since the cake would already be formed in the solid section, the problems encountered with cake formation using fine particles can be overcome. Addition of a third section to the centrifuge unit would not eliminate the need for a feed tank because of the semi-continuous nature of the unit. However, a smaller buffer tank can be used instead of a wide thickening tank. The only downside to using a solid bowl section as part of the hyperbaric centrifuge is that it would need to operate at a very high speed to provide the centrifugal forces necessary to capture ultrafine solids. Calculations suggest that the

required centrifugal field is likely to be in the order to 2,000 to 3,000 g's for the effective capture of minus 0.044 mm solids now lost in standard screenbowl machines operating at 500 g.

3.5 Conclusions

A pilot-scale centrifuge that utilizes pressurized air was built and tested under several conditions. The results showed that higher rotational speeds and longer centrifugation times were needed for producing lower moistures. Also, injecting pressurized air through the cake further improved the moisture.

It was also concluded that thickening was an essential step for centrifugal dewatering, as it increased the recovery of solids. Also, it was found that solids recovery could be further increased when effluent stream was re-circulated back to the feed stream. However, this exercise caused a slime coating to form atop the cake when a non-deslimed feed was used due to the breakage of flocculated agglomerates inside the feed pump. Integration of the thickening process via the addition of a solid bowl section during centrifugation can help with this problem by eliminating the need for this step.

Originally, a more detailed and a complete parametric study of the pilot-scale unit was planned. However, all the attempts for running complete series of tests were unsuccessful due to the fundamental operational problems. For example, the hollow shaft that was used for material feeding and other feed lines and valves could not be designed properly for such a small machine to allow an easy passage of the typical feed material (1 mm x 0). As a result, the lines were plugged several times during testing and led to some failures. Due to the mechanical and design problems faced, it was decided pursue the development of a prototype machine that would include both solid- and screen-bowl sections.

CHAPTER 4 FIELD TESTING OF A PROTOTYPE HYPERBARIC CENTRIFUGE

4.1 Introduction

The laboratory and pilot-scale test programs provided sufficient promising data to warrant the construction of a commercial prototype of the Centribaric™ technology. The one-of-a-kind machine was designed and fabricated by Decanter Machine, Inc., a well-known manufacturer of solid- and screen-bowl centrifuges. The prototype unit was tested at several industrial sites by Decanter Machine. Virginia Tech participated in one of these test programs at Cardinal Plant of Arch Coal.

Cardinal Plant (Figure 4.2) is located near the town of Sharples in Logan County, West Virginia. Plant production is intended mainly for steam coal market. The plant has three 700 tph

Figure 4.1 Prototype hyperbaric centrifuge of Decanter Machine

Figure 4.2 Cardinal Plant

capacity modules. Each module employs single unit operations. Multiple modules provide flexibility of running with one or more modules being idled for maintenance. As shown in Figure 4.3, each module has a 10x20-ft double deck banana screen, which is used as a combined raw coal/deslime screen, cutting at 0.5-inch on the top deck and 1 mm on the bottom deck. The coarse material then goes to a dense medium vessel for density separation. Compound spirals are incorporated for treating 1 x 0.2 mm size fraction, while column flotation is used to clean deslimed fine coal (0.25 x 0.044 mm). Finally, combined deslimed spiral/column concentrate is dewatered by 42x144-inch screenbowl centrifuges. A single thickener is used to treat plant tailings. Thickener underflow is pumped to an established impoundment, while the coarse refuse is hauled to a separate coarse refuse area. (Bethell and DeHart, 2006)

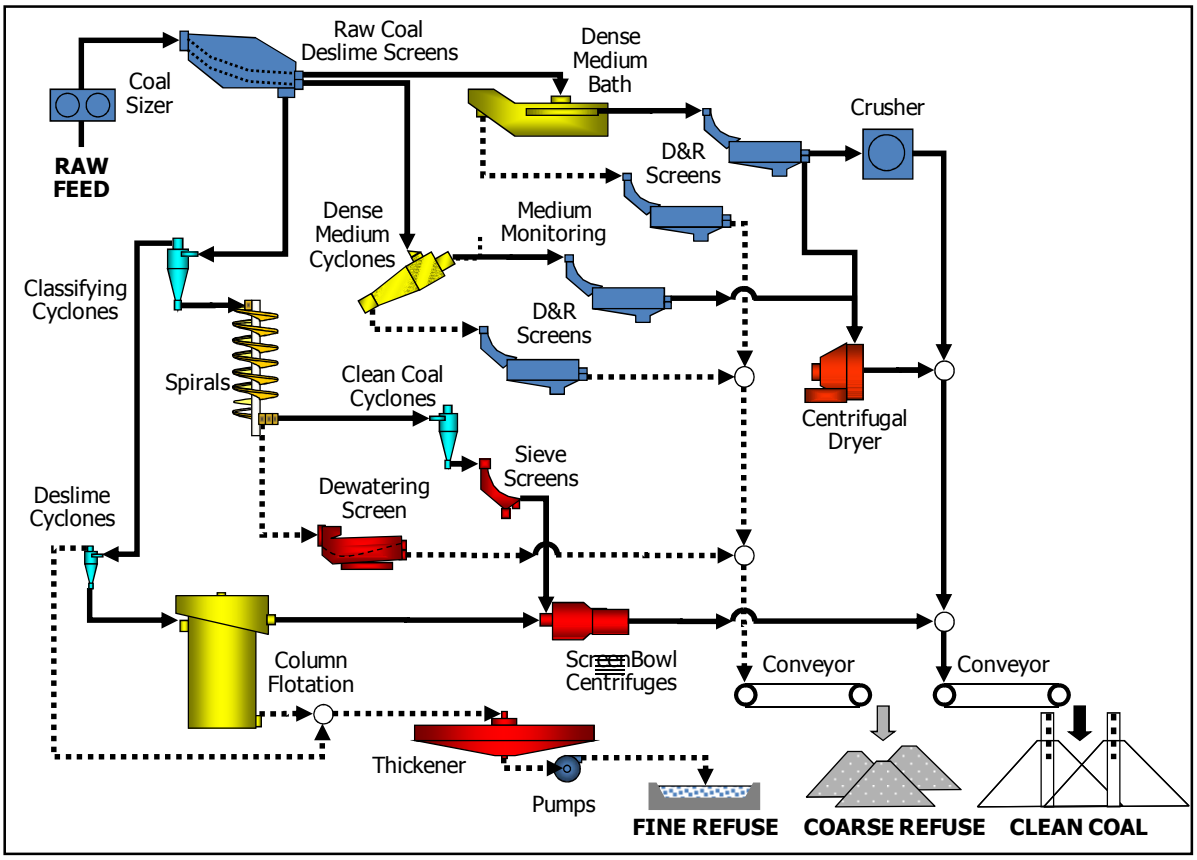

Figure 4.3 Simplified flowsheet of Cardinal Plant (Single Module)

4.2 Experimental

4.2.1 Machine Description

The prototype was designed to handle a volumetric capacity of 120 liter/minute of feed slurry. The prototype unit and all ancillary components were trailer-mounted so the equipment could be easily relocated to different industrial sites (Figure 4.1). The mobile platform included space for a 1,750 liter feed storage tank, tank mixer, slurry pump, gas compressor, discharge collection bin, effluent pump/sump and electrical control systems. While a detailed description of the feed/discharge system, sealing mechanisms and solids transport assemblies cannot be discussed due to the proprietary nature of this patent-pending technology, the basic concept is

similar to other centrifugal dewatering processes in terms of applicability, operation and maintenance. (Figure 4.4).

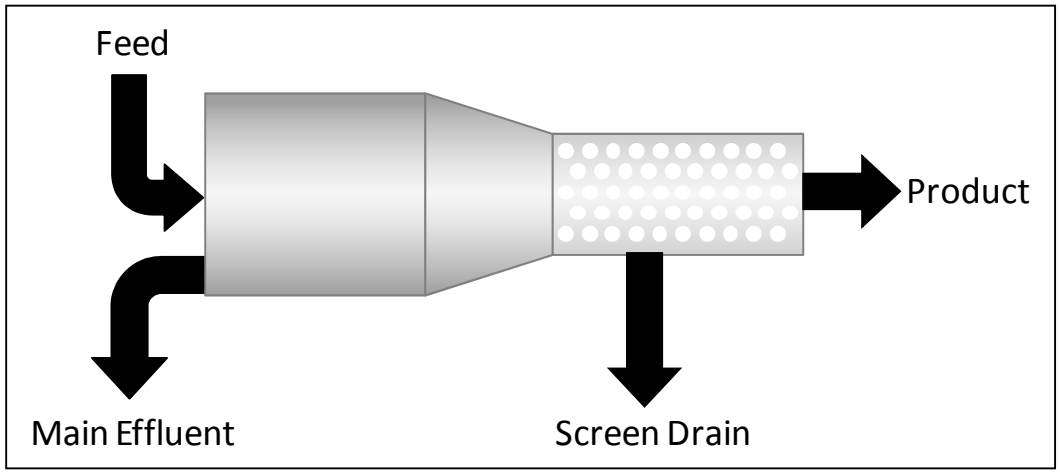

Figure 4.4 Diagram of the prototype hyperbaric centrifuge

4.2.2 Test Procedure

In total, seven different feed mixture combinations were evaluated at this particular test site. The coal used as the feed to the test unit was Alma A coal from the Mountaineer II Mine. The 6-inch cyclone overflow stream (minus 0.044 mm) of the plant was floated with a 20-inchx10-ft pilot scale flotation column, and it was mixed in various proportions, which are given in Table 4.1, with the plant's screenbowl centrifuge screen drain to prepare the feed for every batch. Note that a progressively finer feed stream was used in each subsequent test run. This feeding arrangement made it possible to investigate the effects of a wide range of particle size distributions on dewatering performance and solid/slurry throughput capacity. The mixture was kept agitated in a holding tank during the tests. For the last test, instead of screenbowl screen drain, plant's column flotation concentrate (nominal 0.25 x 0.044 mm) was mixed with leftover slurry from the previous test.

Table 4.1 Feed Mixtures

Test	Mixing Ratio
1	50 % Column concentrate / 50% Screenbowl screen drain
2	60 % Column concentrate / 40% Screenbowl screen drain
3	70 % Column concentrate / 30% Screenbowl screen drain
4	80 % Column concentrate / 20% Screenbowl screen drain
5	90 % Column concentrate / 10% Screenbowl screen drain
6	100 % Column concentrate / 0% Screenbowl screen drain
7	NA% Column concentrate / NA% Plant column concentrate

Timed samples from feed, product, screen effluent and main effluent streams were taken during test runs. While the entire product and screen effluent streams were collected for each test, only 2-4 cuts were taken from feed and main effluent streams to fill up two 5 gallon buckets for each stream. After cutting the sample from the main effluent, a full stream sample of the feed was taken by diverting the feed stream from the centrifuge to a bucket. Feed stream was redirected back to the centrifuge and sufficient time was given to reach steady-state before cutting the next set of samples. The holding tank was filled up before every test at the desired mixing ratio. All the samples were sealed after each test to prevent any evaporation. Analyses of the samples were done by a commercial laboratory. Size distributions and ash data for all the feeds are given in Table 4.2 and Table 4.3, respectively.

Table 4.2 Feed size distributions for all tests

	Weight (%)				
Test	+0.5 mm	0.5 x 0.15 mm	0.15 x 0.044 mm	0.044 x 0.025 mm	-0.025 mm
1	16.63	26.08	20.47	0.58	36.24
2	10.51	17.56	23.28	7.35	41.30
3	8.07	14.63	22.53	8.78	45.99
4	5.52	9.97	21.45	9.20	53.86
5	2.77	7.37	16.58	11.13	62.15
6	0.18	1.40	20.42	3.70	74.30
7	0.01	0.44	3.20	1.89	94.46

Table 4.3 Feed ash values for all tests

	Ash (%)				
Test	+0.5 mm	0.5 x 0.15 mm	0.15 x 0.044 mm	0.044 x 0.025 mm	-0.025 mm
1	7.65	5.43	6.68	20.50	10.21
2	10.59	5.88	5.41	7.68	7.83
3	8.60	6.27	6.47	8.97	8.12
4	10.83	6.80	5.29	6.55	7.94
5	12.90	7.30	4.28	5.03	6.86
6	29.09	7.54	2.33	3.25	6.67
7	28.65	4.61	3.60	3.85	7.19

4.2.3 Performance Analysis

To create a reliable set of data out of the raw data obtained from the laboratory, a steady-state mass balance routine that was set up in an Excel spreadsheet was used. This routine makes the least possible change to the measured values, so that the mass of components (i.e. solid, water, ash, etc.) entering the unit is equal to the mass of components leaving the unit. Different amounts of confidence were given to measured values, using weighted sum-of-squares, to be able to let the routine selectively adjust these values.

It was observed that the feed flow rates calculated from the timed feed samples were higher than the combination of product and effluent stream flow rates. Even though the feed pump was a positive displacement type, it was assumed that there was enough wear on the rotor of the pump that allowed surging while it was operating under pressure. Whereas, when the full feed stream was diverted from the centrifuge to a bucket during sampling, resulting pressure drop on the pump caused the flow rate to increase. Therefore, very little dependence was put on the measured feed flow rate numbers when mass balancing. Also, according to the laboratory analysis, 0.044 x 0.025 mm size fractions of every sample had unrealistically small mass values compared to the upper and lower size fractions. When mass balancing was tried, the routine

made large changes to these values. The coarsest size fraction values were also substantially changed by the mass balance routine. Therefore, these size fractions were combined with other size fractions to obtain a more reliable size distribution. As a result, the input parameters used for mass balances are given below:

- Size distribution (plus 0.15 mm, 0.15 x 0.025 mm and minus 0.025 mm)
- Ash contents (%) of plus 0.15 mm, 0.15 x 0.025 mm and minus 0.025 mm size fractions
- Solids content (%, by weight)
- Slurry rate (kg/hr)

Since screen drain stream was not re-circulated back to the feed stream during testing, there was no experimental data representing the effect of circulating load. To simulate recirculation, combinations of screen drain and feed for every test were calculated by iteration in Excel. New moisture values were predicted using the polynomial curve that was fit to the experimental data (Figure 4.5). Details of the calculations are given in Appendix 1.

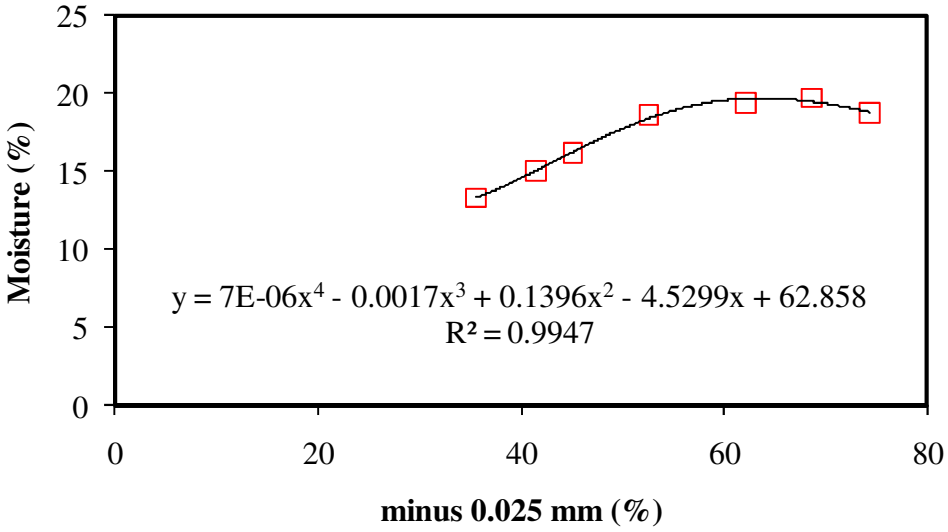

Figure 4.5 Effect of minus 0.025 mm particle amount on cake moisture

4.3 Results

Summary of test results is given in Table 4.4. As can be seen, a low moisture value of 13.7% was achieved at the first test run. This particular run employed a relatively coarse feedstock prepared using a 50/50 mixture of screenbowl screen drain (minus 0.5 mm) and column flotation concentrate (minus 0.044 mm). From this baseline test run, the moisture climbed up to 19.4% as the mass percent of ultra-fines (minus 0.025 mm) increased to its maximum value of 94.5% by weight. The fact that the moisture in the final run was still below 20% was considered to be very impressive given the extreme fineness of the feed material used in the final test run. Conventional dewatering processes (e.g., screenbowl centrifuges) typically generate moistures >50% for this ultrafine size class.

The prototype test data also demonstrated that very high recoveries of ultrafine solids could be achieved while maintaining low moisture contents. The highest recovery of dry solids (i.e., 99.9%) was obtained for the coarsest feed mixture containing only 36.2% minus 0.025 mm, while a slightly lower recovery (i.e., 97.9%) was obtained for the finest feed mixture containing 94.5% minus 0.025 mm.

Table 4.4 Cardinal Plant test results

Test	Condition	No Recirculation (Measured)		With Recirculation (Predicted)	
		Moisture (%)	Solid Recovery (%)	Moisture (%)	Solid Recovery (%)
1	50 / 50 : Col Conc / Scrn Drain	13.3	96.1	13.7	99.9
2	60 / 40 : Col Conc / Scrn Drain	15.0	95.5	15.1	98.9
3	70 / 30 : Col Conc / Scrn Drain	16.2	93.4	17.0	99.9
4	80 / 20 : Col Conc / Scrn Drain	18.6	93.8	18.6	99.2
5	90 / 10 : Col Conc / Scrn Drain	19.4	94.5	19.7	99.4
6	100 / 0 : Col Conc / Scrn Drain	18.7	83.2	18.3	97.3
7	NA/NA : Col Conc / Plant Col Conc	19.7	89.4	19.4	97.9

4.4 Discussion

It was originally anticipated that a linear correlation would be observed between the moisture values and the amount of ultrafine solids in the product. This correlation has been observed for most of conventional dewatering processes used in the coal industry (Arnold, 1999). However, as shown in Figure 4.5, the moisture obtained using the Centribaric^{TM} technology increased linearly until the mass percent of minus 0.025 mm solids reached 60%. The moisture then reached a plateau at about 19.4% and did not increase further as the amount of minus 0.025 mm solids increased. This surprising trend was also found to be reproducible in laboratory tests conducted with air injection. No such plateau was observed in the laboratory tests where no air injection was employed (i.e., the moisture continued to increase in a linear fashion as the amount of ultrafines increased). As such, the Centribaric^{TM} technology appears to be ideally suited for dewatering of ultrafine feeds to low moisture values.

4.5 Conclusions

The prototype hyperbaric centrifuge unit that was built by Decanter Machine Inc. was tested with various feed conditions at Arch Coal's Cardinal Plant. Test results showed that moistures of 13.3-19.7%, which are very low numbers compared to conventional filtration, with high recoveries of 83.2-96.1% were easily achievable when screen drain of the test unit was discarded. Whereas, slightly higher but still low moistures from 13.7% to 19.4% with 97.3-99.9% recoveries were predicted to be achievable if the screen drain was re-circulated. Also, mixing fine (minus 0.044 mm) column concentrate with a coarser stream was found to be effective on reducing moisture and increasing solid recovery. To avoid a substantially higher capacity requirement, a smaller ratio of coarse/fine can be used as the test results show that even

a small amount of coarse material was enough to keep the moisture content low and the recovery high.

4.6 References

1. Arnold, B. J. (1999). Simulation of dewatering devices for predicting the moisture content of coals. Coal Preparation, 20(1-2), 35-54.
2. Bethell, P. J., & DeHart, G. (2006). *Design, Construction and Commissioning of the New 2000 TPH Arch Coal Preparation Plant*. Paper presented at the XV International Coal Preparation Congress, Beijing, China.

CHAPTER 5 MODELING OF A HYPERBARIC FILTER CENTRIFUGE

5.1 Introduction

Coal cleaning is a water based process after which a product with certain amount of moisture is produced. Excess process water is removed by dewatering equipment at the end of the cleaning process. Dewatering is an important step of coal cleaning, because coal producers can only ship a limited amount of moisture due to contractual requirements. Therefore, successfully simulating dewatering equipment using a reliable and accurate model would greatly benefit coal producers, as the value of coal can be estimated under different conditions even before actually running the dewatering equipment.

The final moisture content of a cake depends on many variables such as the physical properties of particles (i.e. size, shape, surface properties, etc.) and operating parameters of the dewatering equipment. Because of the large number of particles involved with randomly distributed sizes and shapes, it is impossible to completely describe this complex system. Instead, the best estimates of process variables can be used to make an accurate prediction.

Dewatering models commonly involve a balance of de-saturating forces that push the water out of the cake and capillary forces that retain water inside the cake. The applied de-saturating forces can be either mechanical as in conventional centrifuge machines or can be hydrodynamic as in pressurized air injection. These forces can also be used in conjunction with each other. Even though there are several empirical and theoretical models developed by researchers to predict moisture content of centrifuge and filter products, there is no model currently available in the technical literature for a hyperbaric centrifuge. Therefore, the purpose

of this chapter was to develop a model for hyperbaric centrifugation. For this purpose, two types of models were developed. The first type of model, which is explained in section 5.2, was developed to explain the pressure distribution inside an HFC cake. This model made it possible to understand why injection of pressurized air helped with dewatering. The second type, which is explained in section 5.3, was intended for prediction of moisture content of HFC products and it involved development of two different models, one of which was a theoretical model and the other one was an empirical model.

5.2 Pressure Distribution Model

The centrifugal dewatering process can be characterized by a filter cake submerged in an annulus of clear liquid (Figure 5.1). Zeitsch (1990) developed a model to predict centrifugal filtration rate based on the first principle considerations. According to Zeitsch, the fundamental law of filtration as formulated by Darcy (1856) is not applicable to centrifugal filtration as it fails to take mass forces into account. Darcy's law suggests that there has to be a pressure difference in order to move a liquid through a porous medium, as follows:

$$Q = \frac{K\Delta PA}{\eta H} \qquad [5.1]$$

where Q is the flow rate of liquid passing through the cake, K is the permeability of the bed, ΔP is the pressure drop across the cake, A is the filter area, η is the viscosity of the fluid and H is the cake thickness. With reference to Figure 5.1, during centrifugation when the liquid layer reaches the cake surface ($r_0 = r_S$), pressures at r_S and r_B will be equal to the ambient pressure. Therefore, according to Eq. [5.1], the liquid should not be flowing at this point because the pressure difference across the cake is zero. However, the liquid will keep flowing because of the acting centrifugal force.

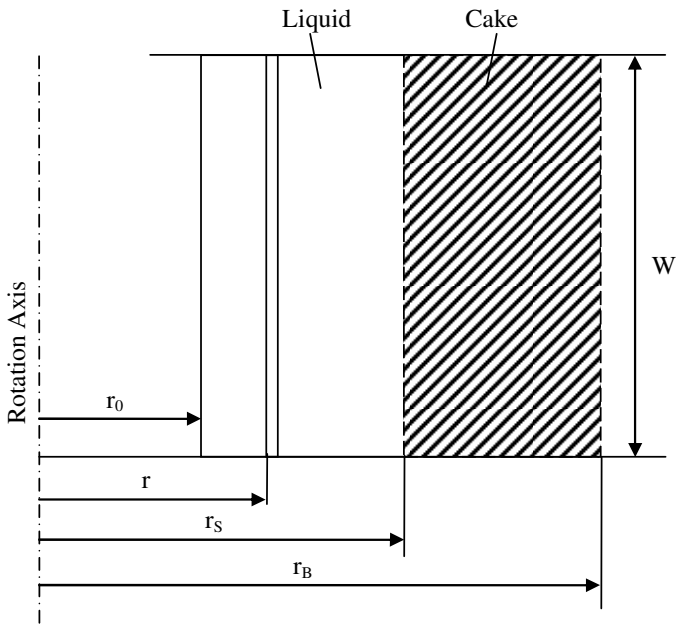

Figure 5.1 Geometry of centrifugal dewatering

Zeitsch (1990) developed the following relationship, which gives the pressure distribution inside a cake during centrifugation, based on the situation given in Figure 5.1:

$$P(r) = \frac{ln(r_B/r)}{ln(r_B/r_S)} P_S + \frac{\rho\omega^2 r_B^2}{2}\left[\frac{ln(r_B/r)}{ln(r_B/r_S)}\left(1 - \frac{r_S^2}{r_B^2}\right) - \left(1 - \frac{r^2}{r_B^2}\right)\right] \quad [5.2]$$

where P_s is the pressure on cake surface, ρ is the liquid density and ω is the angular velocity.

In the current study, this equation was revised to reflect the effect of application of air pressure, as follows:

$$P(r) = \frac{ln(r_B/r)}{ln(r_B/r_S)} (P_S + P_{air}) + \frac{\rho\omega^2 r_B^2}{2}\left[\frac{ln(r_B/r)}{ln(r_B/r_S)}\left(1 - \frac{r_S^2}{r_B^2}\right) - \left(1 - \frac{r^2}{r_B^2}\right)\right] \quad [5.3]$$

A numerical example of Eq. [5.3] is given in Figure 5.2(a). The plot shows that the pressure inside a centrifuge cake drops below ambient pressure when the liquid layer reaches the cake surface. However, the pressure may be increased above the ambient pressure by injecting

pressurized air into the centrifuge (Figure 5.2(b)), thus increasing dewatering kinetics as the total de-saturating force increases.

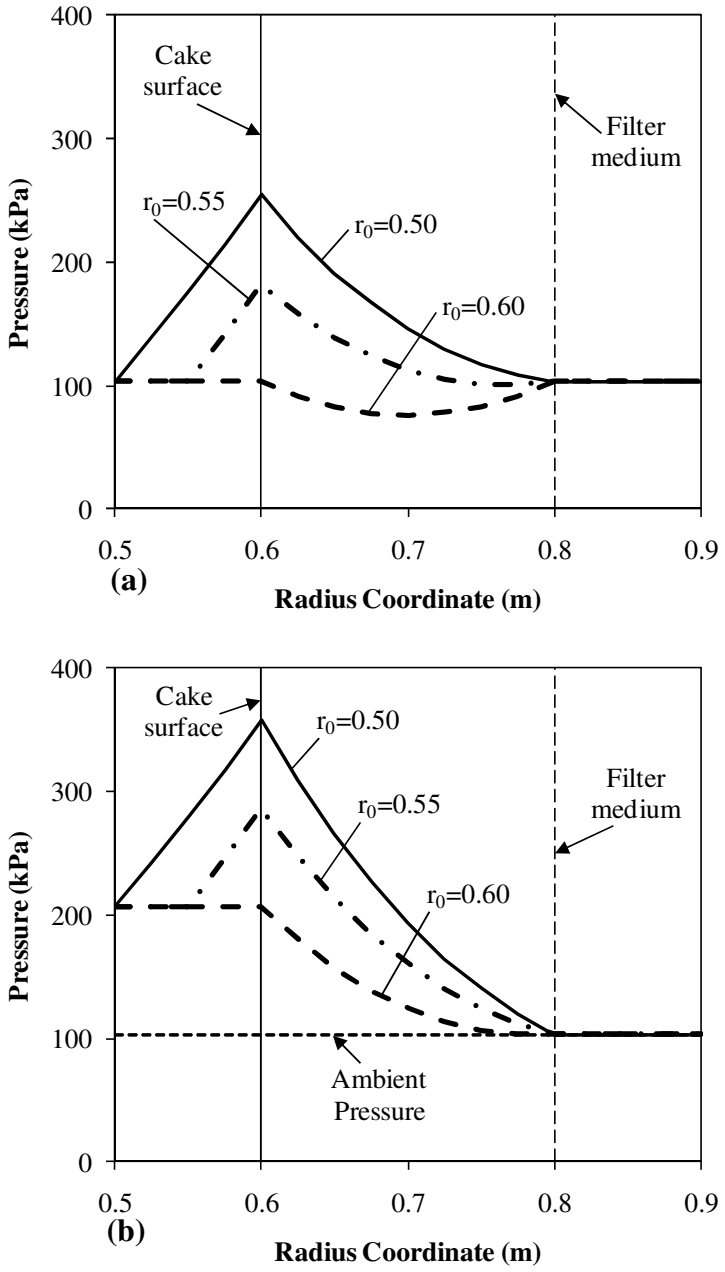

Figure 5.2 Changes in pressure across the filter cake formed on a centrifugal filter: r_B = 0.8 m and r_S = 0.6 m. Calculations were made at r_0 = 0.50, 0.55 and 0.60 m. At r_0 = 0.60 m, the thickness of the water film on the cake become zero. In case (a), pressure in the cake becomes lower than the ambient, as shown by the dotted line. Whereas, in case (b), pressure inside the cake is positive

5.3 Cake Moisture Models

5.3.1 Empirical Dewatering Model

The moisture content of a centrifuge product is calculated in two steps. First, the minimum water content, which is achievable when a de-saturating force acts for a very long time, is calculated and then this value is adjusted upwards to allow for the fact that there is only a finite amount of time available for dewatering. Moreover, when carrying out moisture content calculations, saturation (*S*) values are used instead of moisture values for ease of computation.

The saturation is estimated by using a dimensionless number called capillary number (N_c). The capillary number represents a ratio of de-saturating forces to water retaining forces. Several researchers such as Brownell and Katz (1947), Haruni and Storrow (1953), Dombrowski and Brownell (1954) defined capillary number using the permeability factor *K*, but Wakeman et al. (1976) showed that the capillary number and the previously used permeability expressions to correlate residual saturation data were inadequate because of the inability of Brown (1950) method to calculate *K* for centrifugally spun beds. However, Swindells (1979) replaced permeability term, *K*, with the squared mean particle size term, d_p^2, which resulted in a better correlation:

$$N_c = \frac{\rho_w N_g g d_p^2}{\sigma \cos\theta} \qquad [5.4]$$

where ρ_w is the density of water, N_g is the number of g's, d_p is the mean particle diameter, σ is surface tension of water and θ is the contact angle. In the current study, this equation was modified to allow for pressurized air injection as follows:

$$N_c = \frac{\left(\rho_w N_g g + P_{air}/H\right) d_p^2}{\sigma \cos\theta} \qquad [5.5]$$

where P_{air} is the air pressure and H is the cake thickness. d_p can be calculated using the following equation:

$$d_p = \frac{1}{\sum_{i=1}^{n}\left(\left(\sum_{j=1}^{m} F_{ij}^{*}\right)/A_i\right)} \quad [5.6]$$

Above equation gives the diameter of a particle with the same surface area per unit volume as the total surface are per unit volume of collection of all particles.

It is important to determine the mean particle size accurately, since it greatly affects the simulation results. Size distribution of a particulate system is commonly determined by wet screening. However, because of the limitations of this method the size distribution below 0.025 mm cannot be measured. Moreover, a practical method for determining the size distribution of this size fraction does not exist. Therefore, when conducting simulations, the well known Gates-Gaudin-Schumann (GGS) particle size distribution equation was fitted to size distributions obtained for different feed samples to determine the distribution below 0.025 mm. This allowed for calculating a more realistic mean particle size, especially for the finer size distributions. While fits obtained using GGS equation were not the perfect, it was deemed to be sufficiently accurate for the current study.

Using the data he obtained during his tests and the data available in the literature, Ledger (1999) suggested an empirical relationship that yielded a good correlation between the capillary number and the residual saturation, which is the minimum saturation achievable:

$$S_r = 0.051e^{-N_c/91.3} + 0.0045 \quad [5.7]$$

However, due to the limited amount of time available for dewatering, a higher saturation, which is called effective saturation, S_e, is normally seen in commercial centrifuges. Brown (1950) derived a relationship that defines saturation, S_e, in terms of S_r and S:

$$S_e = \frac{S - S_r}{1 - 2\,S_r + S\,S_r} \quad [5.8]$$

Assuming that the cake is fully saturated at time 0, S_e at any time can be determined by the following equation.

$$S_e^{1-y} = 1 + \frac{2t(y-1)}{C_t((1-S_r)^2 + 1)} \quad [5.9]$$

where t is time and C_t is a parameter given by:

$$C_t = \frac{\eta \varepsilon H}{Kp} \quad [5.10]$$

where η is viscosity of water, ε is porosity of the cake, K is permeability of the cake and p is the pressure differential across the cake. p value can be calculated using the following equation:

$$p = \rho_w N_g g \quad [5.11]$$

Permeability, K, is another important parameter for modeling of the dewatering process. The use of an accurate value of K is crucial for determining the correct moisture content. The best way of determining K is to measure it using one of the available methods in the literature (Zeitsch, 1990). However, when measurement is not possible, the permeability, K, can be estimated using one of the many equations that employ porosity and mean particle size values available in the literature. Brown (1950) proposed the following simple equation for estimating K:

$$K = \frac{\varepsilon^3 d_p^2}{180(1-\varepsilon)^2} \quad [5.12]$$

Panda et al. (1994) also developed the following equation:

$$K = \frac{\varepsilon^3 d_p^2}{72\tau(1-\varepsilon)^2}\left(\frac{S_k C_{D_p}^3 + 3C_{D_p}^2 + 1}{1 + C_{D_p}^2}\right)^2 \quad [5.13]$$

where τ is the tortuosity, S_k is the skewness of the particle size distribution and C_{Dp} is the coefficient of variation of the particle size distribution, which is the standard deviation divided by the mean size. An average value of 3 can be used as the tortuosity. Another equation for predicting permeability was developed by Vidal et al. (2009) as follows:

$$K = \frac{1}{S_0^2(c_1 S_k + c_2)} \frac{\varepsilon^3}{(1-\varepsilon)^{5/3}} \quad [5.14]$$

where c_1 and c_2 are fitting parameters, which were found to be 0.22 and 4.00, respectively, and S_0 is the specific surface area that can be estimated using:

$$S_0 = \frac{6}{d_p} \quad [5.15]$$

Eq. [5.10] was also modified to allow for pressurized air injection, as follows:

$$C_t = \frac{\eta \varepsilon H}{K\left(\rho_w N_g g + P_{air}/H\right)} \quad [5.16]$$

The dimensionless parameter y in Eq. [5.9] is a function of mean particle size, d_p, and can be approximated by:

$$y = 1.4355 + 0.17213 \log d_p + 0.1401 \left(\log d_p\right)^2 \quad [5.17]$$

Residual and effective saturation values obtained using previous equations can be combined using the following equation to determine the total saturation value:

$$S = \frac{S_e - 2S_e S_r + S_r}{1 - S_e S_r} \quad [5.18]$$

Finally, the moisture content of the product is given by:

$$M = \frac{S\varepsilon\rho_w}{S\varepsilon\rho_w + (1-\varepsilon)^2} \quad [5.19]$$

5.3.2 Theoretical Dewatering Model

Zeitsch (1990) developed a theoretical model of centrifugal dewatering using fundamental concepts. For modeling purposes, structure of a filter cake is far too complicated to take size, shape and mutual arrangements of particles into account. However, a filter cake can be characterized as a whole using parameters that are readily measurable, such as the permeability, porosity and volumetric degree of saturation. For his model, Zeitsch assumed that a filter cake would consist of a solid body perforated with cylindrical pores parallel to acting acceleration.

In the current work, modifications were made to Zeitsch's model to allow for pressurized air injection. The velocity of a liquid flowing in a single pore of diameter $s = 2b$ and height H is given by the following differential equation:

$$\pi r^2 P_{air} + \pi r^2 y(t,s)\rho_w N_g g = \pi r^2 \frac{2\sigma\cos\theta}{b} - 2\pi r y(t,s)\eta \frac{\mathrm{d}w}{\mathrm{d}r} \qquad [5.20]$$

where r is the radius coordinate starting at the pore axis and $y(t, s)$ is the height of the liquid at time t. Integrating both sides of this equation yields the radial velocity distribution:

$$w(r) = \frac{b^2 - r^2}{4y(t,s)\eta}\left(P_{air} + \rho_w N_g g\, y(t,s) - \frac{2\sigma\cos\theta}{b}\right) \qquad [5.21]$$

The volume flow between radii r and $(r + \mathrm{d}r)$ during the time interval t is given by:

$$\mathrm{d}V_{r/r+\mathrm{d}r} = 2\pi r \mathrm{d}r w(r)\mathrm{d}t \qquad [5.22]$$

Substituting Eq. [5.21] into Eq. [5.22] results in:

$$\mathrm{d}V_{r/r+\mathrm{d}r} = \frac{\pi \mathrm{d}t}{2y(t,s)\eta}\left(P_{air} + \rho_w N_g g\, y(t,s) - \frac{2\sigma\cos\theta}{b}\right)(b^2 r\mathrm{d}r - r^3\mathrm{d}r) \qquad [5.23]$$

and integration between $r = 0$ and $r = b$ leads to:

$$\mathrm{d}V = \frac{\pi b^4 \mathrm{d}t}{8y(t,s)\eta}\left(P_{air} + \rho_w N_g g\, y(t,s) - \frac{2\sigma\cos\theta}{b}\right) \qquad [5.24]$$

When this volume element leaves the pore, the height of the liquid diminishes, which can expressed using:

$$\mathrm{d}V = -b^2\pi \mathrm{d}y \qquad [5.25]$$

Substituting Eq. [5.24] into Eq. [5.25] yields:

$$\mathrm{d}y = \frac{b^2}{8y(t,s)\eta}\left(\frac{2\sigma\cos\theta}{b} - \rho_w N_g g\, y(t,s) - P_{air}\right) dt \qquad [5.26]$$

Moreover, the introduction of the following three terms:

$$\zeta = \frac{2\sigma\cos\theta}{b\rho_w N_g g H} \qquad [5.27]$$

$$\beta = \frac{b^2\rho_w N_g g}{8\eta} \qquad [5.28]$$

$$X = \frac{P_{air}}{\rho_w N_g g H} \qquad [5.29]$$

leads to a simplified expression given by:

$$\mathrm{d}t = \frac{dy}{\left[\left(\zeta - X - \frac{y(t,s)}{H}\right)\beta\frac{H}{y(t,s)}\right]} \qquad [5.30]$$

Eq. [5.30] can be integrated to give:

$$t = -\frac{\frac{y(t,s)}{H} + (\zeta - X)\ln\left[\left(X + \frac{y(t,s)}{H} - \zeta\right)H\right]}{\frac{\beta}{H}} + C \qquad [5.31]$$

Since the drainage process starts with $y(t, s) = H$ at $t = 0$, it is possible to show that:

$$C = \frac{1 + (\zeta - X)\ln[(X + 1 - \zeta)H]}{\frac{\beta}{H}} \qquad [5.32]$$

Substituting Eq. [5.32] into Eq. [5.31] yields

$$\frac{\beta}{H}t = 1 - \frac{y(t,s)}{H} + (\zeta - X)\ln\left[\frac{1 + X - \zeta}{\frac{y(t,s)}{H} + X - \zeta}\right] \quad [5.33]$$

The well known Laplace equation (1806) was modified to calculate the equilibrium height, h_0, of a liquid in a pore of diameter s when air pressure was present, as follows:

$$h_0 = \frac{4\sigma\cos\theta}{\rho_w g N_g s} - \frac{P_{air}}{\rho_w g N_g} \quad [5.34]$$

Therefore, if the pore diameter is small enough to yield:

$$h_0 = \frac{4\sigma\cos\theta}{\rho_w g N_g s} - \frac{P_{air}}{\rho_w g N_g} > H \quad [5.35]$$

where H is the cake height, the liquid cannot be drained. So, there is a critical pore diameter, s^*

$$s^* = \frac{4\sigma\cos\theta}{\rho_w g N_g H + P_{air}} \quad [5.36]$$

below which the pores remain filled with the liquid. Comparing equations [5.27] and [5.34] shows that:

$$\zeta = \frac{4\sigma\cos\theta}{\rho_w g N_g s H} = \left(\frac{h_0}{H} + \frac{P_{air}}{\rho_w g N_g H}\right) \quad [5.37]$$

Finally, substituting equations [5.27], [5.28], [5.29] and [5.37] into Eq. [5.33] yields:

$$\frac{\beta}{H}t = 1 - \frac{y(t,s)}{H} + \frac{h_0}{H}\ln\left[\frac{1 + \frac{h_0}{H}}{\frac{y(t,s)}{H} - \frac{h_0}{H}}\right] \quad [5.38]$$

This equation gives the relationship between the momentary height, y, of the liquid column in a single pore with time t. Eq. [5.38] does not permit expressing y as an explicit function of t. Therefore, this equation was replaced by the following exponential equation that has the same functional form:

$$\frac{y(t,s)}{H} = \left(1 - \frac{h_0}{H}\right) e^{-\frac{\beta}{H}t} + \frac{h_0}{H} \quad [5.39]$$

Until this point, dewatering of a single pore has been considered. However, it is now possible to model dewatering of a total cake.

The model assumes that a centrifuge cake consists of two types of pores. The first type comprises the pores that cannot be drained at all, while the second type comprises all the other pores. The separation between these two types of pores is defined by the critical pore diameter, s^*, given by Eq. [5.36]. Assuming that pore diameters have a Boltzmann-type distribution, the following equation gives the size distribution of pores in a filter cake:

$$g(s) = \frac{2\varepsilon s}{\pi \hat{s}^4} e^{-\frac{1}{2}\left(\frac{s}{\hat{s}}\right)^2} \quad [5.40]$$

where:

$$\hat{s} = \sqrt{\frac{8K}{\varepsilon}} \quad [5.41]$$

The volume of the liquid contained in the first type pores for a cake with height H and area A can be expressed as:

$$V_R = \int_0^{s^*} g(s) \frac{s^2 \pi}{4} y(t,s) A ds \quad [5.42]$$

Substituting Eq. [5.40] into Eq. [5.42] yields:

$$V_R = \frac{\varepsilon A H}{2\hat{s}^4} \int_0^{s^*} s^3 e^{-\frac{1}{2}\left(\frac{s}{\hat{s}}\right)^2} ds \quad [5.43]$$

After integration and substituting Eq. [5.41] into Eq. [5.43], it can be shown that:

$$\frac{V_R}{\varepsilon A H} = 1 - \left[\frac{\varepsilon}{16K} s^{*2} + 1\right] e^{-\frac{\varepsilon}{16K} s^{*2}} \quad [5.44]$$

where $V_R/\varepsilon AH$ represents the residual saturation of the cake that cannot be drained.

Similarly, the volume of liquid contained in the second type of pores is expressed as:

$$V_E = \int_{s^*}^{\infty} g(s) \frac{s^2 \pi}{4} \frac{y(t,s)}{H} A ds \qquad [5.45]$$

Substituting Eq. [5.39] and Eq. [5.40] into Eq. [5.45] yields:

$$V_E = \frac{\varepsilon A H}{2\hat{s}^4} \int_{s^*}^{\infty} s^3 e^{-\frac{1}{2}\left(\frac{s}{\hat{s}}\right)^2} \left[\left(1 - \frac{h_0}{H}\right) e^{-\frac{\beta}{H}t} + \frac{h_0}{H} \right] ds \qquad [5.46]$$

Integration of this expression gives:

$$\frac{V_E}{\varepsilon A H} = \frac{I_1 - I_2 + I_3 - I_4}{2\hat{s}^4} \qquad [5.47]$$

where $V_E/\varepsilon AH$ represents the additional saturation that is not removed due to the limited amount of time available for drainage. The terms I_1 through I_4 are given by:

$$I_1 = \frac{1 + \left(\frac{\rho_w g N_g t}{32\eta H} + \frac{1}{2\hat{s}^2}\right) s^{*2}}{2\left(\frac{\rho_w g N_g t}{32\eta H} + \frac{1}{2\hat{s}^2}\right)^2} \left(1 + \frac{P_{air}}{\rho_w N_g g H}\right) e^{-\left(\frac{\rho_w g N_g t}{32\eta H} + \frac{1}{2\hat{s}^2}\right) s^{*2}} \qquad (5.48)$$

$$I_2 = \left(\frac{s^*}{2\left(\frac{\rho_w g N_g t}{32\eta H} + \frac{1}{2\hat{s}^2}\right)^2} e^{-\left(\frac{\rho_w g N_g t}{32\eta H} + \frac{1}{2\hat{s}^2}\right) s^{*2}} + \frac{\sqrt{\pi} Erfc\left(\sqrt{\frac{\rho_w g N_g t}{32\eta H} + \frac{1}{2\hat{s}^2}}\, s^*\right)}{4\left(\frac{\rho_w g N_g t}{32\eta H} + \frac{1}{2\hat{s}^2}\right)^{\frac{3}{2}}} \right) \frac{4\sigma \cos\theta}{\rho_w g N_g H} \qquad [5.49]$$

$$I_3 = \left(s^* \hat{s}^2 e^{-\frac{1}{2}\left(\frac{s}{\hat{s}}\right)^2} + \frac{\sqrt{\pi} Erfc\left(\sqrt{\frac{1}{2\hat{s}^2}}\, s^*\right)}{4\left(\frac{1}{2\hat{s}^2}\right)^{\frac{3}{2}}} \right) \frac{4\sigma \cos\theta}{\rho_w g N_g H} \qquad [5.50]$$

$$I_4 = \frac{1 + \frac{1}{2}\left(\frac{s^*}{\hat{s}}\right)^2}{2\left(\frac{1}{2\hat{s}^2}\right)^2} \left(\frac{P_{air}}{\rho_w N_g g H}\right) e^{-\frac{1}{2}\left(\frac{s^*}{\hat{s}}\right)^2} \qquad [5.51]$$

Finally, the total saturation of the cake can be calculated by adding residual and additional saturation values as follows:

$$\frac{V_T}{\varepsilon AH} = \frac{V_E}{\varepsilon AH} + \frac{V_R}{\varepsilon AH} \quad [5.52]$$

This total saturation value can be converted to a moisture value using Eq. [5.19].

5.4 Model Integration and Simulations

5.4.1 Empirical Dewatering Model Simulations

A simulation routine was setup in Microsoft Excel for the empirical model (see Figure 5.3) and was run using different size distributions of coal given in section 2.3.1.4 (see Table 5.2 and Table 5.3 for detailed size distributions). The routine was setup so that cake permeability could be calculated using different methods defined in the previous sections. Simulations were conducted with and without 200 kPa air injection at 500 and 2700 g's. Results obtained with the simulation routine were then compared to experimental results. All the input parameters used in these simulations are summarized in Table 5.1.

Table 5.1 Parameters used in empirical dewatering simulations

Parameter	Unit	Value
k_d	m^{-1}	400
ρ_s	kg/m^3	1400
ρ_w	kg/m^3	1000
ε	--	0.45-0.55
σ	N/m	0.072
μ	Pa.s	0.001
H	m	0.0085
t	s	120
N_g	--	500-2700
P_{air}	kPa	0-200
	(psi)	(0-30)
g	m/s^2	9.81
θ	°	60

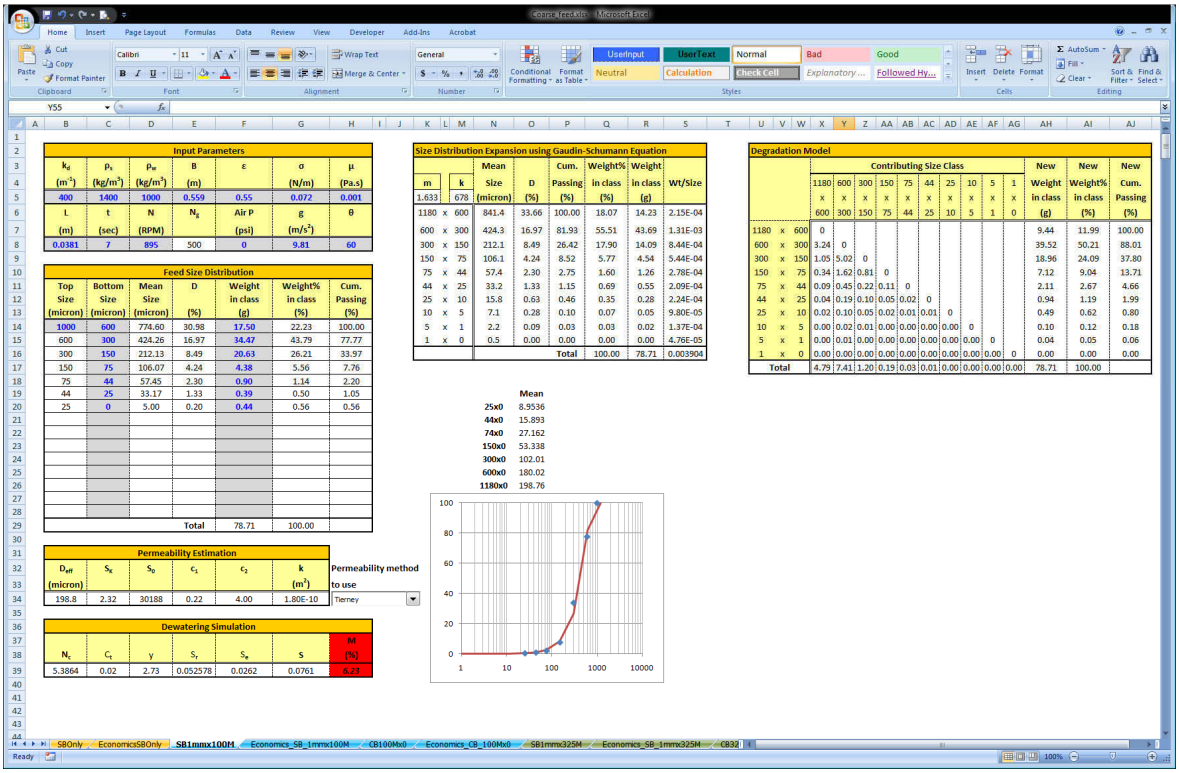

Figure 5.3 Empirical centrifugal dewatering model setup in Excel

Comparisons of simulation results to experimental results obtained at 500 and 2700 g's are given in Figure 5.4 and Tables 5.2 and 5.3. As can be seen, using permeability values calculated by different methods resulted in very similar results at both centrifugal acceleration levels. At 500 g's, very high coefficient of variation (R^2) values, which ranged from 0.996 to 0.998 without air injection and from 0.980 to 0.985 with air injection, obtained using different permeability value calculation methods. At 2700 g's, R^2 values obtained without air injection using permeability values calculated using different methods were identical (i.e. 0.926). However, these values ranged from 0.937 to 0.947 when air was used.

Table 5.2 Measured and predicted moisture values using three different permeability estimation methods at 500 g's

Mass (%)							Measured	Predicted Moistures (%)		
-1.18 mm	-0.6 mm	-0.3 mm	-0.15 mm	-0.075 mm	-0.044 mm	-0.025 mm	Moisture (%)	Panda et al.	Brown	Vidal et al.
(a) Without Air										
100	100	100	100	99.9	99.6	97.8	44.7	43.8	43.5	43.9
100	100	100	99.9	99.1	97.0	84.4	42.1	41.2	40.6	41.2
100	100	100	99.9	96.9	88.6	70.0	40.2	39.3	38.6	39.2
100	100	100	95.5	72.0	58.0	43.6	31.4	31.1	30.3	30.3
100	66.8	48.6	33.0	23.3	18.9	13.8	13.7	14.8	14.3	14.7
(b) With Air										
100	100	100	100	99.9	99.6	97.8	37.8	38.3	37.8	38.5
100	100	100	99.9	99.1	97.0	84.4	30.5	34.2	33.5	34.2
100	100	100	99.9	96.9	88.6	70.0	23.6	25.5	24.8	25.0
100	100	100	95.5	72.0	58.0	43.6	20.3	23.3	22.6	22.6
100	66.8	48.6	33.0	23.3	18.9	13.8	9.8	10.5	10.2	10.4

Table 5.3 Measured and predicted moisture values using three different permeability estimation methods at 2700 g's

Mass (%)							Measured	Predicted Moistures (%)		
-1.18 mm	-0.6 mm	-0.3 mm	-0.15 mm	-0.075 mm	-0.044 mm	-0.025 mm	Moisture (%)	Panda et al.	Brown	Vidal et al.
(a) Without Air										
100	100	99.7	99.6	99.5	99.1	97.2	40.0	35.5	34.9	35.4
100	100	99.9	99.6	98.7	95.6	85.3	32.1	31.5	31.5	31.5
100	100	99.5	96.1	86.4	77.6	63.3	28.3	26.8	26.8	26.8
100	100	99.7	98.3	86.3	74.7	55.5	24.5	21.5	21.5	21.5
100	100	99.5	92.8	76.6	66.3	52.4	21.7	23.0	23.0	23.0
100	99.9	97.9	83.7	62.6	52.7	40.0	18.8	18.6	18.6	18.6
100	97.2	81.6	57.8	43.4	35.6	27.7	14.8	15.5	15.5	15.5
100	88.7	65.4	44.7	31.5	26.3	20.0	11.0	12.5	12.5	12.5
(b) With Air										
100	100	99.7	99.6	99.5	99.1	97.2	27.2	32.5	32.5	32.5
100	100	99.5	96.1	86.4	77.6	63.3	23.7	24.3	24.3	24.3
100	100	99.7	98.3	86.3	74.7	55.5	22.1	21.4	21.4	21.4
100	100	99.9	99.6	98.7	95.6	85.3	21.4	27.3	27.3	27.3
100	100	99.5	92.8	76.6	66.3	52.4	19.8	20.6	20.6	20.6
100	100	97.9	83.7	62.6	52.7	40.0	16.1	16.5	16.5	16.5
100	97.2	81.6	57.8	43.4	35.6	27.7	12.0	13.7	13.7	13.7
100	88.7	65.4	44.7	31.5	26.3	20.0	9.6	11.0	11.0	11.0
100	68.4	49.2	34.1	24.2	20.5	15.9	8.0	9.0	9.0	9.0

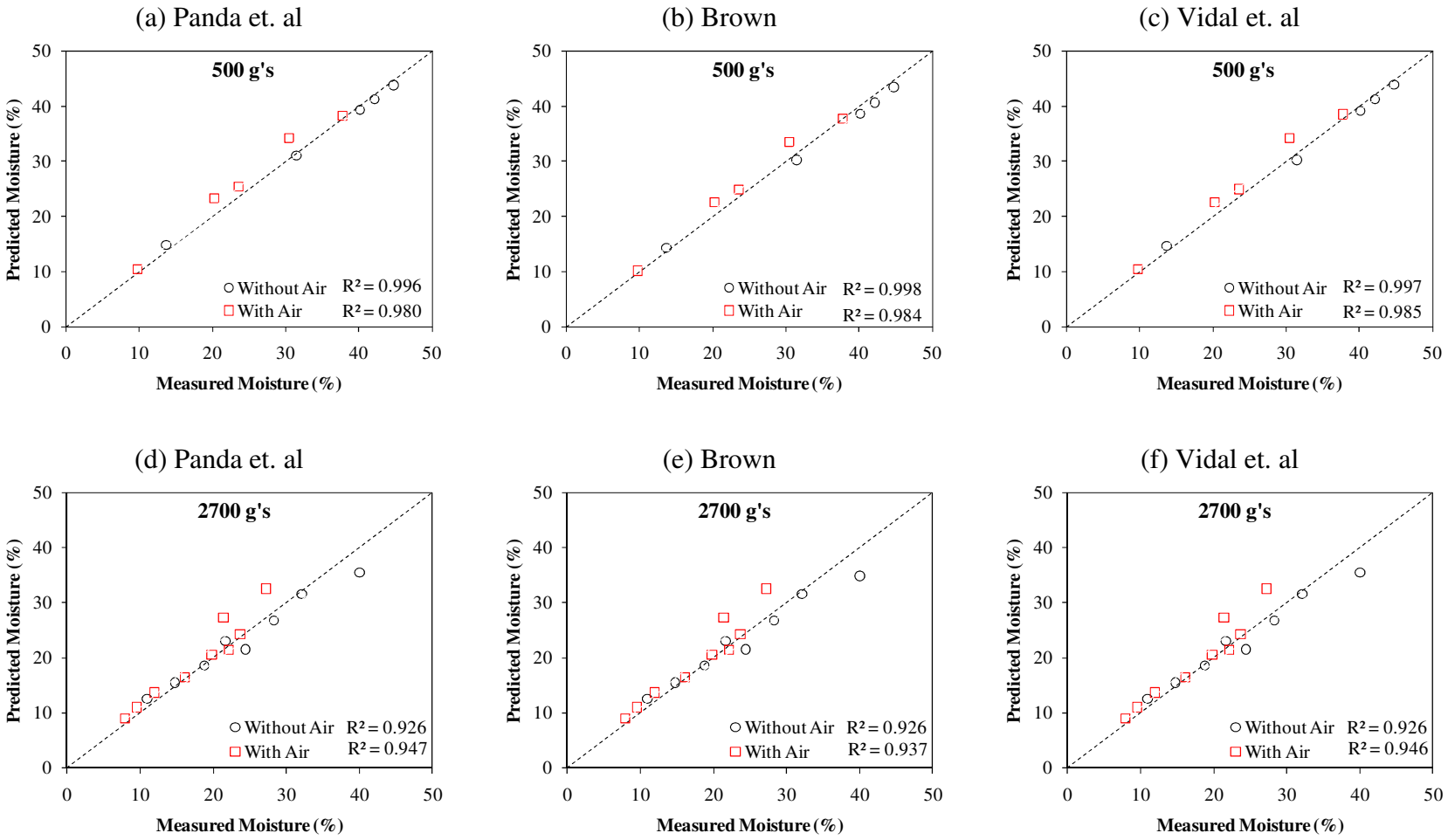

Figure 5.4 Comparison of empirical simulation results and measured moistures using three different methods of permeability calculation at 500 g's and 2700 g's

Another set of simulation runs were conducted to study the synergistic effect of air pressure and centrifugal acceleration on cake moistures. For this set of runs, a fine particle size distribution and a relatively coarse particle size distribution were chosen (see Table 5.4). Air pressure and centrifugal acceleration were varied between 0-400 kPa and 100-3000 g's, respectively, while all the other parameters were kept constant (see Table 5.5).

Table 5.4 Size distributions used in empirical dewatering simulations to study the synergistic effect of air pressure and centrifugal acceleration

Size (mm)	**Coal A (Mass, %)**	**Coal B (Mass, %)**
1.2 x 0.6	0.14	0.00
0.6 x 0.3	1.88	0.06
0.3 x 0.15	13.88	0.20
0.15 x 0.075	20.62	0.69
0.075 x 0.044	9.68	2.25
0.044 x 0.025	12.41	7.50
0.025 x 0	39.05	62.33

Table 5.5 Parameters used in empirical dewatering simulations to study the synergistic effect of air pressure and centrifugal acceleration

Parameter	**Unit**	**Value**
ρ_s	kg/m^3	1400
ρ_w	kg/m^3	1000
ε	--	0. 5
σ	N/m	0.072
μ	Pa.s	0.001
H	m	0.0085
t	s	120
N_g	--	100-3000
P_{air}	kPa	0-400
	(psi)	(0-60)
g	m/s^2	9.81
θ	°	60

Simulation results given in Table 5.6 and Table 5.7 showed that, as expected, for both coarse and fine coals, the highest moisture value would be obtained at the lowest g level without air injection and the lowest moisture value would be obtained at the highest g level with air injection. Moreover, it would be possible to avoid using higher g levels to achieve lower moisture values by application of more air pressure. For example, using 200 kPa of air pressure at 500 g's would produce the same moisture content as 3000 g's would produce without air pressure for both coarse and fine cakes (values highlighted in Table 5.6 and Table 5.7). Experimental results discussed in section 2.3.1.4 that were run at 500 g's and 2700 g's also confirmed this conclusion. In those tests, using 200 kPa air pressure at 500 g's had produced similar moistures to the ones obtained at 2700 g's without air pressure.

Table 5.6 Moisture values obtained with coal A using empirical dewatering simulations at different air pressures and centrifugal accelerations

P_{air} (kPa)\g's	100	300	500	1000	2000	3000
0	32.4	27.4	25.1	22.2	19.6	18.2
67	22.5	21.8	21.1	19.9	18.4	17.4
133	20.1	19.7	19.3	18.6	17.6	16.8
200	18.7	18.4	18.2	17.7	16.9	16.3
267	17.8	17.6	17.4	17.0	16.4	15.9
333	17.1	16.9	16.8	16.5	16.0	15.5
400	16.5	16.4	16.3	16.1	15.6	15.2

Table 5.7 Moisture values obtained with coal B using empirical dewatering simulations at different air pressures and centrifugal accelerations

P_{air} (kPa)\g's	100	300	500	1000	2000	3000
0	40.5	38.7	37.4	35.2	32.7	31.1
67	35.5	34.8	34.2	33.0	31.3	30.1
133	33.2	32.7	32.4	31.6	30.3	29.4
200	31.7	31.4	31.1	30.5	29.5	28.7
267	30.6	30.4	30.2	29.7	28.9	28.2
333	29.7	29.6	29.4	29.0	28.3	27.7
400	16.5	16.4	16.3	16.1	15.6	15.2

The next set of simulation runs were conducted to do a sensitivity analysis of different parameters that were used in the empirical model. The first step of the sensitivity analysis was to establish a baseline moisture value by running the empirical simulation routine using average values of all the input parameters. New moisture values were then predicted by changing each input parameter value by ±10%. Finally, the percent change of the baseline moisture was calculated for each parameter using the new moisture values. Therefore, this study was conducted to determine the magnitude of the influence of different input parameters on moisture prediction of the empirical model.

The results of the sensitivity analysis given in Table 5.8 showed that the most influential parameter was the cake porosity, as a 10% increase in the porosity caused a 16.9% increase in the moisture and a 10% decrease caused a 15.4% decrease in moisture. Moreover, increasing cake thickness by 10% increased the moisture content by 2.7%, while the moisture decreased by 3.0% with a 10% decrease in cake thickness. While the rest of the parameters had similar magnitudes of effects, changing surface tension and contact angle had very small effect on moisture. However, as it was explained in section 1.1.2.2, it is a known fact that lower moisture values can be achieved by adjusting surface tension and contact angle values using dewatering

Table 5.8 Magnitude of change in moisture caused by each parameter

Inputs	Baseline values of parameters	% ΔMoisture with +10% change	% ΔMoisture with -10% change
ε	0.5	16.9	-15.4
σ	0.072	0.0	0.0
μ	0.001	1.6	-1.7
L	0.0127	2.7	-3.0
t	60	-1.5	1.7
N_g	500	-0.4	0.4
Pair	30	-1.2	1.3
θ	60	0.0	0.0
K	10^{-14}	-1.5	1.7

chemicals in accordance with filtration laws. Even though surface tension and contact angle values are included in Eq. [5.4], which is used to calculate the capillary number, these values are rendered ineffective when the capillary number is divided by the value of 91.3 in Eq. [5.7], since the value of the capillary number was usually much lower than 91.3. Therefore, this was found to be one of the shortcomings of the empirical model and further investigation of this shortcoming is suggested for future work.

The final set of simulation runs were conducted to provide a more detailed look at the effects of different parameters on moisture. The results of these runs are shown in Figures 5.5 - 5.11. Since the sensitivity analysis showed that contact angle and surface tension values had very small effects on moisture when the empirical model was used, these parameters were not included in the figures.

It was observed from these plots that the porosity and the moisture content had a straight line relationship, while the correlation of the moisture with other parameters was more in a logarithmic fashion. It was also observed that an increase in porosity, cake thickness and viscosity values caused the moisture content to increase, while an increase in centrifugal acceleration, air pressure, permeability and time values caused the moisture content to decrease. Moreover, as it was observed with the sensitivity analysis, Figure 5.10 and Figure 5.11 showed that increasing air pressure caused a bigger drop of moisture than it was caused by increasing centrifugal acceleration.

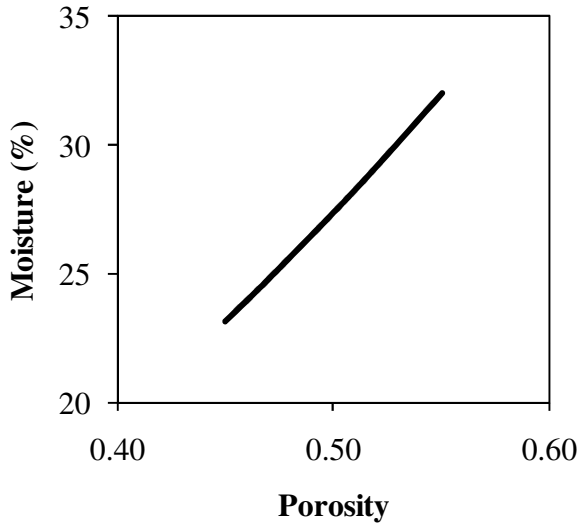

Figure 5.5 Effect of porosity on moisture with empirical model

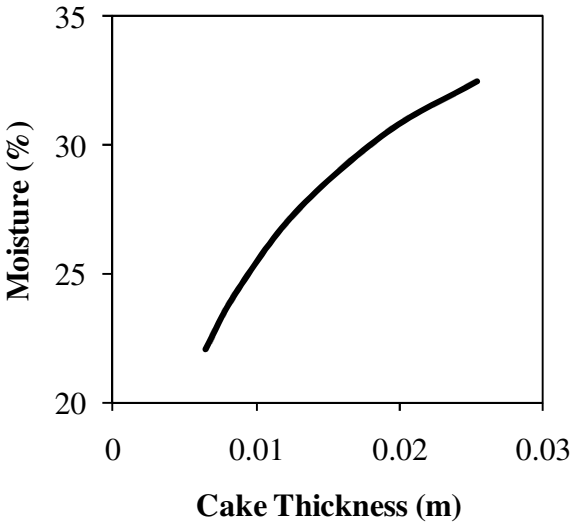

Figure 5.6 Effect of cake thickness on moisture with empirical model

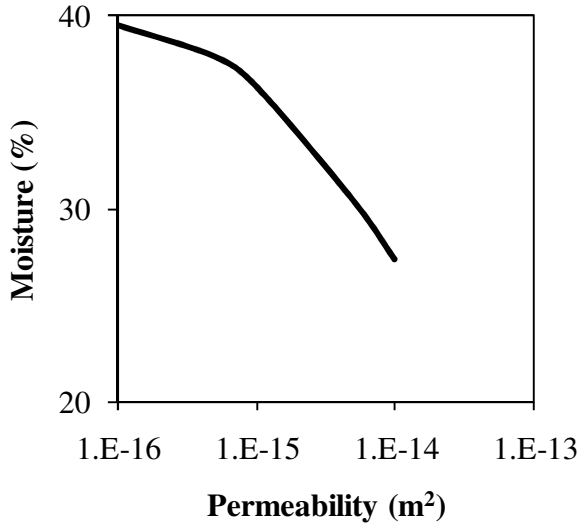

Figure 5.7 Effect of permeability on moisture with empirical model

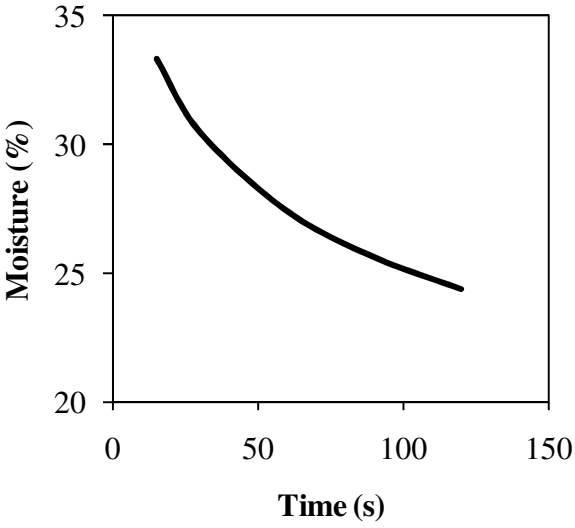

Figure 5.8 Effect of rotation time on moisture with empirical model

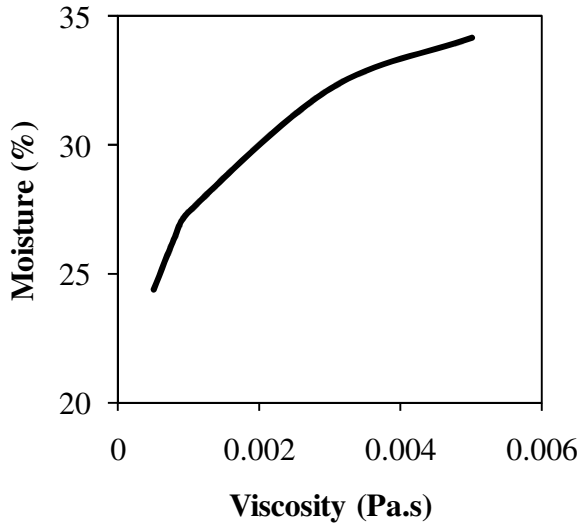

Figure 5.9 Effect of viscosity on moisture with empirical model

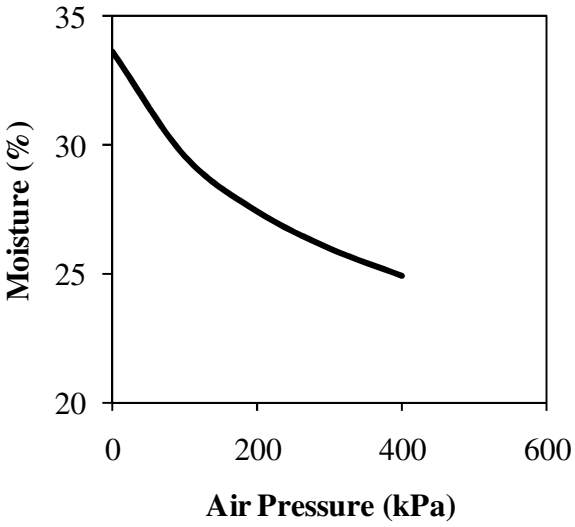

Figure 5.10 Effect of air pressure on moisture with empirical model

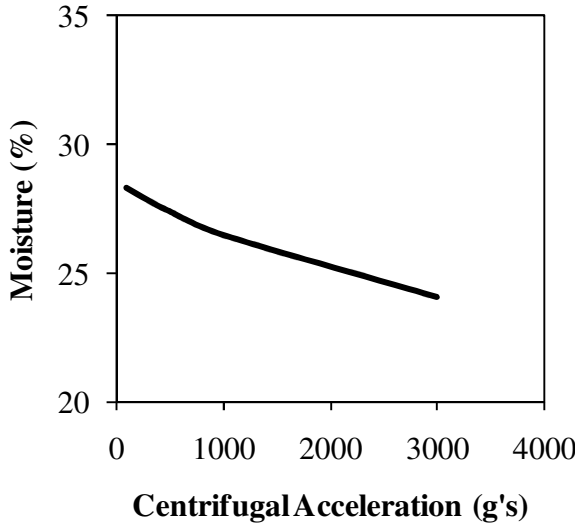

Figure 5.11 Effect of centrifugal acceleration on moisture with empirical model

5.4.2 Theoretical Dewatering Model Simulations

A simulation routine for the theoretical dewatering model was setup in Microsoft Excel using equations described in section 5.4 and was run using the same set of coals and parameters that were used to run the empirical dewatering model. Simulations were conducted with and without 200 kPa air injection at 500 and 2700 g's. Results obtained with simulation routine were then compared to experimental results. All the input parameters used in these simulations are given in Table 5.9.

Table 5.9 Parameters used in dynamic dewatering simulations

Parameter	Unit	Value
ρ_s	kg/m^3	1400
ρ_w	kg/m^3	1000
ε	--	0.45-0.55
σ	N/m	0.072
μ	Pa.s	0.001
H	m	0.0085
t	s	120
N_g	--	500-2700
P_{air}	Pascal	0-206,843
	(psi)	(0-30)
g	m/s^2	9.81
θ	°	60

Conducting simulations using this theoretical model revealed serious issues related to the model. As can be seen from the charts given in Figure 5.12, predicted values were mostly off and did not match the experimental results. The model was able to predict relatively accurate moistures at 2700 g's without air injection with a low R^2 value of 0.794. However, all the other simulations conducted at different conditions (i.e. 500 g's with and without air and 2700 g's with air), produced negative R^2 values, which showed that there was no correlation between predicted and measured values. The model had difficulty with producing decent results, especially with

coarser cakes when air pressure was applied. As can be seen in Tables 5.10 and 5.11, it was not even possible to make any predictions for some of the cakes. The best estimations were obtained at 2700 g's without air injection.

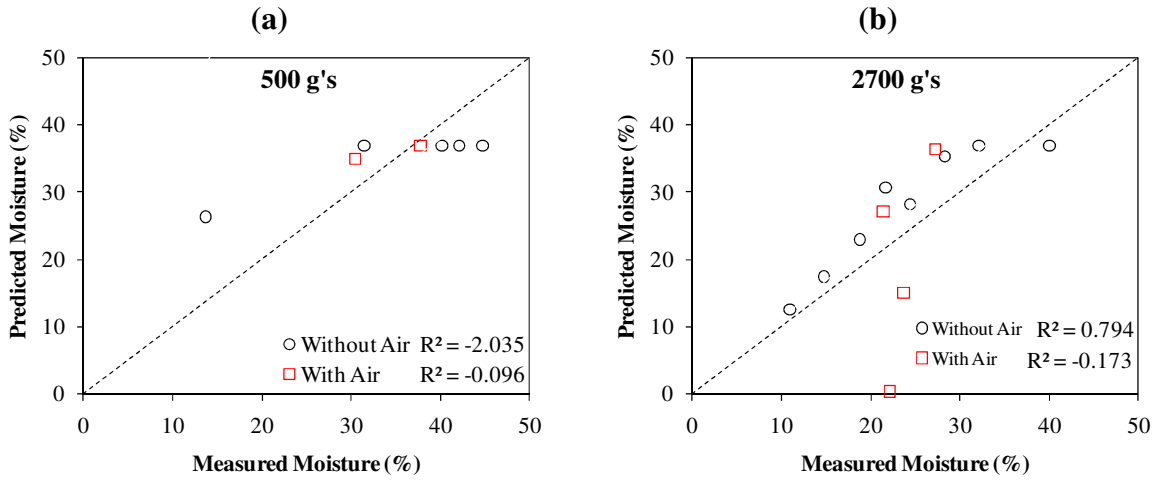

Figure 5.12 Comparison of predicted moistures to measured moistures at (a) 500 g's and (b) 2700 g's using the theoretical dewatering model

Table 5.10 Measured and predicted moisture values using the theoretical dewatering model at 500 g's

Mass (%)							Measured Moisture (%)	Predicted Moisture (%)
-1.18 mm	-0.6 mm	-0.3 mm	-0.15 mm	-0.075 mm	-0.044 mm	-0.025 mm		
(a) Without Air								
100	100	100	100	99.9	99.6	97.8	44.7	36.9
100	100	100	99.9	99.1	97.0	84.4	42.1	36.9
100	100	100	99.9	96.9	88.6	70.0	40.2	36.9
100	100	100	95.5	72.0	58.0	43.6	31.4	36.9
100	66.8	48.6	33.0	23.3	18.9	13.8	13.7	26.3
(b) With Air								
100	100	100	100	99.9	99.6	97.8	37.8	36.9
100	100	100	99.9	99.1	97.0	84.4	30.5	34.9
100	100	100	99.9	96.9	88.6	70.0	23.6	N/A
100	100	100	95.5	72.0	58.0	43.6	20.3	N/A
100	66.8	48.6	33.0	23.3	18.9	13.8	9.8	N/A

Table 5.11 Measured and predicted moisture values using three different permeability estimation methods at 2700 g's

Mass (%)							Measured	Predicted
-1.18 mm	-0.6 mm	-0.3 mm	-0.15 mm	-0.075 mm	-0.044 mm	-0.025 mm	Moisture (%)	Moisture (%)
(a) Without Air								
100	100	99.7	99.6	99.5	99.1	97.2	40.0	36.9
100	100	99.9	99.6	98.7	95.6	85.3	32.1	36.9
100	100	99.5	96.1	86.4	77.6	63.3	28.3	35.2
100	100	99.7	98.3	86.3	74.7	55.5	24.5	28.2
100	100	99.5	92.8	76.6	66.3	52.4	21.7	30.6
100	99.9	97.9	83.7	62.6	52.7	40.0	18.8	22.9
100	97.2	81.6	57.8	43.4	35.6	27.7	14.8	17.4
100	88.7	65.4	44.7	31.5	26.3	20.0	11.0	12.5
(b) With Air								
100	100	99.7	99.6	99.5	99.1	97.2	27.2	36.4
100	100	99.5	96.1	86.4	77.6	63.3	23.7	15.1
100	100	99.7	98.3	86.3	74.7	55.5	22.1	0.39
100	100	99.9	99.6	98.7	95.6	85.3	21.4	27.1
100	100	99.5	92.8	76.6	66.3	52.4	19.8	N/A
100	100	97.9	83.7	62.6	52.7	40.0	16.1	N/A
100	97.2	81.6	57.8	43.4	35.6	27.7	12.0	N/A
100	88.7	65.4	44.7	31.5	26.3	20.0	9.6	N/A
100	68.4	49.2	34.1	24.2	20.5	15.9	8.0	N/A

Another set of simulation runs were conducted to study the effect of different parameters on cake moistures with the theoretical dewatering model. For this purpose, the case that produced the best correlation before (i.e. 2700 g's without air injection) was chosen as the baseline case. While keeping all the other parameters constant, value of only one parameter was changed at a time to demonstrate the effect of that parameter on the cake moisture.

The simulation results given in Figure 5.13 showed that although most of the parameters used in the theoretical dewatering model would affect the kinetics of centrifugal dewatering in an expected way, the predicted equilibrium moistures were unreasonable. Model predictions showed that changing the cake permeability would affect dewatering kinetics immensely.

However, when significantly lower permeability values were used, the model's moisture predictions were as low as 0%. Moreover, increasing contact angle, centrifugal acceleration and air pressure values and decreasing surface tension of the liquid also produced faster dewatering kinetics and lower equilibrium moistures, but again some of the moisture predictions were as low

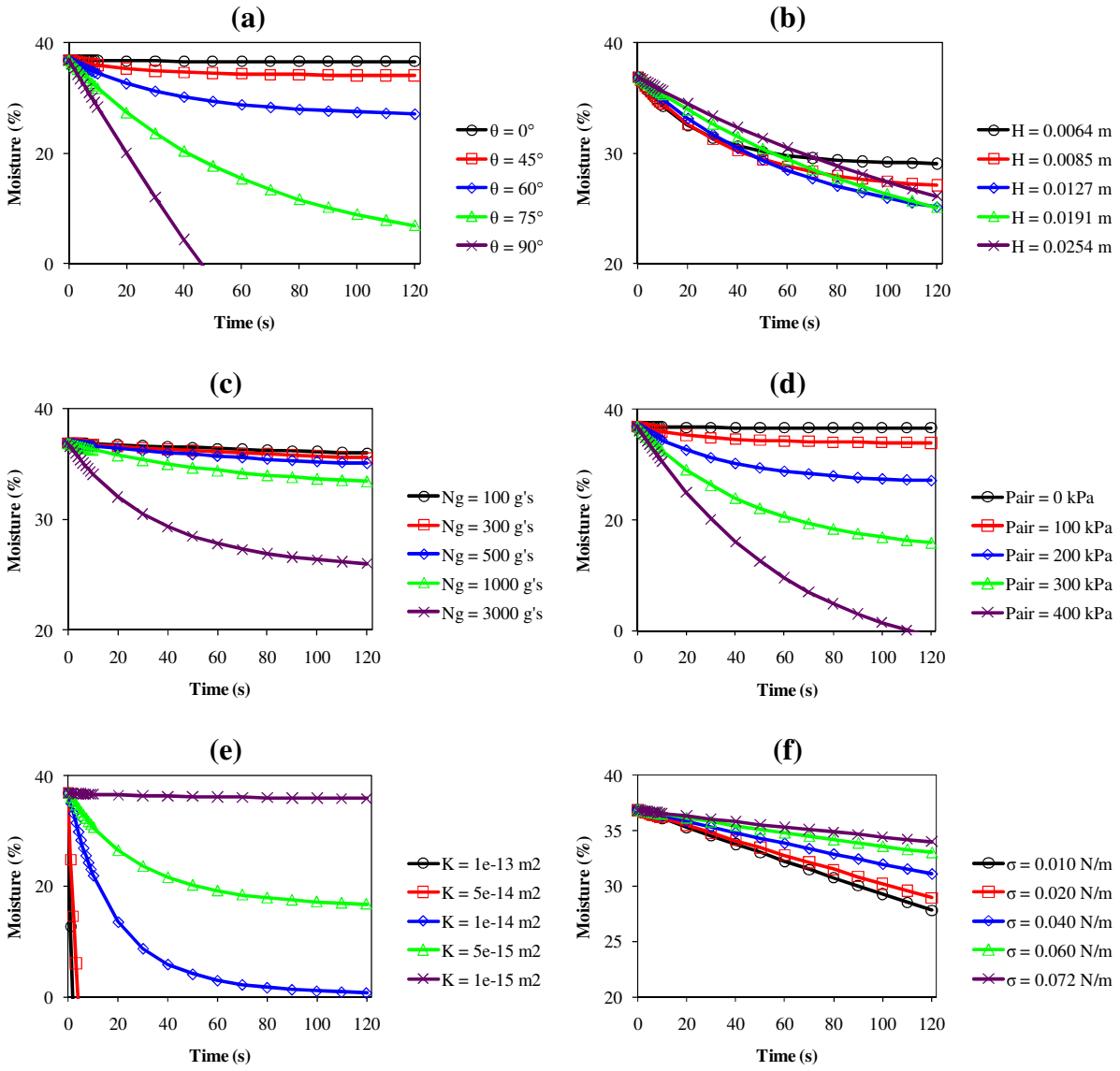

Figure 5.13 Effect of (a) contact angle, (b) cake thickness, (c) centrifugal acceleration, (d) air pressure, (e) cake permeability and (f) liquid surface tension on moisture with theoretical dewatering model

as 0%. Furthermore, according to the model, the equilibrium moisture content first decreased while the cake thickness increased from 0.0064 m to 0.0127 m. However, after this point the moisture increased with increased cake thickness.

As a result, it was concluded that there was a fundamental problem with this model, which could not be solved. While the effects of different parameters on cake moistures were generally reasonable, the equilibrium moisture predictions were unreasonable. An investigation directed at improving the theoretical model is suggested as a topic for future research.

5.5 Mechanical Degradation

Mechanical degradation of particles is unavoidable in centrifugation due to the forces involved in this process. This effect was not taken into consideration when the empirical and theoretical model simulations given in previous sections were conducted, because those size distributions were obtained from products of real HFC tests, which were already degraded. However, it is essential to use a degradation model when dealing with feed size distributions, i.e. size reduction of the feed inside a centrifuge has to be taken into account before any attempt to model centrifugal dewatering process.

Lyons (1951) did a systematic study of mechanical degradation and he found out that larger particles were subject to size reduction more than finer particles. He also found out that the size distribution of newly created fine particles was similar to the ones already existed in the feed.

Particles existing in the feed stream of a centrifuge can be divided into n size ranges, where size 1 is the coarsest size fraction and size n is the finest. It is assumed that the fraction of size class i that can be degraded is linearly related to the average particle size by the following relation:

$$D_i = k_d A_i;\ 0 < D_i < 0.9 \quad [5.53]$$

where D_i is the fraction of size class i degraded, A_i is the average particle size of the size class i and k_d is a parameter unique to the equipment. Tierney and Gottfried (1983) reported that an average k_d value of 98.4 m^{-1} can be used for most centrifuges. However, when simulations given in the following sections were conducted, it was observed that a k_d value of 400 m^{-1} was required to match data from commercially available centrifuges. Therefore, a value of 400 m^{-1} was used for all the empirical simulations conducted in the present work.

The degraded fraction of size class i, given by D_i, is distributed among all size classes that are finer than the size class i, in proportion to the fractions of these size classes in the feed. Moreover, the distribution will be different for each gravity class j. Therefore, the contribution to size class p ($p > i$) due to the degradation of size class i in gravity class j is given by:

$$G_{p,i,j} = F_{i,j} D_i F_{p,j} \Big/ \sum_{k=i+1}^{n} \left(F_{k,j}\right) \quad [5.54]$$

where $F_{i,j}$ is the weight fraction of feed in size class i and gravity class j before degradation. The total contribution to size p from each size class coarser than p can be obtained by summing all $G_{p,i,j}$ values from i = 1 to p - 1. The corrected fraction of feed in size class p and gravity class j after degradation can be determined by adding the summation of $G_{p,i,j}$ values to amount that was not degraded in size class p.

$$F^*_{p,j} = \sum_{i=1}^{p-1} \left(G_{p,i,j}\right) + \left(1 - D_p\right) F_{p,j} \quad [5.55]$$

5.6 Conclusions

An empirical dewatering model and a theoretical dewatering model were developed to describe the process of dewatering during hyperbaric centrifugation. While very accurate results

were obtained using the empirical model, the theoretical model had difficulty in predicting accurate product moistures, which suggested that attempts to precisely model a complicated system such as a filter cake using theoretical equations might lead to inaccurate results due to the vast number of unknowns and assumptions. Consequently, only the empirical model is recommended for predicting the equilibrium moistures obtained during hyperbaric centrifugation.

NOMENCLATURE

A:	Surface area of filter cake, m^2	S_0:	Specific surface area defined by Eq. [5.15]
A_i:	Average size, mean of upper and lower mesh sizes, m	S_K:	Skewness of the particle size distribution
b:	Radius of a capillary, m	S_r:	Residual Saturation
c_1, c_2:	Fitting parameters used in Eq. [5.14]	S_e:	Effective Saturation
C_{DP}:	Coefficient of variation	s:	Diameter of a capillary, m
C_t:	Defined by Eq. [5.10]	s^*:	Critical pore diameter, m
D_i:	Fraction of particles of size i which is degraded	$\hat{s}$:	Predominant pore diameter, m
D_p:	Particle diameter, m	t:	Time, s
$F_{i,j}$ $F^*_{i,j}$:	Weight fraction of feed in size range i and gravity range j before and after degradation	V_R:	Volume of water that cannot be removed from the filter cake, m^3
$g(s)$:	Pore size distribution function	V_E:	Volume of water that is not removed from the filter cake due to time limitation, m^3
g:	Gravitational acceleration, m/s^2	y:	Dimensionless parameter defined by Eq. [5.17]
$G_{p,i,j}$:	Fraction of feed size i and gravity j which appears in size p after degradation	$y(t,s)$:	Momentary height of liquid in a capillary with diameter s at time t, m
h_0:	Equilibrium height of a liquid in a pore, m	η:	Viscosity of the liquid, Pa.s
H:	Cake thickness, m	ρ_w, ρ_s:	Density o water and solids, kg/m^3
k_d:	Degradation constant, dimensionless	σ:	Surface tension of liquid, N/m
K:	Permeability of filter cake, m^2	θ:	Contact angle
N_c:	Capillary number, dimensionless	ε:	Porosity or the void fraction
N_g:	Number of g's	τ:	Tortuosity of particles
P_{air}:	Air pressure, kPa	ζ:	Parameter defined by Eq. [5.27]
P:	Pressure, Pa	β:	Parameter defined by Eq. [5.28]
r:	Radius coordinate starting at the pore axis, m	X:	Parameter defined by Eq. [5.29]
S:	Total Saturation		

5.7 References

1. Brown, G. G., & Associates. (1950). *Unit Operations*: Wiley.
2. Brownell, L. E., & Katz, D. L. (1947). Flow of Fluids Through Porous Media - Part II. *Chemical Engineering Progress, 43*(11), 601-612.
3. Dombrowski, H. S., & Brownell, L. E. (1954). Residual Equilibrium Saturation of Porous Media. *Industrial Engineering Chemistry, 46*(6), 1207-1219.
4. Haruni, M. M., & Storrow, J. A. (1953). Hydroextraction VII: Residual Moisture in Whizzed Cakes. *Chemical Engineering Science, 2*, 203-212.
5. Lyons, O. R. (1951). An Approximate Method of Predicting and Comparing Expected Results When Dewatering Coal by Centrifuge. *Transactions AIME, Mining Engineering, 191*, 417-425.
6. Panda, M. N., & Lake, L. W. (1994). Estimation of single-phase permeability from parameters of particle-size distribution. *American Association of Petroleum Geologists Bulletin, 78*(7), 1028-1039.
7. Swindells, R. J., & White, E. T. (1979). *Drainage of Molasses from Sugar Crystals in a Continuous Centrifuge.* Paper presented at the Seventh Australian Conference on Chemical Engineering.
8. Tierney, J. W., & Gottfried, B. S. (1983). A Simulator for Dewatering of Coal Fines. *Proceedings of the First Conference on Use of Computers in the Coal Industry*, 230-236.
9. Vidal, D., Ridgway, C., Pianet, G., Schoelkopf, J., Roy, R., & Bertrand, F. (2009). Effect of particle size distribution and packing compression on fluid permeability as predicted by lattice-Boltzmann simulations. *Computers and Chemical Engineering, 33*, 256-266.

10. Wakeman, R. J., Rushton, A., & Brewis, L. N. (1976). Residual Saturation Of Dewatered Filter Cakes. *Chemical Engineer-London*(314), 668-670.
11. Zeitsch, K. (1990). Centrifugal Filtration. In L. Svarovsky (Ed.), *Solid-Liquid Separation* (3 ed.). London; Boston: Butterworths.

CHAPTER 6 ECONOMICS OF FINE COAL DEWATERING

6.1 Introduction

Modern coal preparation plants typically incorporate a series of sequential unit operations for sizing, cleaning, and dewatering. This sequence of steps is repeated for each size fraction. This subdivision is necessary since the cleaning processes used in modern plants have a limited range of applicability in terms of particle size. As a result, modern plants may include as many as four separate processing circuits for treating the coarse (plus 50 mm), small (50 x 1 mm), fine (1 x 0.15 mm), and ultrafine (minus 0.15 mm) material.

In the U.S., coarse and small size coal is typically cleaned using dense medium processes such as vessels and cyclones. The coarser products are dewatered using screens, while smaller coal is dewatered using centrifugal dryers. Fine coal is usually upgraded using water-based density separators such as spirals and water-only cyclones. Ultrafine coal is either cleaned using froth flotation or discarded as waste. The fine and ultrafine coal products are dewatered using various combinations of centrifugal dryers, screenbowl centrifuges and/or filters. After dewatering, the clean coal products from the parallel circuits are usually blended together prior to shipment to market.

An important task for plant managers is to select operating points for each plant process to ensure that the coal products from the plant meet quality criteria dictated by sales contracts. These specifications may include limits on ash, sulfur, moisture, heat content, or other quality indicators. Unfortunately, plant operators often choose set points that provide an identical clean coal quality in every plant circuit. As discussed later, operation of all circuits at a constant

product quality typically does not optimize plant yield. Moreover, managers are often forced to select set points that are less than ideal for a given coal due to contractual limitations that may or may not be justified from economic considerations. A mismatch between the inherent cleanability of a given coal (including its tendency to retain moisture) and the specifications in a sales contract can substantially lower overall plant yield and overall profitability.

6.2 Plant Optimization

6.2.1 Optimization by Constant Incremental Ash

Many articles in the technical literature advocate the use of simulation routines to identify optimum set points for processes used in coal preparation plants (Peng and Luckie, 1991; King, 1999). Such data are used to determine the total plant yield and clean coal quality that may be obtained for any combination of operating points. The optimum points are those that provide the highest total plant yield at the desired target quality. However, the simulations require detailed data describing the washability of the feed coals and empirical and/or theoretical partition data describing the separating capabilities of the cleaning equipment. Unfortunately, the lack of such detailed data makes this approach impractical to implement in modern facilities. This trial-and-error approach also provides little insight regarding the underlying principles that control the optimization process.

A more attractive method for plant optimization is to employ constant incremental ash. This concept, which has long been recognized in coal preparation (Mayer, 1950; Dell, 1956; Abbott, 1981; Rayner, 1987), states that the clean coal yield for parallel operations is highest when all circuits are operated at the same incremental ash. This statement is true for any number of parallel circuits and is independent of the size and washability characteristics of the feed coal. Mathematical proof of the incremental ash concept has been done by Luttrell et al. (2003).

However, the fundamental basis for this concept can be easily demonstrated using the simple illustrations provided in Figure 6.1(a) and Figure 6.1(b). In each diagram, the same two feed streams ("A" and "B") are to be treated. The two feeds may represent coal fed to two different cleaning operations in the same plant, the streams fed to two different plants that both service the same customer, or the same cleaning unit at two different points in time. The feed coals are comprised of various amounts of carbonaceous matter (black) and ash-bearing matter (gray). In this example, the washability of Feed "A" makes it relatively easy to upgrade since most of the particles are well liberated. In contrast, Feed "B" has a difficult washability due to the presence of a large percentage of middlings (composite) particles.

Figure 6.1(a) shows the result that is obtained when the separation is conducted to

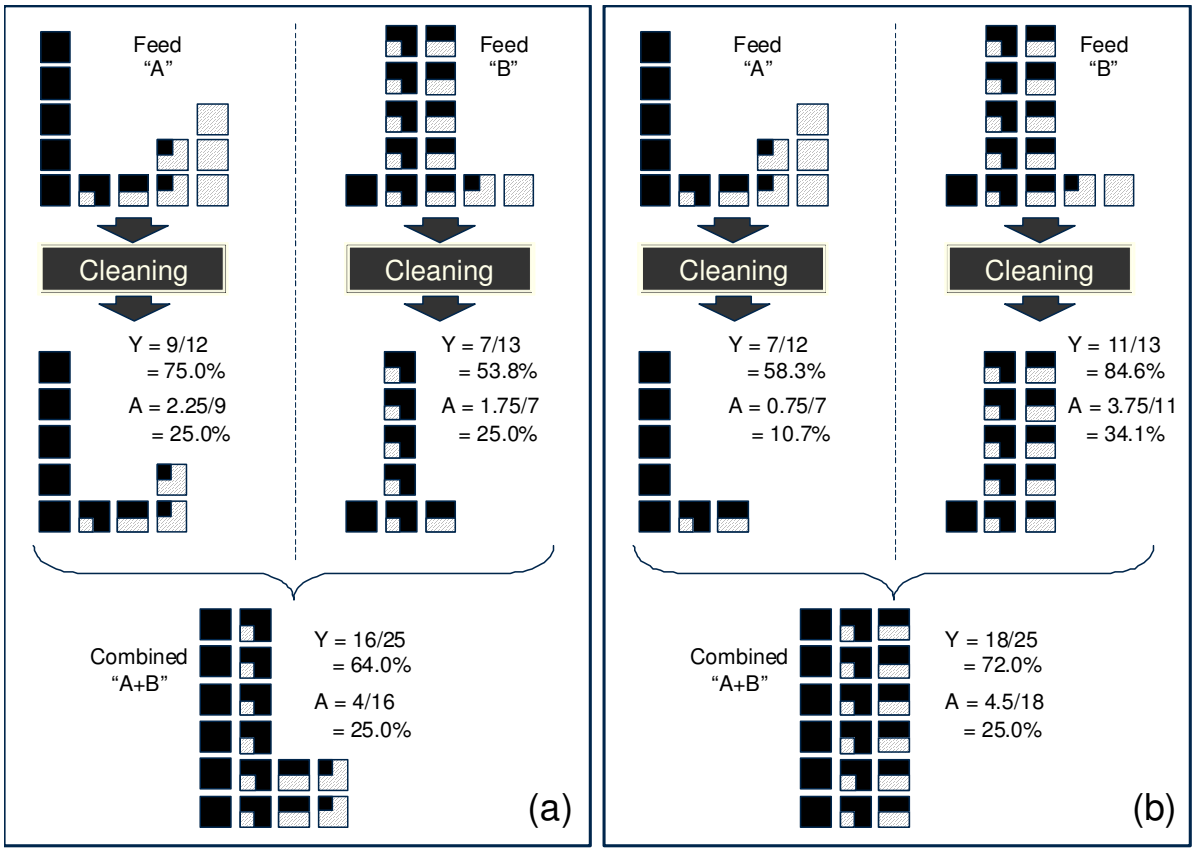

Figure 6.1 Clean coal products obtained by (a) treating parallel streams at constant cumulative ash and (b) treating parallel streams at constant incremental ash

provide a target ash content of 25% for both streams. For Feed “A”, the operating point is raised from left to right until a total of 9 units (blocks) are recovered out of a total of 12 units. This operating point produces a yield of 75% (i.e., 9/12=75%) at the desired target ash of 25% (i.e., 2.25/9 = 25%). For Feed “B”, a yield of only 53.8% (i.e., 7/13=53.8%) can be realized before the target ash of 25% (i.e., 1.75/7=25%) is exceeded. The lower yield is due to the poorer liberation of Feed “B”. The clean products from these two streams are blended together to produce a combined yield of 64% at the desired target ash of 25%. At first inspection, this appears to be an acceptable result since the target grade is met. However, a closer examination shows that particles containing 75% ash reported to clean coal when treating Feed “A”, while at the same time many particles containing just 50% ash were discarded when treating Feed “B”. This combination is obviously not optimum since higher quality particles were discarded so that poorer quality particles could be taken.

The incremental ash concept dictates that maximum yield can only be obtained when the ash content of the last unit recovered from each feed stream is identical. To test this principle, the feed streams shown in Figure 6.1(b) are each separated so that the last unit recovered in both cases contained 50% ash. This combination of operating points decreased the ash content of Feed “A” to 10.7% and increased the ash content of Feed “B” to 34.1%. However, when the two streams are blended together, the combined clean coal product still meets the required target ash of 25%. More importantly, this new set of operating points provides a higher combined yield (i.e., 72% versus 64%). In fact, separation at a constant incremental ash will always provide the maximum yield of coal at a given ash content.

6.2.2 Incremental Ash and Specific Gravity

Incremental ash is a mathematical term that cannot be directly monitored in operating industrial plants. However, this value can be estimated for ideal separations. This approximation assumes that the particles in run-of-mine coals contain only two components, i.e., a low-density ash-free carbonaceous component and a high-density pure-ash mineral component. Under this assumption, the ash content of an individual particle must increase linearly with the reciprocal of the composite particle density (ρ) according to the expression:

$$Ash(\%) = \frac{100}{\rho_c - \rho_a}\left[\frac{\rho_c + \rho_a}{\rho} + \rho_a\right] \qquad [6.1]$$

where ρ_c and ρ_a are the densities of the light (carbonaceous) and dense (ash bearing) components, respectively (Abbot and Miles, 1990). The utility of this expression can be demonstrated by the data shown in Figure 6.2. This illustration shows the ash contents of narrowly partitioned density fractions obtained from experimental float-sink tests conducted on six different size fractions of a run-of-mine coal. For particles coarser than 0.6 mm, the data show that the same individual ash is obtained for any specific gravity regardless of the size fraction treated. The deviation noted for the fractions finer than 0.6 mm can normally be attributed to inefficiencies in the experimental float-sink procedures at finer particle sizes. In any case, plant optimization requires that all parallel circuits be operated at the same incremental

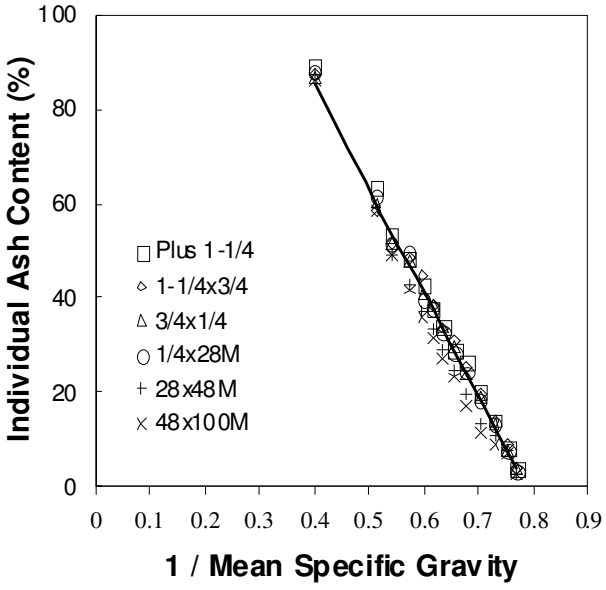

Figure 6.2 Relationship between specific gravity and individual ash content of different size classes

ash. Since Eq. [6.1] shows that incremental ash is fixed by specific gravity, this implies that total plant yield is maximized when all parallel circuits are operated at the same specific gravity cutpoint (Clarkson, 1992). This statement is true regardless of the size distribution or washability characteristics of the feed coal, provided that very efficient separations are maintained in each circuit. If the separation is less efficient (which is typical of fine coal separators), a correction must be made to account for the impacts of misplaced material on the incremental quality. This correction generally requires that less efficient units be operated at a slightly higher specific gravity cutpoint (Luttrell et al., 2003).

6.2.3 Effect of Moisture on Optimization

The incremental ash approach to plant optimization works well for processing metallurgical coals where ash is the primary quality specification. Unfortunately, most coal is sold in the steam (utility) market where other quality specifications are also important (e.g. moisture, heat content, etc.). In particular, the combined ash and moisture content of a coal is very important in this market since this sum dictates the heat content of the coal. Therefore, in the case of steam market, optimization requires that the "incremental value" of the coal be held constant. In other words, the market value of the next particle of coal recovered should be the identical for all circuits. As such, the incremental value concept includes not only incremental ash, but also incremental moisture and, if appropriate, other incremental values that impact the monetary value of the coal product (e.g., sulfur). The inclusion of moisture in the incremental value approach typically dictates that density cutpoints for operations treating coarser particles be set higher than the density cutpoints used to treat finer particles. This difference is due to the fact that moisture content increases (and coal value decreases) as the particle becomes finer. As

can be seen from the following example, the increased moisture can have a dramatic impact on the operating points needed for plant yield optimization.

6.2.4 Incremental Quality and Coal Value

Any discussion of plant optimization must address the issue of coal value. Although coal payments in the steam (utility) market are typically reported on a per ton basis, price adjustments are nearly always applied to compensate for variations in the heat content of the as-received product. For example, consider the tabular analysis illustrated in Table 6.1(a) and Table 6.1(b). In this simplified example, two scenarios for the same cleaning operation are shown. In the first scenario, it is assumed that the product is dry; therefore, moisture has no effect on the coal value. In the second case, the product contains 16.67% moisture, which drives down both the heat content and the market value of the coal. In this example, pure particles of carbonaceous matter (SG=1.3) were assigned a heat value of 15,000 BTU/lb (dry ash-free basis), while pure particles of rock (SG=2.5) were assigned no heat value. The sales agreement for this example dictates a market price of $30.00 per ton of as-received clean coal with quality specifications of 12,500 BTU/lb and 10% ash (as-received). The coal payment schedule is prorated at $0.20 per 100 BTU above/below 12,500 BTU/lb and $0.50 per 1% ash above/below 10% ash. A $10.00 per ton sales related cost has also been applied to account for miscellaneous fees, taxes and other sales expenses associated with the coal production.

The calculations for the first case indicate that pure coal particles carry a $5.00 per ton BTU premium (i.e., [15,000–12,500] x $0.20/100 = $5.00) and $5.00 per ton ash premium (i.e., [10-0] x $0.50/1 = $5.00). After subtracting a sales related cost of $10.00 per ton, the net value of these high grade particles is $30.00 per ton (i.e., $30.00 base + $10.00 premium - $10.00 sales = $30.00). In contrast, the pure rock particles carry a $25.00 per ton BTU penalty (i.e., [0–

12,500]/100 x $0.20 = $25.00) and $45.00 per ton ash penalty (i.e., [10-100]/1 x $0.50 = -$45.00). Thus, after subtracting a sales related cost of $10.00 per ton, these low-grade particles have a net negative value of minus $50.00 per ton (i.e., $30.00 base – $70.00 penalty – $10.00 sales = -$50.00). In other words, the producer gains $30.00 for every ton of pure carbonaceous material shipped to the customer and loses $50.00 per ton of pure rock shipped. Composite particles containing mixed amounts of coal and rock have market values between these two limits. In order to maximize profitability, the coal producer for this example should obviously ship only those particles that have a positive net value and should never ship particles that have a negative net value. In this example, the "zero value" particle, which contains just enough heat content to justify its shipment to market, occurs at a density of 1.75 SG (i.e., an incremental ash of 37.5%). Therefore, for this simplistic example, which does not include the effect of moisture on coal value, the plant operator should set and maintain an effective specific gravity cutpoint of 1.75 SG to ensure that profitability is maximized.

The second scenario is identical to the first except the impact of moisture has been included in the value calculation. In this scenario, the heat value of particles drops with the presence of moisture, thus driving down the net value of each coal particle. The pure particles of carbonaceous matter (SG=1.3) now have a heat value of 12,500 BTU/lb (i.e., 15,000 x [100-16.67]/100 = 12,500 BTU/lb). Therefore, these particles no longer carry a BTU premium. They still carry the same ash premium of $5.00 per ton, since the ash content did not change. (In reality, the presence of moisture would reduce the as-received ash content slightly). Thus, after subtracting the sales cost of $10 per ton, these particles now have a lower net value of $25 per ton (i.e., $30 base + $5 premium – $10 sales = $25.00). The pure rock particles (SG=2.5) still have the same net value of -$50 since moisture does not further reduce the heat value of 0

BTU/lb material. When all these factors are considered, the presence of moisture lowered the optimum density cutpoint for the "zero value" particle from 1.75 to 1.70 SG. In other words, the presence of moisture reduces the optimum density for plant optimization for plants providing coals for the steam market. In fact, very fine particles may contain so much moisture that they have negative value even if they contain no ash. In such cases, the use of desliming circuits to remove and discard ultrafine coal without further processing would be well justified (Bethell and

Table 6.1 Simplified value calculations for particles contained in run-of-mine coal conducted (a) without any moisture and (b) with 16.67% moisture

Scenario (a)

Particle Type						
Specific Gravity	1.30	1.55	1.60	**1.65**	1.70	2.50
Ash Content (%)	0.0	29.2	33.3	**37.5**	41.7	100.0
Moisture Content (%)	0	0	0	**0**	0	0
Heat Content (BTU/lb)	15000	10625	10000	**9375**	8750	0
BTU Value Adjustment	$5.00	-$3.75	-$5.00	**-$6.25**	-$7.50	-$25.00
Ash Value Adjustment	$5.00	-$9.58	-$11.67	**-$13.75**	-$15.83	-$45.00
Sales Cost	-$10.00	-$10.00	-$10.00	**-$10.00**	-$10.00	-$10.00
Net Value	$30.00	$6.67	$3.33	**$0.00**	-$3.33	-$50.00

Scenario (b)

Particle Type						
Specific Gravity	1.30	1.55	**1.60**	1.65	1.70	2.50
Ash Content (%)	0.0	29.2	**33.3**	37.5	41.7	100.0
Moisture Content (%)	16.67	16.67	**16.67**	16.67	16.67	16.67
Heat Content (BTU/lb)	12500	8854	**8333**	7813	7292	0
BTU Value Adjustment	$0.00	-$7.29	**-$8.33**	-$9.37	-$10.42	-$25.00
Ash Value Adjustment	$5.00	-$9.58	**-$11.67**	-$13.75	-$15.83	-$45.00
Sales Cost	-$10.00	-$10.00	**-$10.00**	-$10.00	-$10.00	-$10.00
Net Value	$25.00	$3.13	**$0.00**	-$3.13	-$6.25	-$50.00

Luttrell, 2005).

This above example is important because it shows that the specific gravity for optimum plant operation is controlled by the coal sales agreement and is largely independent of the coal washability. Moreover, penalties attributable to other factors that influence the monetary value of coal such as moisture, sulfur, etc., can shift the optimum density for separations to values that are lower than those predicted by the well-known incremental ash concept. Although this example has been oversimplified, the underlying optimization principle illustrated by this analysis can conceptually be applied to any generalized case if the contractual details are available. Such an example is examined in the following case study.

6.3 Case Study

The optimization of plant yield via proper management of incremental value and the effect of moisture on incremental value can be best illustrated by means of a case study. The study was conducted to evaluate three different circuit designs that treated a minus 1 mm coal stream (see Figure 6.3). The first circuit design was a standard fine coal dewatering circuit used at U.S. coal plants with desliming. In this circuit design, underflow stream of a 15-inch classifying hydrocyclone (nominal 1 x 0.150 mm) was sent to a spiral for cleaning, while the overflow stream (nominal 0.150 x 0 mm) was sent to a 6-inch desliming hydrocyclone. The underflow stream (nominal 0.150 x 0.044 mm) of this hydrocyclone was cleaned with flotation and the clean product was then dewatered using a screenbowl centrifuge along with the spiral product. Moreover, the overflow stream (nominal 0.044 x 0 mm) of the desliming hydrocyclone and the main effluent stream of the screenbowl centrifuge were discarded. In the second circuit configuration, the desliming hydrocyclone was removed and the whole overflow stream of the 15-inch hydrocyclone was cleaned using flotation. Again, the underflow stream of this

hydrocyclone was cleaned using a spiral. However, in this circuit design, while the spiral product (nominal 1 x 0.150 mm) was dewatered using a screenbowl centrifuge, the flotation product and the main effluent of the screenbowl centrifuge (nominal 0.150 x 0 mm) were sent to a Centribaric^{TM} centrifuge for dewatering. Finally, the third circuit design consisted of a 6-inch hydrocyclone similar to the first circuit configuration. However, the overflow stream (nominal 0.044 x 0 mm) of this hydrocyclone was not discarded, but was cleaned with an ultrafine flotation column. While the combined products of the spiral and the deslime flotation (nominal 1 x 0.044 mm) were dewatered using a screenbowl centrifuge, ultrafine flotation product along with the main effluent of the screenbowl centrifuge (nominal 0.044 x 0 mm) were dewatered using a Centribaric^{TM} centrifuge.

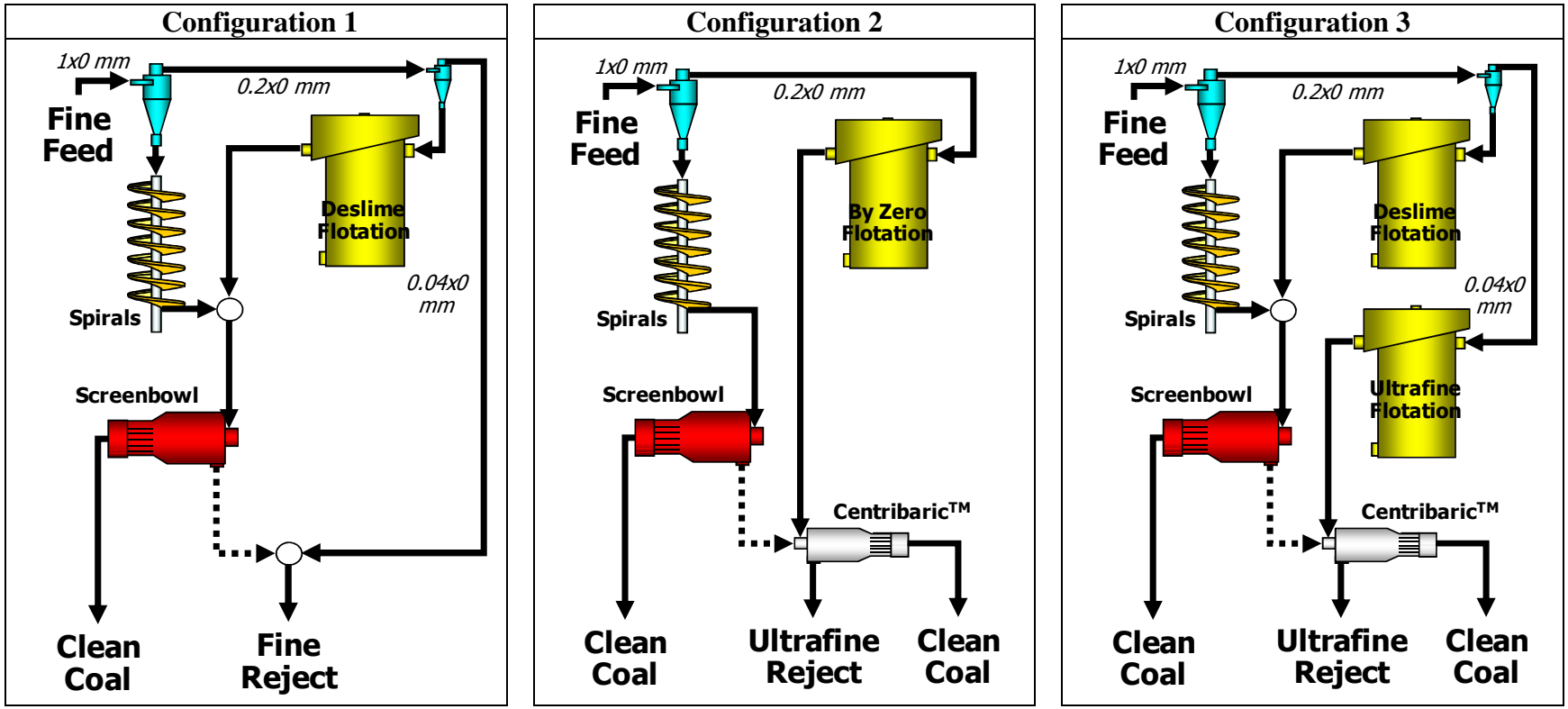

Figure 6.3 Different circuit configurations evaluated for economic analysis

All three circuit configurations were tested with two different coals with size distributions given in Figure 6.4, where coals A and B represent two extreme cases with Hardgrove indexes of 47 and 116, respectively. Assumptions in the analyses include freight charges of $20/ton coal, evaporation costs of $3/ton of water, ash handling expenses of $20/ton of ash, emission penalties of $200/ton of SO_2 emitted, and miscellaneous charges of $1.00/ton of clean coal handled. A constant fuel cost to the boiler of $2.44/MM BTU was maintained for all calculations. Also, the feed stream was assumed to contain clean coal particles with an average of 1.4 SG, which corresponds to about 14.5% dry ash content. All calculations were conducted based on 100 dry tph of feed coal and were performed in a similar fashion to the ones that are given in Table 6.1 (see Appendix 2 for detailed calculations).

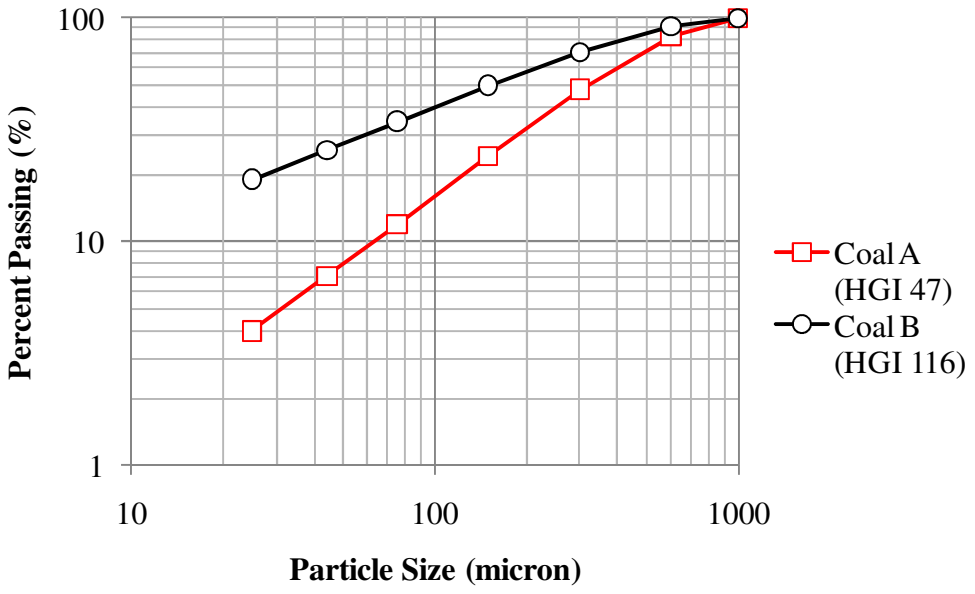

Figure 6.4 Size distributions of coals A and B used for the case study

Since it was assumed that no coal particles would be lost to effluent streams due to re-circulating effluent when the hyperbaric centrifuge was used, both the second and the third

circuit configurations yielded 100% coal to product; whereas some coal particles were lost in the first configuration due to discarding the effluent. Results of the analyses given in Table 6.2 showed that for both coals A and B, the lowest moisture value would be produced when the second circuit configuration is used. While $32.7/ton was the highest product value obtained for coal A, it was a lower value of $29.4 for the coal B because of its higher moisture content due to its finer size distribution. Calculations showed that, if the second circuit configuration is used for coal A, an additional $1,541,735 would be gained per year compared to the first circuit configuration. Similarly, a lower but still a positive gain of $1,081,748 can be achieved with the second configuration for coal B.

Table 6.2 Moisture values and coal worth for (a) the coarse feed and (b) the fine feed with various circuit configurations

Circuit Config.	Moisture (%)	Coal Treated With SB (dry tph)	Coal Treated With HFC (dry tph)	Total Product (dry tph)	Total Product (tph)	Value ($/ton)	Total Value ($/h)	Net Gain ($/h)	Net Gain ($/year)
(a) Coal A									
1	11.1	95.0	--	95.0	106.9	$30.9	$3,304	--	--
2	8.2	92.6	7.4	100.0	109.0	$32.7	$3,561	$257	$1,541,735
3	9.0	94.1	5.9	100.0	109.9	$32.2	$3,539	$236	$1,413,281
(b) Coal B									
1	18.8	85.2	--	85.2	104.9	$26.2	$3,221	--	--
2	13.5	75.8	24.2	100.0	115.6	$29.4	$3,401	$180	$1,081,748
3	14.6	79.5	20.5	100.0	117.1	$28.8	$3,367	$146	$873,832

6.4 References

1. Abbott, J. (1981), "The Optimization of Process Parameters to Maximize the Profitability from a Three-Component Blend," Proceedings First Australian Coal Preparation Conference, Newcastle, Australia, pp. 87-106.
2. Abbott, J. and Miles, N.J. (1990), 'Smoothing and Interpolation of Float-Sink Data for Coals," Inter. Symp. on Gravity Separation, Sept. 12-14, Cornwall, England.
3. Arnold, B. J. (1999), "Simulation of Dewatering Devices for Predicting the Moisture Content of Coals," Coal Preparation, Vol. 20, No. 2, pp. 35-54.
4. Bethell, P.J. and Luttrell, G.H. (2005), "Effects of Ultrafine Desliming on Coal Flotation Circuits," Proceedings, Centenary of Flotation Symposium, Brisbane, Australia, Paper No. 38, June 2005, pp. 719-728.
5. Clarkson, C.J. (1992), "Optimisation of Coal Production from Mine Face to Customer," 3rd Large Open Pit Mining Conference, Aug. 30 – Sept. 3, Makcay, Australia, pp. 433-440.
6. Dell, C.C. (1956), "The Mayer Curve," Colliery Guardian, Vol. 33, pp. 412-414.
7. Kennedy, D.L. (2006), Personal communication.
8. King, R. P. (1999), "Practical Optimization Strategies for Coal-Washing Plants," Coal Preparation Vol. 20, pp. 13-34.
9. Luttrell, G.H., Barbee, C.J., and Stanley, F.L. (2003), "Optimum Cutpoints for Heavy Medium Separations," Advances in Gravity Concentration (R.Q. Honaker and W.R. Forrest, Eds.), Society for Mining, Metallurgy, and Exploration, Inc., Littleton, Colorado, pp. 81-91.
10. Mayer, F.W. (1950), "A New Washing Curve," Gluckauf, Vol. 86, pp. 498-509.

11. Peng, F.F and Luckie, P.T. (1991), “Process Control, Part 1 - Separation Evaluation,” Coal Preparation, 5th Ed., J. Leonard and B. Hardinge, Eds., Society of Mining Engineers, Port City Press, Inc., Baltimore, Maryland, USA, pp. 659-716.
12. Rayner, J.G. (1987), “Direct Determination of Washing Parameters to Maximize Yield at a Given Ash,” Bull. Proc. Australia Inst. Mining and Metallurgy, Vo. 292, No. 8, pp. 67-70.
13. Tierney, J. W., Gottfried, B. S. and Zhao, G.Q. (1983), "A Simulator for Dewatering of Coal Fines," Proceedings, First Conference on Use of Computers in the Coal Industry, SME-AIME, New York, N.Y., pp. 230-236.

CHAPTER 7 SUMMARY AND CONCLUSIONS

Several series of laboratory-scale, pilot-scale and field tests were conducted using a novel fine-particle-dewatering technology called hyperbaric filter centrifugation. Based on the results obtained from this work, Decanter Machine Inc. constructed and sold a full-scale prototype that has now been successfully demonstrated at an industrial plant site. The technology is now marketed under the trade name Centribaric^{TM} centrifuge.

Several laboratory-scale test units were constructed for the purpose of conducting a detailed parametric study of hyperbaric filter centrifugation. Test results obtained with samples containing different size distributions showed that as long as the dewatered product contained less than about 60% minus 0.025 mm particles, centrifugation could be improved through the injection of pressurized air without having to resort to very high centrifugal fields. For example, a centrifugal acceleration of 500 g's with air pressure was found to be as effective for dewatering as a high centrifugal acceleration of 2700 g's without air pressure. Therefore, it was concluded that the use of a costly high-g centrifuge could be avoided when the fines content of a product was below a certain amount. However, when the minus 0.025 mm particle content was above 60%, the use of a high centrifugal acceleration with air pressure was found to be essential to achieve low moisture values. Moreover, tests performed using different coal samples obtained from commercial coal plants showed that it was possible to achieve single-digit moisture values when desliming was performed ahead of hyperbaric centrifugation. Furthermore, tests conducted to study the effects of several surface active dewatering aids and flocculants showed that moisture reductions as large as 60% (compared to no-chemical, and no-air cases) were possible by using chemicals in conjunction with air injection.

Dewatering kinetics tests performed at the laboratory-scale showed that centrifugal dewatering process could be described as a rate process. While the bulk of the water was removed quickly from the cake during centrifugation, a smaller amount was removed at a slower rate. Moreover, a certain amount of water was not removed at all, which represented the final moisture content of the product. The application of air pressure assisted in the removal of water at both fast and slow rates from the cake and lowered the final equilibrium cake moisture.

Pilot-scale test results showed that higher rotational speeds and longer centrifugation times were beneficial for producing lower moistures. Also, injecting pressurized air through the cake further improved the moisture. It was also concluded that thickening was an essential step for centrifugal dewatering, as it increased the recovery of solids. The experiments also showed that solids recovery could be further increased when the effluent stream was re-circulated back to the feed stream. Although a more detailed and a complete parametric study of the pilot-scale unit was originally intended, all attempts to run a complete series of tests were unsuccessful due to the frequent operational issues associated with the use of a small pilot-scale machine.

In light of the problems associated with the pilot-scale tests, a continuous prototype hyperbaric centrifuge was built by Decanter Machine Inc. for use in field testing. The prototype unit successfully demonstrated that low moisture values could be obtained using hyperbaric centrifugation. Low moistures values in the range of 13 to 20% were obtainable with high solid recoveries of 83-96%. Slightly higher, but still low, moistures ranging from 14% to 19% with 97-99% recoveries were predicted to be realistically achievable by circulating the screen drain back to the feed stream. Also, mixing fine (minus 0.044 mm) column concentrate with a coarser stream was found to be effective in reducing moisture and increasing solids recovery. It was concluded that a smaller ratio of coarse-to-fine particles could be used to avoid a substantial

capacity de-rating, as the test results showed that even a very small amount of coarse material was enough to keep the moisture content low and the recovery high.

An empirical dewatering model and a theoretical dewatering model were developed for the hyperbaric centrifugation. While very accurate results were obtained using the empirical model, the theoretical model had difficulty in predicting reliable product moistures. Different centrifugal dewatering circuit configurations employing the hyperbaric centrifuge were simulated using the empirical model and an economic analysis was conducted. Based on the simulation results, it was determined that utilization of hyperbaric centrifuges in a coal plant would likely produce an attractive economic gain compared to utilizing only screenbowl centrifuges.

APPENDIX 1 – Mass Balance Calculations

Evaluation of Hyperbaric Centrifuge - Cardinal Plant

Test Number:	1
Test Date:	September, 16th 2008
Feed:	50% Screen Drain + 50% Column Concentrate
Descripton:	Mass balanced data

	Size Distribution (Mass)				Partition Factors			
Size	Fresh Feed (kg/hr)	Main Effluent (kg/hr)	Screen Drain (kg/hr)	Product (kg/hr)	Fresh Feed --	Main Effluent --	Screen Drain --	Product --
+100 M	125.17	0.00	0.73	124.44	100.00	0.00	0.58	99.42
100x500 M	73.02	0.07	1.87	71.09	100.00	0.09	2.56	97.35
-500 M	116.80	0.36	9.16	107.28	100.00	0.30	7.84	91.85
Overall	314.99	0.42	11.76	302.81	100.00	0.13	3.73	96.13
Slurry Rate	4659.98	4244.39	66.13	349.46				

	Size Distribution (Percent of Stream)				Ash Content			
Size	Fresh Feed (%)	Main Effluent (%)	Screen Drain (%)	Product (%)	Fresh Feed (%)	Main Effluent (%)	Screen Drain (%)	Product (%)
+100 M	39.74	0.05	6.21	41.10	6.36	37.94	6.11	6.36
100x500 M	23.18	16.27	15.90	23.48	7.13	17.32	8.71	7.07
-500 M	37.08	83.68	77.89	35.43	10.03	53.62	11.11	9.79
Overall	100.00	100.00	100.00	100.00	7.90	47.70	10.42	7.74

	Combustible Recovery			
Size	Fresh Feed (%)	Main Effluent (%)	Screen Drain (%)	Product (%)
+100 M	100.00	0.00	0.59	99.41
100x500 M	100.00	0.08	2.52	97.40
-500 M	100.00	0.16	7.75	92.10
Overall	100.00	0.08	3.63	96.29

Stream	Solids SG	Slurry GPM
F. Feed	1.35	20.19
M. Effluent	1.69	18.71
S. Drain	1.37	0.28
Product	1.35	1.19

Measured Moisture (%)	Predicted Moisture (%)
13.35	13.29

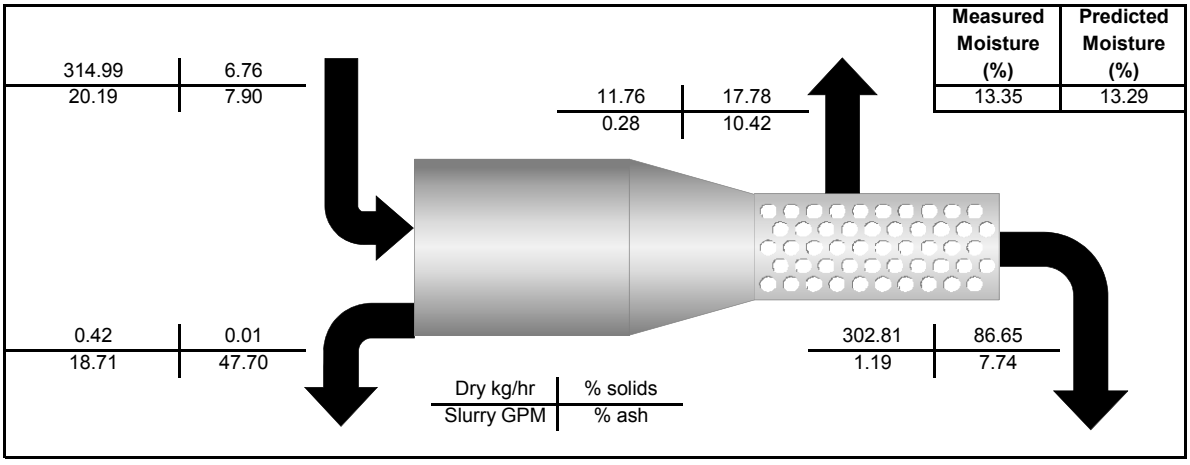

Evaluation of Hyperbaric Centrifuge - Cardinal Plant

Test Number:	1
Test Date:	September, 16th 2008
Feed:	50% Screen Drain + 50% Column Concentrate
Descripton:	Simulated data for screen drain recirculation

	Size Distribution (Mass)				Partition Factors			
Size	Combined Feed (kg/hr)	Main Effluent (kg/hr)	Screen Drain (kg/hr)	Product (kg/hr)	Fresh Feed --	Main Effluent --	Screen Drain --	Product --
+100 M	125.91	0.00	0.73	125.17	100.00	0.00	0.59	100.00
100x500 M	74.94	0.07	1.92	72.95	100.00	0.10	2.63	99.90
-500 M	126.73	0.39	9.94	116.41	100.00	0.33	8.51	99.67
Overall	327.59	0.46	12.59	314.54	100.00	0.14	4.00	99.86
Slurry Rate	4727.06	4295.53	67.08	364.45				

	Size Distribution (Percent of Stream)				Ash Content			
Size	Combined Feed (%)	Main Effluent (%)	Screen Drain (%)	Product (%)	Combined Feed (%)	Main Effluent (%)	Screen Drain (%)	Product (%)
+100 M	38.44	0.05	5.84	39.80	6.36	37.94	6.11	6.36
100x500 M	22.88	15.52	15.24	23.19	7.13	17.32	8.71	7.07
-500 M	38.69	84.43	78.92	37.01	10.03	53.62	11.11	9.79
Overall	100.00	100.00	100.00	100.00	7.95	47.97	10.45	7.80

	Combustible Recovery			
Size	Combined Feed (%)	Main Effluent (%)	Screen Drain (%)	Product (%)
+100 M	100.00	0.00	0.59	100.00
100x500 M	100.00	0.08	2.52	99.96
-500 M	100.00	0.16	7.75	99.93
Overall	100.00	0.08	3.74	99.96

Stream	Solids SG	Slurry GPM
C. Feed	1.35	20.47
M. Effluent	1.69	18.94
S. Drain	1.37	0.28
Product	1.35	1.25

Measured Moisture (%)	Predicted Moisture (%)
---	13.70

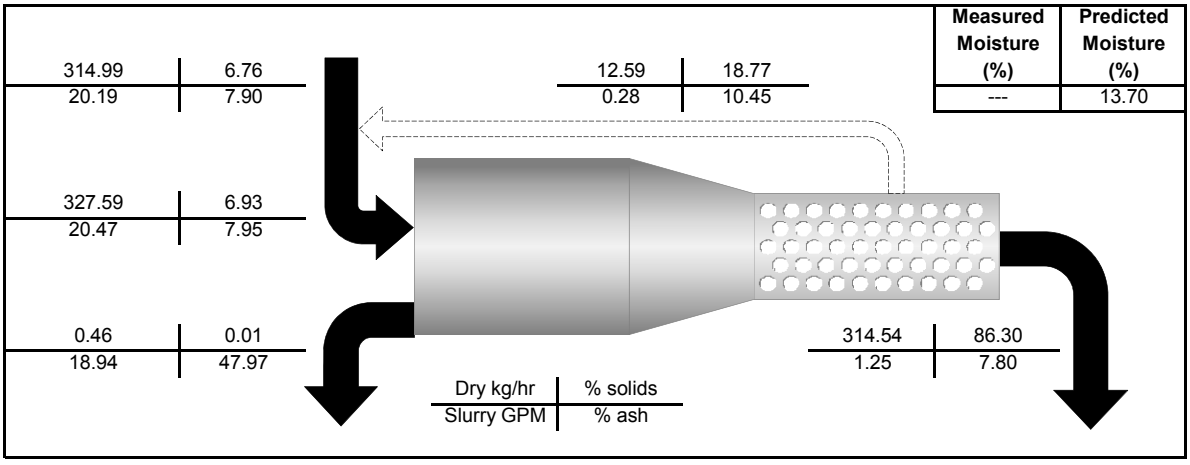

Evaluation of Hyperbaric Centrifuge - Cardinal Plant

Test Number: 2
Test Date: September, 16th 2008
Feed: 40% Screen Drain + 60% Column Concentrate
Description: Mass balanced data

	Size Distribution (Mass)				Partition Factors			
Size	Fresh Feed (kg/hr)	Main Effluent (kg/hr)	Screen Drain (kg/hr)	Product (kg/hr)	Fresh Feed --	Main Effluent --	Screen Drain --	Product --
+100 M	82.18	0.00	0.82	81.36	100.00	0.00	1.00	99.00
100x500 M	86.57	0.01	2.71	83.85	100.00	0.01	3.13	96.86
-500 M	123.46	2.99	6.68	113.80	100.00	2.42	5.41	92.17
Overall	292.21	3.00	10.21	279.00	100.00	1.03	3.50	95.48
Slurry Rate	4707.03	4311.57	67.13	328.33				

	Size Distribution (Percent of Stream)				Ash Content			
Size	Fresh Feed (%)	Main Effluent (%)	Screen Drain (%)	Product (%)	Fresh Feed (%)	Main Effluent (%)	Screen Drain (%)	Product (%)
+100 M	28.12	0.02	8.03	29.16	8.01	28.07	6.98	8.02
100x500 M	29.63	0.19	26.57	30.05	5.76	31.06	6.38	5.74
-500 M	42.25	99.79	65.40	40.79	8.20	55.23	10.55	6.83
Overall	100.00	100.00	100.00	100.00	7.42	55.17	9.16	6.85

	Combustible Recovery			
Size	Fresh Feed (%)	Main Effluent (%)	Screen Drain (%)	Product (%)
+100 M	100.00	0.00	1.01	98.99
100x500 M	100.00	0.00	3.11	96.88
-500 M	100.00	1.18	5.27	93.55
Overall	100.00	0.50	3.43	96.07

Stream	Solids SG	Slurry GPM
F. Feed	1.35	20.42
M. Effluent	1.77	19.01
S. Drain	1.36	0.28
Product	1.34	1.13

Measured Moisture (%)	Predicted Moisture (%)
15.02	14.84

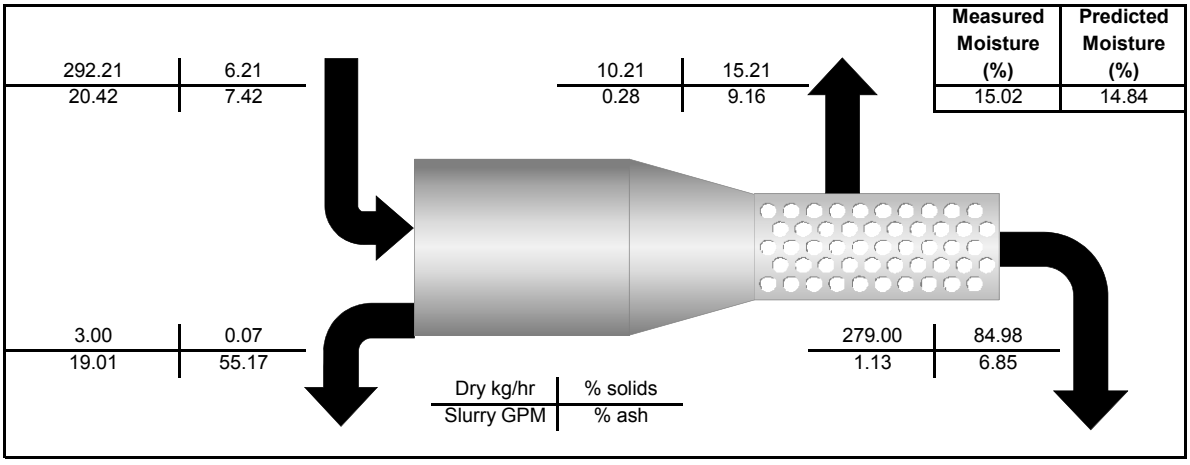

Evaluation of Hyperbaric Centrifuge - Cardinal Plant

Test Number:	2
Test Date:	September, 16th 2008
Feed:	40% Screen Drain + 60% Column Concentrate
Description:	Simulated data for screen drain recirculation

	Size Distribution (Mass)				Partition Factors			
Size	Combined Feed (kg/hr)	Main Effluent (kg/hr)	Screen Drain (kg/hr)	Product (kg/hr)	Fresh Feed --	Main Effluent --	Screen Drain --	Product --
+100 M	83.00	0.00	0.83	82.18	100.00	0.00	1.01	100.00
100x500 M	89.37	0.01	2.80	86.57	100.00	0.01	3.24	99.99
-500 M	130.52	3.16	7.06	120.30	100.00	2.56	5.72	97.44
Overall	302.90	3.17	10.69	289.05	100.00	1.08	3.66	98.92
Slurry Rate	4775.14	4366.53	68.10	340.51				

	Size Distribution (Percent of Stream)				Ash Content			
Size	Combined Feed (%)	Main Effluent (%)	Screen Drain (%)	Product (%)	Combined Feed (%)	Main Effluent (%)	Screen Drain (%)	Product (%)
+100 M	27.40	0.02	7.75	28.43	8.01	28.07	6.98	8.02
100x500 M	29.51	0.19	26.20	29.95	5.76	31.06	6.38	5.74
-500 M	43.09	99.80	66.05	41.62	8.20	55.23	10.55	6.83
Overall	100.00	100.00	100.00	100.00	7.43	55.18	9.18	6.84

	Combustible Recovery			
Size	Combined Feed (%)	Main Effluent (%)	Screen Drain (%)	Product (%)
+100 M	100.00	0.00	1.01	99.99
100x500 M	100.00	0.00	3.11	100.02
-500 M	100.00	1.18	5.27	98.90
Overall	100.00	0.51	3.46	99.54

Stream	Solids SG	Slurry GPM
C. Feed	1.35	20.71
M. Effluent	1.77	19.25
S. Drain	1.36	0.29
Product	1.34	1.18

Measured Moisture (%)	Predicted Moisture (%)
---	15.11

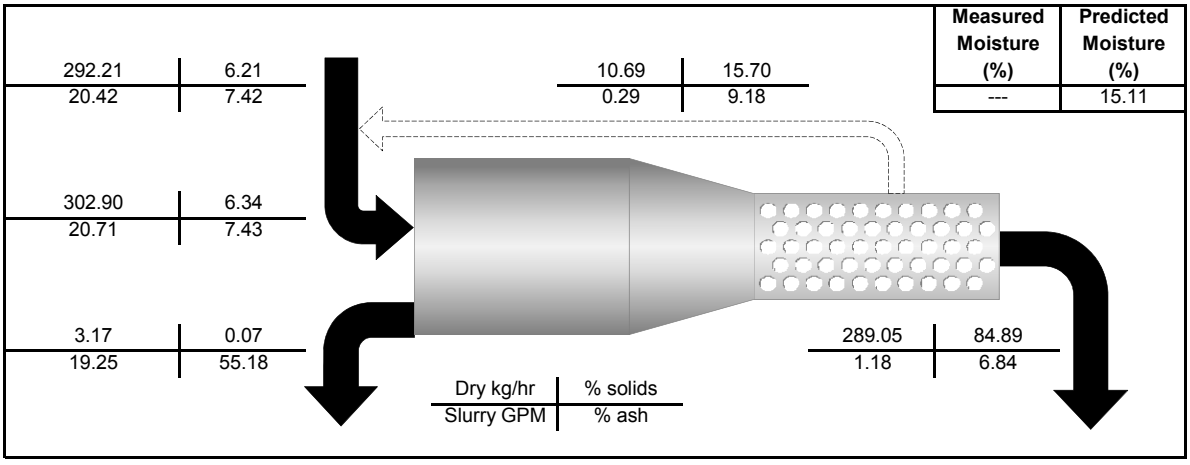

Evaluation of Hyperbaric Centrifuge - Cardinal Plant

Test Number:	3
Test Date:	September, 17th 2008
Feed:	30% Screen Drain + 70% -325 M Column Concentrate
Description:	Mass balanced data

	Size Distribution (Mass)				Partition Factors			
Size	Fresh Feed (kg/hr)	Main Effluent (kg/hr)	Screen Drain (kg/hr)	Product (kg/hr)	Fresh Feed --	Main Effluent --	Screen Drain --	Product --
+100 M	50.11	0.00	0.35	49.76	100.00	0.00	0.70	99.30
100x500 M	58.86	0.00	1.05	57.81	100.00	0.00	1.78	98.22
-500 M	98.51	0.04	12.32	86.15	100.00	0.04	12.51	87.45
Overall	207.49	0.04	13.72	193.72	100.00	0.02	6.61	93.37
Slurry Rate	4756.12	4429.64	95.32	231.17				

	Size Distribution (Percent of Stream)				Ash Content			
Size	Fresh Feed (%)	Main Effluent (%)	Screen Drain (%)	Product (%)	Fresh Feed (%)	Main Effluent (%)	Screen Drain (%)	Product (%)
+100 M	24.15	0.08	2.56	25.69	7.38	17.52	7.81	7.38
100x500 M	28.37	4.27	7.63	29.84	6.96	26.06	7.93	6.94
-500 M	47.48	95.65	89.81	44.47	7.90	51.67	8.47	7.80
Overall	100.00	100.00	100.00	100.00	7.51	50.55	8.41	7.43

	Combustible Recovery			
Size	Fresh Feed (%)	Main Effluent (%)	Screen Drain (%)	Product (%)
+100 M	100.00	0.00	0.70	99.30
100x500 M	100.00	0.00	1.76	98.24
-500 M	100.00	0.02	12.43	87.55
Overall	100.00	0.01	6.55	93.44

Stream	Solids SG	Slurry GPM
F. Feed	1.35	20.73
M. Effluent	1.72	19.53
S. Drain	1.35	0.40
Product	1.35	0.80

Measured Moisture (%)	Predicted Moisture (%)
16.20	16.05

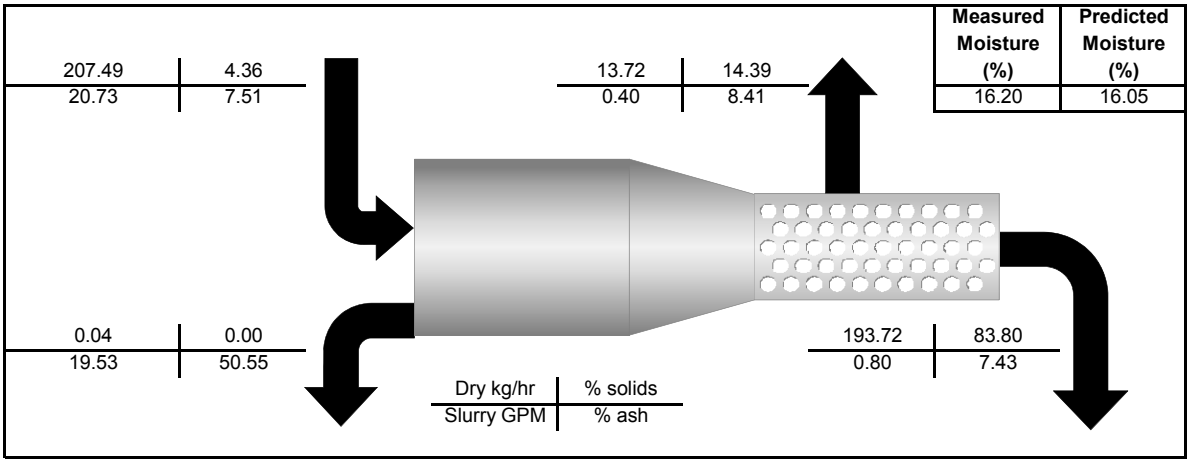

Evaluation of Hyperbaric Centrifuge - Cardinal Plant

Test Number:	3
Test Date:	September, 17th 2008
Feed:	30% Screen Drain + 70% -325 M Column Concentrate
Description:	Simulated data for screen drain recirculation

	Size Distribution (Mass)				Partition Factors			
Size	Combined Feed (kg/hr)	Main Effluent (kg/hr)	Screen Drain (kg/hr)	Product (kg/hr)	Fresh Feed --	Main Effluent --	Screen Drain --	Product --
+100 M	50.46	0.00	0.35	50.11	100.00	0.00	0.71	100.00
100x500 M	59.93	0.00	1.07	58.86	100.00	0.00	1.81	100.00
-500 M	112.60	0.05	14.08	98.47	100.00	0.05	14.30	99.95
Overall	222.99	0.05	15.50	207.44	100.00	0.02	7.47	99.98
Slurry Rate	4853.39	4506.16	97.27	249.97				

	Size Distribution (Percent of Stream)				Ash Content			
Size	Combined Feed (%)	Main Effluent (%)	Screen Drain (%)	Product (%)	Combined Feed (%)	Main Effluent (%)	Screen Drain (%)	Product (%)
+100 M	22.63	0.07	2.28	24.16	7.38	17.52	7.81	7.38
100x500 M	26.88	3.82	6.88	28.38	6.96	26.06	7.93	6.94
-500 M	50.49	96.11	90.84	47.47	7.90	51.67	8.47	7.80
Overall	100.00	100.00	100.00	100.00	7.53	50.67	8.42	7.45

	Combustible Recovery			
Size	Combined Feed (%)	Main Effluent (%)	Screen Drain (%)	Product (%)
+100 M	100.00	0.00	0.70	100.00
100x500 M	100.00	0.00	1.76	100.02
-500 M	100.00	0.02	12.43	100.06
Overall	100.00	0.01	6.89	100.03

Stream	Solids SG	Slurry GPM
C. Feed	1.35	21.15
M. Effluent	1.72	19.87
S. Drain	1.35	0.41
Product	1.35	0.87

Measured Moisture (%)	Predicted Moisture (%)
---	17.01

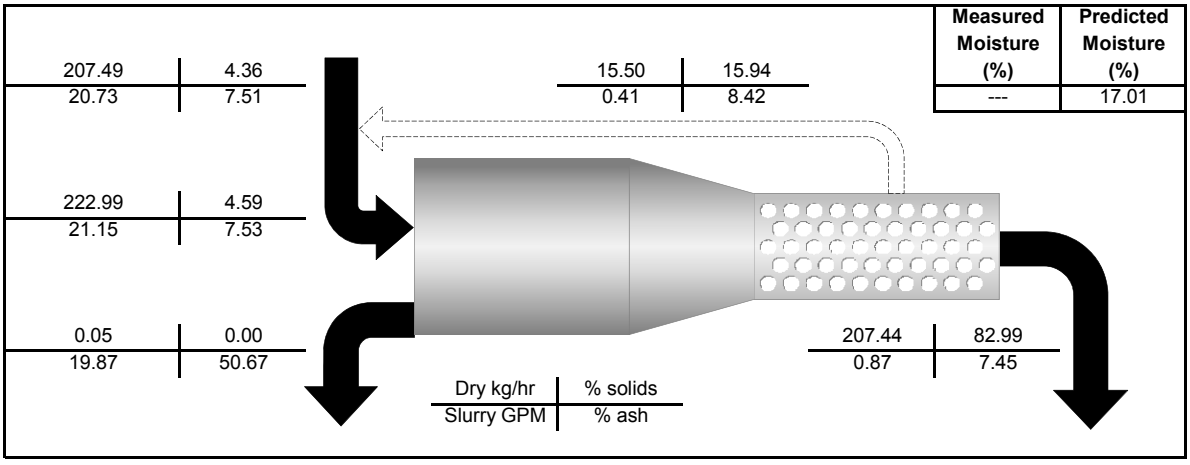

Evaluation of Hyperbaric Centrifuge - Cardinal Plant

Test Number: 4
Test Date: September, 17th 2008
Feed: 20% Screen Drain + 80% Column Concentrate
Description: Mass balanced data

	Size Distribution (Mass)				Partition Factors			
Size	Fresh Feed (kg/hr)	Main Effluent (kg/hr)	Screen Drain (kg/hr)	Product (kg/hr)	Fresh Feed --	Main Effluent --	Screen Drain --	Product --
+100 M	37.51	0.01	0.57	36.93	100.00	0.03	1.52	98.44
100x500 M	73.98	0.01	3.40	70.57	100.00	0.01	4.59	95.39
-500 M	130.25	1.77	9.24	119.24	100.00	1.36	7.09	91.55
Overall	241.74	1.80	13.21	226.74	100.00	0.74	5.46	93.79
Slurry Rate	4867.02	4495.89	92.49	278.65				

	Size Distribution (Percent of Stream)				Ash Content			
Size	Fresh Feed (%)	Main Effluent (%)	Screen Drain (%)	Product (%)	Fresh Feed (%)	Main Effluent (%)	Screen Drain (%)	Product (%)
+100 M	15.52	0.71	4.33	16.29	8.15	28.06	5.99	8.18
100x500 M	30.60	0.56	25.74	31.12	5.23	26.67	5.05	5.23
-500 M	53.88	98.73	69.93	52.59	8.05	58.98	8.32	7.27
Overall	100.00	100.00	100.00	100.00	7.20	58.58	7.38	6.79

	Combustible Recovery			
Size	Fresh Feed (%)	Main Effluent (%)	Screen Drain (%)	Product (%)
+100 M	100.00	0.03	1.56	98.41
100x500 M	100.00	0.01	4.60	95.39
-500 M	100.00	0.61	7.07	92.32
Overall	100.00	0.33	5.45	94.22

Stream	Solids SG	Slurry GPM
F. Feed	1.35	21.19
M. Effluent	1.81	19.82
S. Drain	1.35	0.39
Product	1.34	0.97

Measured Moisture (%)	Predicted Moisture (%)
18.63	18.41

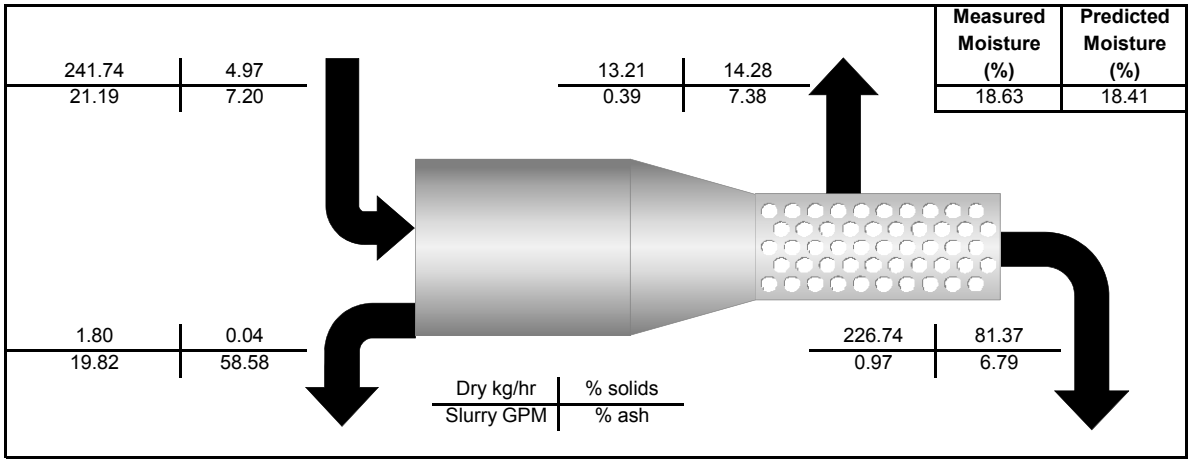

Evaluation of Hyperbaric Centrifuge - Cardinal Plant

Test Number:	4
Test Date:	September, 16th 2008
Feed:	20% Screen Drain + 80% Column Concentrate
Description:	Simulated data for screen drain recirculation

	Size Distribution (Mass)				Partition Factors			
Size	Combined Feed (kg/hr)	Main Effluent (kg/hr)	Screen Drain (kg/hr)	Product (kg/hr)	Fresh Feed --	Main Effluent --	Screen Drain --	Product --
+100 M	38.09	0.01	0.58	37.50	100.00	0.03	1.55	99.97
100x500 M	77.54	0.01	3.56	73.96	100.00	0.01	4.82	99.99
-500 M	140.19	1.91	9.94	128.34	100.00	1.47	7.63	98.53
Overall	255.82	1.93	14.08	239.81	100.00	0.80	5.83	99.20
Slurry Rate	4961.30	4572.34	94.28	294.68				

	Size Distribution (Percent of Stream)				Ash Content			
Size	Combined Feed (%)	Main Effluent (%)	Screen Drain (%)	Product (%)	Combined Feed (%)	Main Effluent (%)	Screen Drain (%)	Product (%)
+100 M	14.89	0.67	4.12	15.64	8.15	28.06	5.99	8.18
100x500 M	30.31	0.55	25.30	30.84	5.23	26.67	5.05	5.23
-500 M	54.80	98.78	70.58	53.52	8.05	58.98	8.32	7.27
Overall	100.00	100.00	100.00	100.00	7.21	58.60	7.40	6.79

	Combustible Recovery			
Size	Combined Feed (%)	Main Effluent (%)	Screen Drain (%)	Product (%)
+100 M	100.00	0.03	1.56	99.94
100x500 M	100.00	0.01	4.60	99.98
-500 M	100.00	0.61	7.07	99.37
Overall	100.00	0.34	5.49	99.65

Stream	Solids SG	Slurry GPM
C. Feed	1.35	21.59
M. Effluent	1.81	20.16
S. Drain	1.35	0.40
Product	1.34	1.03

Measured Moisture (%)	Predicted Moisture (%)
---	18.62

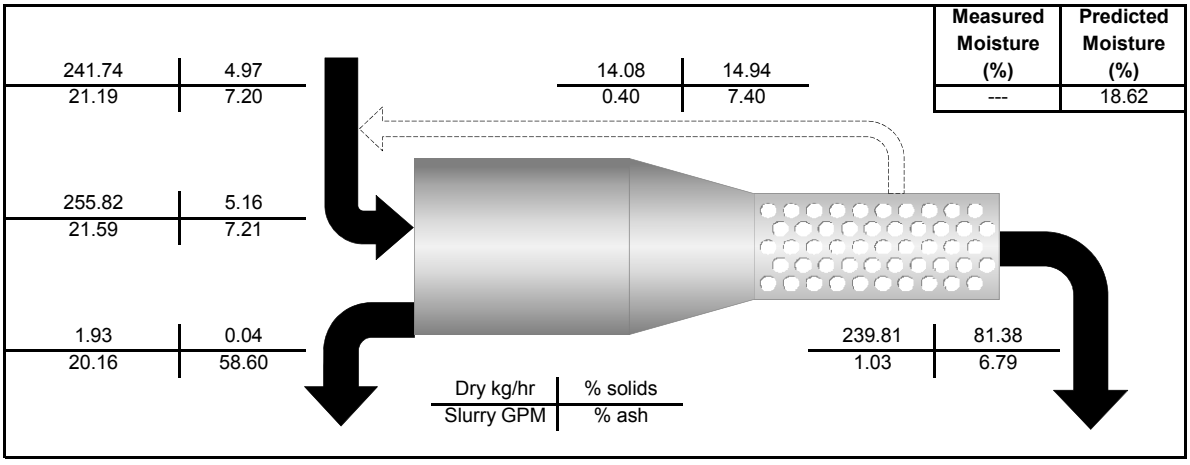

Evaluation of Hyperbaric Centrifuge - Cardinal Plant

Test Number: 5
Test Date: September, 17th 2008
Feed: 10% Screen Drain + 90% Column Concentrate
Description: Mass balanced data

	Size Distribution (Mass)				Partition Factors			
Size	Fresh Feed (kg/hr)	Main Effluent (kg/hr)	Screen Drain (kg/hr)	Product (kg/hr)	Fresh Feed --	Main Effluent --	Screen Drain --	Product --
+100 M	18.08	0.01	0.02	18.05	100.00	0.05	0.11	99.84
100x500 M	49.72	0.01	0.17	49.54	100.00	0.03	0.34	99.63
-500 M	108.13	0.88	8.63	98.62	100.00	0.82	7.98	91.20
Overall	175.93	0.91	8.81	166.21	100.00	0.52	5.01	94.47
Slurry Rate	4805.43	4533.53	65.70	206.20				

	Size Distribution (Percent of Stream)				Ash Content			
Size	Fresh Feed (%)	Main Effluent (%)	Screen Drain (%)	Product (%)	Fresh Feed (%)	Main Effluent (%)	Screen Drain (%)	Product (%)
+100 M	10.28	0.97	0.23	10.86	8.85	18.19	7.37	8.85
100x500 M	28.26	1.65	1.91	29.80	4.26	15.56	4.29	4.26
-500 M	61.46	97.38	97.86	59.33	6.49	45.63	6.34	6.15
Overall	100.00	100.00	100.00	100.00	6.10	44.86	6.30	5.88

	Combustible Recovery			
Size	Fresh Feed (%)	Main Effluent (%)	Screen Drain (%)	Product (%)
+100 M	100.00	0.04	0.11	99.84
100x500 M	100.00	0.03	0.34	99.63
-500 M	100.00	0.48	7.99	91.53
Overall	100.00	0.30	5.00	94.70

Stream	Solids SG	Slurry GPM
F. Feed	1.34	20.99
M. Effluent	1.66	19.99
S. Drain	1.34	0.28
Product	1.34	0.72

Measured Moisture (%)	Predicted Moisture (%)
19.39	19.52

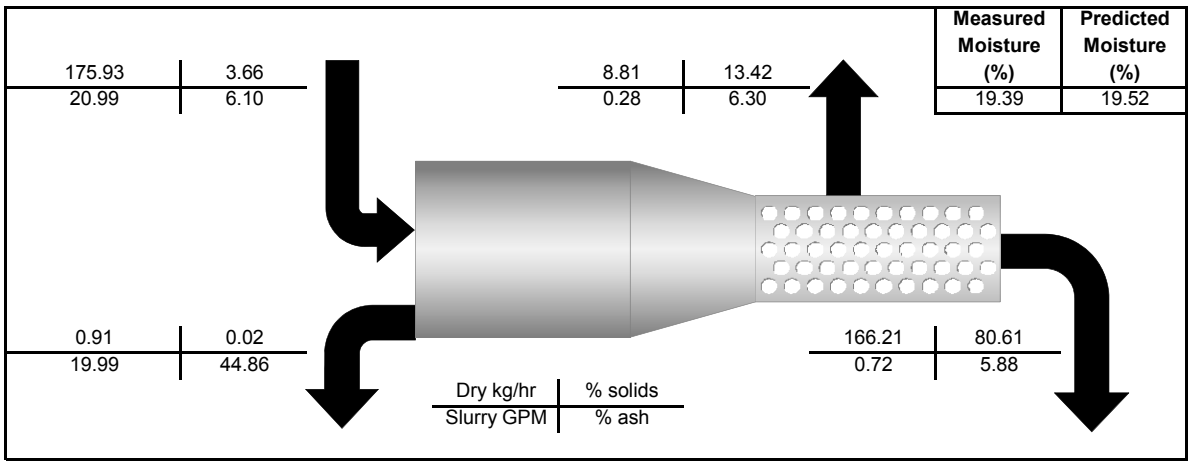

Evaluation of Hyperbaric Centrifuge - Cardinal Plant

Test Number:	5
Test Date:	September, 17th 2008
Feed:	10% Screen Drain + 90% Column Concentrate
Description:	Simulated data for screen drain recirculation

	Size Distribution (Mass)				Partition Factors			
Size	Combined Feed (kg/hr)	Main Effluent (kg/hr)	Screen Drain (kg/hr)	Product (kg/hr)	Fresh Feed --	Main Effluent --	Screen Drain --	Product --
+100 M	18.10	0.01	0.02	18.07	100.00	0.05	0.11	99.95
100x500 M	49.89	0.02	0.17	49.71	100.00	0.03	0.34	99.97
-500 M	117.50	0.96	9.37	107.17	100.00	0.89	8.67	99.11
Overall	185.49	0.99	9.56	174.95	100.00	0.56	5.44	99.44
Slurry Rate	4872.04	4587.69	66.61	217.74				

	Size Distribution (Percent of Stream)				Ash Content			
Size	Combined Feed (%)	Main Effluent (%)	Screen Drain (%)	Product (%)	Combined Feed (%)	Main Effluent (%)	Screen Drain (%)	Product (%)
+100 M	9.76	0.90	0.21	10.33	8.85	18.19	7.37	8.85
100x500 M	26.90	1.53	1.77	28.41	4.26	15.56	4.29	4.26
-500 M	63.35	97.58	98.02	61.26	6.49	45.63	6.34	6.15
Overall	100.00	100.00	100.00	100.00	6.12	44.92	6.30	5.89

	Combustible Recovery			
Size	Combined Feed (%)	Main Effluent (%)	Screen Drain (%)	Product (%)
+100 M	100.00	0.04	0.11	99.95
100x500 M	100.00	0.03	0.34	99.97
-500 M	100.00	0.48	7.99	99.47
Overall	100.00	0.31	5.15	99.66

Stream	Solids SG	Slurry GPM
C. Feed	1.34	21.27
M. Effluent	1.66	20.23
S. Drain	1.34	0.28
Product	1.34	0.77

Measured Moisture (%)	Predicted Moisture (%)
---	19.66

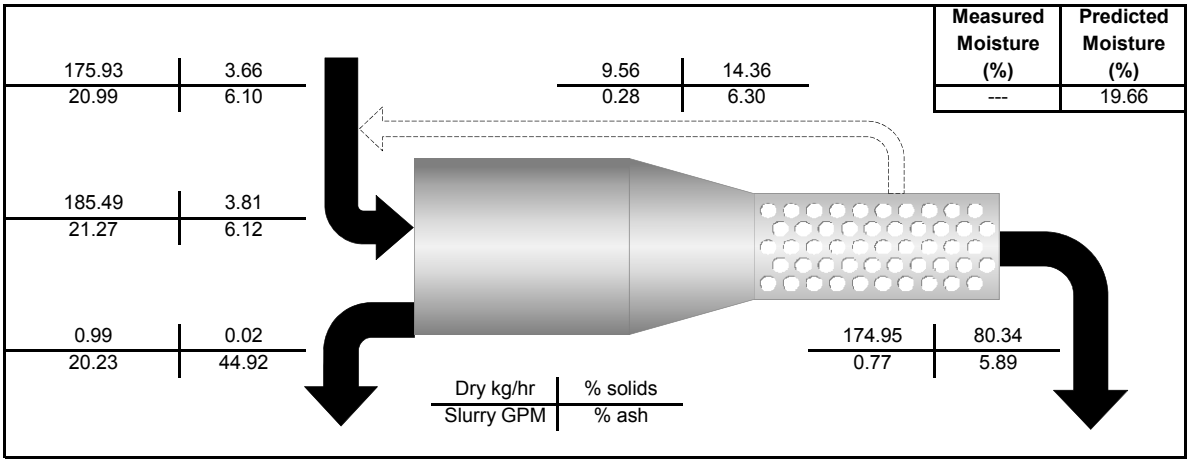

Evaluation of Hyperbaric Centrifuge - Cardinal Plant

Test Number: 6
Test Date: September, 17th 2008
Feed: 100% -325 M Column Concentrate
Description: Mass balanced data

	Size Distribution (Mass)				Partition Factors			
Size	Fresh Feed (kg/hr)	Main Effluent (kg/hr)	Screen Drain (kg/hr)	Product (kg/hr)	Fresh Feed --	Main Effluent --	Screen Drain --	Product --
+100 M	2.11	0.02	0.00	2.09	100.00	0.84	0.06	99.10
100x500 M	35.01	0.01	0.03	34.96	100.00	0.02	0.10	99.88
-500 M	139.91	3.90	25.70	110.31	100.00	2.79	18.37	78.84
Overall	177.02	3.92	25.74	147.36	100.00	2.22	14.54	83.24
Slurry Rate	4704.28	4426.59	96.34	181.35				

	Size Distribution (Percent of Stream)				Ash Content			
Size	Fresh Feed (%)	Main Effluent (%)	Screen Drain (%)	Product (%)	Fresh Feed (%)	Main Effluent (%)	Screen Drain (%)	Product (%)
+100 M	1.19	0.45	0.01	1.42	9.77	42.37	17.51	9.49
100x500 M	19.77	0.20	0.13	23.73	2.48	52.01	3.34	2.46
-500 M	79.03	99.35	99.87	74.86	7.36	60.70	5.89	5.82
Overall	100.00	100.00	100.00	100.00	6.42	60.60	5.89	5.07

	Combustible Recovery			
Size	Fresh Feed (%)	Main Effluent (%)	Screen Drain (%)	Product (%)
+100 M	100.00	0.54	0.06	99.41
100x500 M	100.00	0.01	0.09	99.89
-500 M	100.00	1.18	18.66	80.16
Overall	100.00	0.93	14.62	84.44

Stream	Solids SG	Slurry GPM
F. Feed	1.34	20.54
M. Effluent	1.83	19.51
S. Drain	1.34	0.40
Product	1.33	0.64

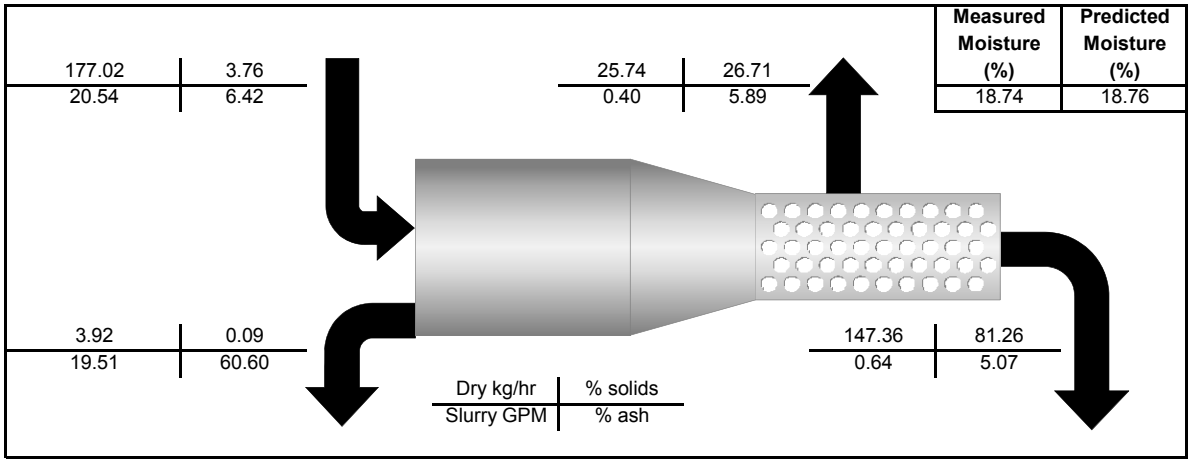

Evaluation of Hyperbaric Centrifuge - Cardinal Plant

Test Number: 6
Test Date: September, 17th 2008
Feed: 100% -325 M Column Concentrate
Description: Simulated data for screen drain recirculation

	Size Distribution (Mass)				Partition Factors			
Size	Combined Feed (kg/hr)	Main Effluent (kg/hr)	Screen Drain (kg/hr)	Product (kg/hr)	Fresh Feed --	Main Effluent --	Screen Drain --	Product --
+100 M	2.11	0.02	0.00	2.09	100.00	0.84	0.06	99.16
100x500 M	35.04	0.01	0.03	35.00	100.00	0.02	0.10	99.98
-500 M	171.39	4.77	31.49	135.13	100.00	3.41	22.51	96.59
Overall	208.54	4.80	31.52	172.22	100.00	2.71	17.81	97.29
Slurry Rate	4802.64	4493.50	98.36	210.78				

	Size Distribution (Percent of Stream)				Ash Content			
Size	Combined Feed (%)	Main Effluent (%)	Screen Drain (%)	Product (%)	Combined Feed (%)	Main Effluent (%)	Screen Drain (%)	Product (%)
+100 M	1.01	0.37	0.00	1.21	9.77	42.37	17.51	9.49
100x500 M	16.80	0.16	0.11	20.32	2.48	52.01	3.34	2.46
-500 M	82.19	99.47	99.89	78.46	7.36	60.70	5.89	5.82
Overall	100.00	100.00	100.00	100.00	6.56	60.62	5.89	5.18

	Combustible Recovery			
Size	Combined Feed (%)	Main Effluent (%)	Screen Drain (%)	Product (%)
+100 M	100.00	0.54	0.06	99.47
100x500 M	100.00	0.01	0.09	99.99
-500 M	100.00	1.18	18.66	98.20
Overall	100.00	0.97	15.23	98.58

Stream	Solids SG	Slurry GPM
C. Feed	1.34	20.94
M. Effluent	1.83	19.80
S. Drain	1.34	0.40
Product	1.33	0.74

Measured Moisture (%)	Predicted Moisture (%)
---	18.29

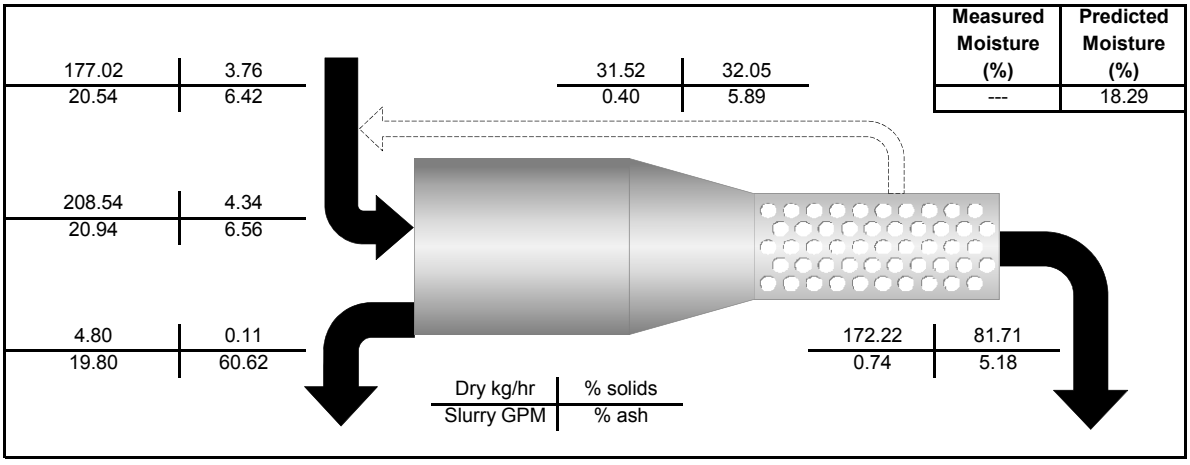

Evaluation of Hyperbaric Centrifuge - Cardinal Plant

Test Number:	7
Test Date:	September, 17th 2008
Feed:	Plant Column Concentrate + Leftover from Test 6
Description:	Mass balanced data

	Size Distribution (Mass)				Partition Factors			
Size	Fresh Feed (kg/hr)	Main Effluent (kg/hr)	Screen Drain (kg/hr)	Product (kg/hr)	Fresh Feed --	Main Effluent --	Screen Drain --	Product --
+100 M	7.38	0.01	0.36	7.01	100.00	0.10	4.92	94.98
100x500 M	48.53	0.01	3.92	44.60	100.00	0.01	8.08	91.90
-500 M	129.04	3.58	11.68	113.77	100.00	2.78	9.06	88.17
Overall	184.94	3.60	15.97	165.37	100.00	1.95	8.64	89.42
Slurry Rate	4860.30	4574.92	79.42	205.96				

	Size Distribution (Percent of Stream)				Ash Content			
Size	Fresh Feed (%)	Main Effluent (%)	Screen Drain (%)	Product (%)	Fresh Feed (%)	Main Effluent (%)	Screen Drain (%)	Product (%)
+100 M	3.99	0.20	2.27	4.24	5.27	23.81	3.78	5.32
100x500 M	26.24	0.17	24.56	26.97	3.25	24.47	2.88	3.28
-500 M	69.77	99.63	73.16	68.79	7.77	61.86	7.84	6.06
Overall	100.00	100.00	100.00	100.00	6.48	61.72	6.53	5.28

	Combustible Recovery			
Size	Fresh Feed (%)	Main Effluent (%)	Screen Drain (%)	Product (%)
+100 M	100.00	0.08	5.00	94.92
100x500 M	100.00	0.01	8.11	91.88
-500 M	100.00	1.15	9.05	89.80
Overall	100.00	0.80	8.63	90.57

Stream	Solids SG	Slurry GPM
F. Feed	1.34	21.22
M. Effluent	1.85	20.16
S. Drain	1.34	0.33
Product	1.33	0.73

Measured Moisture (%)	Predicted Moisture (%)
19.71	19.47

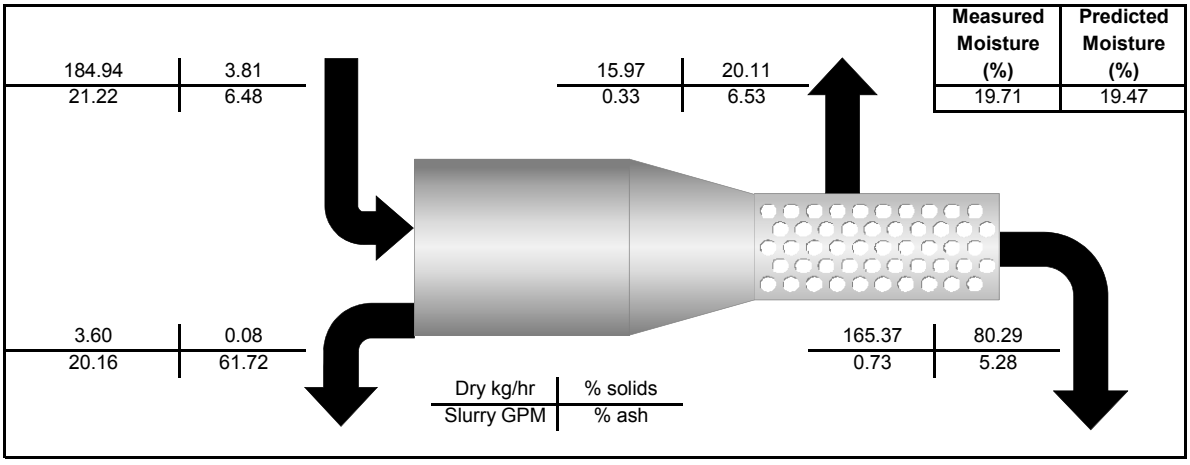

Evaluation of Hyperbaric Centrifuge - Cardinal Plant

Test Number:	7
Test Date:	September, 17th 2008
Feed:	Plant Column Concentrate + Leftover from Test 6
Description:	Simulated data for screen drain recirculation

	Size Distribution (Mass)				Partition Factors			
Size	Combined Feed (kg/hr)	Main Effluent (kg/hr)	Screen Drain (kg/hr)	Product (kg/hr)	Fresh Feed --	Main Effluent --	Screen Drain --	Product --
+100 M	7.76	0.01	0.38	7.37	100.00	0.10	5.18	99.90
100x500 M	52.80	0.01	4.27	48.52	100.00	0.01	8.80	99.99
-500 M	141.88	3.94	12.85	125.10	100.00	3.05	9.96	96.95
Overall	202.44	3.96	17.50	180.99	100.00	2.14	9.46	97.86
Slurry Rate	4941.04	4635.63	80.74	224.67				

	Size Distribution (Percent of Stream)				Ash Content			
Size	Combined Feed (%)	Main Effluent (%)	Screen Drain (%)	Product (%)	Combined Feed (%)	Main Effluent (%)	Screen Drain (%)	Product (%)
+100 M	3.83	0.19	2.18	4.07	5.27	23.81	3.78	5.32
100x500 M	26.08	0.17	24.39	26.81	3.25	24.47	2.88	3.28
-500 M	70.09	99.64	73.43	69.12	7.77	61.86	7.84	6.06
Overall	100.00	100.00	100.00	100.00	6.50	61.72	6.54	5.28

	Combustible Recovery			
Size	Combined Feed (%)	Main Effluent (%)	Screen Drain (%)	Product (%)
+100 M	100.00	0.08	5.00	99.84
100x500 M	100.00	0.01	8.11	99.96
-500 M	100.00	1.15	9.05	98.74
Overall	100.00	0.80	8.64	99.12

Stream	Solids SG	Slurry GPM
C. Feed	1.34	21.56
M. Effluent	1.85	20.43
S. Drain	1.34	0.34
Product	1.33	0.79

Measured Moisture (%)	Predicted Moisture (%)
---	19.44

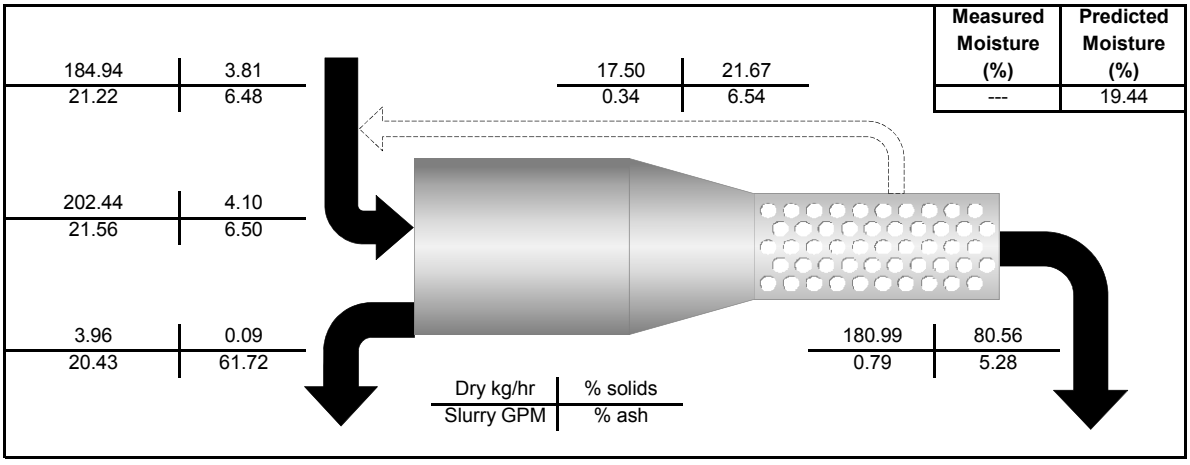

APPENDIX 2 - Economic Calculations

Coal A - Circuit Configuration 1 - Screenbowl Centrifuge Simulation

Input Parameters						
k_d (m^{-1})	ρ_s (kg/m^3)	ρ_w (kg/m^3)	B (m)	ε	σ (N/m)	μ (Pa.s)
400	1400	1000	0.559	0.55	0.072	0.001
L (m)	t (sec)	N (RPM)	N_g	Air P (psi)	g (m/s^2)	θ
0.0508	7	895	500	0	9.81	60

Feed Size Distribution						
Top Size (micron)	Bottom Size (micron)	Mean Size (micron)	D (%)	Weight in class (g)	Weight% in class (%)	Cum. Passing (%)
1000	600	774.60	30.98	17.50	17.50	100.00
600	300	424.26	16.97	34.50	34.50	82.50
300	150	212.13	8.49	24.00	24.00	48.00
150	75	106.07	4.24	12.00	12.00	24.00
75	44	57.45	2.30	5.00	5.00	12.00
44	25	33.17	1.33	3.00	3.00	7.00
25	0	5.00	0.20	4.00	4.00	4.00
			Total	100.00	100.00	

Permeability Estimation						
D_{eff} (micron)	S_K	S_0	c_1	c_2	k (m^2)	Permeability method to use
94.9	1.32	63201	0.22	4.00	4.11E-11	Tierney

Dewatering Simulation						
N_c	C_t	y	S_r	S_e	S	M (%)
1.2289	0.14	3.02	0.054818	0.0980	0.1429	11.09

Size Distribution Expansion using Gaudin-Schumann Equation								
m	k	Mean Size (micron)	D (%)	Cum. Passing (%)	Weight% in class (%)	Weight in class (g)	Wt/Size	
0.904	799							
1180	x 600	841.4	33.66	100.00	22.86	22.86	2.72E-04	
600	x 300	424.3	16.97	77.14	35.92	35.92	8.47E-04	
300	x 150	212.1	8.49	41.22	19.19	19.19	9.05E-04	
150	x 75	106.1	4.24	22.02	10.26	10.26	9.67E-04	
75	x 44	57.4	2.30	11.77	4.50	4.50	7.84E-04	
44	x 25	33.2	1.33	7.26	2.91	2.91	8.77E-04	
25	x 10	15.8	0.63	4.36	2.45	2.45	1.55E-03	
10	x 5	7.1	0.28	1.90	0.89	0.89	1.25E-03	
5	x 1	2.2	0.09	1.02	1.02	1.02	4.55E-03	
1	x 0	0.5	0.00	0.00	0.00	0.00	2.00E-07	
				Total	100.00	100.00	0.012003	

	Mean
5x0	2.231
10x0	3.2718
25x0	5.8921
44x0	8.7412
74x0	16.292
150x0	30.192
300x0	51.366
600x0	81.246
1180x0	94.935

☑ Lose 50% 325 M

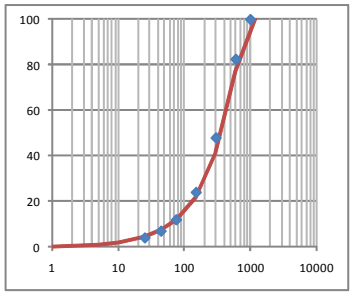

Degradation Model																
	Contributing Size Class										New Weight in class (g)	New Weight after loss (g)	New Weight% in class (%)	New Cum. Passing (%)	Effluent Weight in class (g)
	1180 x 600	600 x 300	300 x 150	150 x 75	75 x 44	44 x 25	25 x 10	10 x 5	5 x 1	1 x 0					
1180 x 600	0										15.16	15.16	15.96	100.00	0.00
600 x 300	3.58	0									33.41	33.41	35.16	84.04	0.00
300 x 150	1.91	2.84	0								22.32	22.32	23.49	48.88	0.00
150 x 75	1.02	1.52	0.76	0							13.12	13.12	13.81	25.38	0.00
75 x 44	0.45	0.67	0.33	0.17	0						6.01	6.01	6.33	11.58	0.00
44 x 25	0.29	0.43	0.22	0.11	0.04	0					3.95	1.98	2.08	5.25	1.98
25 x 10	0.24	0.36	0.18	0.09	0.03	0.02	0				3.38	1.69	1.78	3.17	1.69
10 x 5	0.09	0.13	0.07	0.03	0.01	0.01	0.01	0			1.23	0.61	0.65	1.39	0.61
5 x 1	0.10	0.15	0.08	0.04	0.01	0.01	0.01	0.00	0		1.41	0.71	0.74	0.74	0.71
1 x 0	0.00	0.00	0.00	0.00	0.00	0.00	0.00	0.00	0.00	0	0.00	0.00	0.00	0.00	0.00
Total	7.69	6.10	1.63	0.44	0.10	0.04	0.02	0.00	0.00	0.00	100.00	95.01	100.00		4.99

Coal A - Circuit Configuration 1 - Screenbowl Centrifuge Economics

CALCULATION OF OPTIMUM SIZE CUT

FINANCIAL DATA:		Total Boiler Cost =		$2.44	/MM BTU		Moisture Evap. =		$3.00	/ton H_2O		SO_2 Emission =		$200	/ton SO_2
		Freight Cost =		$20.00	/ton coal		Ash Handling =		$20.00	/ton ash		Other Cost =		$1.00	/ton coal

Size Class		1	2	3	4	5	6	7	Totals
Top Size	µ	**1180**	600	300	150	74	44	25	---
Bottom Size	µ	**600**	**300**	**150**	**74**	**44**	**25**	**0**	---
SG	µ	1.45	1.45	1.45	1.45	1.45	1.45	1.45	---
1/SG	---	0.69	0.69	0.69	0.69	0.69	0.69	0.69	---
Mass	%, dry	**15.96**	**35.16**	**23.49**	**13.81**	**6.33**	**2.08**	**3.17**	100.00
Solid SG		**1.40**	**1.40**	**1.40**	**1.40**	**1.40**	**1.40**	**1.40**	
Ash	%, dry	**14.50**	**14.50**	**14.50**	**14.50**	**14.50**	**14.50**	**14.50**	14.50
Sulfur	%, dry	**1.00**	**1.00**	**1.00**	**1.00**	**1.00**	**1.00**	**1.00**	1.00
BTU/lb	dry	**12825**	**12825**	**12825**	**12825**	**12825**	**12825**	**12825**	12825
BTU/lb	maf	15000	15000	15000	15000	15000	15000	15000	15000
Mass	%, ar	14.63	32.74	22.77	14.53	7.58	2.83	4.92	100.00
Moisture	%, ar	3.02	4.51	8.26	15.50	25.76	34.71	42.78	11.09
Cum. Moisture	%, ar	**11.09**	**12.47**	**17.43**	**24.42**	**32.88**	**39.83**	**42.78**	---
Ash	%, ar	14.06	13.85	13.30	12.25	10.76	9.47	8.30	12.89
Inerts	%, ar	17.08	18.35	21.56	27.75	36.52	44.17	51.08	23.98
Sulfur	%, ar	0.97	0.95	0.92	0.85	0.74	0.65	0.57	0.89
BTU/lb	ar	12438	12247	11766	10837	9522	8374	7338	11403
lb SO2/MM BTU	---	1.56	1.56	1.56	1.56	1.56	1.56	1.56	1.56
Cost to Boiler	$/MM BTU	$2.44	$2.44	$2.44	$2.44	$2.44	$2.44	$2.44	$2.44
Freight Cost	$/MM BTU	$0.80	$0.82	$0.85	$0.92	$1.05	$1.19	$1.36	$0.88
Evap. Cost	$/MM BTU	$0.00	$0.01	$0.01	$0.02	$0.04	$0.06	$0.09	$0.01
Ash Cost	$/MM BTU	$0.11	$0.11	$0.11	$0.11	$0.11	$0.11	$0.11	$0.11
SO2 Cost	$/MM BTU	$0.04	$0.04	$0.04	$0.04	$0.04	$0.04	$0.04	$0.04
Other Cost	$/MM BTU	$0.04	$0.04	$0.04	$0.05	$0.05	$0.06	$0.07	$0.04
Coal Worth	$/MM BTU	$1.44	$1.43	$1.39	$1.30	$1.15	$0.97	$0.77	$1.36
Cost to Boiler	$/ton	$60.70	$59.77	$57.42	$52.89	$46.47	$40.86	$35.81	$55.65
Freight Cost	$/ton	$20.00	$20.00	$20.00	$20.00	$20.00	$20.00	$20.00	$20.00
Evap. Cost	$/ton	$0.09	$0.14	$0.25	$0.46	$0.77	$1.04	$1.28	$0.33
Ash Cost	$/ton	$2.81	$2.77	$2.66	$2.45	$2.15	$1.89	$1.66	$2.58
SO2 Cost	$/ton	$0.89	$0.88	$0.85	$0.78	$0.68	$0.60	$0.53	$0.82
Other Cost	$/ton	$1.00	$1.00	$1.00	$1.00	$1.00	$1.00	$1.00	$1.00
Coal Worth	$/ton	$35.90	$34.98	$32.67	$28.19	$21.86	$16.33	$11.34	$30.92
Individual Tons	dry	15.16	33.41	22.32	13.12	6.01	1.98	3.01	**95.01**
Cum. Tons	dry	95.01	79.85	46.44	24.12	11.00	4.99	3.01	
Individual Tons	ar	15.64	34.99	24.33	15.53	8.10	3.03	5.26	106.86
Cum. Tons	ar	106.86	91.23	56.24	31.91	16.39	8.29	5.26	---
Cum. Mass	%, ar	100.00	85.37	52.63	29.86	15.33	7.76	4.92	---
Cum. Ash	%, ar	14.06	13.91	13.71	13.46	13.24	13.13	12.89	---
Cum. Sulfur	%, ar	0.97	0.96	0.95	0.93	0.91	0.91	0.89	---
Cum. BTU/lb	ar	12438	12350	12221	12067	11929	11834	11759	---
Individual Worth	$	$561.39	$1,223.92	$794.70	$437.69	$177.01	$49.43	$59.66	$3,303.79
Cum. Worth	$	$561.39	$1,785.30	$2,580.00	$3,017.69	$3,194.70	$3,244.13	$3,303.79	---

Coal A - Circuit Configuration 1 - Coarse Cut - Screenbowl Centrifuge Simulation

Input Parameters

k_d (m^{-1})	ρ_s (kg/m^3)	ρ_w (kg/m^3)	B (m)	ε	σ (N/m)	μ (Pa.s)
400	1400	1000	0.559	0.55	0.072	0.001
L (m)	**t (sec)**	**N (RPM)**	**N_g**	**Air P (psi)**	**g (m/s^2)**	**θ**
0.0381	7	895	500	0	9.81	60

Feed Size Distribution

Top Size (micron)	Bottom Size (micron)	Mean Size (micron)	D (%)	Weight in class (g)	Weight% in class (%)	Cum. Passing (%)
1000	600	774.60	30.98	17.50	18.48	100.00
600	300	424.26	16.97	34.50	36.43	81.52
300	150	212.13	8.49	23.98	25.32	45.10
150	75	106.07	4.24	11.63	12.28	19.77
75	44	57.45	2.30	4.14	4.37	7.49
44	25	33.17	1.33	1.84	1.94	3.12
25	0	5.00	0.20	1.12	1.18	1.18
		Total		94.71	100.00	

Permeability Estimation

D_{eff} (micron)	S_K	S_0	c_1	c_2	k (m^2)	Permeability method to use
151.4	2.38	39624	0.22	4.00	1.05E-10	Tierney

Dewatering Simulation

N_c	C_t	y	S_r	S_e	S	M (%)
3.1264	0.04	2.83	0.053783	0.0419	0.0914	*7.39*

Size Distribution Expansion using Gaudin-Schumann Equation

m	k	Mean Size (micron)	D (%)	Cum. Passing (%)	Weight% in class (%)	Weight in class (g)	Wt/Size
1.342	583						
1180 x 600		841.4	33.66	100.00	0.00	0.00	0.00E+00
600 x 300		424.3	16.97	100.00	58.99	55.87	1.39E-03
300 x 150		212.1	8.49	41.01	24.83	23.52	1.17E-03
150 x 75		106.1	4.24	16.17	9.79	9.28	9.23E-04
75 x 44		57.4	2.30	6.38	3.26	3.09	5.68E-04
44 x 25		33.2	1.33	3.12	1.66	1.57	5.00E-04
25 x 10		15.8	0.63	1.46	1.03	0.98	6.54E-04
10 x 5		7.1	0.28	0.43	0.26	0.24	3.66E-04
5 x 1		2.2	0.09	0.17	0.15	0.14	6.66E-04
1 x 0		0.5	0.00	0.02	0.02	0.02	3.88E-04
			Total	100.00	94.71	0.006626	

	Mean
25x0	6.9885
44x0	11.964
74x0	25.452
150x0	50.608
300x0	91.974
600x0	151.42
1180x0	151.42

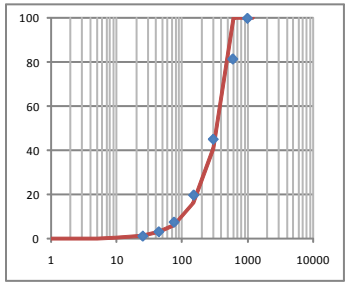

Degradation Model

	Contributing Size Class										New Weight in class (g)	New Weight after loss (g)	New Weight% in class (%)	New Cum. Passing (%)	Effluent Weight in class (g)
	1180 x 600	600 x 300	300 x 150	150 x 75	75 x 44	44 x 25	25 x 10	10 x 5	5 x 1	1 x 0					
1180 x 600	0										0.00	0.00	0.00	100.00	0.00
600 x 300	0.00	0									46.39	46.39	50.13	100.00	0.00
300 x 150	0.00	5.74	0								27.26	27.26	29.46	49.87	0.00
150 x 75	0.00	2.26	1.21	0							12.36	12.36	13.35	20.41	0.00
75 x 44	0.00	0.75	0.40	0.20	0						4.38	4.38	4.73	7.06	0.00
44 x 25	0.00	0.38	0.20	0.10	0.04	0					2.28	1.14	1.23	2.34	1.14
25 x 10	0.00	0.24	0.13	0.06	0.02	0.01	0				1.44	0.72	0.78	1.10	0.72
10 x 5	0.00	0.06	0.03	0.02	0.01	0.00	0.00	0			0.37	0.18	0.20	0.33	0.18
5 x 1	0.00	0.03	0.02	0.01	0.00	0.00	0.00	0.00	0		0.21	0.11	0.11	0.13	0.11
1 x 0	0.00	0.00	0.00	0.00	0.00	0.00	0.00	0.00	0.00	0	0.03	0.01	0.01	0.01	0.01
Total	0.00	9.48	2.00	0.39	0.07	0.02	0.01	0.00	0.00	0.00	94.71	92.55	100.00		2.16

Coal A - Circuit Configuration 1 - Coarse Cut - Screenbowl Centrifuge Economics

CALCULATION OF OPTIMUM SIZE CUT

FINANCIAL DATA:		Total Boiler Cost =		$2.44	/MM BTU		Moisture Evap. =		$3.00	/ton H_2O		SO_2 Emission =	$200	/ton SO_2
		Freight Cost =		$20.00	/ton coal		Ash Handling =		$20.00	/ton ash		Other Cost =	$1.00	/ton coal

Size Class		1	2	3	4	5	6	7	Totals
Top Size	µ	**1180**	600	300	150	74	44	25	---
Bottom Size	µ	**600**	**300**	**150**	**74**	**44**	**25**	**0**	---
SG	µ	1.45	1.45	1.45	1.45	1.45	1.45	1.45	---
1/SG	---	0.69	0.69	0.69	0.69	0.69	0.69	0.69	---
Mass	%, dry	**0.00**	**50.13**	**29.46**	**13.35**	**4.73**	**1.23**	**1.10**	100.00
Solid SG		**1.40**	**1.40**	**1.40**	**1.40**	**1.40**	**1.40**	**1.40**	
Ash	%, dry	**14.50**	**14.50**	**14.50**	**14.50**	**14.50**	**14.50**	**14.50**	14.50
Sulfur	%, dry	**1.00**	**1.00**	**1.00**	**1.00**	**1.00**	**1.00**	**1.00**	1.00
BTU/lb	dry	**12825**	**12825**	**12825**	**12825**	**12825**	**12825**	**12825**	12825
BTU/lb	maf	15000	15000	15000	15000	15000	15000	15000	15000
Mass	%, ar	0.00	48.38	29.04	13.85	5.40	1.61	1.72	100.00
Moisture	%, ar	7.39	4.05	6.04	10.73	18.93	29.20	40.57	7.39
Cum. Moisture	%, ar	**7.39**	**7.39**	**10.52**	**16.28**	**25.09**	**35.08**	**40.57**	---
Ash	%, ar	13.43	13.91	13.62	12.94	11.75	10.26	8.62	13.43
Inerts	%, ar	20.82	17.96	19.66	23.67	30.68	39.47	49.19	20.82
Sulfur	%, ar	0.93	0.96	0.94	0.89	0.81	0.71	0.59	0.93
BTU/lb	ar	11877	12306	12050	11449	10398	9080	7621	11877
lb SO2/MM BTU	---	1.56	1.56	1.56	1.56	1.56	1.56	1.56	1.56
Cost to Boiler	$/MM BTU	$2.44	$2.44	$2.44	$2.44	$2.44	$2.44	$2.44	$2.44
Freight Cost	$/MM BTU	$0.84	$0.81	$0.83	$0.87	$0.96	$1.10	$1.31	$0.84
Evap. Cost	$/MM BTU	$0.01	$0.00	$0.01	$0.01	$0.03	$0.05	$0.08	$0.01
Ash Cost	$/MM BTU	$0.11	$0.11	$0.11	$0.11	$0.11	$0.11	$0.11	$0.11
SO2 Cost	$/MM BTU	$0.04	$0.04	$0.04	$0.04	$0.04	$0.04	$0.04	$0.04
Other Cost	$/MM BTU	$0.04	$0.04	$0.04	$0.04	$0.05	$0.06	$0.07	$0.04
Coal Worth	$/MM BTU	$1.40	$1.43	$1.41	$1.36	$1.25	$1.09	$0.83	$1.40
Cost to Boiler	$/ton	$57.96	$60.05	$58.81	$55.87	$50.74	$44.31	$37.19	$57.96
Freight Cost	$/ton	$20.00	$20.00	$20.00	$20.00	$20.00	$20.00	$20.00	$20.00
Evap. Cost	$/ton	$0.22	$0.12	$0.18	$0.32	$0.57	$0.88	$1.22	$0.22
Ash Cost	$/ton	$2.69	$2.78	$2.72	$2.59	$2.35	$2.05	$1.72	$2.69
SO2 Cost	$/ton	$0.85	$0.88	$0.87	$0.82	$0.75	$0.65	$0.55	$0.85
Other Cost	$/ton	$1.00	$1.00	$1.00	$1.00	$1.00	$1.00	$1.00	$1.00
Coal Worth	$/ton	$33.20	$35.26	$34.03	$31.14	$26.07	$19.73	$12.70	$33.20
Individual Tons	dry	0.00	46.39	27.26	12.36	4.38	1.14	1.02	**92.55**
Cum. Tons	dry	92.55	92.55	46.16	18.89	6.54	2.16	1.02	
Individual Tons	ar	0.00	48.35	29.02	13.84	5.40	1.61	1.72	99.94
Cum. Tons	ar	99.94	99.94	51.59	22.57	8.73	3.33	1.72	---
Cum. Mass	%, ar	100.00	100.00	51.62	22.58	8.73	3.33	1.72	---
Cum. Ash	%, ar	13.43	13.91	13.80	13.67	13.57	13.51	13.43	---
Cum. Sulfur	%, ar	0.93	0.96	0.95	0.94	0.94	0.93	0.93	---
Cum. BTU/lb	ar	11877	12091	12083	12031	11980	11947	11921	---
Individual Worth	$	$0.00	$1,705.01	$987.59	$431.01	$140.72	$31.74	$21.86	$3,317.94
Cum. Worth	$	$0.00	$1,705.01	$2,692.60	$3,123.61	$3,264.34	$3,296.08	$3,317.94	---

Coal A - Circuit Configuration 1 - Coarse Cut - Hyperbaric Centrifuge Simulation

Input Parameters						
k_d (m^{-1})	ρ_s (kg/m^3)	ρ_w (kg/m^3)	B (m)	ε	σ (N/m)	μ (Pa.s)
400	1400	1000	0.381	0.52	0.072	0.001
L (m)	t (sec)	N (RPM)	N_g	Air P (psi)	g (m/s^2)	θ
0.0127	7	2650	2991	0	9.81	60

Feed Size Distribution						
Top Size (micron)	Bottom Size (micron)	Mean Size (micron)	D (%)	Weight in class (g)	Weight% in class (%)	Cum. Passing (%)
1000	600	774.60	30.98	0.00	0.00	100.00
600	300	424.26	16.97	0.00	0.00	100.00
300	150	212.13	8.49	0.02	0.20	100.00
150	75	106.07	4.24	0.37	4.91	99.80
75	44	57.45	2.30	0.86	11.57	94.88
44	25	33.17	1.33	2.30	30.89	83.32
25	0	5.00	0.20	3.91	52.43	52.43
			Total	7.45	100.00	

Permeability Estimation						
D_{eff} (micron)	S_k	S_0	c_1	c_2	k (m^2)	Permeability method to use
13.5	0.75	443725	0.22	4.00	6.20E-13	Tierney

Dewatering Simulation						
N_c	C_t	y	S_r	S_e	S	M (%)
0.1490	0.36	3.93	0.055417	0.2465	0.2784	*17.73*

Size Distribution Expansion using Gaudin-Schumann Equation								
m		k	Mean Size (micron)	D (%)	Cum. Passing (%)	Weight% in class (%)	Weight in class (g)	Wt/Size
0.543		75						
1180	x	600	841.4	33.66	100.00	0.00	0.00	0.00E+00
600	x	300	424.3	16.97	100.00	0.00	0.00	0.00E+00
300	x	150	212.1	8.49	100.00	0.00	0.00	0.00E+00
150	x	75	106.1	4.24	100.00	0.00	0.00	0.00E+00
75	x	44	57.4	2.30	100.00	25.01	1.86	4.35E-03
44	x	25	33.2	1.33	74.99	19.81	1.48	5.97E-03
25	x	10	15.8	0.63	55.18	21.62	1.61	1.37E-02
10	x	5	7.1	0.28	33.56	33.56	2.50	4.75E-02
5	x	1	2.2	0.09	0.00	0.00	0.00	0.00E+00
1	x	0	0.5	0.00	0.00	0.00	0.00	2.00E-07
					Total	100.00	7.45	0.071457

	Mean	Moisture
25x0	8.7614	22.38
44x0	10.841	20.04
74x0	13.522	17.73
150x0	13.522	17.73
300x0	13.522	17.73
600x0	13.522	17.73
1180x0	13.522	17.73

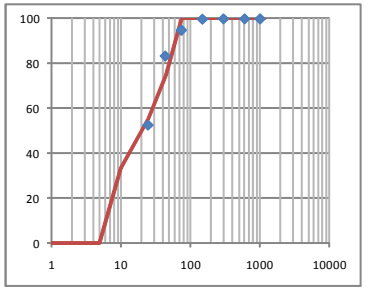

Degradation Model															
			Contributing Size Class										New Weight in class (g)	New Weight% in class (%)	New Cum. Passing (%)
			1180 x 600	600 x 300	300 x 150	150 x 75	75 x 44	44 x 25	25 x 10	10 x 5	5 x 1	1 x 0			
1180	x	600	0										0.00	0.00	100.00
600	x	300	0.00	0									0.00	0.00	100.00
300	x	150	0.00	0.00	0								0.00	0.00	100.00
150	x	75	0.00	0.00	0.00	0							0.00	0.00	100.00
75	x	44	0.00	0.00	0.00	0.00	0						1.82	24.43	100.00
44	x	25	0.00	0.00	0.00	0.00	0.01	0					1.47	19.70	75.57
25	x	10	0.00	0.00	0.00	0.00	0.01	0.01	0				1.62	21.75	55.86
10	x	5	0.00	0.00	0.00	0.00	0.02	0.01	0.01	0			2.53	34.01	34.11
5	x	1	0.00	0.00	0.00	0.00	0.00	0.00	0.00	0.00	0		0.00	0.00	0.09
1	x	0	0.00	0.00	0.00	0.00	0.00	0.00	0.00	0.01	0.00	0	0.01	0.09	0.09
Total			0.00	0.00	0.00	0.00	0.04	0.02	0.01	0.01	0.00	0.00	7.45	100.00	

Coal A - Circuit Configuration 1 - Coarse Cut - Hyperbaric Centrifuge Economics

CALCULATION OF OPTIMUM SIZE CUT

FINANCIAL DATA:		Total Boiler Cost =		$2.44	/MM BTU		Moisture Evap. =		$3.00	/ton H_2O		SO_2 Emission =	$200	/ton SO_2
		Freight Cost =		$20.00	/ton coal		Ash Handling =		$20.00	/ton ash		Other Cost =	$1.00	/ton coal

Size Class		1	2	3	4	5	6	7	Totals
Top Size	µ	**1180**	600	300	150	74	44	25	---
Bottom Size	µ	**600**	**300**	**150**	**74**	**44**	**25**	**0**	---
SG	µ	1.45	1.45	1.45	1.45	1.45	1.45	1.45	---
1/SG	---	0.69	0.69	0.69	0.69	0.69	0.69	0.69	---
Mass	%, dry	**0.00**	**0.00**	**0.00**	**0.00**	**24.43**	**19.70**	**55.86**	100.00
Solid SG		**1.40**	**1.40**	**1.40**	**1.40**	**1.40**	**1.40**	**1.40**	
Ash	%, dry	**14.50**	**14.50**	**14.50**	**14.50**	**14.50**	**14.50**	**14.50**	14.50
Sulfur	%, dry	**1.00**	**1.00**	**1.00**	**1.00**	**1.00**	**1.00**	**1.00**	1.00
BTU/lb	dry	**12825**	**12825**	**12825**	**12825**	**12825**	**12825**	**12825**	12825
BTU/lb	maf	15000	15000	15000	15000	15000	15000	15000	15000
Mass	%, ar	0.00	0.00	0.00	0.00	22.24	18.55	59.21	100.00
Moisture	%, ar	17.73	17.73	17.73	17.73	9.63	12.59	22.38	17.73
Cum. Moisture	%, ar	**17.73**	**17.73**	**17.73**	**17.73**	**17.73**	**20.04**	**22.38**	---
Ash	%, ar	11.93	11.93	11.93	11.93	13.10	12.67	11.25	11.93
Inerts	%, ar	29.65	29.65	29.65	29.65	22.73	25.26	33.63	29.65
Sulfur	%, ar	0.82	0.82	0.82	0.82	0.90	0.87	0.78	0.82
BTU/lb	ar	10552	10552	10552	10552	11590	11211	9955	10552
lb SO2/MM BTU	---	1.56	1.56	1.56	1.56	1.56	1.56	1.56	1.56
Cost to Boiler	$/MM BTU	$2.44	$2.44	$2.44	$2.44	$2.44	$2.44	$2.44	$2.44
Freight Cost	$/MM BTU	$0.95	$0.95	$0.95	$0.95	$0.86	$0.89	$1.00	$0.95
Evap. Cost	$/MM BTU	$0.03	$0.03	$0.03	$0.03	$0.01	$0.02	$0.03	$0.03
Ash Cost	$/MM BTU	$0.11	$0.11	$0.11	$0.11	$0.11	$0.11	$0.11	$0.11
SO2 Cost	$/MM BTU	$0.04	$0.04	$0.04	$0.04	$0.04	$0.04	$0.04	$0.04
Other Cost	$/MM BTU	$0.05	$0.05	$0.05	$0.05	$0.04	$0.04	$0.05	$0.05
Coal Worth	$/MM BTU	$1.27	$1.27	$1.27	$1.27	$1.37	$1.34	$1.20	$1.27
Cost to Boiler	$/ton	$51.49	$51.49	$51.49	$51.49	$56.56	$54.71	$48.58	$51.49
Freight Cost	$/ton	$20.00	$20.00	$20.00	$20.00	$20.00	$20.00	$20.00	$20.00
Evap. Cost	$/ton	$0.53	$0.53	$0.53	$0.53	$0.29	$0.38	$0.67	$0.53
Ash Cost	$/ton	$2.39	$2.39	$2.39	$2.39	$2.62	$2.53	$2.25	$2.39
SO2 Cost	$/ton	$0.76	$0.76	$0.76	$0.76	$0.83	$0.81	$0.72	$0.76
Other Cost	$/ton	$1.00	$1.00	$1.00	$1.00	$1.00	$1.00	$1.00	$1.00
Coal Worth	$/ton	$26.82	$26.82	$26.82	$26.82	$31.82	$29.99	$23.94	$26.82
Individual Tons	dry	0.00	0.00	0.00	0.00	1.82	1.47	4.16	**7.45**
Cum. Tons	dry	7.45	7.45	7.45	7.45	7.45	5.63	4.16	
Individual Tons	ar	0.00	0.00	0.00	0.00	2.01	1.68	5.36	9.05
Cum. Tons	ar	9.05	9.05	9.05	9.05	9.05	7.04	5.36	---
Cum. Mass	%, ar	100.00	100.00	100.00	100.00	100.00	77.76	59.21	---
Cum. Ash	%, ar	11.93	11.93	11.93	11.93	13.10	12.91	11.93	---
Cum. Sulfur	%, ar	0.82	0.82	0.82	0.82	0.90	0.89	0.82	---
Cum. BTU/lb	ar	10552	10552	10552	10552	10760	10820	10740	---
Individual Worth	$	$0.00	$0.00	$0.00	$0.00	$64.09	$50.36	$128.36	$242.81
Cum. Worth	$	$0.00	$0.00	$0.00	$0.00	$64.09	$114.44	$242.81	---

Coal A - Circuit Configuration 1 - Fine Cut - Screenbowl Centrifuge Simulation

Input Parameters

k_d (m^{-1})	ρ_s (kg/m^3)	ρ_w (kg/m^3)	B (m)	ε	σ (N/m)	μ (Pa.s)
400	1400	1000	0.559	0.55	0.072	0.001
L (m)	**t (sec)**	**N (RPM)**	**N_g**	**Air P (psi)**	**g (m/s^2)**	**θ**
0.0381	7	895	500	0	9.81	60

Feed Size Distribution

Top Size (micron)	Bottom Size (micron)	Mean Size (micron)	D (%)	Weight in class (g)	Weight% in class (%)	Cum. Passing (%)
1000	600	774.60	30.98	17.50	18.04	100.00
600	300	424.26	16.97	34.50	35.57	81.96
300	150	212.13	8.49	24.00	24.75	46.38
150	75	106.07	4.24	11.98	12.35	21.64
75	44	57.45	2.30	4.79	4.94	9.29
44	25	33.17	1.33	2.45	2.53	4.35
25	0	5.00	0.20	1.77	1.82	1.82
			Total	96.99	100.00	

Permeability Estimation

D_{eff} (micron)	S_K	S_0	c_1	c_2	k (m^2)	Permeability method to use
126.7	2.34	47346	0.22	4.00	7.33E-11	Tierney

Dewatering Simulation

N_c	C_t	y	S_r	S_e	S	M (%)
2.1897	0.06	2.90	0.054291	0.0557	0.1043	*8.34*

Size Distribution Expansion using Gaudin-Schumann Equation

m	k	Mean Size (micron)	D (%)	Cum. Passing (%)	Weight% in class (%)	Weight in class (g)	Wt/Size
1.201	605						
1180 x 600		841.4	33.66	100.00	1.07	1.03	1.27E-05
600 x 300		424.3	16.97	98.93	55.90	54.22	1.32E-03
300 x 150		212.1	8.49	43.03	24.32	23.58	1.15E-03
150 x 75		106.1	4.24	18.72	10.58	10.26	9.97E-04
75 x 44		57.4	2.30	8.14	3.85	3.73	6.70E-04
44 x 25		33.2	1.33	4.29	2.11	2.05	6.38E-04
25 x 10		15.8	0.63	2.18	1.45	1.41	9.18E-04
10 x 5		7.1	0.28	0.72	0.41	0.40	5.79E-04
5 x 1		2.2	0.09	0.31	0.27	0.26	1.20E-03
1 x 0		0.5	0.00	0.05	0.05	0.04	9.12E-04
				Total	100.00	96.99	0.008395

	Mean
25x0	5.9784
44x0	9.9675
74x0	20.974
150x0	41.896
300x0	75.859
600x0	125.94
1180x0	126.73

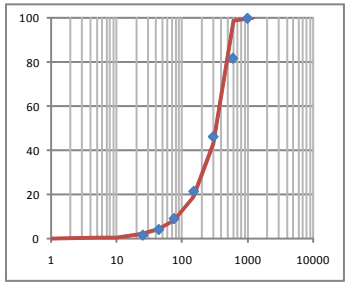

Degradation Model

	Contributing Size Class										New Weight in class (g)	New Weight after loss (g)	New Weight% in class (%)	New Cum. Passing (%)	Effluent Weight in class (g)
	1180 x 600	600 x 300	300 x 150	150 x 75	75 x 44	44 x 25	25 x 10	10 x 5	5 x 1	1 x 0					
1180 x 600	0										0.69	0.69	0.73	100.00	0.00
600 x 300	0.20	0									45.21	45.21	48.07	99.27	0.00
300 x 150	0.09	5.20	0								26.87	26.87	28.56	51.20	0.00
150 x 75	0.04	2.26	1.13	0							13.25	13.25	14.09	22.64	0.00
75 x 44	0.01	0.82	0.41	0.21	0						5.10	5.10	5.43	8.55	0.00
44 x 25	0.01	0.45	0.23	0.11	0.04	0					2.86	1.43	1.52	3.12	1.43
25 x 10	0.01	0.31	0.16	0.08	0.03	0.02	0				2.00	1.00	1.06	1.60	1.00
10 x 5	0.00	0.09	0.04	0.02	0.01	0.01	0.01	0			0.57	0.28	0.30	0.54	0.28
5 x 1	0.00	0.06	0.03	0.01	0.01	0.00	0.00	0.00	0		0.38	0.19	0.20	0.23	0.19
1 x 0	0.00	0.01	0.00	0.00	0.00	0.00	0.00	0.00	0.00	0	0.06	0.03	0.03	0.03	0.03
Total	0.35	9.20	2.00	0.44	0.09	0.03	0.01	0.00	0.00	0.00	96.99	94.05	100.00		2.93

Coal A - Circuit Configuration 1 - Fine Cut - Screenbowl Centrifuge Economics

CALCULATION OF OPTIMUM SIZE CUT

FINANCIAL DATA:		Total Boiler Cost =		$2.44	/MM BTU		Moisture Evap. =		$3.00	/ton H_2O		SO_2 Emission =	$200	/ton SO_2
		Freight Cost =		$20.00	/ton coal		Ash Handling =		$20.00	/ton ash		Other Cost =	$1.00	/ton coal

Size Class		1	2	3	4	5	6	7	Totals
Top Size	µ	**1180**	600	300	150	74	44	25	---
Bottom Size	µ	**600**	**300**	**150**	**74**	**44**	**25**	**0**	---
SG	µ	1.45	1.45	1.45	1.45	1.45	1.45	1.45	---
1/SG	---	0.69	0.69	0.69	0.69	0.69	0.69	0.69	---
Mass	%, dry	**0.73**	**48.07**	**28.56**	**14.09**	**5.43**	**1.52**	**1.60**	100.00
Solid SG		**1.40**	**1.40**	**1.40**	**1.40**	**1.40**	**1.40**	**1.40**	
Ash	%, dry	**14.50**	**14.50**	**14.50**	**14.50**	**14.50**	**14.50**	**14.50**	14.50
Sulfur	%, dry	**1.00**	**1.00**	**1.00**	**1.00**	**1.00**	**1.00**	**1.00**	1.00
BTU/lb	dry	**12825**	**12825**	**12825**	**12825**	**12825**	**12825**	**12825**	12825
BTU/lb	maf	15000	15000	15000	15000	15000	15000	15000	15000
Mass	%, ar	0.69	45.90	27.95	14.62	6.29	2.04	2.51	100.00
Moisture	%, ar	3.10	4.01	6.31	11.69	20.94	31.48	41.77	8.34
Cum. Moisture	%, ar	**8.34**	**8.38**	**12.14**	**18.53**	**27.75**	**37.17**	**41.77**	---
Ash	%, ar	14.05	13.92	13.58	12.80	11.46	9.93	8.44	13.29
Inerts	%, ar	17.15	17.93	19.90	24.49	32.40	41.41	50.22	21.63
Sulfur	%, ar	0.97	0.96	0.94	0.88	0.79	0.69	0.58	0.92
BTU/lb	ar	12428	12311	12015	11326	10140	8788	7468	11755
lb SO2/MM BTU	---	1.56	1.56	1.56	1.56	1.56	1.56	1.56	1.56
Cost to Boiler	$/MM BTU	$2.44	$2.44	$2.44	$2.44	$2.44	$2.44	$2.44	$2.44
Freight Cost	$/MM BTU	$0.80	$0.81	$0.83	$0.88	$0.99	$1.14	$1.34	$0.85
Evap. Cost	$/MM BTU	$0.00	$0.00	$0.01	$0.02	$0.03	$0.05	$0.08	$0.01
Ash Cost	$/MM BTU	$0.11	$0.11	$0.11	$0.11	$0.11	$0.11	$0.11	$0.11
SO2 Cost	$/MM BTU	$0.04	$0.04	$0.04	$0.04	$0.04	$0.04	$0.04	$0.04
Other Cost	$/MM BTU	$0.04	$0.04	$0.04	$0.04	$0.05	$0.06	$0.07	$0.04
Coal Worth	$/MM BTU	$1.44	$1.43	$1.41	$1.35	$1.22	$1.04	$0.80	$1.39
Cost to Boiler	$/ton	$60.65	$60.08	$58.64	$55.27	$49.48	$42.88	$36.44	$57.36
Freight Cost	$/ton	$20.00	$20.00	$20.00	$20.00	$20.00	$20.00	$20.00	$20.00
Evap. Cost	$/ton	$0.09	$0.12	$0.19	$0.35	$0.63	$0.94	$1.25	$0.25
Ash Cost	$/ton	$2.81	$2.78	$2.72	$2.56	$2.29	$1.99	$1.69	$2.66
SO2 Cost	$/ton	$0.89	$0.88	$0.86	$0.81	$0.73	$0.63	$0.54	$0.85
Other Cost	$/ton	$1.00	$1.00	$1.00	$1.00	$1.00	$1.00	$1.00	$1.00
Coal Worth	$/ton	$35.85	$35.29	$33.87	$30.55	$24.83	$18.32	$11.96	$32.61
Individual Tons	dry	0.69	45.21	26.87	13.25	5.10	1.43	1.50	**94.05**
Cum. Tons	dry	94.05	93.37	48.15	21.29	8.04	2.93	1.50	
Individual Tons	ar	0.71	47.10	28.68	15.01	6.46	2.09	2.58	102.62
Cum. Tons	ar	102.62	101.91	54.81	26.13	11.12	4.67	2.58	---
Cum. Mass	%, ar	100.00	99.31	53.41	25.46	10.84	4.55	2.51	---
Cum. Ash	%, ar	14.05	13.92	13.79	13.63	13.49	13.41	13.29	---
Cum. Sulfur	%, ar	0.97	0.96	0.95	0.94	0.93	0.93	0.92	---
Cum. BTU/lb	ar	12428	12369	12295	12206	12128	12077	12038	---
Individual Worth	$	$25.39	$1,662.09	$971.13	$458.35	$160.29	$38.30	$30.85	$3,346.40
Cum. Worth	$	$25.39	$1,687.48	$2,658.60	$3,116.95	$3,277.25	$3,315.55	$3,346.40	---

Coal A - Circuit Configuration 1 - Fine Cut - Hyperbaric Centrifuge Simulation

Input Parameters						
k_d (m^{-1})	ρ_s (kg/m^3)	ρ_w (kg/m^3)	B (m)	ε	σ (N/m)	μ (Pa.s)
400	1400	1000	0.381	0.52	0.072	0.001
L (m)	t (sec)	N (RPM)	N_g	Air P (psi)	g (m/s^2)	θ
0.0127	7	2650	2991	0	9.81	60

Feed Size Distribution						
Top Size (micron)	Bottom Size (micron)	Mean Size (micron)	D (%)	Weight in class (g)	Weight% in class (%)	Cum. Passing (%)
1000	600	774.60	30.98	0.00	0.00	100.00
600	300	424.26	16.97	0.00	0.00	100.00
300	150	212.13	8.49	0.00	0.00	100.00
150	75	106.07	4.24	0.02	0.35	100.00
75	44	57.45	2.30	0.21	3.55	99.64
44	25	33.17	1.33	1.98	33.33	96.09
25	0	5.00	0.20	3.73	62.76	62.76
			Total	5.95	100.00	

Permeability Estimation						
D_{eff} (micron)	S_k	S_0	c_1	c_2	k (m^2)	Permeability method to use
13.0	1.02	463246	0.22	4.00	5.69E-13	Tierney

Dewatering Simulation						
N_c	C_t	y	S_r	S_e	S	M (%)
0.1367	0.40	3.96	0.055424	0.2557	0.2869	*18.17*

Size Distribution Expansion using Gaudin-Schumann Equation								
m	k		Mean Size (micron)	D (%)	Cum. Passing (%)	Weight% in class (%)	Weight in class (g)	Wt/Size
0.753	46							
1180	x	600	841.4	33.66	100.00	0.00	0.00	0.00E+00
600	x	300	424.3	16.97	100.00	0.00	0.00	0.00E+00
300	x	150	212.1	8.49	100.00	0.00	0.00	0.00E+00
150	x	75	106.1	4.24	100.00	0.00	0.00	0.00E+00
75	x	44	57.4	2.30	100.00	3.91	0.23	6.80E-04
44	x	25	33.2	1.33	96.09	33.33	1.98	1.00E-02
25	x	10	15.8	0.63	62.76	31.30	1.86	1.98E-02
10	x	5	7.1	0.28	31.47	31.47	1.87	4.45E-02
5	x	1	2.2	0.09	0.00	0.00	0.00	0.00E+00
1	x	0	0.5	0.00	0.00	0.00	0.00	2.00E-07
					Total	100.00	5.95	0.075025

	Mean	Moisture
25x0	9.4966	21.48
44x0	12.566	18.48
74x0	12.952	18.17
150x0	12.952	18.17
300x0	12.952	18.17
600x0	12.952	18.17
1180x0	12.952	18.17

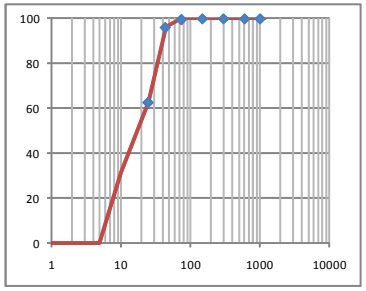

Degradation Model														
			Contributing Size Class										New Weight in class (g)	New Weight% in class (%)	New Cum. Passing (%)
			1180 x 600	600 x 300	300 x 150	150 x 75	75 x 44	44 x 25	25 x 10	10 x 5	5 x 1	1 x 0			
1180	x	600	0										0.00	0.00	100.00
600	x	300	0.00	0									0.00	0.00	100.00
300	x	150	0.00	0.00	0								0.00	0.00	100.00
150	x	75	0.00	0.00	0.00	0							0.00	0.00	100.00
75	x	44	0.00	0.00	0.00	0.00	0						0.23	3.82	100.00
44	x	25	0.00	0.00	0.00	0.00	0.00	0					1.96	32.92	96.18
25	x	10	0.00	0.00	0.00	0.00	0.00	0.01	0				1.86	31.35	63.26
10	x	5	0.00	0.00	0.00	0.00	0.00	0.01	0.01	0			1.89	31.83	31.92
5	x	1	0.00	0.00	0.00	0.00	0.00	0.00	0.00	0.00	0		0.00	0.00	0.09
1	x	0	0.00	0.00	0.00	0.00	0.00	0.00	0.00	0.01	0.00	0	0.01	0.09	0.09
Total			0.00	0.00	0.00	0.00	0.01	0.03	0.01	0.01	0.00	0.00	5.95	100.00	

Coal A - Circuit Configuration 1 - Fine Cut - Hyperbaric Centrifuge Economics

CALCULATION OF OPTIMUM SIZE CUT														
FINANCIAL DATA:		Total Boiler Cost =		$2.44	/MM BTU		Moisture Evap. =		$3.00	/ton H_2O		SO_2 Emission =	$200	/ton SO_2
		Freight Cost =		$20.00	/ton coal		Ash Handling =		$20.00	/ton ash		Other Cost =	$1.00	/ton coal
Size Class		1	2	3	4	5	6	7	Totals					
Top Size	µ	1180	600	300	150	74	44	25	---					
Bottom Size	µ	600	300	150	74	44	25	0	---					
SG	µ	1.45	1.45	1.45	1.45	1.45	1.45	1.45	---					
1/SG	---	0.69	0.69	0.69	0.69	0.69	0.69	0.69	---					
Mass	%, dry	0.00	0.00	0.00	0.00	3.82	32.92	63.26	100.00					
Solid SG		1.40	1.40	1.40	1.40	1.40	1.40	1.40						
Ash	%, dry	14.50	14.50	14.50	14.50	14.50	14.50	14.50	14.50					
Sulfur	%, dry	1.00	1.00	1.00	1.00	1.00	1.00	1.00	1.00					
BTU/lb	dry	12825	12825	12825	12825	12825	12825	12825	12825					
BTU/lb	maf	15000	15000	15000	15000	15000	15000	15000	15000					
Mass	%, ar	0.00	0.00	0.00	0.00	3.45	30.62	65.94	100.00					
Moisture	%, ar	18.17	18.17	18.17	18.17	9.39	12.01	21.48	18.17					
Cum. Moisture	%, ar	18.17	18.17	18.17	18.17	18.17	18.48	21.48	---					
Ash	%, ar	11.86	11.86	11.86	11.86	13.14	12.76	11.38	11.86					
Inerts	%, ar	30.03	30.03	30.03	30.03	22.53	24.77	32.87	30.03					
Sulfur	%, ar	0.82	0.82	0.82	0.82	0.91	0.88	0.79	0.82					
BTU/lb	ar	10495	10495	10495	10495	11621	11285	10070	10495					
lb SO2/MM BTU	---	1.56	1.56	1.56	1.56	1.56	1.56	1.56	1.56					
Cost to Boiler	$/MM BTU	$2.44	$2.44	$2.44	$2.44	$2.44	$2.44	$2.44	$2.44					
Freight Cost	$/MM BTU	$0.95	$0.95	$0.95	$0.95	$0.86	$0.89	$0.99	$0.95					
Evap. Cost	$/MM BTU	$0.03	$0.03	$0.03	$0.03	$0.01	$0.02	$0.03	$0.03					
Ash Cost	$/MM BTU	$0.11	$0.11	$0.11	$0.11	$0.11	$0.11	$0.11	$0.11					
SO2 Cost	$/MM BTU	$0.04	$0.04	$0.04	$0.04	$0.04	$0.04	$0.04	$0.04					
Other Cost	$/MM BTU	$0.05	$0.05	$0.05	$0.05	$0.04	$0.04	$0.05	$0.05					
Coal Worth	$/MM BTU	$1.26	$1.26	$1.26	$1.26	$1.38	$1.34	$1.22	$1.26					
Cost to Boiler	$/ton	$51.22	$51.22	$51.22	$51.22	$56.71	$55.07	$49.14	$51.22					
Freight Cost	$/ton	$20.00	$20.00	$20.00	$20.00	$20.00	$20.00	$20.00	$20.00					
Evap. Cost	$/ton	$0.55	$0.55	$0.55	$0.55	$0.28	$0.36	$0.64	$0.55					
Ash Cost	$/ton	$2.37	$2.37	$2.37	$2.37	$2.63	$2.55	$2.28	$2.37					
SO2 Cost	$/ton	$0.75	$0.75	$0.75	$0.75	$0.84	$0.81	$0.72	$0.75					
Other Cost	$/ton	$1.00	$1.00	$1.00	$1.00	$1.00	$1.00	$1.00	$1.00					
Coal Worth	$/ton	$26.54	$26.54	$26.54	$26.54	$31.97	$30.35	$24.50	$26.54					
Individual Tons	dry	0.00	0.00	0.00	0.00	0.23	1.96	3.76	5.95					
Cum. Tons	dry	5.95	5.95	5.95	5.95	5.95	5.72	3.76						
Individual Tons	ar	0.00	0.00	0.00	0.00	0.25	2.23	4.79	7.27					
Cum. Tons	ar	7.27	7.27	7.27	7.27	7.27	7.02	4.79	---					
Cum. Mass	%, ar	100.00	100.00	100.00	100.00	100.00	96.55	65.94	---					
Cum. Ash	%, ar	11.86	11.86	11.86	11.86	13.14	12.80	11.86	---					
Cum. Sulfur	%, ar	0.82	0.82	0.82	0.82	0.91	0.88	0.82	---					
Cum. BTU/lb	ar	10495	10495	10495	10495	10720	10812	10738	---					
Individual Worth	$	$0.00	$0.00	$0.00	$0.00	$8.01	$67.53	$117.40	$192.93					
Cum. Worth	$	$0.00	$0.00	$0.00	$0.00	$8.01	$75.54	$192.93	---					

Coal A - Circuit Configuration 1 - Summary

Lose 50% 325 M

Send SB effluent to HB

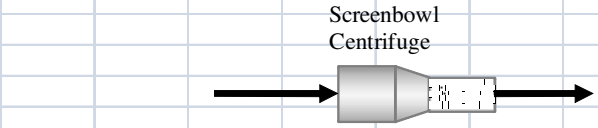

Moisture (%)	Coal Treated (dry tons)	Total Product (dry tons)	Total Product (tons)	Value ($/ton)	Total Value ($)	Net Gain ($/h)	Net Gain ($/year)
11.1	95.0	95.0	106.9	$30.9	$3,304	$0.0	$0.0

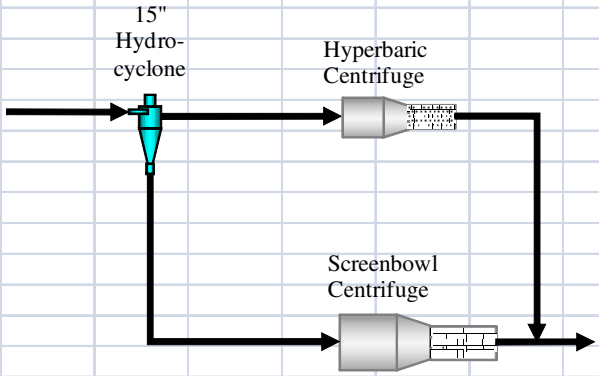

Moisture (%)	Coal Treated With SB (dry tons)	Coal Treated With HFC (dry tons)	Total Product (dry tons)	Total Product (tons)	Value ($/ton)	Total Value ($)	Net Gain ($)	Net Gain ($/year)
8.2	92.6	7.4	100.0	109.0	$32.7	$3,561	$257	$1,541,735

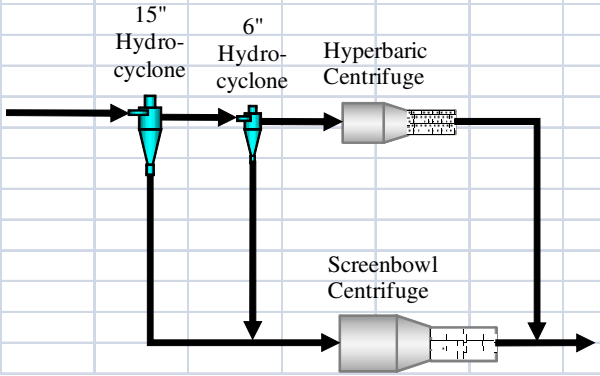

Moisture (%)	Coal Treated With SB (dry tons)	Coal Treated With HFC (dry tons)	Total Product (dry tons)	Total Product (tons)	Value ($/ton)	Total Value ($)	Net Gain ($)	Net Gain ($/year)
9.0	94.1	5.9	100.0	109.9	$32.2	$3,539	$236	$1,413,281

Coal B - Circuit Configuration 1 - Screenbowl Centrifuge Simulation

Input Parameters

k_d (m^{-1})	ρ_s (kg/m^3)	ρ_w (kg/m^3)	B (m)	ε	σ (N/m)	μ (Pa.s)
400	1400	1000	0.559	0.55	0.072	0.001
L (m)	**t (sec)**	**N (RPM)**	**N_g**	**Air P (psi)**	**g (m/s^2)**	**θ**
0.0508	7	895	500	0	9.81	60

Feed Size Distribution

Top Size (micron)	Bottom Size (micron)	Mean Size (micron)	D (%)	Weight in class (g)	Weight% in class (%)	Cum. Passing (%)
1000	600	774.60	30.98	8.0	8.00	100.00
600	300	424.26	16.97	22.0	22.00	92.00
300	150	212.13	8.49	20.0	20.00	70.00
150	75	106.07	4.24	15.5	15.50	50.00
75	44	57.45	2.30	9.0	9.00	34.50
44	25	33.17	1.33	6.5	6.50	25.50
25	0	5.00	0.20	19.0	19.00	19.00
			Total	100.00	100.00	

Permeability Estimation

D_{eff} (micron)	S_K	S_0	c_1	c_2	k (m^2)
46.0	0.95	130384	0.22	4.00	9.67E-12

Permeability method to use: Tierney

Dewatering Simulation

N_c	C_t	y	S_r	S_e	S	M (%)
0.2887	0.59	3.34	0.055339	0.2320	0.2650	*18.79*

Size Distribution Expansion using Gaudin-Schumann Equation

m	k	Mean Size (micron)	D (%)	Cum. Passing (%)	Weight% in class (%)	Weight in class (g)	Wt/Size
0.504	643						
1180 x 600		841.4	33.66	100.00	3.44	3.44	4.09E-05
600 x 300		424.3	16.97	96.56	28.47	28.47	6.71E-04
300 x 150		212.1	8.49	68.09	20.08	20.08	9.46E-04
150 x 75		106.1	4.24	48.01	14.16	14.16	1.33E-03
75 x 44		57.4	2.30	33.86	7.98	7.98	1.39E-03
44 x 25		33.2	1.33	25.88	6.42	6.42	1.93E-03
25 x 10		15.8	0.63	19.46	7.20	7.20	4.55E-03
10 x 5		7.1	0.28	12.26	12.26	12.26	1.73E-02
5 x 1		2.2	0.09	0.00	0.00	0.00	0.00E+00
1 x 0		0.5	0.00	0.00	0.00	0.00	2.00E-07
				Total	100.00	100.00	0.028212

	Mean
5x0	0.5
10x0	6.8498
25x0	8.654
44x0	10.568
74x0	15.232
150x0	22.915
300x0	32.887
600x0	44.851
1180x0	46.018

☑ Lose 50% 325 M

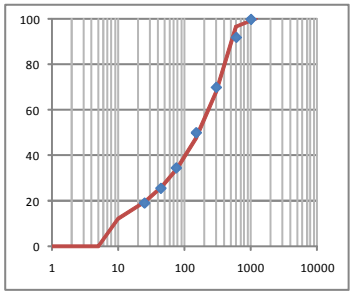

Degradation Model

	Contributing Size Class										New Weight in class (g)	New Weight after loss (g)	New Weight% in class (%)	New Cum. Passing (%)	Effluent Weight in class (g)
	1180 x 600	600 x 300	300 x 150	150 x 75	75 x 44	44 x 25	25 x 10	10 x 5	5 x 1	1 x 0					
1180 x 600	0										2.28	2.28	2.68	100.00	0.00
600 x 300	0.34	0									23.98	23.98	28.14	97.32	0.00
300 x 150	0.24	1.42	0								20.04	20.04	23.52	69.18	0.00
150 x 75	0.17	1.00	0.50	0							15.23	15.23	17.88	45.66	0.00
75 x 44	0.10	0.57	0.28	0.14	0						8.88	8.88	10.42	27.78	0.00
44 x 25	0.08	0.46	0.23	0.11	0.05	0					7.25	3.62	4.25	17.36	3.62
25 x 10	0.09	0.51	0.26	0.13	0.05	0.03	0				8.22	4.11	4.82	13.11	4.11
10 x 5	0.15	0.87	0.44	0.22	0.09	0.05	0.05	0			14.08	7.04	8.26	8.29	7.04
5 x 1	0.00	0.00	0.00	0.00	0.00	0.00	0.00	0.00	0		0.00	0.00	0.00	0.02	0.00
1 x 0	0.00	0.00	0.00	0.00	0.00	0.00	0.00	0.03	0.00	0	0.03	0.02	0.02	0.02	0.02
Total	1.16	4.83	1.70	0.60	0.18	0.09	0.05	0.03	0.00	0.00	100.00	85.21	100.00		14.79

Coal B - Circuit Configuration 1 - Screenbowl Centrifuge Economics

CALCULATION OF OPTIMUM SIZE CUT

FINANCIAL DATA:		Total Boiler Cost =		$2.44	/MM BTU		Moisture Evap. =		$3.00	/ton H_2O		SO_2 Emission =		$200	/ton SO_2
		Freight Cost =		$20.00	/ton coal		Ash Handling =		$20.00	/ton ash		Other Cost =		$1.00	/ton coal

Size Class		1	2	3	4	5	6	7	Totals
Top Size	µ	**1180**	600	300	150	74	44	25	---
Bottom Size	µ	**600**	**300**	**150**	**74**	**44**	**25**	**0**	---
SG	µ	1.45	1.45	1.45	1.45	1.45	1.45	1.45	---
1/SG	---	0.69	0.69	0.69	0.69	0.69	0.69	0.69	---
Mass	%, dry	**2.68**	**28.14**	**23.52**	**17.88**	**10.42**	**4.25**	**13.11**	100.00
Solid SG		**1.40**	**1.40**	**1.40**	**1.40**	**1.40**	**1.40**	**1.40**	
Ash	%, dry	**14.50**	**14.50**	**14.50**	**14.50**	**14.50**	**14.50**	**14.50**	14.50
Sulfur	%, dry	**1.00**	**1.00**	**1.00**	**1.00**	**1.00**	**1.00**	**1.00**	1.00
BTU/lb	dry	**12825**	**12825**	**12825**	**12825**	**12825**	**12825**	**12825**	12825
BTU/lb	maf	15000	15000	15000	15000	15000	15000	15000	15000
Mass	%, ar	2.29	24.52	21.50	17.64	11.32	5.02	17.72	100.00
Moisture	%, ar	4.86	6.80	11.16	17.70	25.21	31.15	39.92	18.79
Cum. Moisture	%, ar	**18.79**	**19.12**	**23.24**	**28.27**	**33.74**	**37.99**	**39.92**	---
Ash	%, ar	13.79	13.51	12.88	11.93	10.84	9.98	8.71	11.77
Inerts	%, ar	18.65	20.31	24.04	29.64	36.05	41.13	48.63	30.56
Sulfur	%, ar	0.95	0.93	0.89	0.82	0.75	0.69	0.60	0.81
BTU/lb	ar	12202	11953	11394	10555	9592	8830	7705	10415
lb SO2/MM BTU	---	1.56	1.56	1.56	1.56	1.56	1.56	1.56	1.56
Cost to Boiler	$/MM BTU	$2.44	$2.44	$2.44	$2.44	$2.44	$2.44	$2.44	$2.44
Freight Cost	$/MM BTU	$0.82	$0.84	$0.88	$0.95	$1.04	$1.13	$1.30	$0.96
Evap. Cost	$/MM BTU	$0.01	$0.01	$0.01	$0.03	$0.04	$0.05	$0.08	$0.03
Ash Cost	$/MM BTU	$0.11	$0.11	$0.11	$0.11	$0.11	$0.11	$0.11	$0.11
SO2 Cost	$/MM BTU	$0.04	$0.04	$0.04	$0.04	$0.04	$0.04	$0.04	$0.04
Other Cost	$/MM BTU	$0.04	$0.04	$0.04	$0.05	$0.05	$0.06	$0.06	$0.05
Coal Worth	$/MM BTU	$1.42	$1.40	$1.35	$1.27	$1.16	$1.05	$0.85	$1.26
Cost to Boiler	$/ton	$59.55	$58.33	$55.60	$51.51	$46.81	$43.09	$37.60	$50.83
Freight Cost	$/ton	$20.00	$20.00	$20.00	$20.00	$20.00	$20.00	$20.00	$20.00
Evap. Cost	$/ton	$0.15	$0.20	$0.33	$0.53	$0.76	$0.93	$1.20	$0.56
Ash Cost	$/ton	$2.76	$2.70	$2.58	$2.39	$2.17	$2.00	$1.74	$2.35
SO2 Cost	$/ton	$0.88	$0.86	$0.82	$0.76	$0.69	$0.63	$0.55	$0.75
Other Cost	$/ton	$1.00	$1.00	$1.00	$1.00	$1.00	$1.00	$1.00	$1.00
Coal Worth	$/ton	$34.76	$33.56	$30.87	$26.83	$22.19	$18.53	$13.11	$26.16
Individual Tons	dry	2.68	28.14	23.52	17.88	10.42	4.25	13.11	**100.00**
Cum. Tons	dry	100.00	97.32	69.18	45.66	27.78	17.36	13.11	
Individual Tons	ar	2.81	30.20	26.47	21.72	13.94	6.18	21.82	123.14
Cum. Tons	ar	123.14	120.32	90.13	63.66	41.93	27.99	21.82	---
Cum. Mass	%, ar	100.00	97.71	73.19	51.69	34.05	22.73	17.72	---
Cum. Ash	%, ar	13.79	13.54	13.24	12.89	12.59	12.43	11.77	---
Cum. Sulfur	%, ar	0.95	0.93	0.91	0.89	0.87	0.86	0.81	---
Cum. BTU/lb	ar	12202	12079	11894	11679	11480	11321	11160	---
Individual Worth	$	$97.83	$1,013.57	$817.23	$582.84	$309.37	$114.47	$285.91	$3,221.21
Cum. Worth	$	$97.83	$1,111.40	$1,928.63	$2,511.46	$2,820.83	$2,935.30	$3,221.21	---

Coal B - Circuit Configuration 1 - Coarse Cut - Screenbowl Centrifuge Simulation

Input Parameters

k_d (m^{-1})	ρ_s (kg/m^3)	ρ_w (kg/m^3)	B (m)	ε	σ (N/m)	μ (Pa.s)
400	1400	1000	0.559	0.55	0.072	0.001
L (m)	**t (sec)**	**N (RPM)**	**N_g**	**Air P (psi)**	**g (m/s^2)**	**θ**
0.0381	7	895	500	0	9.81	60

Feed Size Distribution

Top Size (micron)	Bottom Size (micron)	Mean Size (micron)	D (%)	Weight in class (g)	Weight% in class (%)	Cum. Passing (%)
1000	600	774.60	30.98	8.00	9.79	100.00
600	300	424.26	16.97	22.00	26.91	90.21
300	150	212.13	8.49	19.99	24.45	63.30
150	75	106.07	4.24	15.03	18.38	38.86
75	44	57.45	2.30	7.45	9.11	20.47
44	25	33.17	1.33	3.98	4.87	11.36
25	0	5.00	0.20	5.31	6.49	6.49
			Total	81.75	100.00	

Permeability Estimation

D_{eff} (micron)	S_K	S_0	c_1	c_2	k (m^2)	Permeability method to use
88.7	1.65	67653	0.22	4.00	3.59E-11	Tierney

Dewatering Simulation

N_c	C_t	y	S_r	S_e	S	M (%)
1.0725	0.12	3.05	0.054904	0.0935	0.1388	*10.81*

Size Distribution Expansion using Gaudin-Schumann Equation

m	k	Mean Size (micron)	D (%)	Cum. Passing (%)	Weight% in class (%)	Weight in class (g)	Wt/Size
0.843	556						
1180 x 600		841.4	33.66	100.00	0.00	0.00	0.00E+00
600 x 300		424.3	16.97	100.00	40.54	33.14	9.56E-04
300 x 150		212.1	8.49	59.46	26.31	21.51	1.24E-03
150 x 75		106.1	4.24	33.15	14.67	11.99	1.38E-03
75 x 44		57.4	2.30	18.48	6.69	5.47	1.16E-03
44 x 25		33.2	1.33	11.79	4.47	3.65	1.35E-03
25 x 10		15.8	0.63	7.32	3.94	3.22	2.49E-03
10 x 5		7.1	0.28	3.38	3.38	2.76	4.78E-03
5 x 1		2.2	0.09	0.00	0.00	0.00	0.00E+00
1 x 0		0.5	0.00	0.00	0.00	0.00	2.00E-07
				Total	100.00	81.75	0.013362

	Mean
25x0	9.8493
44x0	13.376
74x0	22.376
150x0	38.118
300x0	61.141
600x0	88.688
1180x0	88.688

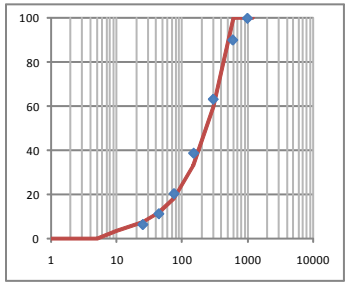

Degradation Model

	Contributing Size Class										New Weight in class (g)	New Weight after loss (g)	New Weight% in class (%)	New Cum. Passing (%)	Effluent Weight in class (g)
	1180 x 600	600 x 300	300 x 150	150 x 75	75 x 44	44 x 25	25 x 10	10 x 5	5 x 1	1 x 0					
1180 x 600	0										0.00	0.00	0.00	100.00	0.00
600 x 300	0.00	0									27.52	27.52	36.29	100.00	0.00
300 x 150	0.00	2.49	0								22.18	22.18	29.25	63.71	0.00
150 x 75	0.00	1.39	0.81	0							13.68	13.68	18.04	34.46	0.00
75 x 44	0.00	0.63	0.37	0.18	0						6.53	6.53	8.61	16.43	0.00
44 x 25	0.00	0.42	0.25	0.12	0.05	0					4.44	2.22	2.93	7.81	2.22
25 x 10	0.00	0.37	0.22	0.11	0.04	0.03	0				3.97	1.98	2.61	4.88	1.98
10 x 5	0.00	0.32	0.19	0.09	0.04	0.02	0.02	0			3.43	1.72	2.26	2.27	1.72
5 x 1	0.00	0.00	0.00	0.00	0.00	0.00	0.00	0.00	0		0.00	0.00	0.00	0.01	0.00
1 x 0	0.00	0.00	0.00	0.00	0.00	0.00	0.00	0.01	0.00	0	0.01	0.00	0.01	0.01	0.00
Total	0.00	5.62	1.83	0.51	0.13	0.05	0.02	0.01	0.00	0.00	81.75	75.83	100.00		5.92

Coal B - Circuit Configuration 1 - Coarse Cut - Screenbowl Centrifuge Economics

CALCULATION OF OPTIMUM SIZE CUT

FINANCIAL DATA:		Total Boiler Cost =		$2.44	/MM BTU		Moisture Evap. =		$3.00	/ton H_2O		SO_2 Emission =	$200	/ton SO_2
		Freight Cost =		$20.00	/ton coal		Ash Handling =		$20.00	/ton ash		Other Cost =	$1.00	/ton coal

Size Class		1	2	3	4	5	6	7	Totals
Top Size	µ	**1180**	600	300	150	74	44	25	---
Bottom Size	µ	**600**	**300**	**150**	**74**	**44**	**25**	**0**	---
SG	µ	1.45	1.45	1.45	1.45	1.45	1.45	1.45	---
1/SG	---	0.69	0.69	0.69	0.69	0.69	0.69	0.69	---
Mass	%, dry	**0.00**	**36.29**	**29.25**	**18.04**	**8.61**	**2.93**	**4.88**	100.00
Solid SG		**1.40**	**1.40**	**1.40**	**1.40**	**1.40**	**1.40**	**1.40**	
Ash	%, dry	**14.50**	**14.50**	**14.50**	**14.50**	**14.50**	**14.50**	**14.50**	14.50
Sulfur	%, dry	**1.00**	**1.00**	**1.00**	**1.00**	**1.00**	**1.00**	**1.00**	1.00
BTU/lb	dry	**12825**	**12825**	**12825**	**12825**	**12825**	**12825**	**12825**	12825
BTU/lb	maf	15000	15000	15000	15000	15000	15000	15000	15000
Mass	%, ar	0.00	33.75	27.96	18.26	9.52	3.57	6.95	100.00
Moisture	%, ar	10.81	4.11	6.71	11.87	19.29	26.75	37.29	10.81
Cum. Moisture	%, ar	**10.81**	**10.81**	**14.22**	**19.71**	**26.86**	**33.72**	**37.29**	---
Ash	%, ar	12.93	13.90	13.53	12.78	11.70	10.62	9.09	12.93
Inerts	%, ar	23.74	18.01	20.23	24.65	30.99	37.37	46.39	23.74
Sulfur	%, ar	0.89	0.96	0.93	0.88	0.81	0.73	0.63	0.89
BTU/lb	ar	11439	12299	11965	11303	10351	9395	8042	11439
lb SO2/MM BTU	---	1.56	1.56	1.56	1.56	1.56	1.56	1.56	1.56
Cost to Boiler	$/MM BTU	$2.44	$2.44	$2.44	$2.44	$2.44	$2.44	$2.44	$2.44
Freight Cost	$/MM BTU	$0.87	$0.81	$0.84	$0.88	$0.97	$1.06	$1.24	$0.87
Evap. Cost	$/MM BTU	$0.01	$0.01	$0.01	$0.02	$0.03	$0.04	$0.07	$0.01
Ash Cost	$/MM BTU	$0.11	$0.11	$0.11	$0.11	$0.11	$0.11	$0.11	$0.11
SO2 Cost	$/MM BTU	$0.04	$0.04	$0.04	$0.04	$0.04	$0.04	$0.04	$0.04
Other Cost	$/MM BTU	$0.04	$0.04	$0.04	$0.04	$0.05	$0.05	$0.06	$0.04
Coal Worth	$/MM BTU	$1.36	$1.43	$1.41	$1.35	$1.25	$1.13	$0.92	$1.36
Cost to Boiler	$/ton	$55.82	$60.02	$58.39	$55.16	$50.51	$45.85	$39.25	$55.82
Freight Cost	$/ton	$20.00	$20.00	$20.00	$20.00	$20.00	$20.00	$20.00	$20.00
Evap. Cost	$/ton	$0.32	$0.12	$0.20	$0.36	$0.58	$0.80	$1.12	$0.32
Ash Cost	$/ton	$2.59	$2.78	$2.71	$2.56	$2.34	$2.12	$1.82	$2.59
SO2 Cost	$/ton	$0.82	$0.88	$0.86	$0.81	$0.74	$0.68	$0.58	$0.82
Other Cost	$/ton	$1.00	$1.00	$1.00	$1.00	$1.00	$1.00	$1.00	$1.00
Coal Worth	$/ton	$31.09	$35.23	$33.62	$30.44	$25.85	$21.25	$14.73	$31.09
Individual Tons	dry	0.00	27.52	22.18	13.68	6.53	2.22	3.70	**75.83**
Cum. Tons	dry	75.83	75.83	48.31	26.13	12.46	5.92	3.70	
Individual Tons	ar	0.00	28.70	23.77	15.52	8.09	3.03	5.91	85.02
Cum. Tons	ar	85.02	85.02	56.32	32.55	17.03	8.94	5.91	---
Cum. Mass	%, ar	100.00	100.00	66.25	38.29	20.03	10.51	6.95	---
Cum. Ash	%, ar	12.93	13.90	13.73	13.51	13.32	13.22	12.93	---
Cum. Sulfur	%, ar	0.89	0.96	0.95	0.93	0.92	0.91	0.89	---
Cum. BTU/lb	ar	11439	11869	11893	11819	11728	11655	11581	---
Individual Worth	$	$0.00	$1,010.94	$799.21	$472.38	$209.16	$64.44	$86.99	$2,643.12
Cum. Worth	$	$0.00	$1,010.94	$1,810.16	$2,282.54	$2,491.69	$2,556.13	$2,643.12	---

Coal B - Circuit Configuration 1 - Coarse Cut - Hyperbaric Centrifuge Simulation

Input Parameters						
k_d (m^{-1})	ρ_s (kg/m^3)	ρ_w (kg/m^3)	B (m)	ε	σ (N/m)	μ (Pa.s)
400	1400	1000	0.381	0.52	0.072	0.001
L (m)	t (sec)	N (RPM)	N_g	Air P (psi)	g (m/s^2)	θ
0.0127	7	2650	2991	0	9.81	60

Feed Size Distribution						
Top Size (micron)	Bottom Size (micron)	Mean Size (micron)	D (%)	Weight in class (g)	Weight% in class (%)	Cum. Passing (%)
1000	600	774.60	30.98	0.00	0.00	100.00
600	300	424.26	16.97	0.00	0.00	100.00
300	150	212.13	8.49	0.01	0.05	100.00
150	75	106.07	4.24	0.47	1.96	99.95
75	44	57.45	2.30	1.55	6.42	97.99
44	25	33.17	1.33	4.74	19.61	91.58
25	0	5.00	0.20	17.40	71.97	71.97
			Total	24.17	100.00	

Permeability Estimation						
D_{eff} (micron)	S_k	S_0	c_1	c_2	k (m^2)	Permeability method to use
9.9	2.39	606248	0.22	4.00	3.32E-13	Tierney

Dewatering Simulation						
N_c	C_t	y	S_r	S_e	S	M (%)
0.0798	0.68	4.10	0.055455	0.3179	0.3442	*21.03*

Size Distribution Expansion using Gaudin-Schumann Equation								
m		k	Mean Size (micron)	D (%)	Cum. Passing (%)	Weight% in class (%)	Weight in class (g)	Wt/Size
0.282		73						
1180	x	600	841.4	33.66	100.00	0.00	0.00	0.00E+00
600	x	300	424.3	16.97	100.00	0.00	0.00	0.00E+00
300	x	150	212.1	8.49	100.00	0.00	0.00	0.00E+00
150	x	75	106.1	4.24	100.00	0.00	0.00	0.00E+00
75	x	44	57.4	2.30	100.00	13.30	3.22	2.32E-03
44	x	25	33.2	1.33	86.70	12.79	3.09	3.86E-03
25	x	10	15.8	0.63	73.91	16.85	4.07	1.07E-02
10	x	5	7.1	0.28	57.05	57.05	13.79	8.07E-02
5	x	1	2.2	0.09	0.00	0.00	0.00	0.00E+00
1	x	0	0.5	0.00	0.00	0.00	0.00	2.00E-07
					Total	100.00	24.17	0.097518

	Mean	Moisture
25x0	7.8282	23.64
44x0	8.808	22.32
74x0	9.8969	21.03
150x0	9.8969	21.03
300x0	9.8969	21.03
600x0	9.8969	21.03
1180x0	9.8969	21.03

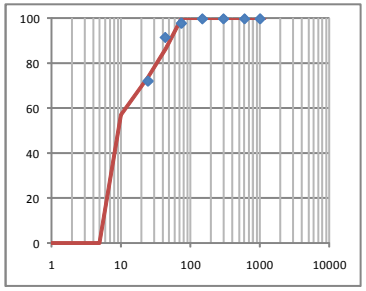

Degradation Model														
			Contributing Size Class										New Weight in class (g)	New Weight% in class (%)	New Cum. Passing (%)
			1180 x 600	600 x 300	300 x 150	150 x 75	75 x 44	44 x 25	25 x 10	10 x 5	5 x 1	1 x 0			
1180	x	600	0										0.00	0.00	100.00
600	x	300	0.00	0									0.00	0.00	100.00
300	x	150	0.00	0.00	0								0.00	0.00	100.00
150	x	75	0.00	0.00	0.00	0							0.00	0.00	100.00
75	x	44	0.00	0.00	0.00	0.00	0						3.14	13.00	100.00
44	x	25	0.00	0.00	0.00	0.00	0.01	0					3.06	12.67	87.00
25	x	10	0.00	0.00	0.00	0.00	0.01	0.01	0				4.07	16.84	74.34
10	x	5	0.00	0.00	0.00	0.00	0.05	0.03	0.03	0			13.86	57.33	57.49
5	x	1	0.00	0.00	0.00	0.00	0.00	0.00	0.00	0.00	0		0.00	0.00	0.16
1	x	0	0.00	0.00	0.00	0.00	0.00	0.00	0.00	0.04	0.00	0	0.04	0.16	0.16
Total			0.00	0.00	0.00	0.00	0.07	0.04	0.03	0.04	0.00	0.00	24.17	100.00	

Coal B - Circuit Configuration 1 - Coarse Cut - Hyperbaric Centrifuge Economics

CALCULATION OF OPTIMUM SIZE CUT

FINANCIAL DATA:		Total Boiler Cost =		$2.44	/MM BTU		Moisture Evap. =		$3.00	/ton H_2O		SO_2 Emission =	$200	/ton SO_2
		Freight Cost =		$20.00	/ton coal		Ash Handling =		$20.00	/ton ash		Other Cost =	$1.00	/ton coal

Size Class		1	2	3	4	5	6	7	Totals
Top Size	µ	**1180**	600	300	150	74	44	25	---
Bottom Size	µ	**600**	**300**	**150**	**74**	**44**	**25**	**0**	---
SG	µ	1.45	1.45	1.45	1.45	1.45	1.45	1.45	---
1/SG	---	0.69	0.69	0.69	0.69	0.69	0.69	0.69	---
Mass	%, dry	**0.00**	**0.00**	**0.00**	**0.00**	**13.00**	**12.67**	**74.34**	100.00
Solid SG		**1.40**	**1.40**	**1.40**	**1.40**	**1.40**	**1.40**	**1.40**	
Ash	%, dry	**14.50**	**14.50**	**14.50**	**14.50**	**14.50**	**14.50**	**14.50**	14.50
Sulfur	%, dry	**1.00**	**1.00**	**1.00**	**1.00**	**1.00**	**1.00**	**1.00**	1.00
BTU/lb	dry	**12825**	**12825**	**12825**	**12825**	**12825**	**12825**	**12825**	12825
BTU/lb	maf	15000	15000	15000	15000	15000	15000	15000	15000
Mass	%, ar	0.00	0.00	0.00	0.00	11.55	11.57	76.87	100.00
Moisture	%, ar	21.03	21.03	21.03	21.03	11.18	13.55	23.64	21.03
Cum. Moisture	%, ar	**21.03**	**21.03**	**21.03**	**21.03**	**21.03**	**22.32**	**23.64**	---
Ash	%, ar	11.45	11.45	11.45	11.45	12.88	12.53	11.07	11.45
Inerts	%, ar	32.48	32.48	32.48	32.48	24.06	26.08	34.71	32.48
Sulfur	%, ar	0.79	0.79	0.79	0.79	0.89	0.86	0.76	0.79
BTU/lb	ar	10128	10128	10128	10128	11391	11087	9794	10128
lb SO2/MM BTU	---	1.56	1.56	1.56	1.56	1.56	1.56	1.56	1.56
Cost to Boiler	$/MM BTU	$2.44	$2.44	$2.44	$2.44	$2.44	$2.44	$2.44	$2.44
Freight Cost	$/MM BTU	$0.99	$0.99	$0.99	$0.99	$0.88	$0.90	$1.02	$0.99
Evap. Cost	$/MM BTU	$0.03	$0.03	$0.03	$0.03	$0.01	$0.02	$0.04	$0.03
Ash Cost	$/MM BTU	$0.11	$0.11	$0.11	$0.11	$0.11	$0.11	$0.11	$0.11
SO2 Cost	$/MM BTU	$0.04	$0.04	$0.04	$0.04	$0.04	$0.04	$0.04	$0.04
Other Cost	$/MM BTU	$0.05	$0.05	$0.05	$0.05	$0.04	$0.05	$0.05	$0.05
Coal Worth	$/MM BTU	$1.22	$1.22	$1.22	$1.22	$1.35	$1.33	$1.18	$1.22
Cost to Boiler	$/ton	$49.42	$49.42	$49.42	$49.42	$55.59	$54.11	$47.79	$49.42
Freight Cost	$/ton	$20.00	$20.00	$20.00	$20.00	$20.00	$20.00	$20.00	$20.00
Evap. Cost	$/ton	$0.63	$0.63	$0.63	$0.63	$0.34	$0.41	$0.71	$0.63
Ash Cost	$/ton	$2.29	$2.29	$2.29	$2.29	$2.58	$2.51	$2.21	$2.29
SO2 Cost	$/ton	$0.73	$0.73	$0.73	$0.73	$0.82	$0.80	$0.70	$0.73
Other Cost	$/ton	$1.00	$1.00	$1.00	$1.00	$1.00	$1.00	$1.00	$1.00
Coal Worth	$/ton	$24.78	$24.78	$24.78	$24.78	$30.86	$29.40	$23.17	$24.78
Individual Tons	dry	0.00	0.00	0.00	0.00	3.14	3.06	17.97	**24.17**
Cum. Tons	dry	24.17	24.17	24.17	24.17	24.17	21.03	17.97	
Individual Tons	ar	0.00	0.00	0.00	0.00	3.54	3.54	23.53	30.61
Cum. Tons	ar	30.61	30.61	30.61	30.61	30.61	27.07	23.53	---
Cum. Mass	%, ar	100.00	100.00	100.00	100.00	100.00	88.45	76.87	---
Cum. Ash	%, ar	11.45	11.45	11.45	11.45	12.88	12.71	11.45	---
Cum. Sulfur	%, ar	0.79	0.79	0.79	0.79	0.89	0.88	0.79	---
Cum. BTU/lb	ar	10128	10128	10128	10128	10381	10487	10407	---
Individual Worth	$	$0.00	$0.00	$0.00	$0.00	$109.14	$104.13	$545.11	$758.38
Cum. Worth	$	$0.00	$0.00	$0.00	$0.00	$109.14	$213.27	$758.38	---

Coal B - Circuit Configuration 1 - Fine Cut - Screenbowl Centrifuge Simulation

Input Parameters						
k_d (m^{-1})	ρ_s (kg/m^3)	ρ_w (kg/m^3)	B (m)	ε	σ (N/m)	μ (Pa.s)
400	1400	1000	0.559	0.55	0.072	0.001
L (m)	t (sec)	N (RPM)	N_g	Air P (psi)	g (m/s^2)	θ
0.0381	7	895	500	0	9.81	60

Feed Size Distribution						
Top Size (micron)	Bottom Size (micron)	Mean Size (micron)	D (%)	Weight in class (g)	Weight% in class (%)	Cum. Passing (%)
1000	600	774.60	30.98	8.00	9.11	100.00
600	300	424.26	16.97	22.00	25.06	90.89
300	150	212.13	8.49	20.00	22.78	65.83
150	75	106.07	4.24	15.47	17.62	43.05
75	44	57.45	2.30	8.62	9.82	25.43
44	25	33.17	1.33	5.31	6.05	15.61
25	0	5.00	0.20	8.40	9.57	9.57
			Total	87.80	100.00	

Permeability Estimation						
D_{eff} (micron)	S_K	S_0	c_1	c_2	k (m^2)	Permeability method to use
71.4	1.50	83977	0.22	4.00	2.33E-11	Tierney

Dewatering Simulation						
N_c	C_t	y	S_r	S_e	S	M (%)
0.6961	0.18	3.14	0.055113	0.1239	0.1664	12.69

Size Distribution Expansion using Gaudin-Schumann Equation								
m		k	Mean Size (micron)	D (%)	Cum. Passing (%)	Weight% in class (%)	Weight in class (g)	Wt/Size
0.716		573						
1180	x	600	841.4	33.66	100.00	0.00	0.00	0.00E+00
600	x	300	424.3	16.97	100.00	37.09	32.57	8.74E-04
300	x	150	212.1	8.49	62.91	24.62	21.62	1.16E-03
150	x	75	106.1	4.24	38.29	14.98	13.16	1.41E-03
75	x	44	57.4	2.30	23.30	7.40	6.50	1.29E-03
44	x	25	33.2	1.33	15.90	5.30	4.65	1.60E-03
25	x	10	15.8	0.63	10.61	5.11	4.48	3.23E-03
10	x	5	7.1	0.28	5.50	5.50	4.83	7.78E-03
5	x	1	2.2	0.09	0.00	0.00	0.00	0.00E+00
1	x	0	0.5	0.00	0.00	0.00	0.00	2.00E-07
					Total	100.00	87.80	0.017343

	Mean
25x0	9.41
44x0	12.315
74x0	19.643
150x0	32.258
300x0	50.004
600x0	71.448
1180x0	71.448

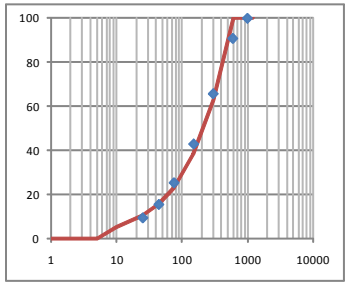

Degradation Model																
			Contributing Size Class										New Weight in class (g)	New Weight after loss (g)	New Weight% in class (%)	New Cum. Passing (%)	Effluent Weight in class (g)
			1180 x 600	600 x 300	300 x 150	150 x 75	75 x 44	44 x 25	25 x 10	10 x 5	5 x 1	1 x 0					
1180	x	600	0										0.00	0.00	0.00	100.00	0.00
600	x	300	0.00	0									27.04	27.04	34.02	100.00	0.00
300	x	150	0.00	2.16	0								21.95	21.95	27.61	65.98	0.00
150	x	75	0.00	1.32	0.72	0							14.63	14.63	18.41	38.36	0.00
75	x	44	0.00	0.65	0.35	0.18	0						7.53	7.53	9.47	19.95	0.00
44	x	25	0.00	0.47	0.25	0.13	0.05	0					5.48	2.74	3.45	10.48	2.74
25	x	10	0.00	0.45	0.24	0.12	0.05	0.03	0				5.35	2.67	3.36	7.03	2.67
10	x	5	0.00	0.48	0.26	0.13	0.05	0.03	0.03	0			5.81	2.90	3.65	3.66	2.90
5	x	1	0.00	0.00	0.00	0.00	0.00	0.00	0.00	0.00	0		0.00	0.00	0.00	0.01	0.00
1	x	0	0.00	0.00	0.00	0.00	0.00	0.00	0.00	0.01	0.00	0	0.01	0.01	0.01	0.01	0.01
Total			0.00	5.53	1.83	0.56	0.15	0.06	0.03	0.01	0.00	0.00	87.80	79.48	100.00		8.33

Coal B - Circuit Configuration 1 - Fine Cut - Screenbowl Centrifuge Economics

CALCULATION OF OPTIMUM SIZE CUT

FINANCIAL DATA:		Total Boiler Cost =		$2.44	/MM BTU		Moisture Evap. =		$3.00	/ton H_2O		SO_2 Emission =	$200	/ton SO_2
		Freight Cost =		$20.00	/ton coal		Ash Handling =		$20.00	/ton ash		Other Cost =	$1.00	/ton coal

Size Class		1	2	3	4	5	6	7	Totals
Top Size	µ	**1180**	600	300	150	74	44	25	---
Bottom Size	µ	**600**	**300**	**150**	**74**	**44**	**25**	**0**	---
SG	µ	1.45	1.45	1.45	1.45	1.45	1.45	1.45	---
1/SG	---	0.69	0.69	0.69	0.69	0.69	0.69	0.69	---
Mass	%, dry	**0.00**	**34.02**	**27.61**	**18.41**	**9.47**	**3.45**	**7.03**	100.00
Solid SG		**1.40**	**1.40**	**1.40**	**1.40**	**1.40**	**1.40**	**1.40**	
Ash	%, dry	**14.50**	**14.50**	**14.50**	**14.50**	**14.50**	**14.50**	**14.50**	14.50
Sulfur	%, dry	**1.00**	**1.00**	**1.00**	**1.00**	**1.00**	**1.00**	**1.00**	1.00
BTU/lb	dry	**12825**	**12825**	**12825**	**12825**	**12825**	**12825**	**12825**	12825
BTU/lb	maf	15000	15000	15000	15000	15000	15000	15000	15000
Mass	%, ar	0.00	31.08	26.04	18.47	10.40	4.16	9.86	100.00
Moisture	%, ar	12.69	4.41	7.42	12.94	20.45	27.50	37.78	12.69
Cum. Moisture	%, ar	**12.69**	**12.69**	**16.42**	**21.89**	**28.65**	**34.73**	**37.78**	---
Ash	%, ar	12.66	13.86	13.42	12.62	11.53	10.51	9.02	12.66
Inerts	%, ar	25.35	18.27	20.84	25.57	31.98	38.01	46.80	25.35
Sulfur	%, ar	0.87	0.96	0.93	0.87	0.80	0.72	0.62	0.87
BTU/lb	ar	11198	12259	11874	11165	10203	9298	7980	11198
lb SO2/MM BTU	---	1.56	1.56	1.56	1.56	1.56	1.56	1.56	1.56
Cost to Boiler	$/MM BTU	$2.44	$2.44	$2.44	$2.44	$2.44	$2.44	$2.44	$2.44
Freight Cost	$/MM BTU	$0.89	$0.82	$0.84	$0.90	$0.98	$1.08	$1.25	$0.89
Evap. Cost	$/MM BTU	$0.02	$0.01	$0.01	$0.02	$0.03	$0.04	$0.07	$0.02
Ash Cost	$/MM BTU	$0.11	$0.11	$0.11	$0.11	$0.11	$0.11	$0.11	$0.11
SO2 Cost	$/MM BTU	$0.04	$0.04	$0.04	$0.04	$0.04	$0.04	$0.04	$0.04
Other Cost	$/MM BTU	$0.04	$0.04	$0.04	$0.04	$0.05	$0.05	$0.06	$0.04
Coal Worth	$/MM BTU	$1.34	$1.43	$1.40	$1.33	$1.23	$1.12	$0.90	$1.34
Cost to Boiler	$/ton	$54.65	$59.83	$57.94	$54.49	$49.79	$45.37	$38.94	$54.65
Freight Cost	$/ton	$20.00	$20.00	$20.00	$20.00	$20.00	$20.00	$20.00	$20.00
Evap. Cost	$/ton	$0.38	$0.13	$0.22	$0.39	$0.61	$0.83	$1.13	$0.38
Ash Cost	$/ton	$2.53	$2.77	$2.68	$2.52	$2.31	$2.10	$1.80	$2.53
SO2 Cost	$/ton	$0.80	$0.88	$0.85	$0.80	$0.73	$0.67	$0.57	$0.80
Other Cost	$/ton	$1.00	$1.00	$1.00	$1.00	$1.00	$1.00	$1.00	$1.00
Coal Worth	$/ton	$29.93	$35.04	$33.18	$29.77	$25.14	$20.78	$14.43	$29.93
Individual Tons	dry	0.00	27.04	21.95	14.63	7.53	2.74	5.58	**79.48**
Cum. Tons	dry	79.48	79.48	52.44	30.49	15.86	8.33	5.58	
Individual Tons	ar	0.00	28.29	23.70	16.81	9.46	3.78	8.98	91.02
Cum. Tons	ar	91.02	91.02	62.74	39.03	22.22	12.76	8.98	---
Cum. Mass	%, ar	100.00	100.00	68.92	42.88	24.41	14.02	9.86	---
Cum. Ash	%, ar	12.66	13.86	13.66	13.41	13.18	13.06	12.66	---
Cum. Sulfur	%, ar	0.87	0.96	0.94	0.92	0.91	0.90	0.87	---
Cum. BTU/lb	ar	11198	11729	11766	11683	11576	11485	11389	---
Individual Worth	$	$0.00	$991.22	$786.61	$500.41	$237.90	$78.58	$129.52	$2,724.24
Cum. Worth	$	$0.00	$991.22	$1,777.83	$2,278.24	$2,516.14	$2,594.73	$2,724.24	---

Coal B - Circuit Configuration 1 - Fine Cut - Hyperbaric Centrifuge Simulation

Input Parameters						
k_d (m^{-1})	ρ_s (kg/m^3)	ρ_w (kg/m^3)	B (m)	ε	σ (N/m)	μ (Pa.s)
400	1400	1000	0.381	0.52	0.072	0.001
L (m)	t (sec)	N (RPM)	N_g	Air P (psi)	g (m/s^2)	θ
0.0127	7	2650	2991	0	9.81	60

Feed Size Distribution						
Top Size (micron)	Bottom Size (micron)	Mean Size (micron)	D (%)	Weight in class (g)	Weight% in class (%)	Cum. Passing (%)
1000	600	774.60	30.98	0.00	0.00	100.00
600	300	424.26	16.97	0.00	0.00	100.00
300	150	212.13	8.49	0.00	0.00	100.00
150	75	106.07	4.24	0.03	0.13	100.00
75	44	57.45	2.30	0.38	1.85	99.87
44	25	33.17	1.33	3.93	19.16	98.02
25	0	5.00	0.20	16.18	78.85	78.85
			Total	20.52	100.00	

Permeability Estimation						
D_{eff} (micron)	S_k	S_0	c_1	c_2	k (m^2)	Permeability method to use
9.7	2.07	615646	0.22	4.00	3.22E-13	Tierney

Dewatering Simulation						
N_c	C_t	y	S_r	S_e	S	M (%)
0.0774	0.70	4.11	0.055457	0.3217	0.3477	*21.20*

Size Distribution Expansion using Gaudin-Schumann Equation								
m	k	Mean Size (micron)	D (%)	Cum. Passing (%)	Weight% in class (%)	Weight in class (g)	Wt/Size	
0.385	46							
1180	x 600	841.4	33.66	100.00	0.00	0.00	0.00E+00	
600	x 300	424.3	16.97	100.00	0.00	0.00	0.00E+00	
300	x 150	212.1	8.49	100.00	0.00	0.00	0.00E+00	
150	x 75	106.1	4.24	100.00	0.00	0.00	0.00E+00	
75	x 44	57.4	2.30	100.00	1.98	0.41	3.46E-04	
44	x 25	33.2	1.33	98.02	19.16	3.93	5.78E-03	
25	x 10	15.8	0.63	78.85	23.43	4.81	1.48E-02	
10	x 5	7.1	0.28	55.42	55.42	11.37	7.84E-02	
5	x 1	2.2	0.09	0.00	0.00	0.00	0.00E+00	
1	x 0	0.5	0.00	0.00	0.00	0.00	2.00E-07	
				Total	100.00	20.52	0.099317	

	Mean	Moisture
25x0	8.1956	23.12
44x0	9.5884	21.38
74x0	9.7459	21.20
150x0	9.7459	21.20
300x0	9.7459	21.20
600x0	9.7459	21.20
1180x0	9.7459	21.20

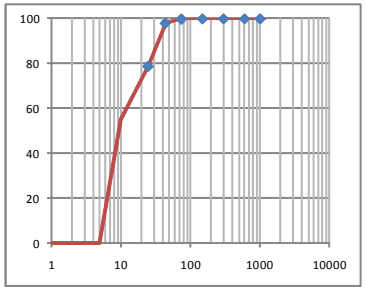

Degradation Model														
	Contributing Size Class										New Weight in class (g)	New Weight% in class (%)	New Cum. Passing (%)	
	1180 x 600	600 x 300	300 x 150	150 x 75	75 x 44	44 x 25	25 x 10	10 x 5	5 x 1	1 x 0				
1180 x 600	0										0.00	0.00	100.00	
600 x 300	0.00	0									0.00	0.00	100.00	
300 x 150	0.00	0.00	0								0.00	0.00	100.00	
150 x 75	0.00	0.00	0.00	0							0.00	0.00	100.00	
75 x 44	0.00	0.00	0.00	0.00	0						0.40	1.94	100.00	
44 x 25	0.00	0.00	0.00	0.00	0.00	0					3.88	18.92	98.06	
25 x 10	0.00	0.00	0.00	0.00	0.00	0.02	0				4.80	23.37	79.14	
10 x 5	0.00	0.00	0.00	0.00	0.01	0.04	0.03	0			11.41	55.61	55.77	
5 x 1	0.00	0.00	0.00	0.00	0.00	0.00	0.00	0.00	0		0.00	0.00	0.16	
1 x 0	0.00	0.00	0.00	0.00	0.00	0.00	0.00	0.03	0.00	0	0.03	0.16	0.16	
Total	0.00	0.00	0.00	0.00	0.01	0.05	0.03	0.03	0.00	0.00	20.52	100.00		

Coal B - Circuit Configuration 1 - Fine Cut - Hyperbaric Centrifuge Economics

CALCULATION OF OPTIMUM SIZE CUT

FINANCIAL DATA:		Total Boiler Cost =		$2.44	/MM BTU		Moisture Evap. =		$3.00	/ton H_2O		SO_2 Emission =	$200	/ton SO_2
		Freight Cost =		$20.00	/ton coal		Ash Handling =		$20.00	/ton ash		Other Cost =	$1.00	/ton coal

Size Class		1	2	3	4	5	6	7	Totals
Top Size	µ	**1180**	600	300	150	74	44	25	---
Bottom Size	µ	**600**	**300**	**150**	**74**	**44**	**25**	**0**	---
SG	µ	1.45	1.45	1.45	1.45	1.45	1.45	1.45	---
1/SG	---	0.69	0.69	0.69	0.69	0.69	0.69	0.69	---
Mass	%, dry	**0.00**	**0.00**	**0.00**	**0.00**	**1.94**	**18.92**	**79.14**	100.00
Solid SG		**1.40**	**1.40**	**1.40**	**1.40**	**1.40**	**1.40**	**1.40**	
Ash	%, dry	**14.50**	**14.50**	**14.50**	**14.50**	**14.50**	**14.50**	**14.50**	14.50
Sulfur	%, dry	**1.00**	**1.00**	**1.00**	**1.00**	**1.00**	**1.00**	**1.00**	1.00
BTU/lb	dry	**12825**	**12825**	**12825**	**12825**	**12825**	**12825**	**12825**	12825
BTU/lb	maf	15000	15000	15000	15000	15000	15000	15000	15000
Mass	%, ar	0.00	0.00	0.00	0.00	1.72	17.16	81.12	100.00
Moisture	%, ar	21.20	21.20	21.20	21.20	10.96	13.14	23.12	21.20
Cum. Moisture	%, ar	**21.20**	**21.20**	**21.20**	**21.20**	**21.20**	**21.38**	**23.12**	---
Ash	%, ar	11.42	11.42	11.42	11.42	12.91	12.59	11.15	11.42
Inerts	%, ar	32.62	32.62	32.62	32.62	23.87	25.73	34.27	32.62
Sulfur	%, ar	0.79	0.79	0.79	0.79	0.89	0.87	0.77	0.79
BTU/lb	ar	10106	10106	10106	10106	11420	11141	9860	10106
lb SO2/MM BTU	---	1.56	1.56	1.56	1.56	1.56	1.56	1.56	1.56
Cost to Boiler	$/MM BTU	$2.44	$2.44	$2.44	$2.44	$2.44	$2.44	$2.44	$2.44
Freight Cost	$/MM BTU	$0.99	$0.99	$0.99	$0.99	$0.88	$0.90	$1.01	$0.99
Evap. Cost	$/MM BTU	$0.03	$0.03	$0.03	$0.03	$0.01	$0.02	$0.04	$0.03
Ash Cost	$/MM BTU	$0.11	$0.11	$0.11	$0.11	$0.11	$0.11	$0.11	$0.11
SO2 Cost	$/MM BTU	$0.04	$0.04	$0.04	$0.04	$0.04	$0.04	$0.04	$0.04
Other Cost	$/MM BTU	$0.05	$0.05	$0.05	$0.05	$0.04	$0.04	$0.05	$0.05
Coal Worth	$/MM BTU	$1.22	$1.22	$1.22	$1.22	$1.36	$1.33	$1.19	$1.22
Cost to Boiler	$/ton	$49.32	$49.32	$49.32	$49.32	$55.73	$54.37	$48.12	$49.32
Freight Cost	$/ton	$20.00	$20.00	$20.00	$20.00	$20.00	$20.00	$20.00	$20.00
Evap. Cost	$/ton	$0.64	$0.64	$0.64	$0.64	$0.33	$0.39	$0.69	$0.64
Ash Cost	$/ton	$2.28	$2.28	$2.28	$2.28	$2.58	$2.52	$2.23	$2.28
SO2 Cost	$/ton	$0.73	$0.73	$0.73	$0.73	$0.82	$0.80	$0.71	$0.73
Other Cost	$/ton	$1.00	$1.00	$1.00	$1.00	$1.00	$1.00	$1.00	$1.00
Coal Worth	$/ton	$24.67	$24.67	$24.67	$24.67	$31.00	$29.65	$23.48	$24.67
Individual Tons	dry	0.00	0.00	0.00	0.00	0.40	3.88	16.24	**20.52**
Cum. Tons	dry	20.52	20.52	20.52	20.52	20.52	20.13	16.24	
Individual Tons	ar	0.00	0.00	0.00	0.00	0.45	4.47	21.13	26.05
Cum. Tons	ar	26.05	26.05	26.05	26.05	26.05	25.60	21.13	---
Cum. Mass	%, ar	100.00	100.00	100.00	100.00	100.00	98.28	81.12	---
Cum. Ash	%, ar	11.42	11.42	11.42	11.42	12.91	12.62	11.42	---
Cum. Sulfur	%, ar	0.79	0.79	0.79	0.79	0.89	0.87	0.79	---
Cum. BTU/lb	ar	10106	10106	10106	10106	10369	10496	10420	---
Individual Worth	$	$0.00	$0.00	$0.00	$0.00	$13.86	$132.56	$496.19	$642.60
Cum. Worth	$	$0.00	$0.00	$0.00	$0.00	$13.86	$146.41	$642.60	---

Coal B - Circuit Configuration 1 - Summary

☑ Lose 50% 325 M

☑ Send SB effluent to HB

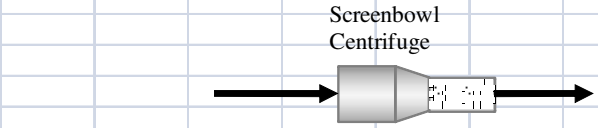

Moisture (%)	Coal Treated (dry tph)	Total Product (dry tph)	Total Product (tph)	Value ($/ton)	Total Value ($/h)	Net Gain ($/h)	Net Gain ($/year)
18.8	85.2	85.2	104.9	$26.2	$3,221	$0.0	$0.0

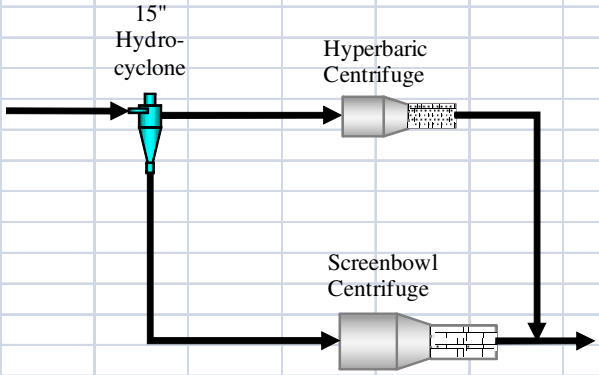

Moisture (%)	Coal Treated With SB (dry tph)	Coal Treated With HFC (dry tph)	Total Product (dry tph)	Total Product (tph)	Value ($/ton)	Total Value ($)	Net Gain ($)	Net Gain ($/year)
13.5	75.8	24.2	100.0	115.6	$29.4	$3,401	$180	$1,081,748

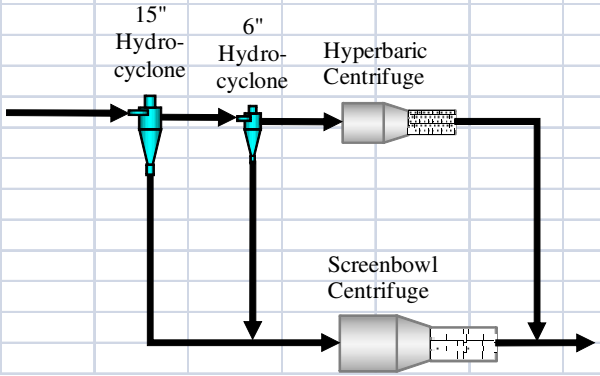

Moisture (%)	Coal Treated With SB (dry tph)	Coal Treated With HFC (dry tph)	Total Product (dry tph)	Total Product (tph)	Value ($/ton)	Total Value ($)	Net Gain ($)	Net Gain ($/year)
14.6	79.5	20.5	100.0	117.1	$28.8	$3,367	$146	$873,832